Osteoclasts are multinucleated cells that degrade cartilage as well as bone

Quitterie C Larrouture

Wolfson College

Supervisors: Helen Knowles and Sarah Snelling



Department of Musculoskeletal Sciences

University of Oxford

A thesis submitted for the degree

Doctor of Philosophy

Michaelmas Term 2019

Acknowledgements

I would like to thank my supervisors, Dr. Helen Knowles and Dr. Sarah Snelling for their support, their guidance and assistance in my research. I feel very lucky to have these supervisors who made these few years so enjoyable. I would also like to thank my many colleagues in the Botnar Research Centre especially to the Edwards research lab taking care of me as if I was part of their group. In particular, I am very grateful to Dr. Emma Morris for answering my questions and for offering much needed support. I had so much fun with you in the tissue culture. Thanks also to my friends; Dr. Sam Olechnowicz, Dr. Jessica Whitburn, Aneka Sowman, Laura Diment, Po Chang, Akira Wiberg, Hajjar and Rob Staruch for sharing the highs and lows of completing a DPhil and for making it so enjoyable along the way. I would also like to thank Dr. Afsie Sabokbar for always being there for a chat and offering a sympathetic ear. I can never thank you enough for your help.

Thank you to Mr. Max Gibbons for the provision of GCTB tissue samples from the Nuffield Orthopaedic Hospital, Oxford. Thank you to Jolet Mimpen and Louise Appleton for helping to collect the TKA from the Nuffield Orthopaedic Hospital, Oxford. Thank you to Dr. Adam Cribbs for the analysis of the sequencing. Thank you to the patients who so kindly gave their permission for us to use their blood and tissue samples for research. I would like to thank Prof. Paul Wordsworth for allowing me to work in his lab for a year and half. In addition to the financial help I had a lot of fun with Dr Matteo Vecellio from his lab. Thank you to my thesis

committee Prof. James Edwards and Dr. James Dunford, your input during the meetings and your positivity were very important to me.

I would like to thank Dr. Srinivasa Rao for the long chats that we had, how to resist his office was in front of the lab…More seriously, thank you for discussing ideas and experiments and your help in this thesis. I would like to thank Florentine Timmer, definitely my time in Oxford will not have been the same without you. Thank you to Dr. Beatriz Gamez Molina for everything, I really enjoyed going to the gym with you and chatting for hours, does not matter what. It has been great going to work with friends every day and I will miss the Pub Night on Fridays with you.

Thanks for the encouragement from my family, I really enjoyed the smile and the excitement of my dad seeing me at the airport. Thank you to my mother for her help and support. I would like to thank my sister Maylis which was present every single day. Thanks to my grandmother and my aunt to have listened to my complaints, doubts and for being able to give me strength when I needed it. Coming to see you in France were important moments for me. Lastly, thank you to my best friend Julia for our endless conversations. Tom, Ben and Anne-So thank you for your support and jokes.

Finally, I would like to say thank you to my partner Emon who has supported me throughout this DPhil in every possible way. You have always had the right words and your help has been invaluable. This thesis is surely a stage of life and I am happy to have done it in your company.

Abstract

Osteoclasts are essential for bone remodelling and are normally found at the bone surface where they create resorption pits. Osteoclasts are present in diseased cartilage in osteoarthritis and rheumatoid arthritis as well as in primary bone sarcomas including osteosarcoma, giant cell tumour of bone and osteochondroma. Whether osteoclasts can also degrade cartilage has been little explored. The aim of this thesis was to characterise how osteoclasts can affect cartilage degradation.

Diseased human cartilage and elephant dentine (positive control) were compared as substrates for osteoclasts. It has been observed by SEM that the cartilage surface around osteoclasts was damaged, suggesting their ability to degrade cartilage. The capacity of CD14+ monocyte-derived osteoclasts and primary human osteoclasts to release glycosaminoglycan and collagen from cartilage was observed in this thesis. Glycosaminoglycan release was reduced by both a pan-MMP inhibitor (GM6001) and TIMP1, suggesting that osteoclasts use soluble MMPs to degrade cartilage by release of proteoglycans. To find the key candidate(s), RT-qPCR and RNA sequencing were performed on osteoclasts cultured on plastic, dentine or cartilage. MMP-8 and MMP-9 genes and proteins were highly expressed in osteoclasts on cartilage and gelatin zymography and siRNA experiments confirmed their activity and involvement in proteoglycan degradation. Finally, we confirmed the presence of MMP-8 and MMP-9 in tissue sections from conditions characterised by OA.

This thesis highlights the morphological, immunophenotypic and gene expression differences when osteoclasts are cultured on different substrates. This thesis also highlights the necessity for contact between osteoclasts and cartilage for direct proteoglycan degradation whilst indirect interaction with osteoclasts degrading bone significantly decreases collagen release from cartilage. Direct and indirect chondrocyte and osteoclast co-culture experiments demonstrated the ability of chondrocytes to control osteoclast formation and activity, potentially via an increase in OPG and RANKL expression. Understanding and controlling the activity of osteoclasts might represent an interesting perspective for pathologies characterized by cartilage degeneration and would present an attractive target for further research.

Contents

Chapter 1 Introduction 1

1.1 Articular cartilage 2

1.1.1 Type and function of joints 2

1.1.2 Structure of articular cartilage 3

1.1.3 Composition of articular cartilage 5

1.2 Cartilage remodelling 12

1.2.1 ECM formation 12

1.2.2 ECM degradation 14

1.2.3 History of the proteolytic enzymes 15

1.2.4 Matrix Metalloproteinases 17

1.2.5 Stromelysins 20

1.2.6 Matrilysins 20

1.2.7 A disintegrin and metalloproteinase with thrombospondin motifs 21

1.2.8 Tissue inhibitors of metalloproteinases 23

1.3 Cartilage pathologies 25

1.3.1 Osteoarthritis (OA) 26

1.3.2 Rheumatoid arthritis (RA) 27

1.4 Bone tissue 28

1.4.1 Function of the skeleton 28

1.4.2 Bone composition 28

1.4.3 Bone development 29

1.4.4 Bone structure 30

1.4.5 Bone remodelling and cells of the skeletal system 32

1.4.6 Osteoclastogenesis 40

1.4.7 Mechanisms of bone resorption 42

1.4.8 Dysregulation of bone remodelling 46

1.5 Bone-cartilage interface 47

1.5.1 Structure and organisation 47

1.6 Hypothesis and aims 53

Chapter 2 Materials and methods 55

2.1 Tissue culture 56
2.1.1 Cell culture conditions 56
2.1.2 Preparation of the surface used to culture osteoclasts 56
2.1.3 Primary cells 59
2.1.4 Co-culture 62
2.1.5 Culture of osteoclasts with cartilage without contact 63
2.2 Biochemistry of osteoclasts 64
2.2.1 Cell viability 64
2.2.2 Proteoglycan detection 65
2.2.3 Collagen detection 66
2.3 Cytochemical assessment of osteoclast formation 67
2.3.1 Tartrate resistant acid phosphatase (TRAP) staining 67
2.3.2 Vitronectin receptor immunohistochemical staining 68
2.3.3 Lacunar resorption staining 70
2.3.4 Immunofluorescence staining (F-actin rings) 70
2.4 Histology of dentine and cartilage 71
2.4.1 Fixation, decalcification and sectioning 71
2.4.2 Haematoxylin and Eosin staining 72
2.4.3 Immunohistochemistry 72
2.4.4 Scanning electron microscopy (SEM) 73
2.4.5 Phenotypic analysis from tissue section 73
2.5 Gene expression 74
2.5.1 RNA extraction 74
2.5.2 RNA quality and concentration 74
2.5.3 Reverse transcription 74
2.5.4 Polymerase chain reaction (PCR) 75
2.5.5 Real-time PCR (RT-qPCR) 77
2.5.6 Primer list 80
2.5.7 RNA sequencing 82

2.6 Protein expression 84
2.6.1 Zymography 84
2.6.2 Western blotting 88
2.7 SiRNA for MMP-8 and MMP-9 92
2.7.1 SiRNA optimization 92
2.8 Statistics 99
Chapter 3 Osteoclasts are present in diseased joints and degrade cartilage *in vitro* 100
Introduction 101
3.1 Joint-related pathologies 101
3.1.1 Osteoclasts in osteoarthritis (OA) 101
3.1.2 Rheumatoid arthritis (RA) 103
3.1.3 Giant Cell Tumour of Bone (GCTB) 105
3.1.4 Osteosarcomas 105
3.1.5 Osteochondroma 106
3.1.6 Chondroblastoma 106
3.1.7 Chondromyxoid fibroma 107
3.2 Osteoclasts and cartilage 108
3.2.1 Chondroclasts 108
3.2.2 Culturing osteoclasts on cartilage 109
3.3 Objectives 110
Results 111
3.4 Osteoclasts in joint pathologies 111
3.4.1 Osteoclasts are observed in the deep zone of OA articular cartilage 111
3.4.2 Osteoclasts are found in the pannus in rheumatoid arthritis (RA) 112
3.4.3 Osteoclasts of Giant Cell Tumour of Bone (GCTB) invade cartilage 113
3.4.4 Giant cell rich osteosarcoma in proximity with cartilage 114

3.4.5 Osteoclasts were observed at the junction of the cartilage cap and the cancellous bone in osteochondroma 115
3.4.6 Benign chondroblastoma contains osteoclast-like cells 116
3.4.7 Chondromyxoid fibroma also contains osteoclast-like cells 117
3.5 Development and testing of the osteoclast-cartilage culture system 118
3.5.1 Increase of aggrecan release in osteoclast-acellular cartilage culture 123
3.5.2 Type II collagen degradation by osteoclasts 125
3.5.3 Bone resorption *in vitro:* collagen release 127
3.6 Mature and active osteoclasts degrade bone and cartilage 130
3.7 Morphological and immunophenotypic characteristics of osteoclast-cartilage culture compared with osteoclast-dentine culture 131
3.7.1 Osteoclasts cultured on cartilage do not have a sealing zone 132
3.7.2 TRAP and VNR positive osteoclasts on articular cartilage 133
3.7.3 Osteoclasts degrading articular cartilage matrix *in vitro* 136
3.7.1 Osteoclasts resorbing bone *in vitro* 139
3.7.2 The expression of osteoclasts markers varies depending on the substrate 142
Discussion 144
Conclusion 151
Chapter 4 Osteoclasts use MMPs to degrade cartilage and contact with their substrate is essential 152
Introduction 153
4.1 Acidification by V-ATPase 153
4.2 Cathepsin K 154

4.3 MMPs 155
4.4 Interaction between bone and cartilage 155
4.4.1 Communication between osteoblasts and chondrocytes *in vitro* 157
4.4.2 Communication of monocytes and macrophages with chondrocytes 158
4.4.3 Communication between osteoclasts and chondrocytes 158
4.5 Objectives 159
Results **161**
4.6 Osteoclasts degrade cellular cartilage 161
4.6.1 Osteoclast-driven proteoglycan degradation is increased on cellular compared to acellular cartilage explants 161
4.6.2 Live chondrocytes do not increase collagen degradation by osteoclasts 164
4.7 Use of inhibitors to find the mechanism of degradation used by osteoclasts 167
4.7.1 Acidification is not required for cartilage digestion 167
4.7.2 Cathepsin K is not required for proteoglycan degradation 169
4.7.3 Osteoclasts use MMPs to degrade cartilage 171
4.7.4 Osteoclasts also degrade cellular cartilage via MMPs 173
4.7.5 Similar trend with mature and active osteoclasts and inhibitors 175
4.8 Direct contact between osteoclasts and cartilage is necessary for GAG release 177
4.9 The interaction between osteoclasts and chondrocytes exists and is modified according to the surface on which osteoclasts are cultured 180

4.9.1 Osteoclasts interact with chondrocytes to stimulate collagen release from cartilage 180
4.9.2 Direct co-culture of osteoclasts and chondrocytes on coverslips 182
4.9.3 Effect of chondrocytes on the morphology and resorption activity of osteoclasts differentiated on dentine 184
4.9.4 Expression levels of OPG and RANKL by chondrocytes change when they are cultured on plastic or dentine 187
Discussion 189
Conclusion 203
Chapter 5 Osteoclasts secrete MMP-8 and MMP-9 to degrade cartilage 204
Introduction 205
5.1 MMPs 206
5.1.1 Collagenases 206
5.1.2 Gelatinases 209
5.1.3 Membrane-type MMPs 210
5.2 ADAMTS 211
5.2.1 ADAMTS-1 211
5.2.2 ADAMTS-4 and ADAMTS-5 211
5.2.3 Other ADAMTSs 212
5.3 Cleavage of aggrecan by MMPs and ADAMTSs 213
5.4 TIMPs 216
5.5 Objectives 218
Results 219
5.1 *MMP8* and *MMP9* are the key candidates responsible for cartilage degradation 219
5.1.1 Osteoclasts degrade cartilage via soluble MMPs 219
5.1.2 RNA sequencing and its validation 223
5.2 Effect of substrate on osteoclast gene expression 228

5.2.1 Gene expression differences between osteoclasts cultured on plastic and osteoclasts cultured on dentine 229
5.2.2 Gene expression differences between osteoclasts cultured on plastic and osteoclasts cultured on cartilage 232
5.2.3 Analysis of the protein expression and activity of secreted MMP-8 and MMP-9 using Western blot and gelatin zymography 235
5.2.4 MMP-8 and MMP-9 contribute to cartilage degradation by osteoclasts 238
5.2.5 MMP-8 cleaves aggrecan at MMP and aggrecanase cleavage sites. 240
5.2.6 MMP-8 and MMP-9 are expressed by osteoclasts in contact with cartilage *in vivo* 242
Discussion **246**
Conclusion **253**
Chapter 6 Summary, Limitations and Future directions **254**
Summary **255**
6.1 Osteoclasts degrade cartilage via MMP-8 and MMP-9 257
6.1.1 Osteoclasts are in contact with cartilage in diseased joints 257
6.1.2 Osteoclast cultured on cartilage degrade the cartilage ECM 257
6.1.3 Osteoclasts express MMP-8 and MMP-9 that are the key candidates responsible for proteoglycan degradation from cartilage 258
6.2 Osteoclast can affect the integrity of cartilage also via paracrine factors 262
6.2.1 Decrease in proteoglycan release by chondrocytes in response to paracrine factors 262
6.2.2 Paracrine factors released by osteoclasts increase collagen degradation from cartilage 264

6.2.3 Chondrocytes affect osteoclasts formation and activity *in vitro* via OPG and RANKL 265
6.3 Osteoclasts activity is altered by substrate they are cultured on 267
Limitations and Future Directions 270
6.4 Further exploration into mechanisms of cartilage degradation by osteoclasts 270
6.4.1 Further validation that osteoclasts are responsible for cartilage degradation 270
6.4.2 Expression and secretion of MMP-8 and MMP-9 271
6.4.3 What is the role of osteoclasts in collagen degradation from cartilage? 271
6.4.4 Do osteoclasts use an MMP independent mechanism to degrade collagen? 272
6.5 Do osteoclasts in normal joints behave the same as in diseased joints? 273
6.5.1 Are MMP-8 and MMP-9 present in other diseased joints? 273
6.5.2 Cartilage degradation in normal joints? 273
6.5.3 Developing a model system *in vitro* to understand the importance of the substrate for osteoclast formation and activity 274
6.6 Interaction between osteoclasts and chondrocytes 275
6.6.1 Is direct contact between chondrocytes and osteoclasts important for the regulation of their formation and activity? 275
6.6.2 Will the same thing happen between healthy chondrocytes and osteoclasts? 276
6.6.3 Can chondrocytes induce osteoclast formation via RANKL secretion? 277
6.7 Can other cells degrade cartilage? 278
6.8 Is the presence of blood vessels important for osteoclasts invasion and activity? 279

Summary statement **281**

Appendix **282**

References **292**

Figures

Figure 1.1 Synovial joints with the articular capsule. Subchondral bone is covered by articular cartilage 3

Figure 1.2 Cells and collagen fibres organisation in articular cartilage (Fox et al, Sports health, 2009)[5]**.** 5

Figure 1.3 Composition of articular cartilage (Chen et al, Nature Review Rheumatology, 2006)[14]**.** 7

Figure 1.4 Structure and organisation of collagen (Knupp et al, Scientific World journal, 2003)[17]. 8

Figure 1.5 Aggrecans are the most abundant proteoglycans in articular cartilage (Iozzo et al, Matrix biology, 2015)[25]**.** 10

Figure 1.6 Domain structure of metalloproteinases. 19

Figure 1.7 Domain structure of ADAMTs and ADAMs. 22

Figure 1.8 Bone structure of growing (a) and mature (b) long bone (Betts et al, Anatomy and Physiology, 2013)[118]. 31

Figure 1.9 Organisation of compact bone; an osteon contains within the central canal blood and lymphatic vessels as well as nerves (Betts et al, Anatomy and Physiology, 2013)[118]**.** 32

Figure 1.10 Osteoclast differentiation is stimulated by M-CSF and RANKL (Kim et al, Chonnam medical journal, 2016)[147]**.** 39

Figure 1.11 The stages of osteoclast differentiation and activation 41

Figure 1.12 Attachment and polarization are key steps for osteoclasts activation 43

Figure 1.13 Osteoclast consumes large amounts of energy to drive HCl secretion that produce calcium, water and phosphate from the mineral comprising the bone matrix. 44

Figure 1.14 Dissolution of organic matrix by proteolysis and waste products are endocytosed 45

Figure 1.15 Representation in 3D of articular cartilage and subchondral bone. 50
Figure 1.16 Diagram representing the hypothesis and the aims of this thesis. 54
Figure 2.1 Pieces collected from a patient undergoing total knee arthroplasty 57
Figure 2.2 Cartilage was peeled A. The piece between the forceps will be cut to approximately 6x6 mm squares B. 59
Figure 2.3 Improving the understanding of osteoclasts cultured on different surfaces 59
Figure 2.4 Improving the understanding of the cartilage transwell experiment. 64
Figure 2.5 Example of gel electrophoresis ran after PCR at 60°C for 5 primers in osteoclasts. 77
Figure 2.6 Example of melting curve with a narrow peak. The primer used is the β-actin in osteoclasts at 60 °C 79
Figure 2.7 Analysis of Zymography in Image J 88
Figure 2.8 PVDF membrane stained with Ponceau S solution to see the protein bands 91
Figure 2.9 The passenger-strand is degraded whereas the guide-strand is used to find the mRNA that has a complementary sequence leading to the cleavage of the mRNA (Dana et al, International journal of biomedical science , 2017)[192] 94
Figure 2.10 Optimization of siRNA, mRNA levels was monitored with 2 osteoclasts preparation. 95
Figure 2.11 Optimization of MMP-8 siRNA, protein levels monitored with 4 osteoclasts preparation in conditioned media (A.) and cells (B.). 96
Figure 2.12 Optimization of MMP-9 siRNA, protein levels monitored with 4 osteoclasts preparation in conditioned media (A.) and cells (B.). 96

Figure 2.11 Decrease of MMP-8 and MMP-9 protein secreted by osteoclasts on cartilage after transfection of siRNA. 98
Figure 3.1 H&E staining of a damaged knee joint of OA patient containing osteoclasts. 112
Figure 3.2 H&E staining of RA tissue section. 113
Figure 3.3 H&E staining of GCTB tissue sections. 114
Figure 3.4 H&E staining of giant cell rich osteosarcoma tissue sections extending through the subchondral plate. 115
Figure 3.5 Osteochondroma sections stained with H&E. 116
Figure 3.6 H&E tissue section of chondroblastoma with osteoclasts. 117
Figure 3.7 Multinucleated osteoclast-like cells in chondromyxoid fibroma with chondroid lobules. 118
Figure 3.8 Osteoclast characterization on dentine. 120
Figure 3.9 Characterization of cartilage explants used for the experiment. 121
Figure 3.10 Cell viability of monocytes differentiated into osteoclasts on dentine, cellular and acellular cartilage. 123
Figure 3.11 GAG release in culture media by osteoclasts on acellular cartilage at day 10, day 13 and over time. 125
Figure 3.12 Collagen release in culture media in presence of osteoclasts on cartilage. 127
Figure 3.13 Collagen release into culture media by osteoclasts on dentines. 129
Figure 3.14 Osteoclasts isolated from GCTB cultured on dentine or cartilage. 131
Figure 3.15 Immunofluorescence staining of actin (Phalloidin) and nuclei (DAPI) in osteoclasts on different substrates. 133
Figure 3.16 Monocytes can differentiate into osteoclasts on cartilage. 135
Figure 3.17 SEM images of osteoclasts on cartilage. 137

Figure 3.18 Transverse sections of osteoclasts degrading cartilage *in vitro*. 139
Figure 3.19 SEM images of osteoclasts on dentine. 140
Figure 3.20 H&E transversal section of active osteoclasts on dentine. 141
Figure 3.21 RT-qPCR of classical osteoclast genes expressed by osteoclasts on plastic, dentine or cartilage. A. Individual 143
Figure 3.22 Summary of the particularities of osteoclasts cultured on plastic, dentine and cartilage. 148
Figure 4.1 GAG release in the presence of osteoclasts on cellular cartilage. 163
Figure 4.2 Collagen release in culture media in the presence of osteoclasts on cartilage. 166
Figure 4.3 Osteoclasts cultured on dentine and cartilage in presence of bafilomycin. 168
Figure 4.4 Osteoclasts cultured on dentine and cartilage in presence of cathepsin K inhibitor. 170
Figure 4.5 Osteoclasts cultured on dentine and cartilage in presence of MMP inhibitor. 172
Figure 4.6 Osteoclasts cultured on cellular cartilage in the presence of inhibitors. 174
Figure 4.7 GCTB-derived osteoclasts cultured on dentine and cartilage in presence of inhibitors. 176
Figure 4.8 Osteoclasts cultured on plastic or on dentine with pieces of cartilage in the transwell. 179
Figure 4.9 Presence of paracrine factors modifying chondrocyte activity in the ECM. 181
Figure 4.10 Actin cytoskeleton and nuclear staining of osteoclasts and chondrocytes. 182
Figure 4.11 Co-culture of osteoclasts and chondrocytes on coverslips. 184

Figure 4.12 Osteoclasts cultured with or without chondrocytes on dentine. 186
Figure 4.13 Expression levels of OPG and RANKL. 188
Figure 4.14 Schematic representation of the results of Chapter 4. 197
Figure 4.15 Schematic representation of the results of Chapter 4. 201
Figure 5.1 Aggrecanase (in red) and MMP (in blue) cleavage sites found within aggrecans. 216
Figure 5.2 Soluble MMPs are involved in cartilage degradation. 221
Figure 5.3 mRNA expression of MMPs in osteoclasts cultured on dentine and acellular cartilage. 223
Figure 5.4 Volcano plot highlighting significantly different genes between osteoclasts on dentine and cartilage. 225
Figure 5.5 The top 15 over-expressed genes. 226
Figure 5.6 RT-qPCR validating gene expression differences between osteoclasts on dentine and osteoclasts on cartilage. 227
Figure 5.7 Principal Component Analysis (PCA) plot of osteoclasts on cartilage, dentine and plastic (no substrate). 229
Figure 5.8 Volcano plot highlighting significantly different genes between osteoclasts on plastic and osteoclasts on dentine. 230
Figure 5.9 The top 15 over-expressed genes. 231
Figure 5.10 Volcano plot highlighting significantly different genes between osteoclasts on plastic and on cartilage. 233
Figure 5.11 The top 15 over-expressed genes. 234
Figure 5.12 MMP-8 is secreted by osteoclasts on cartilage and actively degrades gelatin. 236
Figure 5.13 Expression of the protein MMP-9 by osteoclasts on cartilage and its gelatinase activity. 237

Figure 5.14 Osteoclasts cultured on acellular cartilage use MMP-8 and MMP-9 to degrade the ECM. 239
Figure 5.15 Osteoclasts degrade the ECM via the aggrecanase cleavage site Glu^{373}~^{374}Ala. 241
Figure 5.16 Protein expression of ADAMTS-1 in osteoclasts 242
Figure 5.17 MMP-8 immunohistochemistry in OA tissue. 244
Figure 5.18 MMP-9 immunohistochemistry in OA tissue. 245
Figure 6.1 Diagram representing the hypothesis of this thesis. 256
Figure 6.2 Summary of findings: Identification of the key proteins driving osteoclast-mediated cartilage degradation disease. 261
Figure 6.3 Summary of the results of Aim 2: to determine whether the effects of osteoclasts on cartilage degradation are due to direct degradation, the release of paracrine factors or interaction with chondrocytes. 263
Figure 6.4 Summary of Aim 4: to characterise the differences between osteoclasts cultured on plastic, dentine and cartilage. 269

Appendixes

Appendix A.1 Collagen assay giving the total amount of collagen released in culture media. 282

Appendix A.2 Acellular cartilage cultured in the presence of inhibitors. 283

Appendix A.3 Total amount of GAG released by cellular and acellular cartilage cultured with or without cells. 284

Appendix A.4 Cellular cartilage cultured in the presence of inhibitors. 285

Appendix A.5 Expression levels of OPG and RANKL. 286

Appendix A.6 Soluble MMPs and MT1-MMP are not released by cartilage. 287

Appendix A.7 No compensation effect when cells were transfected with MMP-8 and MMP-9 siRNAs. 288

Appendix A.8 GAG and collagen release by osteoclasts on coated plate. 289

Appendix A.9 Co-culture of monocytes and chondrocytes on coverslips. 290

Tables

Table.1. List of the reagents used for the GAG assay: all the reagents were purchased from Sigma 66
Table.2. List of the reagents used for the collagen assay: all the reagents were purchased from Sigma 67
Table.3. List of the reagents used for the TRAP staining, all the reagents were purchased from Sigma 68
Table.4. Protocol for deparaffinization and rehydration 72
Table.5. Constituents of the reverse transcription reaction mix 75
Table.6. Cycling conditions used for the reverse transcription 75
Table.7. Constituents of the PCR reaction mix 76
Table.8. Cycling conditions used for the PCR 76
Table.9. Constituents of the RT-qPCR reaction mix using SYBR Green 78
Table.10. Constituents of the RT-qPCR reaction mix using TaqMan 78
Table.11. Cycling conditions used for real-time qPCR 78
Table.12. Osteoclasts primer list 80
Table.13. MMPs primer list 80
Table.14. Sequencing validation primer list 80
Table.15. Qiagen primer list 81
Table.16. Primer design primer list 81
Table.17. Taqman primer list 82
Table.18. List of the solutions used for silver staining. All the components were ordered from Sigma 87
Table.19. Composition of 1X laemmili buffer 90
Table.20. Primary antibodies list abbreviations: all primary antibodies were purchased from Abcam 92
Table.21. Secondary antibodies list abbreviations: all secondary antibodies were purchased from ThermoFisher 92
Table.22. List of siRNA used for the experiment 94

α-MEM- alpha minimal essential medium

ABC- avidin-biotin complex

ACP5- tartrate-resistant acid phosphatase type 5

ACTB-Actin β

ADAM- a disintegrin and metalloproteinase)

ADAMTS- a disintegrin metalloproteinases with thrombospondin type I like motifs

ADGRE1- Adhesion G Protein-Coupled Receptor E1

AE2- anion exchanger 2

ALK- activin-like kinase

ALP- alkaline phosphatase

ATP- adenosine triphosphate

BCA - bicinchonic acid

BMP- bone morphogenetic proteins

BSA - bovine serum albumin

C2M- Collagen type II degraded by MMPs

C3- complement component 3

CAII- carbonic anhydrase

CDMP- Cartilage-derived morphogenetic proteins

cDNA - complementary DNA

CFU-G- colony-forming unit granulocyte

CFU-GM- granulocyte-macrophage colony-forming unit

CFU-M- colony-forming unit macrophage

Cl- chloride

CLC7- chloride channel 7

CLP- common lymphoid progenitor

CMP- common myeloid progenitor

CO_2- carbon dioxide

COMP- cartilage oligomeric matrix protein

CTSK- cathepsin K

CTX-I- C-terminal telopeptide I

CTX-II- C-terminal telopeptide II

CysR- cysteine-rich domain

DAB- dimethylaminobenzaldehyde

DABz- 3,3′-Diaminobenzidine

DAPI- 4′,6-diamidino-2-phenylindole

DKK- Dickkopf WNT Signalling Pathway Inhibitor-1

DMEM- dublecco's modified eagle media

DMMB- 1,9-dimethylmethylene blue

DNA - deoxyribonucleic acid

EBI3- Epstein Barr virus induced 3

ECM- extracellular matrix

EDTA- Ethylenediaminetetraacetic acid

EGF- epidermal growth factor

ELISA - enzyme-linked immunosorbent assay

ERK- extracellular signal regulated kinase

FBS - fetal bovine serum

FGF- fibroblast growth factors

FLIP- fluorescence loss in photobleaching

FLS- fibroblast-like-synoviocyte

GAG- glycosaminoglycan

GCK- glucokinase

GCTB- Giant cell tumour of bone

H&E- hematoxylin and eosin

HIF-1α- Hypoxia inducible factor

H_2CO_3- carbonic acid

H_2O-water

HEPES- 4-(2-hydroxyethyl)-1-piperazineethanesulfonic acid

HSC- hematopoietic stem cells

IGF- insulin-like growth factor

IgG – immunoglobulin G

IL- interleukin

ITGAL- the integrin subunit alpha L

JNK- c-Jun N-terminal kinase

LGI2- Leucine-rich repeat glioma-inactivated family member 2

LIGHT- Lymphotoxins exhibiting Inducible expression and competing with herpes simplex virus Glycoprotein D for Herpesvirus entry mediator, a receptor expressed by T lymphocytes

LRP- lipoprotein receptor

M-CSF- macrophage colony-stimulating factor

MAPK- mitogen-activated protein kinases

miRNA- microRNA

MITF- Microphthalmia-associated transcription factor

MMP- matrix metalloproteinase

MSC- mesenchymal stem cells

NFATC1- nuclear factor of activated T cells, cytoplasmic1

NFKB- nuclear factor kappa B

OA- osteoarthritis

OCP- osteoclast precursors

ODF- osteoclast differentiation factor

OPG- osteoprotegerin

OPGL- OPG ligand

PBMC- peripheral blood mononuclear cell

PBS - phosphate buffered saline

PCA- principal component analysis

PE2- prostaglandin E_2

PI3/AKT- phosphatidylinositol-3-kinase/ protein kinase

PTH- parathyroid hormone

PTH- parathyroid hormone

PVDF - polyvinylidene difluoride membrane

qPCR- qPCR - quantitative real-time polymerase chain reaction

RA- rheumatoid arhritis

RANK- receptor activator of nuclear factor κB

RANKL- receptor activator of nuclear factor κB ligand

REDOX- oxidation-reduction

RGD- arginine-glycine-aspartic acid

RNA - ribonucleic acid

RNA Seq - RNA-Sequencing

RUNX2- runt-related transcription factor 2

SDS-PAGE - sodium dodecyl sulphate-polyacrylamide

SEM- scanning electron microscopy

SIGLEC- sialic acid binding immunoglobulin-like lectin

siRNAs - small interfering RNAs

SOST- sclerostin

SOX9- sex determining region Y box 9

Sp- spacer region

STAT3- signal transducer and activator of transcription 3

TBS - tris-buffered saline

TEA- tris-acetate-EDTA

TGF-β- transforming growth factor beta

TIMPS- Tissue inhibitors of metalloproteinases

TNFR – Tumour necrosis factor receptor

TNSF14- TNF superfamily member 14

TRAF- TNF receptor-associated factor

TRANCE- TNF-related activation-induced cytokine

TRAP- tartrate-resistant acid phosphate

TRITC- Tetramethylrhodamine

VNR- vitronectin receptor

Chapter 1

INTRODUCTION

1.1 Articular cartilage

1.1.1 Type and function of joints

Joints are formed where the extremities of bones meet and articulate with each other. Healthy joints allow precise movement, flexibility and help in supporting the weight of the body. There are three main types of joints; fibrous, cartilaginous and synovial joints. Found between the bones in the skull, the fibrous, or fixed joints do not allow any movement[1]. The two extremities of bones are in direct contact with each other and are connected by dense connective tissue. The cartilaginous joint allows more movement than fibrous joints since the dense connective tissue is replaced by cartilage[2]. This type of joint is found in the intervertebral disc. The synovial joints are found where the two extremities of bones are never in direct contact; the knee is the largest synovial joint in the human body. There are 4 important characteristics of the knee; a fibrous joint capsule, which encompasses the distal femur and proximal tibia, the synovium, which is a soft tissue lining of the joint, and the synovial fluid[1]. The synovial fluid increases joint motility and is secreted by the synovial membrane. The synovial fluid is responsible for joint lubrication and providing nutrition to the articular cartilage[3] that coats the end of the bones. (**Figure 1.1**).

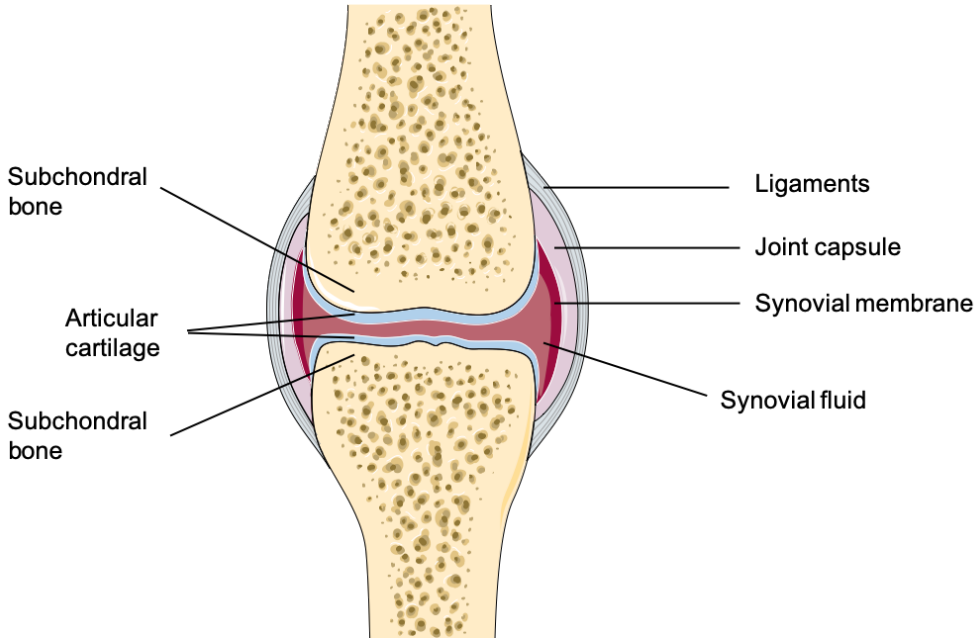


Figure 1.1 Synovial joints with the articular capsule. Subchondral bone is covered by articular cartilage

1.1.2 Structure of articular cartilage

A thin layer of articular cartilage covers the extremities of bones giving high flexibility to the synovial joint and an important resistance to compressive forces. Articular cartilage is hyaline cartilage; there are no blood vessels, nerves or lymphatics[4]. Articular cartilage is composed of a dense extracellular matrix (ECM) containing fibroblast-like cells called chondrocytes. The articular cartilage ECM is mostly composed of water, collagen, proteoglycans and other noncollagenous proteins and glycoproteins[5].

The structure of this cartilage can be divided into 4 zones according to the cell organization and the orientation of the collagen fibres (**Figure 1.2**). The content of proteoglycans and the concentration of water is also different

between cartilage zones[6]. The shape, number and size of chondrocytes varies according to the depth of the zone.

- The superficial zone (10% to 20% of articular thickness) has elongated and flattened chondrocytes and collagen fibres are aligned parallel to the surface, strengthens tensile properties and enhances resistance properties against shear and compressive forces. The superficial zone contains a high concentration of water, no proteoglycans, and type II and type IX collagen fibrils[7].
- The middle zone (40% to 60% of articular thickness) is characterised by round and randomly distributed chondrocytes, and the thicker collagen fibres are in oblique orientation allowing resistance to compressive forces. Type II, IX and XI of collagen are found in this zone.
- The deep zone (30% to 40% of articular thickness) is in contact with the subchondral bone and harbours a few hypertrophic chondrocytes. The largest diameter collagen fibrils (mostly type X of collagen) are perpendicular to the joint surface and parallel to cell columns. This layer is the most resistant to compressive forces since it contains the highest proteoglycan content and the lowest water concentration.
- The tidemark is the interface where uncalcified cartilage in the deep zone meets calcified cartilage in contact with subchondral bone. The calcified zone is a boundary between cartilage and subchondral bone. Collagen fibrils span across these zones and appear to anchor cartilage to subchondral bone.

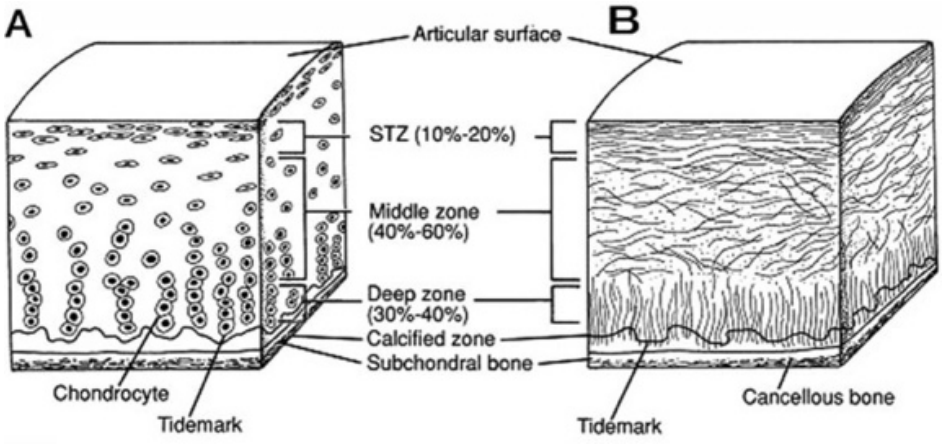


Figure 1.2 Cells and collagen fibres organisation in articular cartilage (Fox et al, Sports health, 2009)[5]**.** The calcified cartilage is on the top of subchondral bone. STZ = superficial zone.

1.1.3 Composition of articular cartilage

1.1.3.1 Chondrocytes

Chondrocytes are the only cell type present in articular cartilage making them responsible for development, synthesis and turnover of the ECM[8]. Chondrocytes have extremely low proliferation rates, but they are metabolically active and respond to a number of environmental stimuli including mechanical load. Stimulation and communication between chondrocytes occurs via soluble mediators that can diffuse through the ECM[9]. Integrins expressed by chondrocytes binds to the ECM proteins that provide signals regulating cell proliferation, survival, differentiation and matrix remodelling also, these integrins are also mechanotransducers and therefore play a role in the biomechanical communication between chondrocytes and the matrix[10].

Chondrogenesis is the transformation of mesenchymal stem cells (MSCs) into chondrocytes. The first step is called condensation; the MSCs differentiate into chondroprogenitors forming a compact cell mass with rounded cells and resulting in the deposition of pre-cartilaginous ECM[11]. Chondroprogenitors express high levels of the transcription factor SOX9 encouraging their proliferation and differentiation to chondroblasts and repressing the expression of the transcription factor RUNX2[12,13]. Chondrocytes differentiate and mature while the matrix, which is initially rich in fibronectin and type I collagen, is replaced by type II collagen and proteoglycans as the main components.

1.1.3.2 Extracellular matrix

The main component of articular cartilage is water found within the intrafibrillar space between collagen fibers. The collagen is the most abundant macromolecule in ECM conferring tensile stiffness and strength to cartilage (**Figure 1.3**).

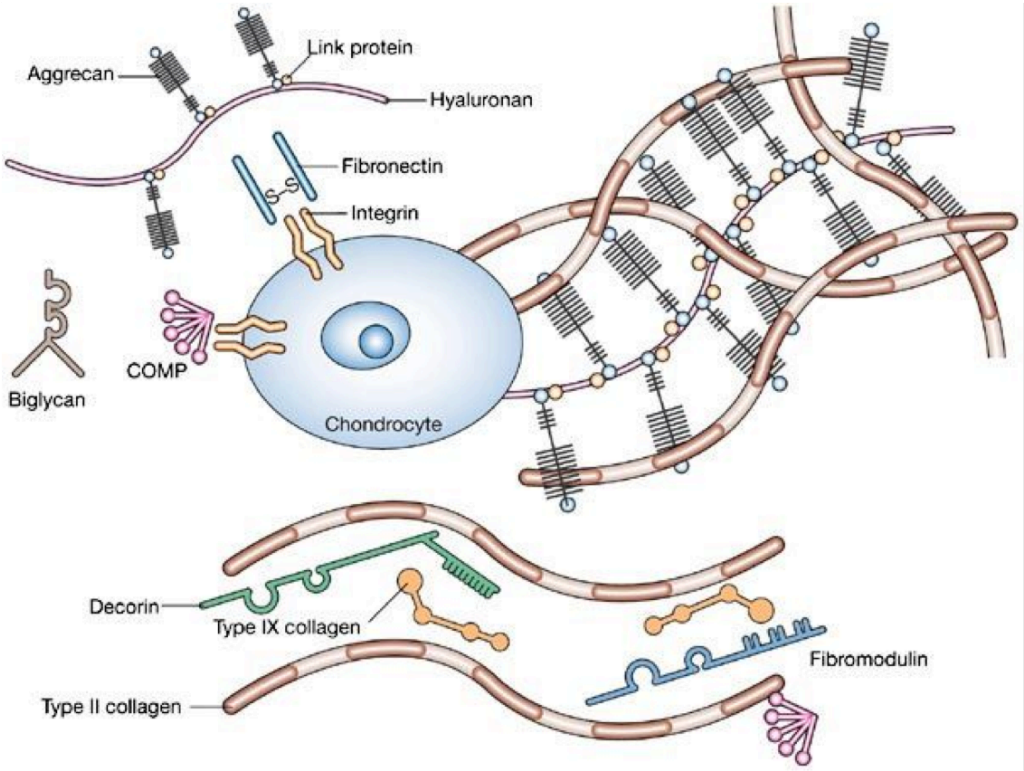


Figure 1.3 Composition of articular cartilage (Chen et al, Nature Review Rheumatology, 2006)[14]**.** Aggrecan is the most abundant proteoglycan. Collagen fibers are intertwined with proteoglycans.

All members of the collagen family contain a region of 3 polypeptide α-chains wound into a characteristic triple helix structure[15] (**Figure 1.4**). Collagen α-chain is characterised by a Glycine-X-Y repeating triplet sequence motif (where X is usually proline and Y is often hydroxyproline) and can undergo post-translational modifications[16]. The triple helical structure is highly resistant to most proteinases. Intercalated between the triplet sequence motifs a glycine-isoleucine or glycine-leucine amino acids can be found. These are the sites of recognition for MMP cleavage. The N- and C-telopeptides of the procollagen are cleaved rapidly by specific

proteases to form a collagen molecule. Collagen molecules are assembled to form fibrils that are parallel and overlap each other[17].

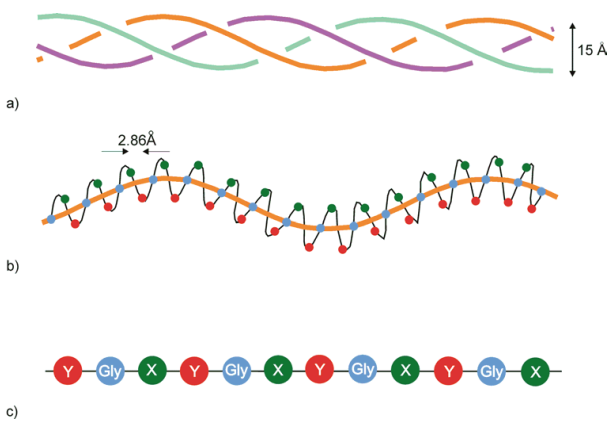


Figure 1.4 Structure and organisation of collagen (Knupp et al, Scientific World journal, 2003)[17].The collagen triple helix is represented in a). The collagen α-chain structure is represented in b) and the α- chain composition is represented in c) with X: proline, Y: hydroxyproline and Gly: glycine.

Type II collagen is the dominant form of collagen forming a fibrillar network in articular cartilage. Collagens can be distinguished by their ability to associate into fibrils or cross-link with different collagen or proteins. In articular cartilage, type IX collagen fibrils cross-linked with type II collagen fibrils binds to non-collagenous protein. This provide a cohesion framework where proteoglycans are intertwined[18]. Type XI collagen makes a critical contribution to the organization and mechanical stability of type II collagen. The network of collagen fibres provides the capacity to contain the swelling pressure. Collagens types I, IV, V and VI are also present acting to form and stabilize the network of collagen[19,20].

Proteoglycans are heavily glycosylated protein monomers and are the second largest macromolecule in articular cartilage. A proteoglycan is attached to a backbone of hyaluronic acid via a link protein, and the complex is referred to as hyaluronan proteoglycan[21] (**Figure 1.5**). A variety of proteoglycans are essential for normal function, including aggrecan, decorin, biglycan and fibromodulin. Aggrecan is the most abundant proteoglycan in articular cartilage (80 %), and it is composed of chains of glycosaminoglycan (GAG). Each chain of GAG is composed of more than 100 monosaccharides[22] and the most common GAG found in aggrecan is chondroitin sulphate and keratan sulphate in smaller quantities. The particularity of aggrecan is that 100 GAGs can be attached to the core protein. Proteoglycans are subdivided into at least three distinct domains. The amino-terminal end of the protein core forms two globular domains G1 and G2, which are separated by a short interglobular domain. The function of the G2 domain is unclear; the interglobular domain contains most of the oligosaccharides, but few or no glycosaminoglycans chains and is a common site for proteolysis. The amino-terminal globular domain (G1) of the core interacts specifically with hyaluronate and cartilage link protein in the formation of proteoglycan aggregates. Link protein stabilises the proteoglycan aggregate and protects the aggrecan from degradation by hyaluronidase of free radical degradation[23]. An intermediate region contains a large part of the keratan sulphate chains and oligosaccharides. A long region containing numerous proteoglycans attachment sites separates the G2 and G3 domains. The attachments of chondroitin sulphate chains are closer to the domain G2 whereas the keratan sulphate chains are closer to the domain G3

at the carboxy-terminal domain of the core protein[24]. The chondroitin sulphate chains are extended and are responsible for the hydrophilic nature and large molecular size/weight of the proteoglycan [25]. The G3 domain is composed of 2 epidermal growth factor (EGF) like repeats and 1 C-type lectin like domain and 1 complementary regulatory protein like domain. Zhen et al. suggested the G3 domain is required for normal trafficking of aggrecan to the ECM[26] and Aspberg et al. highlighted the ability of the lectin like domain to interact with other molecules of the ECM showing the role in anchoring aggrecan in the tissue[27].

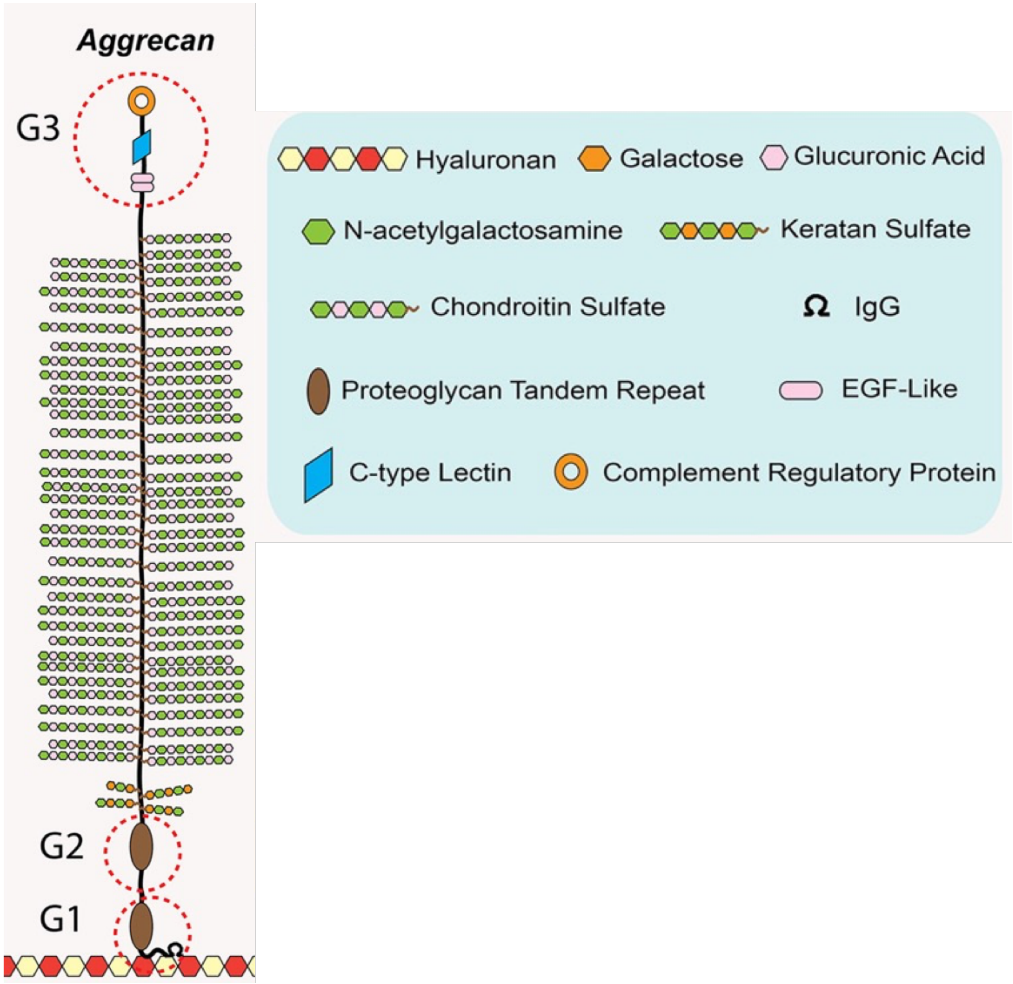


Figure 1.5 Aggrecans are the most abundant proteoglycans in articular cartilage (Iozzo et al, Matrix biology, 2015)[25]**.** The composition of the chains

between the domain G2 and G3 vary but chondroitin sulphate and keratan sulphate are the most common.

The overall negative charge of chondroitin sulphate and keratan sulphate imparts the control of the hydration of the ECM. GAGs are hydrated and when compressed, the water is extruded from the molecules. There is a subsequent return of water when the compressive force is released and the inflexible collagen component resists the swelling pressure and prevents over-hydration of the proteoglycan[28].

The ECM contains a large number of noncollagenous proteins and glycoproteins and several of them play a structural role in the matrix. These proteins may have a role in cell-matrix interactions or in matrix-matrix interactions. Cartilage oligomeric matrix protein (COMP) belongs to the thrombospondin family and is one of the most studied. Its importance was illustrated by the presence of pseudo chondroplasia in individuals bearing a mutation in the COMP gene. These proteins might interact with type IX collagen fibrils and therefore provide stability to the network. The proteins termed cartilage intermediate-layer protein, fibronectin and chondro-adherin are involved in cell-matrix interactions and thought to influence cell proliferation or metabolism in response to a stress. Other proteins are important during the development of the ECM or in juvenile cartilage[29].

Collagen that has been denatured by collagenases can be hydrolysed to form a biodegradable polypeptide called gelatin. Fibronectin is a glycoprotein that is present at low levels in the ECM. Laminin is another glycoprotein with three subunits including α-, β- and γ-chains. These glycoproteins contain

binding sites to collagen and proteoglycans that help to reinforce the ECM structure and improve the organisation of the ECM. The tripeptide arginine-glycine-aspartic acid (RGD) site is recognised by RGD-directed receptors that belong to the integrin superfamily of proteins. Receptors are located at the cell surface allowing a cell-matrix adhesion forming a network[30].

The cartilage matrix also contains a number of cytokines, growth factors, associated ECM proteinases and their inhibitors that are important in tissue remodelling.

1.2 Cartilage remodelling

1.2.1 ECM formation

Articular cartilage turnover is often represented as a balance between anabolic pathways (cartilage formation) and catabolic pathways (cartilage degradation)[9].

A number of essential growth factors and anabolic cytokines are involved in chondrocyte maturation and cartilage formation including transforming growth factor beta (TGF-β) family proteins, bone morphogenetic proteins (BMPs), cartilage-derived morphogenetic proteins, fibroblast growth factors (FGFs) and insulin-like growth factor.

The TGF-β superfamily regulates the early commitment of mesenchymal cells to the chondrogenic pathways during cartilage development and endochondral bone formation[31]. Three isoforms of TGF-β; TGF-β1, TGF-β2 and TGF-β3 are found in articular cartilage and are involved in early chondrogenesis and collagen synthesis. TGF-β signals via

receptors called activin-like kinase (ALK) 1 and ALK5. ALK5 activation causes the phosphorylation of Smad 2/3 that represses hypertrophic differentiation of chondrocytes and maintains collagen and proteoglycan production[32]. ALK1 activate Smads 1/5/8 pathways that stimulate hypertrophic differentiation followed by the production of collagen X, matrix metalloproteinases and bone markers. BMPs are a group of multi-functional growth factors that belong to the TGF-β superfamily. BMPs interact with cellular membrane receptors and act through Smads to increase ECM formation[33]. BMPs are also involved in chondrogenesis, more specifically, BMP2 up-regulates the expression of SOX9 and N-cadherin, promoting cell-cell interaction during the condensation stage of chondrogenesis[31,34]. Cartilage-derived morphogenetic proteins (CDMP) are another subfamily of the TGF-β superfamily and contribute to the formation of the chondroprogenitors and differentiation of chondrocytes[35].

FGFs are known to play a key role in chondrocyte proliferation and differentiation. FGF-2 is often used in tissue culture to differentiate MSCs into chondrocytes and impedes their dedifferentiation process in monolayer culture[36,37]. Mutation in the receptor of FGF-2 results in chondrodysplasia[33]. FGFs are suspected to be inhibitors of hypertrophic chondrocyte differentiation. In mature cartilage, insulin-like growth factor (IGF)-1 is believed to participate in ECM anabolism by enhancing aggrecans, proteoglycans and collagen type II synthesis[31]. Natural mutations in the IGF1 gene result in severe retardation of skeletal development in human and mouse. Studies showed the combination of TGF-β1 with IGF1 enhance total cartilage

production compared with IGF1 alone[38] and affect the proliferation and differentiation of chondrocytes[39]. TGF-β acts early to induce chondrogenesis whereas IGF1 enhances and maintains proliferation.

1.2.2 ECM degradation

Catabolic cytokines interleukin-1β (IL-1β), interleukin-6 (IL-6) and tumour necrosis factor-α (TNF-α) stimulate chondrocyte secretion of proteinases causing ECM degradation such as the matrix metalloproteinase (MMPs) and a disintegrin metalloproteinases with thrombospondin type I like motifs (ADAMTSs)[34] will be discussed in section 1.3.1 and 1.3.2 respectively.

With increasing age, there are changes in the distribution of chondrocytes with dissipation at the superficial zone and increase in the deep zone. There is also a decrease in hydration of the matrix with an increase of stiffness[5,9]. The size of proteoglycans decreases and the proportion of keratan sulphate increases over that of chondroitin sulphate. The composition and structural integrity of ECM in articular cartilage is responsible for the ability of joints to withstand joint forces.

The maintenance of ECM depends on the chondrocyte to mediate synthesis, assembly, and degradation of matrix proteins. A physiological imbalance induced by factors present within the chemical and mechanical environment of the ECM will induce dramatic changes in chondrocyte metabolic activities and degradation of the ECM[11,40]. For example, if loading becomes excessive or if there is inflammation or an injury the pro-inflammatory cytokines TNF-α and IL-1β will increase synthesis of MMPs

and decrease the synthesis of TIMPs. In arthritis, pro-inflammatory cytokines play an important role in cartilage degradation.

1.2.3 History of the proteolytic enzymes

In a study in 1956, it was observed that injection of crude papain into rabbit ears caused the ears to lose rigidity and remain limp for 18 hours after injection. The ear rigidity was returned after 3-4 days but was again lost if papain was re-injected. Papain is a proteinase that cleaves aggrecans by releasing chondroitin sulphate into the microenvironment. This experiment showed that cartilage proteoglycans are susceptible to proteolytic degradation[41]. A similar observation was made when large doses of vitamin A were injected into the rabbit[42]. Lucky et al. and Fell et al. have shown that lysosomal proteases play a part in the degradation of embryonic chick cartilage matrix[43,44]. The action of excess vitamin A results in the secretion of increased amounts of a lysosomal protease named cathepsin D, which has an acid pH optimum (around pH 5)[45]. Synovial fluid in rheumatoid arthritis is more acidic than normal joints however, osteoarthritic joints have a proteolytic activity at neutral pH [46,47]. To confirm the importance of cathepsin D in the breakdown of cartilage and due to the absence of a specific chemical inhibitor, blocking antibodies were used. At pH 5, over 90 % inhibition of degradation was obtained in bovine nasal cartilage. The optimal activity of purified cathepsin D on proteoglycans is at pH 5. Pepstatin or chloroquine, which are potent inhibitors of cathepsins, inhibited proteoglycan degradation at pH 5 but had no effect at neutral pH[48]. While the amount of cathepsin D is high in human cartilage, the action must be limited to an environment where

an acid pH might be produced[49]. All these observations suggested the presence of an unidentified neutral proteinase historically called proteoglycanase[50,51].

In 1976, Sapolsky et al. described three enzymes: a neutral protease that digests proteoglycan subunits optimally at pH 7.2 and two acid enzymes distinct from cathepsins that could digest proteoglycan subunits at pH 4.5 and 5.5. After inhibition by o-phenanthroline (chelator), their activity was restored by zinc or ferrous ions[52]. These metal-dependent properties earned them the name of metalloproteinases or matrixins. One year later, Ehrlich et al. demonstrated that an enzyme preparation, extracted from human OA cartilage, was able to degrade collagen and aggrecan since resulting fragments contained chondroitin sulphate and keratan sulphate[53]. From this time, the metalloproteases were not only believed to degrade proteoglycans but also type IV collagen, laminin, fibronectin and procollagen[54]. Matrix metalloproteinase 3 (MMP-3) was isolated from human articular cartilage and found to cleave aggrecan between G1 and G2 domains at Asn^{341}-Phe^{342} [55]. At that time, it was believed that MMPs were the main aggrecan-degrading enzymes in osteoarthritis. In 1992, Sandy et al. showed that synovial fluid purified from OA patients contained aggrecan fragments that were cleaved, in a large majority, at a different location (Glu^{373}-Ala^{373}) between G1 and G2 domains. This new location was also shown in cytokine-stimulated chondrocyte and cartilage explant cultures[56,57]. The endogenous MMP inhibitors (Tissue inhibitors of metalloproteinases (TIMP)-1 and TIMP-2) did not inhibit the release of these fragments suggesting that MMP activity was not responsible for "aggrecanase" activity[58]. The aggrecanase 1, also called a

disintegrin metalloproteinases with thrombospondin type I like motifs (ADAMTS)-4, was purified for the first time from Il-1 stimulated bovine nasal cartilage by researchers at DuPont Pharmaceuticals in 1999[59]. MMPs and ADAMTSs are considered as the major mediators of collagen and proteoglycan cleavage[60,61].

1.2.4 Matrix Metalloproteinases

The first MMP was discovered in 1962 when skin from the resorbing tail of metamorphosing tadpoles was cultured on a collagen gel, and an enzyme able to degrade triple helical collagen at neutral pH was observed[62]. This enzyme was called MMP-1 and is now part of a large family with 24 members. MMPs are classified into 6 subgroups; collagenases, gelatinases, stromelysins, matrilysins, membrane-type MMPs and other non-classified MMPs. A typical MMP consist of several domains: the pre-domain also called signal peptide, pro-peptide domain, catalytic domain and hemopexin domain (**Figure 1.6Figure 1.6**). The pro-peptide is 80 amino acids long with a cysteine switch motif (PRCGXPD) that interacts with the catalytic zinc ion, thereby controlling the enzyme activity[63]. The catalytic domain is 170 amino acids long and contains the zinc-binding motif (HEXXHXXGXXH) and the active site. The type of amino acids at the active site varies according to the substrate and enhances the catalytic efficiency towards the substrate. A linker peptide of variable length, known as the hinge region, is present between the catalytic domain and the hemopexin domain. The hemopexin domain, composed of 200 amino acids, is responsible for the interaction with substrates and other MMPs or the binding to inhibitors or cell surface[64].

Except the membrane-type MMPs that are anchored to the plasma membrane, other MMPs are soluble and therefore secreted as extracellular protein.

The catalytic activity of MMPs is regulated at four points: gene expression, the storage of the enzyme, the activation of the pro-enzyme and inactivation by the formation of a complex with inhibitor[65]. Growth factors, inflammatory cytokines, hormones, other MMPs, cell or ECM interactions will modify the signalling pathways that in turn stimulate or reduce the transcription of MMPs[66]. MMP expression is also regulated via natural silencing machineries such as microRNA (miRNA) and through inhibiting the translation of the prepro-enzyme into pro-enzyme[67]. The compartmentalisation can be intracellular or pericellular. MMPs are either confined to pericellular compartments such as secretion vesicle or anchored to the matrix or cell membrane ensuring a sufficiently high enzyme concentration within the defined location. MMPs are synthesised and secreted as inactive pro-MMPs[68]. The cysteine switch maintains the protein in an inactive state. Activation of the enzyme requires either proteolytic processing of the pro-peptide domain by other MMPs or a physical or a steric disruption of the pro-peptide conformation. The presence of inhibitors is the last stage where proteinases are physiologically controlled, and it will be discussed in section 1.2.6.

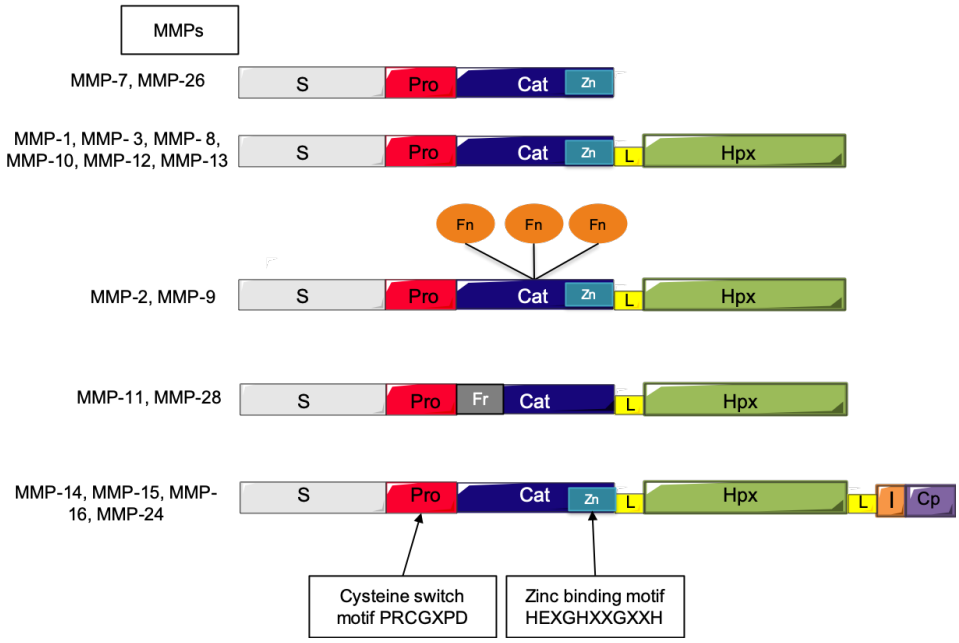


Figure 1.6 Domain structure of metalloproteinases. S: Signal sequence, Pro: Pro-domain, Fr: Furin cleavage, Cat: Catalytic domain, Fn: Fibronectin repeat, Zn: Zinc cleavage L: Linker, Hpx: Hemopexin domain, I: Transmembrane domain (Type 1) and Cp: Cytoplasmic tail.

More and more studies show that MMPs are not only capable of degrading all components of the ECM but also participate in physiological processes such as inflammation, angiogenesis, bone remodelling and embryogenesis. Understanding the exact role of MMP in angiogenesis is important for cancer therapy because it is necessary for tumour growth, tumour invasion and metastasis[69,70]. Except other pro-proteases and protease inhibitors, MMPs also act on a wide range of non-matrix extracellular proteins such as cytokines, receptors, membrane proteins and antimicrobial peptidest[71,72].

1.2.5 Stromelysins

In 1986, a neutral metalloproteinase was isolated from the culture medium of human rheumatoid synovial cells stimulated with rabbit macrophage-conditioned medium. This metalloproteinase was different from the collagenase and gelatinase already described. The enzyme was able to cleave proteoglycans, collagen type IV, gelatin and laminin. A similar enzyme was purified from rabbit fibroblasts and has been named stromelysin[73]. The name stromelysins refers to their ability to degrade multiple components of the ECM or stroma. MMP-3, MMP-10 and MMP-11 are now known as stromelysin 1, stromelysin 2 and stromelysin 3, respectively. MMP-11 is structurally and functionally divergent to MMP-3 and MMP-10, and it can be activated intracellularly. MMP-3 and MMP-10 are structurally similar to collagenases but fail to cleave the triple helical regions of type II and I collagen. The stromelysins participate in pro-MMP activation of pro-collagenases (pro-MMP-1 and pro-MMP-13) and pro-gelatinases (pro-MMP-9). MMP-3 has been described as an important factor in the development of arthritis: it is a marker of progression of joint degradation in rheumatoid arthritis and might be an indicator of early diagnosis of osteoarthritis[74]. The physiological function of MMP-10 and MMP-11 is still unclear.

1.2.6 Matrilysins

MMP-7 was first described as a putative uterine metalloproteinase-1 in 1988. MMP-7 and MMP-26 lack a hemopexin domain and can degrade collagen type IV, fibronectin and laminin. The matrilysins are the smallest of

the MMPs; they contain only the pro-peptide and catalytic domains and are unable to cleave intact collagen. However, MMP-7 can degrade most of the ECM components such as elastin, gelatin, laminin and fibronectin. MMP-7 knockout mice highlight its role in innate immunity; the mice show a decreased resistance to bacterial gastrointestinal infection[75]. As with other MMPs, MMP-7 has been identified in tumours and correlates with aggressiveness of the tumour. For example, the degradation of E-cadherin decreases cellular adhesion promoting tumour invasion. MMP-26 is less active in the ECM degradation since it cannot cleave collagens, laminin and elastin[76].

1.2.7 A disintegrin and metalloproteinase with thrombospondin motifs

The ADAMTSs are a family of 19 members secreted metalloproteinases involved in various developmental and homeostatic processes such as angiogenesis, coagulation and arthritis[60,77]. The first aggrecanase purified from IL-1-stimulated bovine nasal cartilage was called aggrecanase 1 or ADAMTS-4[59]. This was quickly followed by the purification of aggrecanase-2 or ADAMTS-5. ADAMTSs proteins are also secreted as a prepro-enzyme including a signal peptide, pro-domain, catalytic domain, disintegrin-like domain, a central thrombospondin type I-like (TS) repeat, a cysteine-rich domain (CysR), a spacer region (Sp) and a variable number of C-terminal TS repeats[78] **(Figure 1.7).**

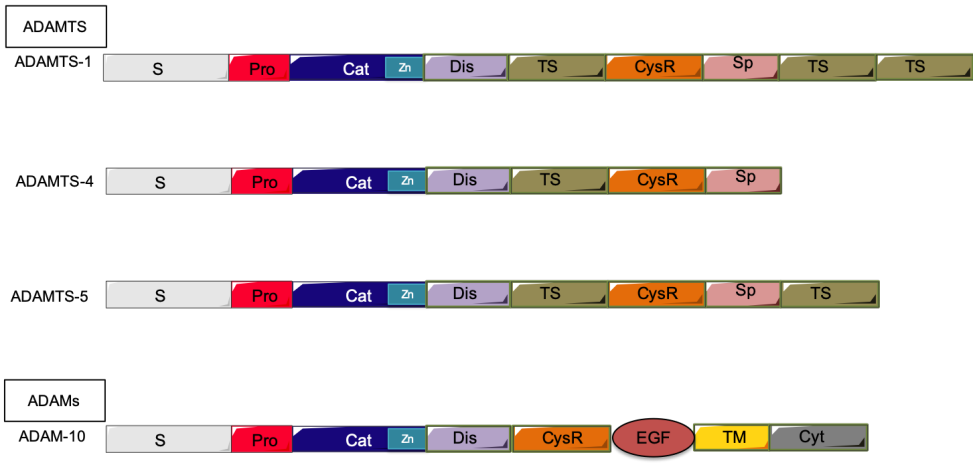


Figure 1.7 Domain structure of ADAMTs and ADAMs. S: Signal sequence, Pro: Pro-domain, Cat: Catalytic domain, Zn: Zinc cleavage, Dis: Disintegrin domain, TS: Thrombospondin type 1, CysR: Cysteine rich domain, Sp: Spacer domain, EGF: Epidermal growth factor-like repeat, TM: Transmembrane domain and Cyt: Cytoplasmic domain.

Another member of the metalloproteinase family named a disintegrin and metalloproteinase (ADAMs) are expressed and participate widely to a variety of biological processes. 21 ADAMs are found in humans and 13 of them are proteolytically active. Most ADAMs have an EGF-like domain between the cysteine-rich domain and the transmembrane region with a cytoplasmic tail (**Figure 1.7**). The length and the sequence of the tail vary between different ADAM family members[79]. 8 ADAMs are non-haematopoietic and non-testis specific, among them ADAM-9, ADAM-10, ADAM-15 and ADAM-17 have been characterised in joint homeostasis and arthritis. ADAM-10 is low in normal cartilage and increased during osteoarthritis development and in response to pro-inflammatory cytokines[80]. It has only been shown that ADAM-10 can cleave collagen type IV *in vitro*[81].

1.2.8 Tissue inhibitors of metalloproteinases

In 1975, Bauer et al determined that an inhibitor produced by human skin fibroblasts and present in their conditioned medium was able to abolish over 90 % of the collagenase activity[82]. A second study found that a single inhibitor isolated from human serum inhibited 4 human collagenases from skin, rheumatoid synovium, gastric mucosa and granulocytes[83]. In 1976, Kuettner et al demonstrated that a collagenase inhibitor isolated from human cartilage and bovine cartilage and aorta was an effective inhibitor of human skin collagenase. They suggested that collagen turnover in cartilage might be under a "strict control via an enzyme-inhibitor-complex" and deficiency in inhibition may be related to cartilage collagen degradation in disease[84]. Murphy et al observed that collagenase inhibitory activity was detected in skin, bone, and uterine cultures and therefore proposed that all connective tissues synthesize collagenase inhibitors in order to control local enzyme activity[85]. In 1979, two studies showed that the purified inhibitor inhibited collagenase activity with 1:1 stoichiometry and that the inhibitor ranged in size from 25-31 kDa[86,87]. Finally, in 1981 this endogenous inhibitor was found to inhibit multiple metalloproteinases, including collagenase, gelatinase, proteoglycanase and was termed tissue inhibitor of metalloproteinase[88].

TIMPs are 4 genes encoding TIMPs (*TIMP-1*, *TIMP-2*, *TIMP-3* and *TIMP-4*) resulting with 184-194 amino acids long proteins. Mammalian TIMPs contain an N-terminal domain of 125 residues approximately and a C-terminal domain of 65 residues. Each domain contains 6 conserved cysteine residues, which form 3 disulphide bridges per domain that stabilise the domain structure. Four residues at the N-terminal domain of the substrate will

bind to four residues attached in TIMP-1 by a disulphide. The structure will be interposed in the active site of the MMPs and a residue Cys1 located at the N-terminal bound to the zinc atom in the catalytic domain[89]. The sequence identity of the 4 TIMPs shows similarities especially between TIMP-2 and TIMP-4 or between TIMP-2 and TIMP-3[90,91]. Despite their similarities, differences do exist between the 4 TIMPS in their inhibitory range, tissues in which they are expressed and localization within tissues.

TIMP-2 inhibits all MMPs including MT-MMPs and is important in the cell-surface activation of pro-MMP-2. A complex is formed between pro-MMP-2, TIMP-2 and MT1-MMP to cleave the pro-domain of the zymogen. *Timp2* null mice confirmed that TIMP-2 is required for pro-MMP-2 activation *in vivo* and *in vitro*. It is important to note that exogenous addition of TIMP-2 could restore activation of pro-MMP-2 *in vitro*[92]. Another study showed that *Timp2* null mice exhibit phenotypes associated with the central nervous system. They display symptoms of altered motor dysfunction due to peripheral and central nerve defects resulting from abnormal ECM turnover and reduced neuronal differentiation[92]. TIMP-3 is the only one tightly bound to the ECM and has the broadest inhibition spectrum as it inhibits several numbers of the MMPs, ADAMs and ADAMTSs families. *Timp3* null mice showed an increase in cartilage degradation with aging due to increased ECM degradation by MMPs and ADAMTSs, in particular ADAMTS-5 and MMP-13[93]. ADAMTS-4 and ADAMTS-5 are effectively inhibited only by TIMP-3. TIMP-3 protein expression is less present in human osteoarthritis cartilage compared to normal cartilage[94]. Intra-articular injection of N-terminal or full-length TIMP-3 inhibited cartilage degradation in a rat meniscal tear model.

This indicates that TIMP-3 has the capacity to block cartilage degradation[95]. *Timp3* null mice show a metalloproteinase activity in the lung during development leading to impaired branching of the bronchiole compared to the wild type due to a reduction in fibronectin abundance. GM6001, a broad inhibitor of MMPs decreased the degradation of fibronectin and rescued the impaired bronchiole[96]. TIMP-4 is the least studied of the TIMP family. TIMP-4 binds to pro-MMP-2 as TIMP-2 does and is also a strong inhibitor of MT1-MMP but TIMP-4 cannot activate pro-MMP-2[97]. TIMP-4 is expressed primarily in the heart and lower levels of expression in the kidney, placenta, colon, testes and adipose tissue. *TIMP-4* null mice display various cardiac defects, reflecting the expression profile of this inhibitor[98]. TIMP-4 promotes high fat-induced obesity and fatty liver suggesting that targeted inhibition of TIMP-4 could be a therapeutic target against obesity[99].

1.3 Cartilage pathologies

There are many diseases that affect cartilage osteoarthritis (OA), inflammatory arthritis including rheumatoid arthritis (RA), cartilaginous tumours, chondrocalcinosis and other rare genetic disorders. The avascular nature of cartilage presents a challenge for delivery of treatments to cartilage itself[100]. A short description of osteoarthritis and rheumatoid arthritis is described here since OA and RA are the most common cartilage-related diseases and will be used as a comparison with normal joints in this introduction. Other cartilage pathologies will be discussed in detail in chapter 3.

1.3.1 Osteoarthritis (OA)

Osteoarthritis (OA) is the most common type of arthritis. It is a progressive joint disease associated with pain and stiffness. OA is a disease of the whole joint characterised by a progressive loss of articular cartilage, synovial inflammation and thickening of the subchondral bone. The degeneration of cartilage is associated with mechanical stress and systemic inflammation induced by obesity, joint injury and genetic predisposition[8]. The progression of OA can be described in two phases, the biosynthetic phase with repair of cartilage damage and proliferation of chondrocytes. Hypertrophic chondrocytes are proliferative and more active, they increase the production of both; matrix proteins and matrix-degrading proteins. Cartilage formed by hypertrophic chondrocytes is different from normal articular cartilage; collagen type II is replaced by type I and collagen type X accompanied by a calcification of the matrix. This is progressively followed by their apoptosis and a vascular infiltration of the cartilage[101]is produced. The second is the degradative phase with remodelling of the matrix, hypertrophic chondrocytes, cartilage vascularization and calcification and subchondral bone formation. Despite this increased activity, the repair of matrix components is limited and the production of proinflammatory mediators, including interleukin (IL)-1β and TNFα, directly induces the catabolic activity of chondrocytes. Interleukin (IL)-1β is upregulated in OA and increases the production of matrix degrading enzymes such as MMP-1, MMP-3 and MMP-13 in chondrocytes. At the same time IL-1β was shown to

downregulate SOX9 which decreases the expression of collagen type II and aggrecan[102].

1.3.2 Rheumatoid arthritis (RA)

Rheumatoid arthritis (RA) is the second most common arthritis. It is an autoimmune disorder involving chronic inflammatory polyarthritis. Several risk factors are known to be involved in the development of RA including genetics, female sex, and environmental factors (smoking or infectious agents). The progression of RA consists of a primary inflammatory response with swelling and stiffness, then the cartilage and bone are degraded which starts to decrease the mobility of the joint and will eventually end up with a total loss of function[103]. After entering the joint, immune cells (T cells and B cells) induce a further inflammatory response by activating macrophages, osteoclasts, neutrophils and blood monocytes. Cytokines such as TNF, IL-1, IL-6 and IL-17 contribute to inflammation and activate fibroblast-like-synoviocyte (FLS) cells. The activation of FLS increases their expression of the receptor activator of nuclear factor κB (RANK) ligand (RANKL) that, associated with other inflammatory cytokines, stimulates osteoclast activity. The T cells promote inflammation and produce IL-17 that will increase macrophage activity as well as stimulate the FLS cells. The proliferative FLS invade and penetrate the joint space to form a pannus, spreading across the cartilage surface and producing degrading matrix enzymes which erode the cartilage tissue as well as bone[104,105].

1.4 Bone tissue

1.4.1 Function of the skeleton

Skeletal tissue includes bones, cartilage as well as ligaments and tendons. Bone is a complex and vital structure that serves essential functions. It mechanically supports the body by facilitating movement and locomotion as well as protecting internal organs. Bone marrow is the main source for white and red blood cells and its reservoir of minerals and fats metabolically supports the body.

1.4.2 Bone composition

Bone's unique combination of organic and inorganic phases provides both tensile and loading strength[106]. The organic phase (20 % - 40 %) is mainly composed of collagen type I where each layer of collagen fibrils is oriented at a different angle to the previous layer. In addition to providing structural strength and flexibility to the bone, the collagen fibrils determine the structural organization for other proteins and act as a template for mineral deposition. Lipids and water are also present in bone. There are smaller but significant amounts of non-collagenous proteins such as enzymes, growth factors, proteoglycans, glycoprotein, calcium binding proteins, and adhesion molecules[107]. These proteins are involved in cell activity and proliferation, cell-cell interaction, cell-ECM interaction, ECM organisation and mineralisation[108,109].

The inorganic phase (50 % - 70 %) is composed of hydroxyapatite crystals around the collagen composite providing mechanical resistance to the tissue and also serving as a source of calcium and phosphate for mineral

homeostasis[110,111].

1.4.3 Bone development

The embryonic skeleton is derived from three cell lineages[112,113]. The neural crest cells form the craniofacial skeleton, the sclerotome cells from the somites form the axial skeleton and the lateral plate mesoderm cells form the limbs. The mesenchymal cells that differentiate from these cell lineages condense and form regions of high cell density. The skeleton at the embryo stage consists of fibrous membrane and hyaline cartilage. At this point, the tissue can form bone by two different processes: intramembranous ossification or endochondral ossification to replace the cartilage template[114]. Intramembranous ossification involves the regions of mesenchymal condensations differentiating directly into bone forming cells called osteoblasts and thereby synthesising bone matrix called osteoid[113,115]. This bone matrix is highly vascularised with irregular and disorganised collagen fibres. The secretion of the osteoid is inward toward ossification trapping osteoblasts within bone matrix. A few days later, the osteoid calcifies and hardens forming the final woven trabecular bone. The periosteum formation allows a lamellar bone replacement of the woven bone at the outer edge. Intramembranous ossification occurs mostly in flat bones such as the cranial bones and clavicle.

Endochondral ossification involves the replacement of cartilage 'bone' models with bone. Long bones mainly develop by endochondral ossification and are characterised by longitudinal growth driven by a specific layer of cartilage called the growth plate[115]. These models are formed when the

mesenchymal cells differentiate into chondroblasts, which secrete a cartilaginous matrix. The outer layer of cartilage tissue in the forming bone, the perichondrium, is vascularised delivering nutrients to this area stimulating the remaining MSCs to differentiate into osteoblasts. Chondrocytes continue to proliferate and contribute to the overall elongation of the structure. The periosteal bud consists of blood vessels; nerves, lymphatics and osteogenic cells will appear in the middle of the bone. The chondrocytes in this growth plate undergo a cycle of proliferation, differentiation, hypertrophy and death, allowing the long bones to lengthen. When the chondrocytes become hypertrophic, they secrete an extracellular matrix, which is then calcified and partially resorbed by osteoclasts (specialist bone-resorbing cells) allowing blood vessels to penetrate the avascular cartilage. Osteoblasts are then recruited to remodel the cartilage into woven bone and subsequently mature lamellar bone[112,116].

When the long bones have grown to their full length the growth plate is calcified and remodelled. A secondary ossification centre appears after birth resulting in the ossification of the epiphyses.

1.4.4 Bone structure

The long bone is divided into three zones: the epiphysis, the metaphysis and the diaphysis[117] (**Figure 1.8**). The epiphysis is located at either end of the bone and is connected by the metaphysis to the central diaphysis. The internal space enclosed by the epiphysis and metaphysis contains trabecular bone. This bone is characterised by a network of fine bone structures that resemble the structure of a sponge. The spaces in this fine network are filled with bone

marrow. This sponge-like structure maximises the surface area of the bone in contact with the marrow, fulfilling a primarily metabolic role. Cortical bone is a thick dense layer of bone. This bone is often organised into concentric structures that surround blood vessels and nerves called Haversian systems or osteons. Thus, the diaphysis, which is subjected to high stress, tends to have a thick cortical layer that encloses the bone marrow cavity while the epiphysis has only a thin cortical layer.

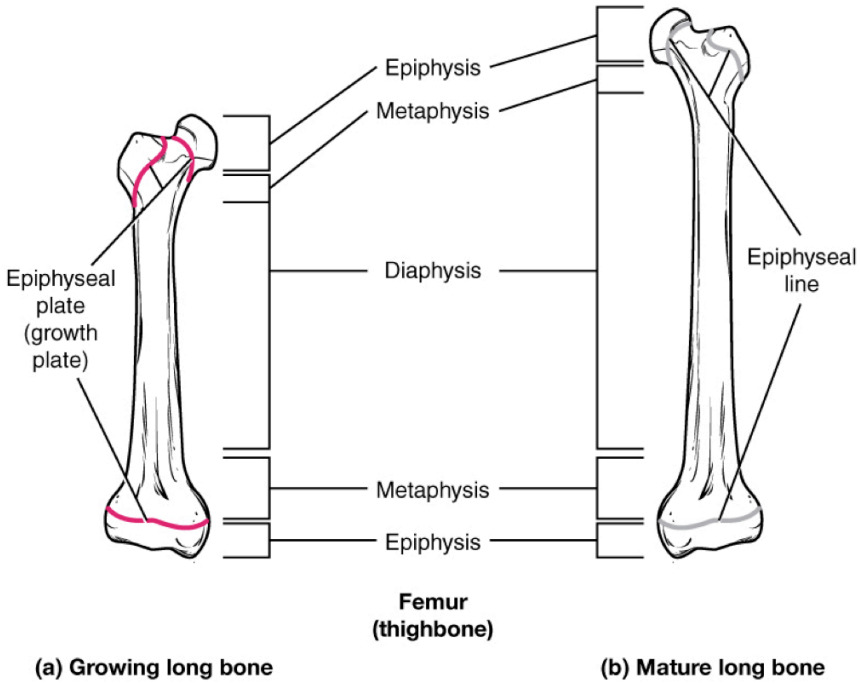


Figure 1.8 Bone structure of growing (a) and mature (b) long bone (Betts et al, Anatomy and Physiology, 2013)[118].

The osteon consists of a central canal called the Haversian canal, which contains blood and lymphatic vessels and nerves (**Figure 1.9**). This canal is surrounded by concentric rings (lamellae) of matrix, which correspond to a linear deposition of dense mineral and collagen. Bone cells (osteocytes) are located between the rings of matrix, in the lacunae. Small channels (canaliculi) radiate from the lacunae to the Haversian canal forming a system

of interconnected canals. An external layer of bone covering the surface is called the periosteum and the inner layer that lines bone is called the endosteum. These deep layers are non-specialised connective tissue that hosts osteoclasts and osteoblasts[107].

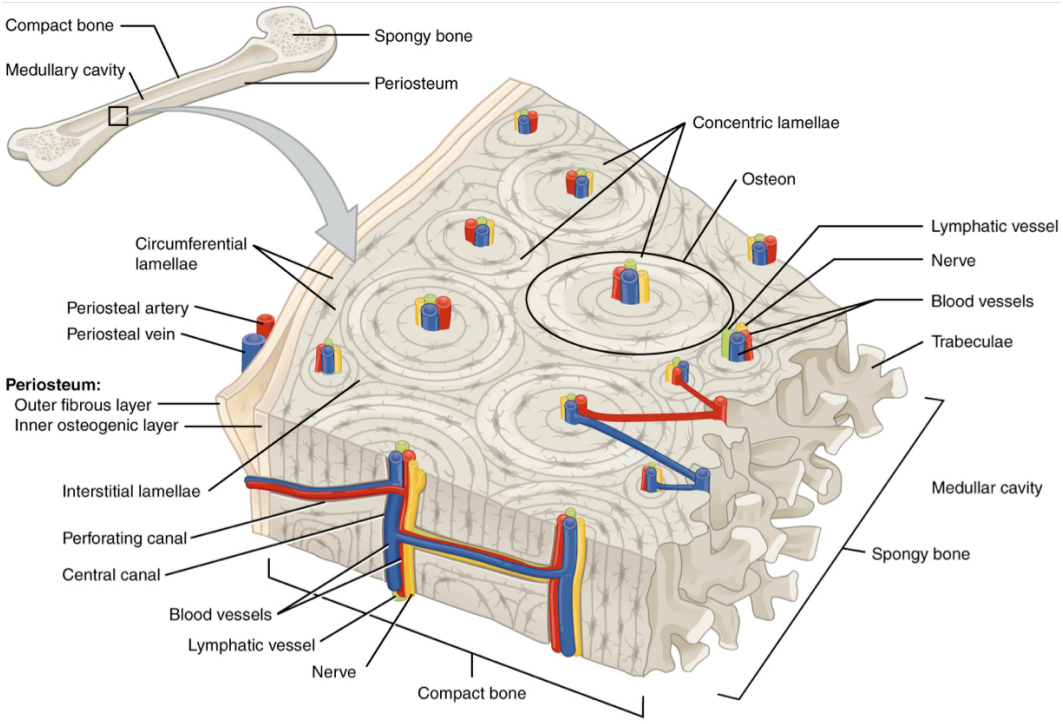


Figure 1.9 Organisation of compact bone; an osteon contains within the central canal blood and lymphatic vessels as well as nerves (Betts et al, Anatomy and Physiology, 2013)[118]**.** (Micrograph provided by the Regents of University of Michigan Medical School © 2012)

1.4.5 Bone remodelling and cells of the skeletal system

10 % of the adult skeleton is renewed each year. Two cell types, osteoclasts that resorb bone matrix and osteoblasts that synthesize new matrix, ensure the remodelling. The balance between destruction and formation of bone is regulated by complex interactions between bone cells, as well as chemical and mechanical change in the local microenvironment.

Skeletal diseases are attributable to an imbalance in the differentiation and/or activity of these cellular components. Therefore, understanding factors influencing their biology and the signalling pathways that control their formation and function has a therapeutic value. Bone marrow contains two distinct populations of stem cells: one is hematopoietic stem cells (HSCs) and the other is MSCs. Bone forming cells, osteoblasts and osteocytes, are derived from MSCs while bone resorbing cells, osteoclasts, are derived from HSCs[119].

1.4.5.1 Osteoblasts and mineralization

Osteogenesis is characterised by cessation of MSC division followed by their differentiation into functional osteoblasts responsible for the synthesis and mineralization of bone matrix. Osteoblasts, located at the outer and inner surfaces of the bone tissue, produce a bone mineralised ECM. Mature osteoblasts are cuboidal cells with a large endoplasmic reticulum and prominent Golgi apparatus[119]. Tight and gap junctions between osteoblasts form a tight epithelium-like cell layer that separates the general extracellular fluid from the bone matrix. Mature osteoblasts express osterix and secrete bone matrix proteins such as collagen type I, osteocalcin and bone sialoprotein. They control, on their apical surface, the matrix environment during mineralisation with an important alkaline phosphatase (ALP) activity. ALP enzyme activity is necessary to supply phosphate for bone mineral, although it should be noted that ALP alone is not sufficient for mineralisation *in vitro*[120,121]

Mineralization takes place underneath osteoblasts with the precipitation by alkaline phosphatase of calcium and phosphate minerals producing hydroxyapatite crystals. Mineral will intercalate within the gaps between type I collagen fibrils that have been produced by osteoblasts. It is a complex

process controlled by many factors including mineral concentrations, enzyme activity and the composition of the bone matrix[120].

1.4.5.2 Bone lining cells

Lining cells are quiescent osteoblasts, which, if necessary, can be activated to re-differentiate into osteoblasts. They line the majority of adult bone surfaces, resting on the mineralised bone. The role of bone lining cells includes protecting bone surfaces from osteoclasts attaching to the bone matrix in areas that are not required for resorption, retraction from the bone surface when osteoclasts are recruited for bone resorption, linking resorption phase to formation phase. In contrast to osteoblasts, these cells have a flattened shape with few organelles[112,119,122].

1.4.5.3 Osteocytes

Osteocytes are the most numerous bone cells (90 – 95 %) and have a half-life of 25 years. The activity of bone formation osteoblasts ends with their differentiation into osteocytes, when the osteoblastic cells are completely surrounded by calcified matrix. The volume of the cells is reduced and has numerous cellular processes that project through the canaliculi[112,115]. These dendritic projections extend through the osteoid to the vascular space or bone surface, making connections via gap junctions, with other embedded cells or cells on the bone surface[123]. The mechanisms and components by which osteocytes convert mechanical stimuli to biochemical signals are not well known[119].

Mature osteocytes negatively regulate osteoblast formation and activity by expressing dickkopf (DKK)-1 and sclerostin (SOST). SOST acts as an

antagonist against lipoprotein receptor 5 (LRP5) and a mutation in the gene causes sclerosteosis with high bone mass in humans. The function of osteocytes includes the detection of mechanical stimuli and micro-damage and initiation of tissue repair. Osteocyte apoptosis is necessary for repairing microdamage; prior to apoptosis, the osteocytes release sclerostin and RANKL at the microcrack, allowing the recruitment of osteoclasts to the site. Wijenayaka et al. showed that addition of exogenous sclerostin increased RANKL mRNA expression and decreased the expression of osteoprotegerin (OPG) in both cultures of primary osteocyte-like cells and in MLO-Y4 cells (an osteocyte-like cell line). OPG inhibit osteoclastogenesis and is secreted osteoblasts and stromal cells. Other factors can stimulate apoptosis such as lack of oxygen, glucocorticoid treatment and withdrawal of oestrogen. Osteocytes are also involved in the regulation of phosphate metabolism via the hormone FGF-23.

Two studies suggest that osteocytes, and not osteoblasts, are the primary source of RANKL. Nakashima *et al.* measured a 10 times higher concentration of RANKL in purified osteocytes compared with osteoblasts or bone marrow stromal cells[124]. Co-culture of osteocytes with osteoclast precursor cells resulted in a higher amount of differentiation to osteoclasts, compared to co-culture with osteoblasts. However, osteocytes were unable to induce osteoclastogenesis without 1,25(OH)2D3 and prostaglandin E2 (PE2) highlighting the importance of OPG downregulation. In addition to these *in vitro* experiments, Nakashima et al generated osteocyte-specific $RANKL^{-/-}$ mice, which were normal at birth but developed postnatal osteopetrosis.

Osteopetrosis is a rare heritable disorder caused by defective osteoclasts and result in a general increase in bone mass. The bone of patients with osteopetrosis contains large areas of un-remodelled mineralised cartilage. However, Nakashima et al could not rule out the possibility that other cell types, including osteoblasts, are involved in developmental stages and might produce soluble forms of RANKL.

1.4.5.4 Osteoclasts

The main function of osteoclasts is to resorb bone matrix by dissolving hydroxyapatite minerals and degrading, by proteolysis, the organic components.

The osteoclast was first recognised in 1873 as a multinuclear cell that was able to resorb bone[125]. Until the late 1970s the dominant theory was that osteoclasts and osteoblasts were derived from the same lineage. The final indisputable proof of the haematopoietic origin of osteoclasts was demonstrated with the transplantation of histocompatible haematopoietic cells, derived from the bone marrow/spleen, to the osteopetrotic murine model $^{op/op}$ which corrected the pathological bone phenotype[126]. This was confirmed in humans when a child with malignant osteopetrosis was cured following a bone marrow transplant[127]. It was also shown that osteoclasts belong to the macrophage/monocyte lineage[128]. The next stage in the investigation of osteoclasts was to identify the different cellular stages of osteoclast differentiation thereby facilitating the development of *in vitro* methods of generating osteoclasts. Burger *et al.* co-cultured murine bone marrow cells and stripped fetal bone, which induced the formation of osteoclasts; without the bone no osteoclasts were formed[129]. This system was

developed further with the substitution of the bone rudiments for pure populations of osteoblastic cells such as the ST2 cell line[130]. By using osteoblast cell lines this reduced the heterogeneity of the cell populations in the cultures, making it easier to identify osteoclast precursors. Variations of this co-culture system led to the identification of osteoclastogenic factors[131], notably macrophage colony-stimulating factor (M-CSF), 1,25 dihydroxyvitamin D3 (1,25(OH)2D3)[132], parathyroid hormone (PTH), prostaglandin E2[133], interleukin 1 (IL-1) and RANKL. The activation of resorption by "functionally pure" osteoclast cultures could be produced by the transfer of conditioned medium from osteoblasts leading to the conclusion that osteoblastic cells were needed for osteoclast activity. Udagawa *et al.* determined that cells positive for tartrate-resistant acid phosphate (TRAP) activity could be generated from monocyte-enriched populations, whereas they could not be formed from monocyte-depleted fractions of peripheral blood[134]. Furthermore, Fujikawa *et al.* found that it was possible to generate human osteoclasts from the peripheral blood mononuclear cell (PBMC) population in the monocyte fraction when cultured with M-CSF and 1,25(OH)2D3[135]. Massey *et al.* cultured a selected population of PBMCs, the $CD14^+$ fraction, which they found to be able to produce 2-4 times more resorption than unselected PBMCs[136]. These studies and others indicated that osteoclasts were derived from monocyte found within the $CD14^+$ fraction of PBMCs[137].

Osteoclast formation *in vitro* minimally requires the exposure of cells to cytokines derived from osteolineage cells: M-CSF and RANKL[138–140]. The

role of M-CSF in bone was established by studies using osteopetrotic ($^{op/op}$) mutant mice that possesses an inactivating mutation in the colony-stimulating factor-1 gene which result in the absence of M-CSF[141,142] and rats with the toothless osteopetrotic mutation ($^{tl/tl}$)[143] giving an osteopetrotic phenotype due to the absence of osteoclasts[144,145]. However, the addition of exogenous M-CSF was able to resolve the bone disorder[146]. Osteoblasts and bone marrow stromal cells produce M-CSF that binds to its receptor c-Fms present on the surface of osteoclast precursors and mature osteoclasts. This cytokine regulates the survival, proliferation and differentiation of macrophages and osteoclast precursors through the extracellular signal regulated kinase (ERK) and PI3K/AKT pathways[147,148] (**Figure 1.10**).

RANKL is a type II transmembrane protein member of the tumour necrosis factor (TNF) superfamily. RANKL is a single-pass transmembrane protein with an extracellular C-terminus and cytoplasmic N-terminus[139]. It is a crucial factor for osteoclastogenesis and is expressed by osteoblasts, osteocytes, and stromal cells[119]. *In vitro* experiments of mouse bone marrow or spleen cells co-cultured with a feeder layer of primary stromal cells or calvarium-derived osteoblasts helped towards better understanding of osteoclast development[149,150]. These two studies showed that osteoclast differentiation is dependent on contact with stromal stem cells and the subsequent factors/cytokines derived from the osteolineage cells. RANKL exists in a membrane-bound form and as a soluble protein, where it is cleaved at the cell surface by metalloprotease-disintegrin TNF-α convertase. The membrane-bound form is the most abundant found *in vivo*. RANKL was first

identified in T cells and was previously called OPGL, ODF and TRANCE. Mice deficient in RANK or RANKL lack osteoclasts and present osteopetrotic bone phenotypes highlighting their role in osteoclast development and bone homeostasis[151,152]. The binding of RANKL to RANK activates the TNF receptor-associated factor (TRAF) adaptor proteins (**Figure 1.10**). TRAF-6 is the most critical for osteoclast formation and function by activating multiple downstream signalling pathways such as nuclear factor kappa B (NF-κB), c-Jun N-terminal kinase (JNK), ERK, p38, mitogen-activated protein kinases (MAPKs) pathways[140] and nuclear factor of activated T cells, cytoplasmic1 (NFATc1). Various hormones and cytokines such as 1,25 dihydroxyvitamin D3 (1,25(OH)2D3), (PTH), PE_2, IL-1 and IL-6 can increase the expression level of RANKL, which is decreased in the presence of interferon-β and -γ.

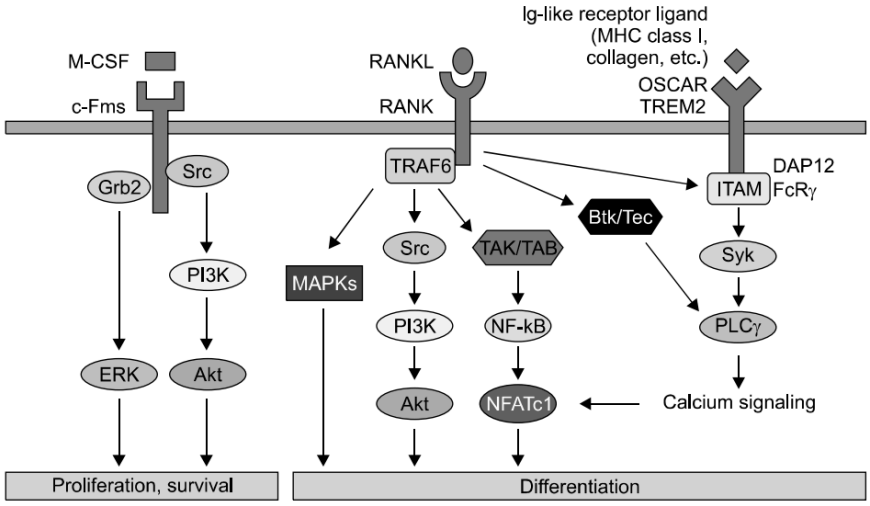


Figure 1.10 Osteoclast differentiation is stimulated by M-CSF and RANKL (Kim et al, Chonnam medical journal, 2016)[147]**.**

1.4.6 Osteoclastogenesis

Osteoblasts, chondrocytes, stromal and endothelial cells produce the cytokines and provide the microenvironment for homing osteoclastogenesis. Mature osteoclasts are large multinucleated cells (60 - 100 μm in diameter) and have a morphology highly specialised for their bone-resorbing function[119,131].

The first osteoclast differentiation stage for the HSCs is to become either a common lymphoid progenitor (CLP) or common myeloid progenitor (CMP). The CLP loop gives rise to T cells, B cells and natural killer cells[153]. The CMP pool does not express IL-7Rα and gives rise to megakaryocytes, erythrocytes and granulocytes/macrophages. The earliest identifiable hematopoietic precursor able to form osteoclasts is the granulocyte-macrophage colony-forming unit (CFU-GM). The principal transcription factors that are involved are PU.1, MITF and c-FOS. Osteoblasts and stromal cells produce M-CSF that provides the signal for macrophage survival and proliferation. C-Fms, the receptor of M-CSF, is expressed by the CFU-GM cells and cells that are able to interact with M-CSF directing the cells to enter the macrophage progenitor pool (CFU-M) instead of the granulocyte pool (CFU-G)[154–156]. The cells in presence of M-CSF can further differentiate to macrophage, osteoclast or dendritic cells precursors[147] (**Figure 1.11**). The commitment of the CFU-M cells to the osteoclast lineage starts when the cytokine RANKL is present in the microenvironment and induces the rearrangement of the cytoskeleton[113]. The CFU-M cells are called osteoclast

precursors (OCPs). M-CSF and the presence of c-Fms also induces RANK up-regulation on OCPs, rendering them responsive to RANKL[157].

The RANKL-RANK binding pushes the OCPs to differentiate into pre-osteoclasts and the presence of RANKL and M-CSF induces their fusion into multinucleated cells. NFATc1 is a master transcription factor for the terminal differentiation of osteoclasts since its induction activates the expression of osteoclast-specific genes.

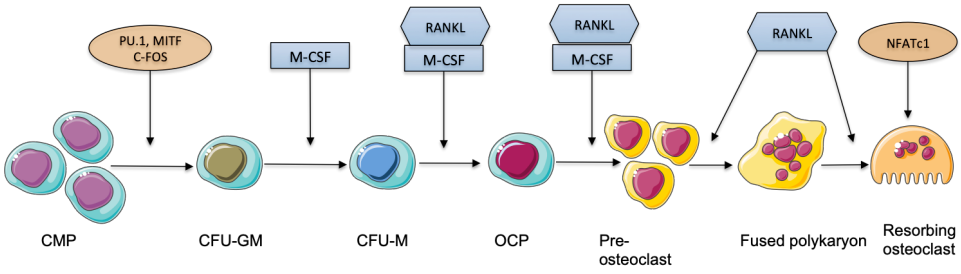


Figure 1.11 The stages of osteoclast differentiation and activation

OPG is an osteoclastogenesis inhibitory factor and is secreted by osteoblasts and stromal cells. OPG belongs to the TNF receptor superfamily. However, unlike other members of the superfamily, OPG is secreted as a soluble protein. OPG is a soluble decoy receptor to RANKL competing with RANK for RANKL binding. The OPG knockout mouse develops severe osteoporosis with a marked increase in osteoclast formation and resorption[158,159]. The absence of interaction between RANK and RANKL inhibits osteoclast differentiation and function. Cell-cell contact, hormones, matrix proteins and vitamins can also influence osteoclast differentiation and function[140]. OPG can be used to treat tumour-induced bone destruction [160].

1.4.7 Mechanisms of bone resorption

Bone resorption is the first step of bone remodelling; it precedes bone formation. Osteoclasts migrate to the target area in response to various resorptive stimuli. A resorption cycle involves five stages: attachment of the osteoclast to the bone matrix, polarization, reorganization, resorption, and detachment of the osteoclasts. One osteoclast can repeat several resorption cycles before entering the apoptosis pathway[115,161].

Before resorption, a sealing zone is formed between the membrane of the osteoclast and the underlying bone; this tight attachment is mediated mainly by integrins able to bind to the RGD sequence present in a variety of bone-residing proteins such as vitronectin, collagen, osteopontin and bone sialoprotein. The principal integrins are vitronectin receptor (VNR) $\alpha v\beta 3$, collagen/laminin receptor $\alpha 2\beta 1$ and vitronectin/fibronectin receptor $\alpha v\beta 1$[162,163].

The polarisation and reorganisation of the cytoskeleton occurs once the osteoclast is attached to the bone matrix. Highly polarised osteoclasts reorganise their membrane into three distinct domains: the first domain is the sealing zone located at the extremity of the osteoclast, the second one is the ruffled border centrally positioned between the sealing zone at the apical membrane in contact with bone matrix. Finally, the basolateral membrane is reorganise with the functional secretory domain in contact with the extracellular fluid[119,164].

During the attachment and polarisation phases, the cells spread and reorganise their cytoskeleton (**Figure 1.12**). Podosomes are composed of a

dense F-actin core, which is surrounded by molecules important in adhesion and regulation. At the beginning of the differentiation and activation of the osteoclast, podosomes are in clusters, which will evolve to a ring belt organisation. This dynamic actin ring and the integrins isolate the ruffled border from the extracellular environment. The membrane at the ruffled border develops numerous folds in its surface due to the directional insertion of vesicles that contain protons and lysosomal enzymes. All these structural modifications are a hallmark of active osteoclasts[165].

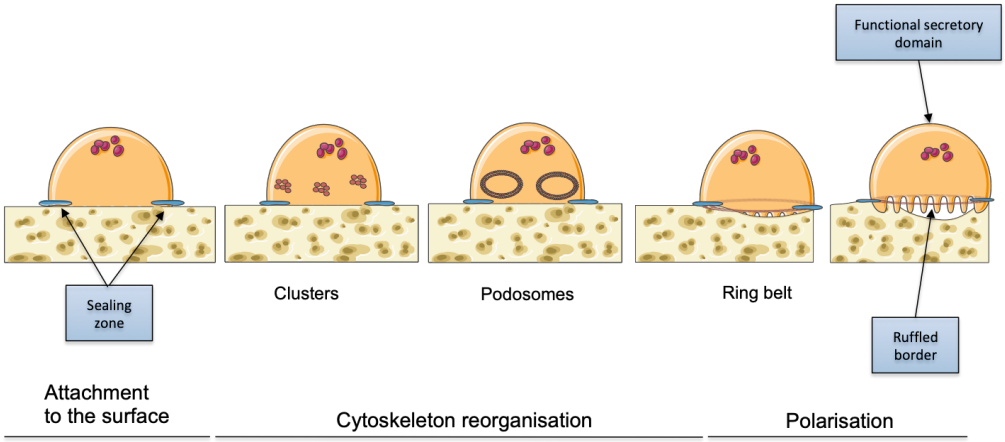


Figure 1.12 Attachment and polarization are key steps for osteoclasts activation

The first part of bone resorption is secretion of acid to dissolve the minerals (**Figure 1.13**). The resorption lacuna is an acidic microenvironment (pH drops to 4.5) created between the sealing zone, the ruffled border and the bone matrix. A vacuolar type of electrogenic H^+-ATPase pump, present at the ruffled border, secretes protons into the lacuna. A GLUT2 transporter in mitochondria supports the source of energy during oxidative phosphorylation of glucose. In parallel, chloride is passively transported to the apical side and

passes the ruffled border via the CLC7 channel. The production of H^+ and Cl^- ions depends on carbonic anhydrase II that catalysis the conversion of CO_2 and H_2O into H_2CO_3, which ionizes into H^+ and HCO_3^-. The H^+ are transported to the sealing zone via the pump and one chloride-bicarbonate is exchanged at the basolateral side against one chloride by the anion exchanger 2 (AE2) [164,166].

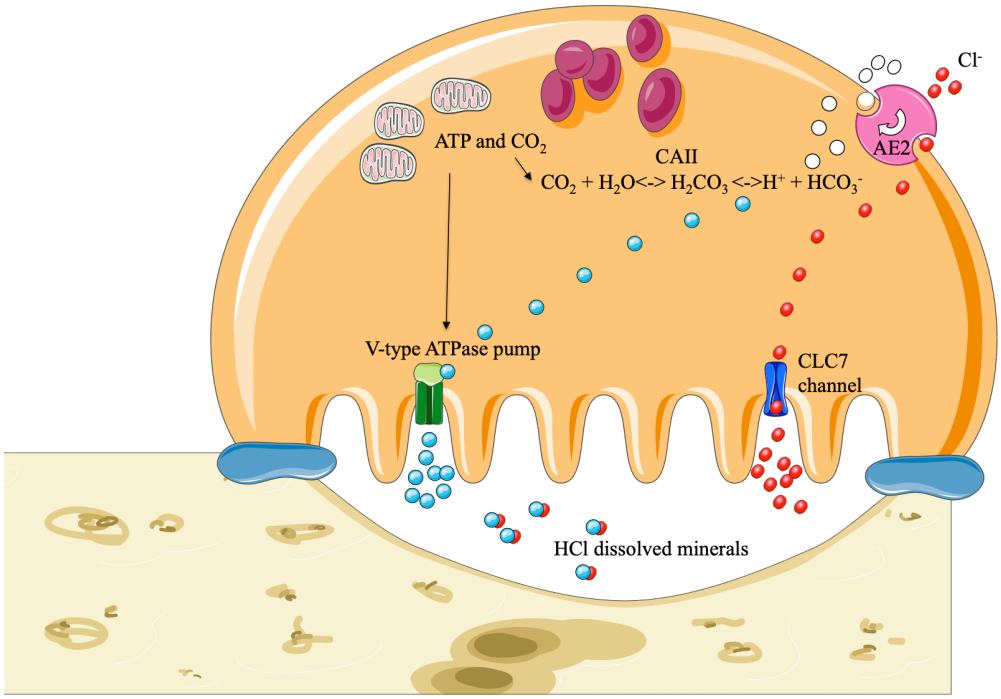


Figure 1.13 Osteoclast consumes large amounts of energy to drive HCl secretion that produce calcium, water and phosphate from the mineral comprising the bone matrix.CAII: carbonic anhydrase II, AE2: anion exchanger 2, CLC7: Chloride channel 7.

Acidification of the lacuna solubilizes minerals and makes the organic matrix available to proteinases. Lysosomal enzymes such as cathepsins catalyse the organic matrix (**Figure 1.14**). Cathepsin K is the predominant proteinase in human osteoclasts and is transported to the resorption area in vesicles which fuse with the ruffled border releasing the enzymes into the

resorption lacuna. The low pH activates cathepsin K and they degrade key components of bone such as type I collagen by cleaving the triple helix at multiple sites: telopeptides and helical region[167]. In addition, a variety of MMPs are also released into the resorption lacuna such as MMP-9 and MMP-14. After cleavage, the triple helix unwinds and becomes available to gelatinolytic proteinases for degradation.

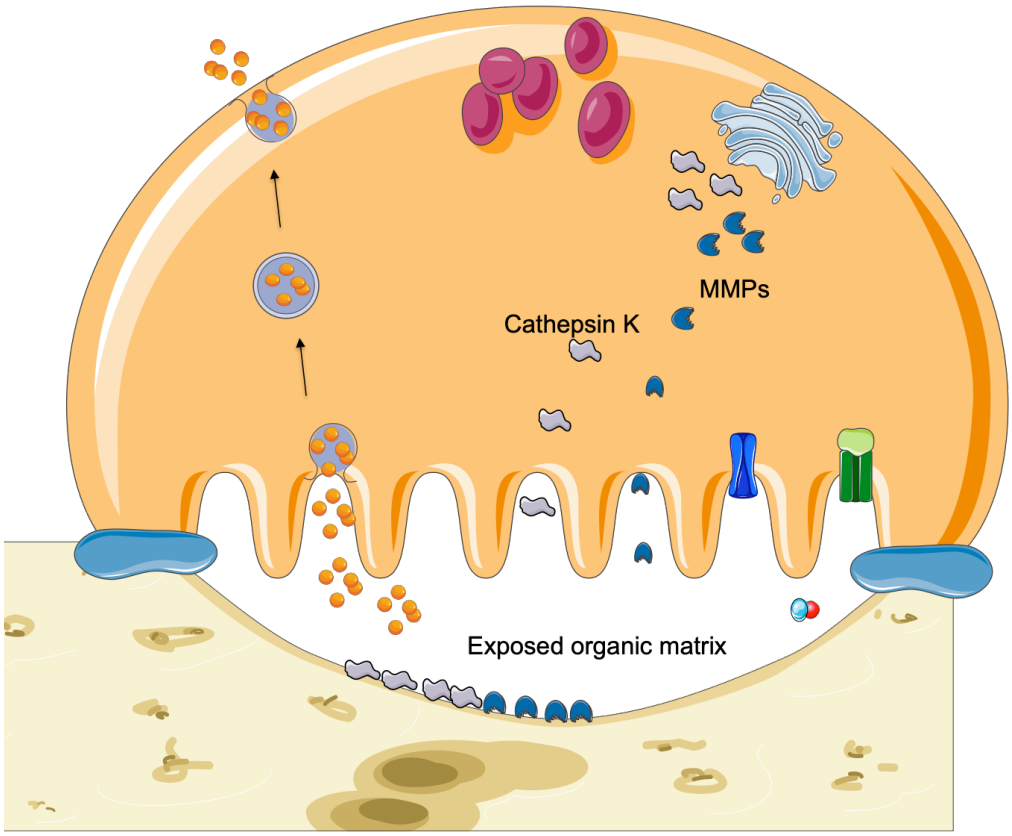


Figure 1.14 Dissolution of organic matrix by proteolysis and waste products are endocytosed

The resorbed products are endocytosed at the ruffled border and transported to the functional secretory domain by transcytosis vesicles. It has also been suggested that degradation products can be continuously released

from the sealing zone. After completion of a resorption cycle the osteoclast can either repeat a few more such cycles or undergo apoptosis.

1.4.8 Dysregulation of bone remodelling

The intricate balance between bone formation and resorption is essential to ensure the precise replacement of bone. When this process is deregulated bone pathologies manifest. There are numerous bone diseases and cancers that can impact bone metabolism. In Paget's disease, osteoporosis and rheumatoid arthritis osteoclast activity is abnormally enhanced. Conversely in osteopetrosis, osteoclasts are unable to acidify decreases the rate of bone and cartilage resorption[168]. Bone marrow transplantation is a treatment option for osteopetrosis to obtain mature and functioning osteoclasts.

In addition to these bone diseases there a number of cancers that have a similar detrimental effect on bone. Several cancers, such as breast cancer and prostate cancer, often metastasize to the bone. The tumor cells release a number of cytokines including RANKL thereby stimulating osteoclast formation. Bone cancers are especially distressing for patients not only because of the significant destruction of bone but also because of the associated crippling pain.

Giant cell tumour of bone (GCTB) is a locally aggressive bone tumour most commonly found in individuals over 30-40 years of age. GCTB is primarily located in the epiphyseal region of the long bones mostly in the knee. Approximatively 80% of these tumours are benign but have a recurrence rate of 20-50%, with 10% of the recurrences undergoing malignant

transformation. GCTB is composed of sheets of mononuclear cells interspersed with uniformly distributed large osteoclast-like giant cells. Current treatment options involve surgical intervention either by curettage or resection of the tumour-bearing part of bone. Curettage is combined with various adjuvants with specific thermal or chemical effects against any remaining tumour cells. These adjuvants include liquid nitrogen, phenol, hydrogen peroxide and alcohol. Bisphosphonates and Denosumab are also currently being used to inhibit osteolysis in problematic GCTB cases. Bisphosphonates is a pyrophosphate that bind to the hydroxyapatite inhibiting their degradation by osteoclasts and denosumab is a monoclonal human antibody that binds to RANKL.

Pathologies where osteoclasts affect the joint are discussed in detail in Chapter 3.

1.5 Bone-cartilage interface

1.5.1 Structure and organisation

Historically, the bone-cartilage interface was considered to act as an impermeable barrier, however, there is an increasing amount of research suggesting that these tissues can communicate. The bone-cartilage interface appears during endochondral ossification when the initial cartilaginous model of long bones is degraded by osteoclasts and replaced by true bony matrix. Any alteration at the osteochondral interface may disrupt the mechanical and chemical interactions between bone and cartilage which may affect cell physiology and tissue homeostasis.

The bone-cartilage interface contains the deep layer of articular cartilage, the tidemark, the calcified cartilage and the underlying subchondral bone (**Figure 1.15**). The main function of the cartilage-bone interface is to transmit the tensile, compressive and shear forces from the articular cartilage to the mineralised bone. Collagen type II fibres in the calcified cartilage are cemented to collagen type I present in the subchondral bone. The calcified cartilage is a zone of transition composed of the main components of each tissue; minerals and type I collagen for bone matrix and GAG and type II collagen for cartilage matrix. The chemical characteristics of articular cartilage, calcified cartilage and subchondral bone in 40 healthy human knees were analysed by amino acid assay and X-ray diffraction. Although the quantity of each component is not as high as it is in the original tissue; Zhang et al show that the percentage of dry weight of hydroxyapatite is around 65% in calcified cartilage and 85% in bone. The quantity of type II collagen in the calcified cartilage is around 20% and around 61% in hyaline cartilage[169]. Duer et al used a 2-dimensional nuclear magnetic resonance spectroscopy and X-ray diffraction to analyse the mineral composition of powdered calcified cartilage samples from phalanx and distal radius of mature horses. The hydroxyapatite present in calcified cartilage is similar to bone but the crystals are smaller in calcified cartilage. The presence of GAG in calcified cartilage provides a more hydrated matrix than bone matrix. Also, finding osteocalcin in calcified cartilage testifies to the abundance of minerals; it is a mineral-binding protein with a Gla residue which is normally found in bone matrix[170]. Variation in the degree of mineralisation within the calcified cartilage is likely to facilitate transport of molecules and cellular crosstalk.

Subchondral bone can be separated into two distinct anatomic entities: subchondral bone plate and subchondral trabecular bone. The subchondral bone plate is composed of cortical bone and is between the calcified cartilage and the subchondral trabecular bone. In some places, the bone marrow located inside the subchondral bone or the subchondral bone itself are in direct contact with cartilage. Various terms are used to describe this; vascular channels, subchondral cracks or pits. The channels can extend beyond the tidemark in the articular cartilage or remain within the calcified cartilage. This direct contact allows molecules to spread out between the two components. The subchondral bone plate and the subchondral trabecular bone attenuates and absorb the forces generated by movement. It also has a supportive function; the presence of vascular canals located beneath the calcified cartilage provides nutrients and other molecules to the articular cartilage. Imhof et al proposed that blood vessels in the subchondral bone plate provide more than 50 % of oxygen, glucose and water[171]. Kim et al performed an acute ischemic injury to create a hypoxic environment at the epiphysis. The abrupt disruption of oxygen and nutrients induced cell death in underlying bone and the deep layer of cartilage. These observations confirmed the importance of blood vessels in the subchondral bone plate for cartilage function[172]. It becomes evident that diffusion of cytokines and growth factors from subchondral bone to the articular cartilage is important in normal and diseased joints.

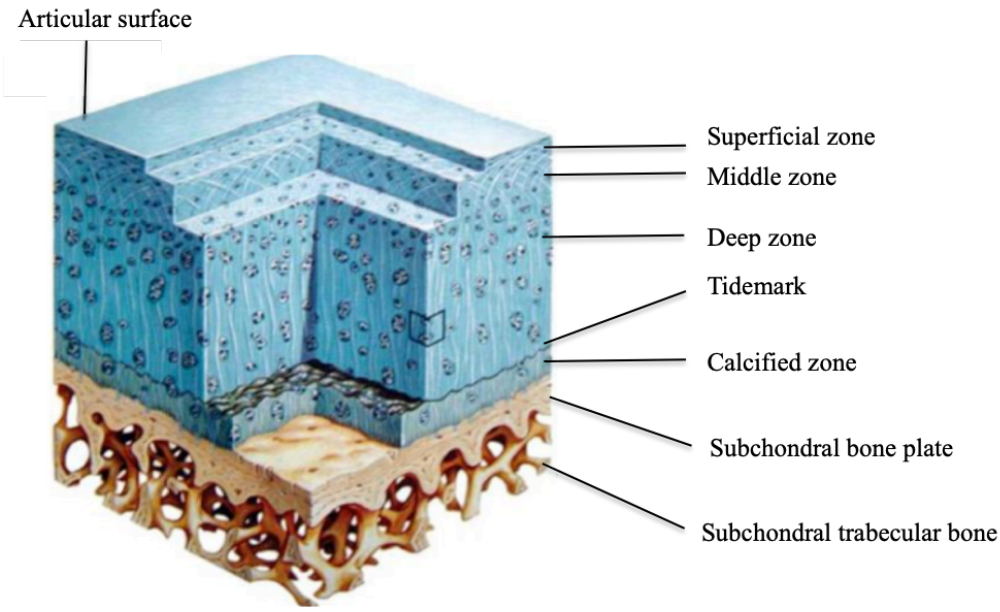


Figure 1.15 Representation in 3D of articular cartilage and subchondral bone.
Adapted from Landinez-Parra et al, Injury and skeletal biomechanics, 2012 [173]. Interaction between bone cells and cartilage

1.1.1.1 Diffusion of factors between bone-cartilage *in vitro*

The measure of small molecules; rhodamine and sodium fluorescein perfusing in calcified cartilage were measured first in equine calcified cartilage. After 1.5 hours the tracer was found in the synovial fluid suggesting that it diffused from the subchondral channels thru the cartilage[174]. In 2009, a study using a fluorescence loss in photobleaching (FLIP) method showed the diffusion *in vivo* of tracer through the bone-cartilage interface[175]. Briefly, a fluorescent zone of tissue is repeatedly photobleached within a small region while the whole zone is continuously imaged. The permeability of both tissues is quantified according to the loss of fluorescence induced by photobleaching. Hwang et al reported that the hydraulic conductance of the articular cartilage and subchondral bone plate increases with OA progression.

They postulated that fluid movement can act as a mechanical signal to the cells and enhance the transport of diffusible factors that may mediate the crosstalk between cartilage and bone[176]. Pan et al used photobleaching in two murine models of OA and normal joints. They found that the crosstalk was increased in OA models compared to normal joints and suggested that microcracks and vascular invasion facilitate the diffusion of small molecules[177].

1.5.1.1 Molecular interaction between bone and cartilage in OA

The initiating event responsible for the degradation of cartilage in OA is still unclear. There is more and more evidence that subchondral bone remodelling plays an important role in the early stages preceding cartilage degradation. The calcified cartilage and the subchondral bone plate are thickening along with abnormal tidemark duplication. *In vivo* micro-CT combined with histology on an instability-induced OA mouse model showed an increase in bone remodelling with high osteoblast and osteoclast activity and loss of subchondral bone compared to normal joints. The plate porosity increases and blood vessels penetrate into the calcified cartilage allowing a direct crosstalk between bone and cartilage[178]. *In vivo* molecular interactions in the bone-cartilage interface provide insight into the specific mechanisms underlying the effects of crucial biological factors and signalling pathways on cartilage-bone pathophysiology. The metabolic homeostasis and interface integrity are maintained by TGF-β signalling. Knockout of TGF-β1 or interruption of TGF-β signalling in murine cartilage increase its degeneration with a loss of proteoglycans[179]. Zhen et al used mice where only osteoblastic

cells were expressing TGF-β1 since it was under the promoter of type I collagen. The high concentration of TGF-β1 in subchondral bone initiated changes and induced cartilage degradation confirming the crosstalk between subchondral bone and articular cartilage[180]. Wnt/B-catenin is another pathway that is important for bone and cartilage homeostasis. Antagonists and agonists of this pathway including sclerostin, secreted Frizzled-related protein 3 (sFRP-3) and Dickkopf (DKK1) have been shown to protect against excessive bone remodelling and cartilage destruction *in vitro* and *in vivo*. Weng et al used a rat model of OA that was treated with antisense oligonucleotide DKK-1. Blocking expression of DKK-1, which is a Wnt inhibitor mostly expressed in osteocytes, prevented chondrocyte apoptosis, showed less cartilage degradation and reduced bone remodelling[181].

1.5.1.2 Bone degrading cells and cartilage

There are two situations where osteoclasts are known to degrade calcified cartilage; endochondral ossification and fracture healing. Multinucleated cells in contact with mineralised cartilage were described in normal development of the epiphyseal plate of growing rats[182]. Also, during fracture healing, the cartilaginous callus is degraded by osteoclasts and then replaced by lamellar bone. Ota et al investigated the cartilage degradation during bone fracture healing in OPG deficient mice. Local OPG acts as a negative regulator for chondrocytes and osteoclasts[183]. Fracture healing in $OPG^{-/-}$ mice showed a faster union of the fractured bone and degradation of the cartilaginous callus with an increase in osteoclast number.

1.6 Hypothesis and aims

The interaction between osteoclasts and cartilage is gaining attention since the mechanism of cartilage degradation is poorly understood and osteoclasts can be seen in contact with cartilage in diseased joints such as OA, RA and GCTB. In the literature it is increasingly hypothesised that osteoclasts can drive cartilage degradation[184–188]. If this is the case, controlling the activity of osteoclasts would present an attractive target for further research and might represent an interesting perspective for diseases characterized by cartilage degeneration.

The overall goal of this thesis was to characterise the role of osteoclasts in the cartilage turnover that occurs in diseased joints.

1. The first aim of this thesis was to establish whether proteoglycans and collagen degradation occurred and to ascertain pathologies where osteoclasts and cartilage interactions are relevant.
2. The second aim of this thesis was to determine whether the effects of osteoclasts on cartilage degradation was due to direct degradation, the release of paracrine factors or an interaction with chondrocytes. A possible cross talk between chondrocytes and osteoclasts was hypothesised.
3. The last aim was to characterise if the substrate to which osteoclasts attach affects osteoclast formation and activity. It was hypothesised that osteoclasts cultured on plastic, bone and cartilage will not be identical. More specifically, osteoclast activity and their morphology would be different.

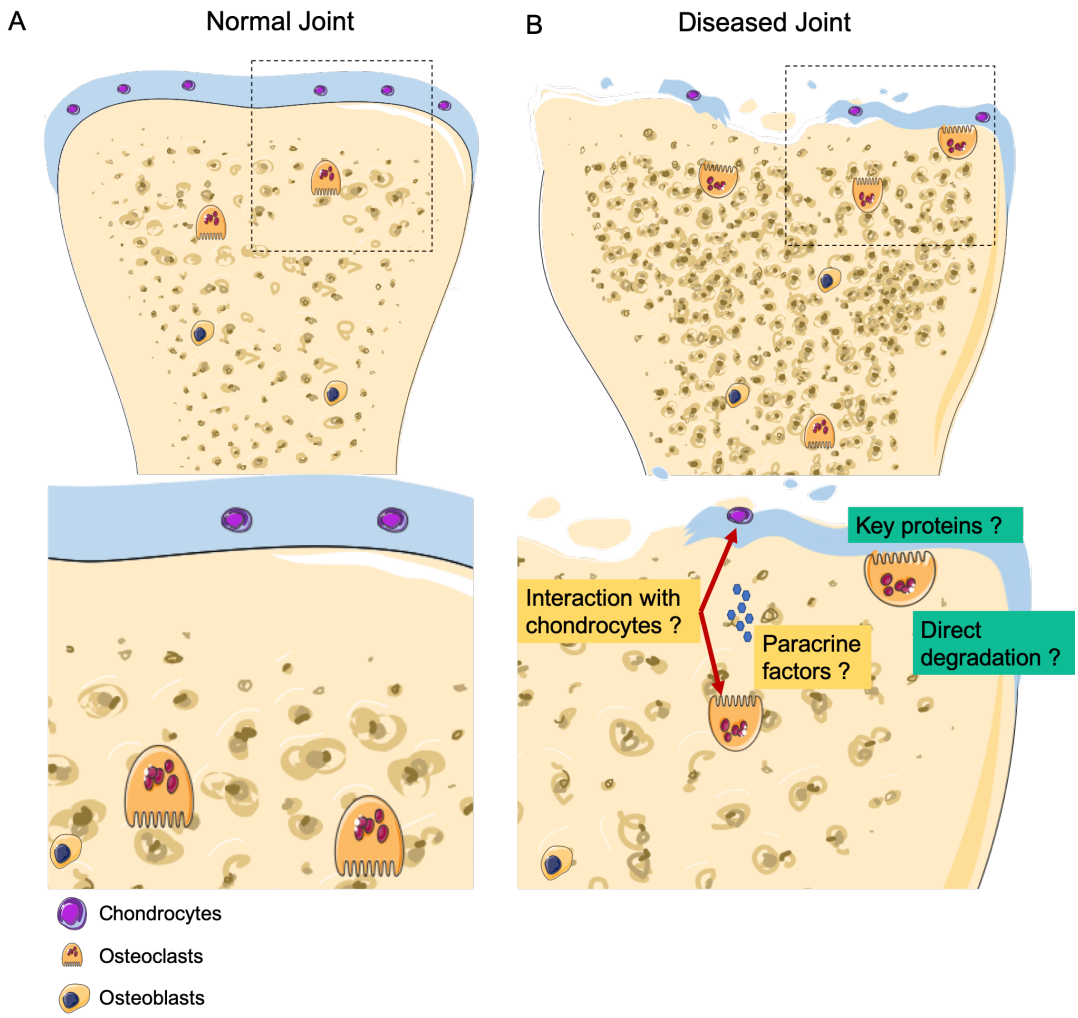


Figure 1.16 Diagram representing the hypothesis and the aims of this thesis. A. Osteoclasts maintaining bone homeostasis with osteoblasts and chondrocytes embedded into cartilage. **B.** Osteoclasts degrading bone and in contact with cartilage in diseased joints

Chapter 2

MATERIALS AND METHODS

2.1 Tissue culture

2.1.1 Cell culture conditions

Monocytes, chondrocytes and osteoclasts were maintained in complete alpha minimal essential medium (complete α-MEM) (Lonza, Wokingham, UK) supplemented with 10% heat-inactivated foetal calf serum (FCS) (Gibco, Paisley, UK), 50 IU/ml Penicillin, 50 µg/ml streptomycin sulphate (Invitrogen, Paisley, UK) and 2 mM L-glutamine (Lonza) in a humidified atmosphere of 5% CO_2 at 37°C. The complete medium was refreshed every 2-3 days for 10-13 days. All cytokines and receptor antibodies were from R&D Systems (Abingdon, UK) except RANKL (London, UK)

Bafilomycin (CST, Hitchin, UK) was added at 10 and 50 nM, E64 (LKT, Cambridge, UK) at 5 and 50 µM and GM6001 (Selleckchem, Muchen, DE) at 50 and 250 µM. The choice of specific concentration for the individual inhibitors was based on previous studies[185,189]. The control for this experiment was the cells with M-CSF and RANKL.

2.1.2 Preparation of the surface used to culture osteoclasts

2.1.2.1 Coverslips and dentine preparation

Glass coverslips (Knittel Glaser, DE) of 6 mm diameter were placed in 8.5 cm petri dishes in a tissue culture hood and sterilised in 70 % ethanol (Fisher, Loughborough, UK) until completely dry.

Elephant ivory discs (dentine) were prepared by cutting 250 µm thick transverse wafers using a low-speed saw with a diamond-edged blade (Buehler, Coventry, U.K.). A hole punch was used to cut out small circular

discs of 4 mm diameter which were cleaned by sonication in distilled water (dH_2O) for 5 min at 7 watts and washed in dH_2O. Dentines were sterilised in the same way as coverslips.

2.1.2.2 Cartilage tissue preparation

Cartilage tissues were obtained at the time of surgery from patients undergoing total knee arthroplasty replacement for OA at the Nuffield Orthopaedic Centre, Oxford (**Figure 2.1**).

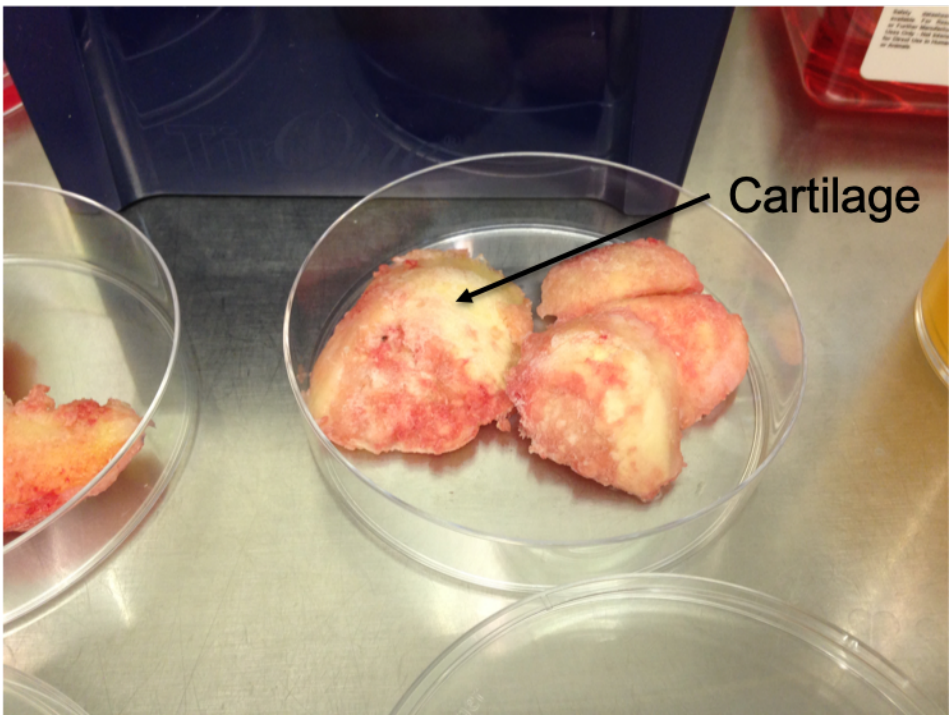


Figure 2.1 Pieces collected from a patient undergoing total knee arthroplasty

Directly after reception, the tissue was washed in plain media to remove blood and the non-cartilage debris. Cartilage pieces were cut to approximately 6x6 mm squares before being placed in the wells of a 48-well tissue culture plate (Greiner Bio-One, Stonehouse, UK) (**Figure 2.2**). In this thesis the cartilage was made either acellular or maintained cellular.

To generate acellular cartilage, explants were frozen/thawed at -80˚C and prior to be use for the experiment, the explants were snap frozen in liquid nitrogen to make sure that chondrocytes were not active even after freezing.

The experiment using cellular cartilage consisted in placing the cartilage pieces to rest for 4 days in the cell culture incubator before use.

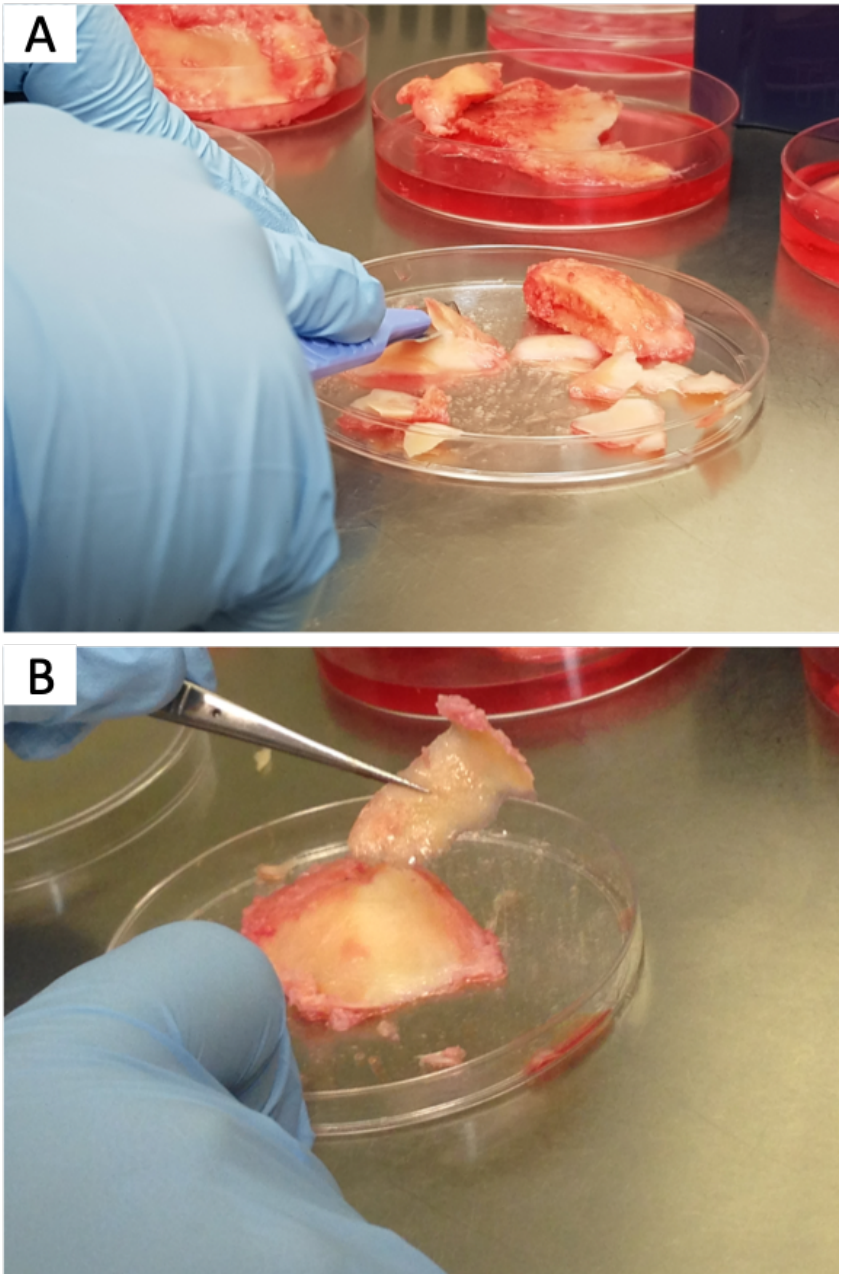


Figure 2.2 Cartilage was peeled A. The piece between the forceps will be cut to approximately 6x6 mm squares B.

2.1.2.3 Establishing colour code and diagrams for easier understanding

To improve the understanding of this thesis diagrams will be used all along, osteoclasts cultured on dentine will be represented on an orange surface, frozen or acellular cartilage on a red surface and cellular cartilage on a green surface (**Figure 2.3**).

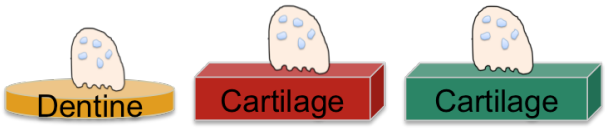


Figure 2.3 Improving the understanding of osteoclasts cultured on different surfaces

2.1.3 Primary cells

2.1.3.1 Isolation of monocytes and culture of osteoclasts

Peripheral blood mononuclear cells (PBMC) were isolated from healthy male human volunteers' human leucocyte cones (NHS Blood and Transplant, Bristol, UK)

Buffy coat was diluted 1:1 in unsupplemented α-MEM (Lonza). This mixture was layered on top of Histopaque (Sigma-Aldrich, Poole, UK) and centrifuged at a speed of 2,300 rpm for 25 min at 4°C. The resulting middle white layer containing PBMCs was isolated and mixed with unsupplemented α-MEM. The mixture was centrifuged twice at 1,500 rpm for 10 min and the pellet was resuspended in 10 ml of unsupplemented α-MEM. PBMC cell number was determined by mixing the cells with 5% (v/v) of acetic acid (Sigma) to lyse the red blood cells and counted with a TC20 automated cell

counter (Bio-Rad, Watford, UK). Cells were resuspended in 80 µl of filtered running buffer (0.5% bovine serum albumin (BSA, Sigma), 2 mM EDTA (Amresco, Lutterworth, UK), 1X phosphate buffered saline (PBS) (Sigma)) per 10^7 total cells. 20 µl of MACS Microbeads (Miltenyi Biotech, Surrey, UK) conjugated with a monoclonal mouse anti-human CD14 antibody, per 10^7 total cells was added and incubated for 15 min at 4°C. Cells were washed with 20 ml of running buffer and centrifuged at 1,500 rpm for 10 min at 4°C. Cells were resuspended in 500 µl of running buffer per 10^8 cells. The cell suspension was added to large positive selection (LS) columns (Miltenyi Biotech) mounted on a magnetic separator. When the columns are placed on a permanent magnet a strong magnetic field is formed. Outside of the magnet, the magnetic columns can no longer retain the labelled cells and they can be eluted. The $CD14^+$ cell population were washed with 3 x 3 ml of running buffer. The column was removed from the magnetic separator and the $CD14^+$ cell fraction was flushed through with 5 ml of running buffer. Cells were counted and seeded at 0.25 x 10^6 cells/well into 96-well tissue culture plates containing dentine slices, at 1 x 10^6 cells/well into 24-well tissue culture plates or containing coverslips and at 1 x 10^6 cells/well into 48-well tissue culture plate containing cartilage pieces.

Following 18 hr, dentines and cartilage pieces were transferred to a new plate to remove the non-adherent cells. Adherent cells on dentine and cartilage were cultured in 24-well or 48-well tissue culture plates with 1,000 or 750 µl/well (respectively) of complete α-MEM with 25 ng/ml M-CSF and 50 ng/ml RANKL for up to 13 days to obtain osteoclasts. M-CSF and RANKL

were respectively dissolved in α-MEM and dH_2O and stored at -20°C. Osteoclasts start to appear after 7-8 days of cell culture and are actively resorbing until the 13th day of cell culture. To obtain macrophages the adherent cells were cultured in the presence of M-CSF only for 13 days.

2.1.3.2 Isolation and culture of human articular chondrocytes

Cartilage tissues were obtained at the time of surgery from patients undergoing total knee arthroplasty replacement for OA at the Nuffield Orthopaedic Centre, Oxford. Chondrocytes were isolated and cultured by Jolet Mimpen, Botnar Research Centre, Oxford. Briefly, the cartilage was dissected and digested overnight with collagenase solution (1 mg/ml collagenase, 0.4% (w/v) HEPES (Sigma), DMEM GlutaMax (Gibco) and 1,000 IU/ml penicillin /100 µg/ml streptomycin). The digestion mixture was passed through a 70-µm-cell strainer (Falcon Becton Dickinson, Oxford, UK) and centrifuged twice at 1,500 rpm for 5 min to wash the cell pellet. Cells were resuspended and counted in 5 ml complete DMEM/F12 (10% FCS, and 1,000 IU/ml penicillin /100 µg/ml streptomycin (Gibco)). $4x10^4$ cells/cm^2 were seeded and allowed to adhere and proliferate over 7-9 days. Chondrocytes were grown until 80 % confluence and used for further experiments until a maximum of passage 3.

2.1.3.3 Isolation and culture of mature osteoclasts

GCTB is a tumour that contains numerous osteoclast-like giant cells, which are known to be mature osteoclasts. GCTB tissues from patients were obtained at the time of surgery at the Nuffield Orthopaedic Centre, Oxford. Fresh GCTB tissue was washed in a sterile petri-dish with 1X PBS to wash out the blood and placed in complete α-MEM. Tumours were cut into small

fragments using scissors, and the number of giant cells released was counted by light microscope (OlympusBX40 microscope with an Olympus DP70 camera). The volume of media was adjusted to obtain approximately 50 giant cells per drop (100 µl). The cell suspension was then seeded on dentine in a 96-well plate or on cartilage in a 48-well plate. After 3 hr of incubation, the dentine and cartilage were transferred to new wells to remove the non-adherent cells. Adherent cells on dentine and cartilage were cultured in 24-well or 48-well tissue culture plates with 1,000 or 750 µl/well (respectively) of complete α-MEM without M-CSF and RANKL. Cells were cultured for 48 hr in the presence or absence of inhibitors (see section 2.1.1).

2.1.3.4 Ethics

The London - Fulham Research Ethics Committee approved all work on human tissue. Samples were obtained from the Oxford Musculoskeletal Biobank and were collected with informed donor consent in full compliance with national and institutional ethical requirements, the United Kingdom Human Tissue Act, and the Declaration of Helsinki (HTA Licence 12217 and Oxford REC C 09/H0606/11+5). The ethics number for the diseased tissue was 07/H0706/81 and 11/H0711/7 for the leucocyte cones.

2.1.4 Co-culture

2.1.4.1 Osteoclast-chondrocyte direct co-culture

Osteoclasts were seeded as monocytes at 1 x 10^6/well and chondrocytes were seeded at 4 x 10^4/well in the same well of a 24-well plate. For the control groups, osteoclasts were seeded without chondrocytes and chondrocytes were seeded without monocytes. In the co-culture, cells were seeded on coverslips or on dentines. Cells cultured with α-MEM containing M-CSF and RANKL

for 10 days corresponded to the osteoclasts-chondrocytes co-culture experiment.

2.1.4.2 Osteoclasts-chondrocytes transwell

Transwell cell culture inserts (Corning Costar, Cambridge, MA) with 0.4 μm pore-size filters were placed in individual wells of 24-well plates. Monocytes were seeded at 1 x 10^6/well in the lower chamber and chondrocytes were seeded at 4 x 10^4/well in the upper chamber. Monocytes and osteoclasts cultured in the lower chamber were cultured on coverslips or on dentines. After 24 hr of adhesion, the transwells were moved to the 24-well plates. For the control group, monocytes were seeded in the lower chamber with empty transwell inserts on top. Another control was to seed the chondrocytes in the upper chamber without cells in the lower cavity of the 24-well plates. Cells were cultured with α-MEM containing M-CSF and RANKL for 10 days corresponding to the osteoclasts-chondrocytes transwell experiment.

The cell culture of chondrocytes in complete DMEM/F12 or in complete α-MEM, containing M-CSF and RANKL were identical. For this reason and to make the experiment easier, all cells were grown in complete α-MEM, containing M-CSF and RANKL.

2.1.5 Culture of osteoclasts with cartilage without contact

2.1.5.1 Cartilage transwell

Transwell cell culture inserts (Corning Costar) with 0.4 μm pore-size filters were placed in individual wells of 24-well plates. Monocytes were seeded at 1 x 10^6/well in the lower cavity directly on the bottom of the well

or on dentine slices. Cellular or acellular cartilage pieces were placed in the upper chambers (**Figure 2.4**). For no-cell controls, lower chambers were left empty and cartilage pieces were placed in the upper chamber. To make sure that monocytes were able to differentiate into osteoclasts, another control was to seed the monocytes in the lower chamber without cartilage in the upper chamber. Monocytes were differentiated to osteoclasts with complete α-MEM with M-CSF and RANKL for 10 days.

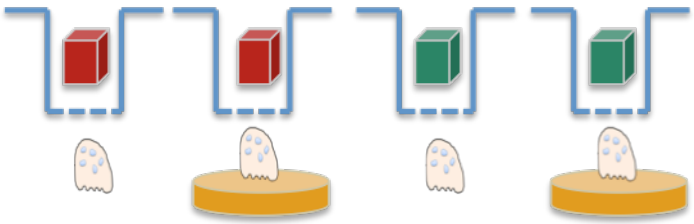


Figure 2.4 Improving the understanding of the cartilage transwell experiment. Osteoclasts are either on plastic or on dentine and the cartilage pieces are placed in the upper chamber.

2.2 Biochemistry of osteoclasts

2.2.1 Cell viability

The alamar blue assay is a fluorometric growth indicator based on detection of metabolic activity. Specifically, the system incorporates an oxidation-reduction (REDOX) indicator that both fluoresces and changes colour in response to chemical reduction relating to cellular metabolic reduction. At excitation of 530 and an emission at 590, resazurin sodium salt (oxidised form) is blue and non-fluorescent whereas resofurin sodium salt (reduced form) is pink and highly fluorescent. Alamar blue solution

(Invitrogen) was diluted 1 to 10 in the cell culture media and, after 4 hr of incubation at 37˚C, 200 µl of media was transferred to a white 96-well microplate (Greiner Bio-one). The fluorescence was measured using a microplate reader (FLUOstar Omega, BMG Labtech, Aylesbury, UK). Medium without cells was used as background.

2.2.2 Proteoglycan detection

The most widely used method for proteoglycan quantification is the 1,9-dimethylmethylene blue (DMMB) assay that quantifies the amount of sulphated GAGs (chondroitin 4 and 6 sulphates, heparin, keratin and dermatan sulphates). Hyaluronic acid is not detected therefore it will not interfere with the assay.

The binding between the dye and the repeated negative charges of the sulphates shift the absorption spectrum (from dark blue to pink colour). This shift is directly proportional to the number of sulphated GAGs present in the media.

The phosphate buffer solution (at pH 6.5) is a combination of solution A and B (**Table.1**); more precisely, 137 ml of solution A was mixed with 63 ml of solution B. At each time point the conditioned media was collected and frozen until needed. At the time of the experiment, 40 µl of conditioned media was diluted with phosphate buffer solution if necessary and transferred into a transparent 96-well microplate (Greiner Bio-One) and 250 µl of DMMB solution was added to each well. The standard curve was prepared with shark chondroitin sulphate (0 – 50 µg/ml) diluted in the phosphate buffer solution

and the absorbance was directly measured at 530 nm with a microplate reader (FLUOstar).

Table.1. List of the reagents used for the GAG assay: all the reagents were purchased from Sigma

Name of the solution	Component
Solution A	100 mM sodium dihydrogen phosphate
Solution B	120 mM sodium hydrogen phosphate
DMMB solution at pH 3	16 mg of DMMB 50 mM of glycine 40 mM of NaCl 0.1 M HCl

2.2.3 Collagen detection

The collagen α-chain is characterised by a Glycine-X-Y repeating triplet sequence motif (where X is usually proline and Y is hydroxyproline). The amount of collagen was quantified by measuring the hydroxyproline content via dimethylaminobenzaldehyde (DAB) and chloramine T assay.

At each relevant time point the conditioned media was collected and kept in -80 ˚C until needed. An aliquot of culture media was combined with an equal volume of concentrated HCl in safe lock tubes (Fisher Scientific) to generate a 6N HCl solution and hydrolysed for 18 hr at 105˚C. Free hydroxyproline is released from proteins and peptides by acid hydrolysis. After cooling down, samples were centrifuged and kept open until dry at room temperature. The precipitate was resuspended in 100 µl dH_2O and 40 µl was aliquot in a 96-well plate. 25 µl of solution A (**Table.2**) was added for 4 min, the free hydroxyproline is oxidised to a pyrrole with chloramine T. Directly after, 150 µl of the solution B was added and sealed to avoid evaporation

during the run and incubated at 65˚C for 35 min. The pyrrole reacts with the DAB to give a reddish colour. The standard curve (0 - 60 µg/ml) was made from the stock solution of hydroxyproline diluted in dH_2O. Absorbance was directly measured at 560 nm with a microplate reader.

Table.2. List of the reagents used for the collagen assay: all the reagents were purchased from Sigma

Name of the solution	Component
4X Acetate-citrate buffer	57 g sodium acetate 37.5 g tri-sodium citrate 5.5 g citric acid 386 ml propan-2-ol 1 L of dH_2O
DAB solution	20 g DAB 30 ml of 70% perchloric acid
Chloramine T solution	140 mg chloramine T 2 ml of dH_2O
Solution A	2 ml chloramine T solution 8 ml acetate-citrate buffer
Solution B	30 ml of prpan-2-ol 10 ml DAB solution

2.3 Cytochemical assessment of osteoclast formation

2.3.1 Tartrate resistant acid phosphatase (TRAP) staining

TRAP, also known as 5-acid-phosphatase, is an iron-containing enzyme strongly secreted by osteoclasts during bone resorption correlating with their resorptive behaviour. Light staining for TRAP can be seen with other type of cells, e.g. with chondrocytes.

Cell preparations were washed in 1X PBS and fixed in 4% formalin (Sigma). Cells were stained for acid phosphatase with an equal volume of

solution A and B (**Table.3**). The naphthol AS-BI phosphate is used as a substrate and the product reacted with the fast violet B salt. After incubation, for 3 hr at 37˚C and a wash with dH_2O, dentines or coverslips were dried and mounted onto microscope slides (VWR, Lutterworth, UK) with DPX glue.

Table.3. List of the reagents used for the TRAP staining, all the reagents were purchased from Sigma

Name of the solution	Component
Tartrate solution at pH 5	0.2 M Acetic acid 0.2 M Sodium acetate 10 mM of sodium tartrate
Solution A	1.5 M Naphthol AS-BI phosphate 0.4 M of DMSO
Solution B	3.5 mM of fast violet B salt 0.4 M of DMSO

The cells were visualised by light microscopy and those cells positive for the TRAP stain containing three or more nuclei were considered as osteoclasts and counted in the following categories: 3-5 nuclei, 6-9 nuclei and more than 10 nuclei.

2.3.2 Vitronectin receptor immunohistochemical staining

The alpha V and beta 3 vitronectin receptor is an integrin strongly expressed by active osteoclasts. This αVβ3-integrin recognise and binds to the RGD sequence expressed by matrix proteins. The antibody CD51/CD61 used for this staining recognises the intact the vitronectin receptor. The staining was visualised using an indirect immunoperoxidase technique with the 3,3′-Diaminobenzidine (DABz) staining.

Cell preparations were washed with 1X PBS and placed into a glass tray and fixed in ice-cold acetone (Fisher) for 10 min and allowed to dry. Samples were washed in 1X PBS and incubated for 10 min in 3% hydrogen peroxide (Sigma) to completely inhibit endogenous peroxidase activity. Samples were washed and incubated with normal horse serum (Vectastain ABC HRP kit, Peterborough, UK) to prevent nonspecific antibody binding. 200 µl of unlabelled primary antibody against CD51/61 (Cat number MCA757G, AbD Serotec, Oxford, UK) diluted in 1X PBS (1:200) was applied for 30 min. After three rinses, the biotinylated secondary antibody raised in horse against mouse IgG was added for 30 min (Cat number PK-7200) and rinsed three times with 1X PBS. A preformed avidin-biotinylated-horseradish peroxidase complex (ABC) was applied for 30 min. The tetravalent avidin/streptavidin structure in the ABC complex offers multiple binding opportunities to the biotinylated secondary antibodies.

After three rinses, the DAB solution, prepared according to the instructions provided (DAB substrate kit for peroxidase, Vector laboratories, Peterborough, UK), was added for 3-5 min. This solution oxidizes (brown coloration) in the presence of the horseradish peroxidase enzyme (HRP). After multiple rinses, dentine slices were dried and mounted on microscope slides with DPX glue.

The VNR positive cells, considered as osteoclasts, were visualised by light microscopy by photographing each dentine slice. Two different areas of each dentine slice were counted using the ImageJ software

(National Health Institute, Bethesda, USA) to have the average number of osteoclasts per dentine slice.

2.3.3 Lacunar resorption staining

Functional evidence of osteoclast activity was determined by a lacunar resorption assay using cell cultures on dentine slices; the latter provide a smooth-surfaced mineralised substrate. Dentine slices with cells were washed with 1X PBS and sonicated for 5 min at 7 watts to remove adherent cells. The slices were then washed with dH_2O, stained with the toluidine blue solution (0.5% (w/v) toluidine blue and 0.5% (w/v) boric acid, pH 7.2-7.4 (Sigma)) for 5 min. After multiple rinses, dentines were dried and mounted on microscope slides with DPX glue.

Resorption pits were visualised by light microscopy and measured by photographing each dentine slice and assembling the images in Adobe Photoshop (Adobe, Montain View, USA). The resorption pits were then coloured in black using the Photoshop software and the image was converted to grayscale. The threshold filter converted the grayscale image into a high-contrast, black-and-white image that ensured only the coloured resorption pits remained. The black and white colours were inverted and the mean white area (mean resorbed area) was measured using ImageJ software.

2.3.4 Immunofluorescence staining (F-actin rings)

The cytoskeleton is composed of a series of filamentous structures including actin filaments (F-actin). Phalloidin is a peptide that binds specifically and with high affinity to the polymerised form of F-actin. Coverslips, dentines or cartilage pieces were washed in 1X PBS and fixed in

4% formalin for 10 min. After three washes with 1X PBS, the cells were permeabilised with 0.5% Triton X-100 (Sigma) for 6 min. The coverslips, dentines and cartilage pieces were stained in the dark with TRITC-conjugated phalloidin antibody (1:200, Sigma) for 30 min. The coverslips, dentine and cartilage pieces were washed with 1X PBS and mounted on microscope slides with Fluoroshield with DAPI mounting media (Sigma). This media preserves the fluorescence and contains DAPI, which is a counterstain for DNA. The osteoclasts' F-actin rings were visualised using a Zeiss Axio Imager M1 fluorescence microscope (Carl Zeiss microscopy, Cambridge, UK) (F-actin: 450-480 nm and DAPI: 360-460 nm). This technique was also used for the co-culture experiments.

2.4 Histology of dentine and cartilage

2.4.1 Fixation, decalcification and sectioning

Osteoclasts cultured on dentine and cartilage pieces were fixed in 4% formalin (Sigma) for 10 min and washed in 1X PBS. Dentines were decalcified in 0.5 M EDTA solution pH 8 for 24 hr at 4°C. Samples were processed by the Histology Facility at the Kennedy Institute of Rheumatology, Oxford for paraffin embedding. Transverse sections of the samples (5 μm thickness) were made with the microtome (Leica Biosystems RM2125, Milkon Keynes, UK). Microscope slides were used to pick the sections out of the water bath (Leica Biosystems) and the slide rack was placed into an oven overnight at 37°C to improve attachment to the microscope slide before the staining procedure.

2.4.2 Haematoxylin and Eosin staining

Before proceeding with the staining, the samples were deparaffinised and rehydrated. Incomplete removal of paraffin can lead to poor staining in the section. The deparaffinization and rehydration are described in **Table.4**.

Samples were stained for 1 min in Mayers Haematoxylin solution (Sigma) and rinsed with tap water until the water is clear. After a wash in 80% ethanol for 1 min the slides were placed in Eosin (Sigma) for 2 min and directly dehydrated and mounted with DPX under a coverslip. Pictures of the sample were taken with a light microscope.

Table.4. Protocol for deparaffinization and rehydration

Name of the solution	Component
Xylene	3 x 3 min
100 % ethanol	3 x 3 min
95 % ethanol	1 min
70 % ethanol	1 min
50 % ethanol	1 min

2.4.3 Immunohistochemistry

All sections were rinsed in 1X PBS twice followed by a peroxidase block (3 % hydrogen peroxide in methanol) for 10 min to block endogenous peroxidases and washed 3 times in 1X PBS. The antigen retrieval was carried out by the immersion of the sections in a hot citric acid solution for 20 min. Citric acid solution was pre-warmed at 95°C. After a rinse in PBS, the sections were incubated with horse blocking serum for 30 minutes. The primary antibody (diluted in 1X PBS) was incubated overnight at 4°C in a humidity chamber. The primary antibodies for MMP-8 and MMP-9 are listed

in ***Table.20***. This was followed by two rinses with 1X PBS for 5 min each and an HRP-link reagent for 30 min. Sections were rinsed twice and the biotinylated secondary antibody raised in horse against rabbit IgG was added for 30 min (Cat number PK-7200) and rinsed three times with 1X PBS. A preformed avidin-biotinylated-horseradish peroxidase complex (ABC) was applied for 30 min. After three rinses, the DABz solution, prepared according to the instructions provided (DAB substrate kit for peroxidase), was added for 3-5 min. The sections were then immersed in distilled water and counterstained with Mayer's Haematoxylin for 2 minutes. After multiple rinses, slices were dehydrated and covered with a coverslip with DPX glue. Pictures were taken with a light microscope.

2.4.4 Scanning electron microscopy (SEM)

Samples fixed in 4% formalin in 1X PBS were washed with dH_2O. Samples were coated with gold and imaged using a Philips XL 30/SEM with field emission gun, operating in SEM mode. The pictures were taken under the supervision of Dr Kalin Dragnevski, Department of Engineering Science, University of Oxford, Oxford.

2.4.5 Phenotypic analysis from tissue section

Pathological bone and joint specimens showing evidence of cartilage resorption by multinucleated cells were identified from files of the Nuffield Orthopaedic Centre, Oxford. These specimens included cases of RA and OA of the knee, GCTB, osteosarcoma, osteochondroma, benign chondroblastoma and chondromyxoid fibroma.

The fixation, embedding, sectioning and staining were performed by the bone and soft tissue pathology lab at the Nuffield Hospital Centre, Oxford. Briefly, 5 μm sections of paraffin-embedded tissue were stained with H&E prior to light microscopic observations.

2.5 Gene expression

2.5.1 RNA extraction

TRIzol reagent (Invitrogen) was used to lyse the cells according to the manufacturer's recommendations. TRIzol maintains RNA integrity during cell lysis, and the RNA is precipitated with ethanol. Ethanol induces conformational changes to the nucleic acid structure that will aggregate. Samples were then DNase-treated to degrade any DNA present in the sample and purified using the Direct-Zol RNA Miniprep kit (Zymo Research, Cambridge, UK).

2.5.2 RNA quality and concentration

Samples were eluted with DNase/RNase-Free water and the total amount of RNA was quantified using a NanoDrop TM 1000 Spectrophotometer (ThermoFisher, Hertfordshire, UK) at an absorbance of 260 nm. The 260/280 nm absorbance ratio was used to assess purity of the samples (≥ 1.7 represented a good quality uncontaminated sample of RNA). All RNA preparations were stored at -80˚C for further experiments.

2.5.3 Reverse transcription

RNA was diluted in DNase/RNase-Free water to get a final concentration of 10 μg/ml in 10 μl. A reverse transcription master mix (High-

capacity cDNA Reverse transcription kits (AB Applied Biosystems, California, USA)) was prepared as described in **Table.5**. The cycle conditions were used on a thermal cycler (Veriti Thermal cycler) as described in **Table.6** and the resulting cDNA was stored at -20 ˚C until use.

Table.5. Constituents of the reverse transcription reaction mix

Component	Volume (µL)/Reaction kit
10X RT Buffer	2
25X dNTP Mix (100mM)	0.8
10X RT Random Primers	2
Multiscribe Reverse Transcriptase	1
Nuclease-free H2O	4.2
Total per Reaction	**10**

Table.6. Cycling conditions used for the reverse transcription

Step	Temperature	Time
Step 1	25°C	10 min
Step 2	37°C	120 min
Step 3	85°C	5 min
Step 4	4 °C	∞

2.5.4 Polymerase chain reaction (PCR)

2.5.4.1 PCR

To confirm the length and the specificity of the primers with gel electrophoresis, the Platinum PCR SuperMix High Fidelity (Invitrogen) was used for PCR amplification of cDNA templates. The solution was prepared as described in **Table.7** and the cycle conditions were used on a thermal cycler as described in **Table.8**

Table.7. Constituents of the PCR reaction mix

Component	Amount for 12-µl reaction
Platinum PCR SuperMix High Fidelity	9 µl
Primer solution	1 µl
Template DNA solution	2 µl

Table.8. Cycling conditions used for the PCR

Step	Temperature	Time	Cycles
Denature	94°C	30 sec	1
Anneal	55°C	30 sec	40
Extend	68°C	1 min	

2.5.4.2 Gel electrophoresis of PCR products

PCR amplification products were observed on a gel electrophoresis. Agarose (New England BioLabs Ltd., Hertfordshire, UK) was added to 200 ml of 1X tris-acetate-EDTA (TEA) buffer (Sigma) at a 2% concentration. The solution was heated in a microwave until the agarose was dissolved. The mixture was allowed to cool and 11 µl of ethidium bromide (Sigma) was added to the liquid mixture to enable nucleic acid visualisation. The liquid was then poured onto a gel mould with a comb. Each sample was mixed with 5X DNA loading dye (New England BioLabs) then loaded into the wells of the solidified gel. Electrophoretic separation of the products was carried out at 100 volts for 80 min, in parallel with 1 kilobase 5X DNA ladder (ThermoFisher) or Gene ruler Mix (ThermoFisher) at 1 µg/µl to determine the relative size of the PCR products. Gels were run at 100 V for 45 min and the bands were visualised under 365 nm UV light and images were recorded using a UVITEC gel documentation imaging system.

Primer dimers are the product of nonspecific annealing and primer elongation events. They will appear as a smear or band of smaller amplicons (**Figure 2.5**). Pure and homogenous produce appeared as a single, sharply defined band at the corresponding base pair size.

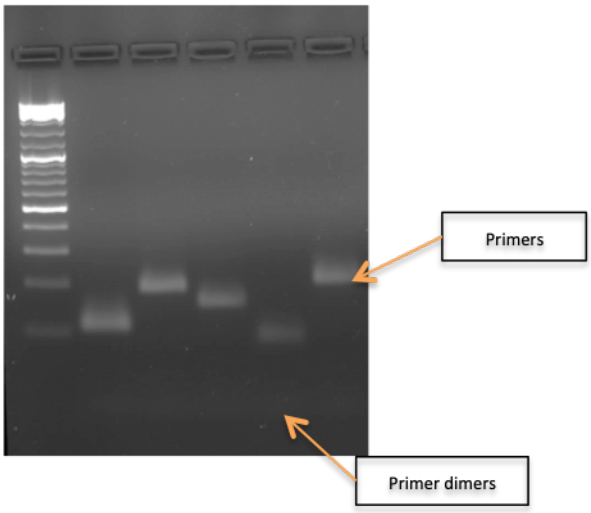


Figure 2.5 Example of gel electrophoresis ran after PCR at 60°C for 5 primers in osteoclasts. Primer dimers arrow shows the expected location, but no primer was dimerised. Respectively from left to the right; DNA ladder and β-actin, ACP5, 16S, 21S, 70S primers.

2.5.5 Real-time PCR (RT-qPCR)

2.5.5.1 Preparation of RT-qPCR

Primers were used in a FAST SYBR Green real-time PCR reaction (Applied Biosystems) or in a TaqMan Fast Advanced reaction (Applied Biosystem). A master mix (per sample) was prepared as described in **Table.9** and

Table.*10* respectively.

Table.9. Constituents of the RT-qPCR reaction mix using SYBR Green

Component	Volume (µL) for 10 µL reaction
Fast SYBR Green Master Mix (2X)	5
Forward and reverse primers	1
cDNA template	1
Nuclease-free water	3
Total volume	**10**

Table.10. Constituents of the RT-qPCR reaction mix using TaqMan

Component	Volume (µL) for 10 µL reaction
TaqMan Fast Advanced Master Mix (2X)	5
TaqMan Gene Expression Assay (20X)	0.5
cDNA template	1
Nuclease-free water	3.5
Total volume	**10**

2.5.5.2 Conditions used for RT-qPCR

All conditions were plated with 3 technical repeats in optical 384-well plates (Life Technologies, Paisley, UK) protected with an optical adhesive cover (Life Technologies) to avoid evaporation during the run. Quantitative PCR was performed using an Applied Biosystems ViiA7 instrument (Life Technologies). The cycle conditions are described in **Table.11** but the temperature of 60°C was varied according to the primer melting temperature (Tm) of the primers used.

Table.11. Cycling conditions used for real-time qPCR

Step	Temperature	Time	Cycles
Enzyme activation	95°C	20 sec	Hold

Denature	95°C	1 sec	40
Anneal/Extend	60°C	20 sec	

2.5.5.3 RT- qPCR calculations and data analysis

A melting curve analysis was performed to check for primer dimers and for a single amplification product. The primer dimers are the product of nonspecific annealing and primer elongation events. Pure and homogenous products show a single, sharply defined melting curve with a narrow peak (**Figure 2.6**).

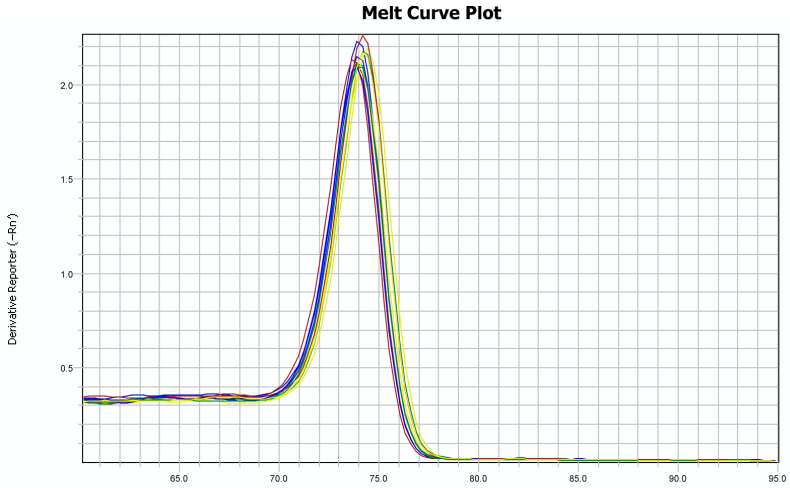


Figure 2.6 Example of melting curve with a narrow peak. The primer used is the β-actin in osteoclasts at 60 °C

A gene was not considered to be expressed when the average cycle threshold (Ct) value per condition was higher than 34. The average cycle threshold value per condition was determined and gene expression was analysed by the ΔΔCt method in Excel (Microsof Office):

$$\Delta Ct = Ct_{\text{target}} - Ct_{\text{housekeeping}}$$

$$\text{Relative expression level} = 2^{-\Delta Ct}$$

Finally, the expression of individual mRNAs was calculated relative to expression of β-actin using the ($2^{-\Delta Ct}$) method.

2.5.6 Primer list

A part of SYBR green primers (**Table.12**, **Table.13** and **Table.14**) were designed using NCBI primer blast and purchased from Sigma.

Table.12. Osteoclasts primer list

Gene Name	Forward	Reverse	Product size
CLCN7	CTAAGAAGGTGTCCTGGTCCG	GGAGGGTCCATATCCTGGCG	142
CA2	GGACAAAGCAGCTTCACTTGG	CCTAGAACGGCCAGTCCATC	91
STAT3	TCCTGAAGCTGACCCAGGTA	TATTGCTGCAGGTCGTTGGT	83
ATP6V1A 16S	GGACTTCATGATCTGCTCCG	CCCGAGTATGCTTCGTTTTT	144
ATP6V1A 21S	CCATCGGAACTACCATGCAGG	TCCACAGAAGAGGTTAGACAGG	76
ATP6V1A 70S	GCCTTTGGCTGTGGAAAGAC	TGGCTACCAAAGCTGTCCTC	190
ACP5	TGAGGACGTATTCTCTGACCG	CACATTGGTCTGTGGGATCTTG	175
CTSK	GCAGAAGAACCGGGGTATTGA	GAAGGAGGTCAGGCTTGCAT	202
OPG	CAATGAACAACTTGCTGTGCTG	ATGAGAGGTTTCTTCGTCATAATGAA	113
RANKL	AAAGATGTATATAGGTGTGTGAGACT	CTCCCACTGGCTGTAAATACG	113

Table.13. MMPs primer list

Gene Name	Forward	Reverse	Size
MMP-2	TACAGGATCATTGGCTACACACC	GGTCACATCGCTCCAGACT	90
MMP-7	GAGTGAGCTACAGTGGGAACA	CTATGACGCGGGAGTTTAACAT	158
MMP-8	AAGTGGGAACGCACTACTTG	GGATTCCATTGGGTCCATCAAAT	220
MMP-10	TGCTTTGTCCTTCGATGCCA	AAAACGGTGTCCCTGCTGTT	183
MMP-12	AACCAACGCTTGCCAAATCC	TTTCCCACGGTAGTGACAGC	86
MMP-14	ATCTGCCTCTGCCTCACCTA	AAGCCCCATCCAAGGCTAAC	126
MMP-15	GGCCGACATCATGGTACTCT	GAGGTTGTTTCCATGCAGGT	178
MMP-21	TTCACTTTGACGACGACGAG	GATCCCTCACAGGAGCCATA	168
MMP-25	CCACACTCACCCTGAATCCT	ACTGAGGCTGGACAGCAACT	221
MMP-28	TACCAACAGTTATGCGGCCTG	CAAAGCGTTTCTTACGCCTCA	86

Table.14. Sequencing validation primer list

Gene Name	Forward	Reverse	Size
CEACAM8	TGCTCAGCTCACTATTGAAGC	CCTATAATTCGACGGTTGGCAT	144

LGI2	CTGAGCCTGGTAAATGGGACG	CCCGGATGATCGTGAATGAGTT	109
EBI3	TCATTGCCACGTACAGGCTC	GGGTCGGGCTTGATGATGTG	208
ITGAL	TGCTTATCATCATCACGGATGG	CTCTCCTTGGTCTGAAAATGCT	112
IL1A	AGATGCCTGAGATACCCAAAACC	CCAAGCACACCCAGTAGTCT	147
TNF	TCCTTCAGACACCCTCAACC	AGGCCCCAGTTTGAATTCTT	91
NFKB1	AACAGAGAGGATTTCGTTTCCG	TTTGACCTGAGGGTAAGACTTCT	104
MAPK1	TCTGGAGCAGTATTACGACCC	CTGGCTGGAATCTAGCAGTCT	134
AKT1	AGCGACGTGGCTATTGTGAAG	GCCATCATTCTTGAGGAGGAAGT	96

The rest of SYBR green primers (**Table.15**) were purchased from Qiagen and Primer design (**Table.16**)

Table.15. Qiagen primer list

Gene Name	Probe number
ACTB	Hs_ACTB_2_SG
MMP-1	Hs_MMP1_1_SG
MMP-3	Hs_MMP3_1_SG
MMP-9	Hs_MMP9_1_SG
MMP-13	Hs_MMP13_1_SG
TIMP1	Hs_TIMP1_1_SG

Table.16. Primer design primer list

Gene Name	Probe number
ADAMTS1	JN171532
ADAMTS4	JN171533
ADAMTS5	JN171534
COL2A1	JN150926
MMP-8	JN215643
MMP-21	JN215646
MMP-20	JN215645

All Taqman primers (***Table.17***) were purchased from ThermoFisher.

Table.17. Taqman primer list

Gene Name	Probe number	Dye	Size
MMP-8-1	Hs01029057	FAM	67
MMP-8-2	Hs01029061	FAM	90
ACTB	Hs01060665	VIC	63

2.5.7 RNA sequencing

2.5.7.1 NEBNext Ultra II RNA library prep for Illumina

RNA was DNase I treated, cleaned and concentrated according to the manufacturer's instructions using Zymo RNA Clean and Concentrator -5 (R1013, Zymo). mRNA was enriched from total RNA according to the manufacturer's instructions using a NEBnext poly(A) mRNA magnetic isolation module. Firstly, mRNA was isolated and fragmented from total RNA using oligo dT beads and a magnetic rack. Beads were mixed with 1µg RNA and then washed twice. Samples were then heated to 65˚C for 5mins before being washed. Tris buffer was added, and samples were heated once again to 80˚C and held at 25˚C to perform the first elution of the mRNA from the beads. Beads were subsequently washed, and mRNA was eluted and fragmented with the addition of first strand synthesis reaction buffer and random primer mix. Samples were heated to 94˚C for 15 min and held at 4˚C Sequencing libraries were prepared according to the manufacturer's recommendations using the NEBNext Ultra II RNA Library Prep kit (E7770S, NEB). Briefly, first and second strand cDNA synthesis was performed using mRNA isolated as above. Double strand cDNA was purified using NEBNext sample purification beads, and DNA was eluted in 0.1X TE buffer. End prep reaction and adaptor ligation was performed, and

purification was done using sample purification beads. RNA and DNA quantification was performed using HS RNA and HS DNA assay kits (Q32852, Q32851, Invitrogen) Qubit fluorometer (Life Tech) according to the manufacturer's instructions. RNA and DNA quality was determined using High Materials and Methods 76 Sensitivity RNA Screentape and D1000 High Sensitivity DNA Screentape respectively on Agilent 4200 tapestation system according to the manufacturer's instructions.

2.5.7.2 Illumina Sequencing

Single-indexed and multiplexed samples were run on an Illumina Next Seq 500 sequencer using a NextSeq 500 v2 kit (150 cycles) (FC-404-2005) for paired-end sequencing (75 bases x 2). Results from RNA-Seq were aligned to the human genome assembly version 38 (hg38 or GRCh38). At least 14 million aligned reads were obtained per sample.

2.5.7.3 Bioinformatic Analysis

Bioinformatic analysis for the RNA-Seq was performed by Dr. Adam Cribbs, University of Oxford. Briefly, sequencing reads were de-multiplexed based on the sample index and aligned to the human genome (hg38) using the STAR (Spliced Transcipts Alignment to a Reference) aligner157. Differential expression analysis was performed using DESeq2158 between three groups designated as no substrate (osteoclasts cultured on plastic), dentine (osteoclasts cultured on dentine) and cartilage (osteoclasts cultured on cellular cartilage)

2.6 Protein expression

2.6.1 Zymography

Zymography, also called substrate-containing polyacrylamide gel electrophoresis (PAGE), is a method for determining the activity of different MMP isoenzymes. Proteins are separated in sodium dodecyl sulphate (SDS) polyacrylamide gels containing a copolymerised MMP substrate (gelatin). After incubation to remove the SDS and reactivate the proteins, the substrate is cleaved by MMPs. MMP activities are detected after the gel staining as transparent bands against a dark-blue background (Coomassie staining) or dark-grey bands against light brown background (Silver staining). The detection of enzyme activity is possible because this experiment is performed under non-reducing and non-denaturing conditions.

2.6.1.1 Preparation of conditioned media

Pieces of acellular cartilage were covered with 1 x 10^6 monocytes in a 24-well plate. For 9 days, the monocytes were differentiated to osteoclasts with complete media with M-CSF and RANKL. At day 9, the media was changed with FBS-free media with M-CSF and RANKL and the conditioned media was collected at day 10. It is crucial to remove all serum for the cellculture because serum contains MMPs and it may confound the results. 3 pieces of cartilage were used for each osteoclast preparation (PBMC), 3 x 1 ml of conditioned media were collected for each osteoclast and kept at -20°C until use. The conditioned media was centrifuged at 1, 500 g during 7 min to pellet the cells. The conditioned media was then transferred to a new tube and stored at -80°C until use.

2.6.1.2 Electrophoresis

1 part of conditioned media was mixed with 2 parts of loading buffer (Bio-Rad). The 10% acrylamide gel containing gelatin with 10 well and 1 mm thickness were used (ThermoFisher). 10 µl of conditioned media was loaded per well. Active recombinant human protein MMP-9 was used as a positive control. For MMP-8 and MMP-9 positive controls recombinant MMP-8 (cat # 908-MP-010, R&D systems) and MMP-9 (cat # 911-MP-010, R&D systems) were used respectively. An additional positive control for all collagenase activity was a "crude" collagenase (Sigma). After loading the samples to each well, a protein molecular weight marker was used in one well (Bio-Rad). The tank was filled with 1X running buffer. 10X running buffer at pH8 was prepared with Glycine: 192 mM, Tris-HCl: 25mM and 0.1 % SDS (Sigma) and diluted in ddH_2O. The gel was run at 150 V until the loading buffer reached the bottom of the gel (≈ 2 hr).

2.6.1.3 Washing and incubation gels

1X renaturation buffer was prepared with 10X renaturation buffer (Bio-Rad) and ddH_2O. Gels were washed for 40 min in renaturation buffer at room temperature to remove SDS from the gel. Then gels were washed with development buffer for 5 min to remove the renaturation buffer. The development buffer (pH 7.6) was prepared with 50 mM Tris, 10 mM CaCl2, 50 mM NaCl and 0.05 % Brij 35 (Sigma) in ddH_2O. The development buffer was replaced with fresh buffer and incubated for 24 hr at room temperature. The development buffer contains cofactors necessary for the activation of MMPs. For negative control, the gel was incubated in a solution containing EGTA that binds to calcium ions that inhibit the activation of MMPs. This

solution was prepared with 10 mM EGTA (Sigma) in 90 ml of ddH_2O and 10 ml of development buffer.

2.6.1.4 Gel staining

Silver staining of polyacrylamide gels detect most proteins (in the nanogram range) which makes this staining 100 times more sensitive than Coomassie brilliant blue staining[190]. Differences in protein migration patterns can be seen when various enzymes are examined, there is also a better resolution of high and low molecular weight and the proteases that remain near the origins of substrate-containing gels can still be detected.

The gel was soaked in fixing solution for 20-30 min with gentle agitation and washed in 50 % methanol for at least 10 min with 3 changes (**Table.18**). Removing the acetic acid is important to reduce the background and increase the sensitivity. The gel was sensitised for a maximum duration of 1 min with the sensitizing solution and washed in distilled water for 20 sec with 3 changes. Longer times decrease the detection of small proteins. The gel was immersed into the silver staining solution for 20 min and washed in distilled water for 30 sec with 2 changes. To remove any residual silver nitrate the gel was transferred to a new container. Finally, the gel was incubated in the developing solution until the staining was sufficient (usually 1 min). To stop the reaction the gel was rinsed and stored in fixing solution.

Table.18. List of the solutions used for silver staining. All the components were ordered from Sigma

Solution	Composition
Fixing solution	40 % ethanol, 10 % acetic acid and 50 % dH_2O
Sensitizing solution	0.02 % sodium thiosulphate (Sigma) in dH_2O
Staining solution	0.2 % silver nitrate (Sigma) in dH_2O. 74 µl of formaldehyde (Sigma) was added just before use
Developing solution	6 % sodium carbonate (Sigma) in dH_2O. 50 µl 35 % formaldehyde and 4 ml sensitizing solution added just before use

2.6.1.5 Imaging and analysis

Gels were scanned with Epson V700 Photo scanner using Epsonscan software. The protein intensity was quantified using the analysis of gels option in ImageJ software as shown in the example in

Figure 2.7.

Briefly, images were converted into grayscale and large rectangles were drawn around each band of interest. Subsequently, a profile plot was created for each selected area and a straight line was drawn at the base of each peak, from one side to the other to enclose the area of the peak (the tails to either side of the peak were the background signal). Finally, the peak area could be expressed as a percentage of the total size of all the measured peaks. If a loading control was present, the percentage value of the protein of interest was divided by the loading control percentage to get a relative intensity (2^{nd} label below).

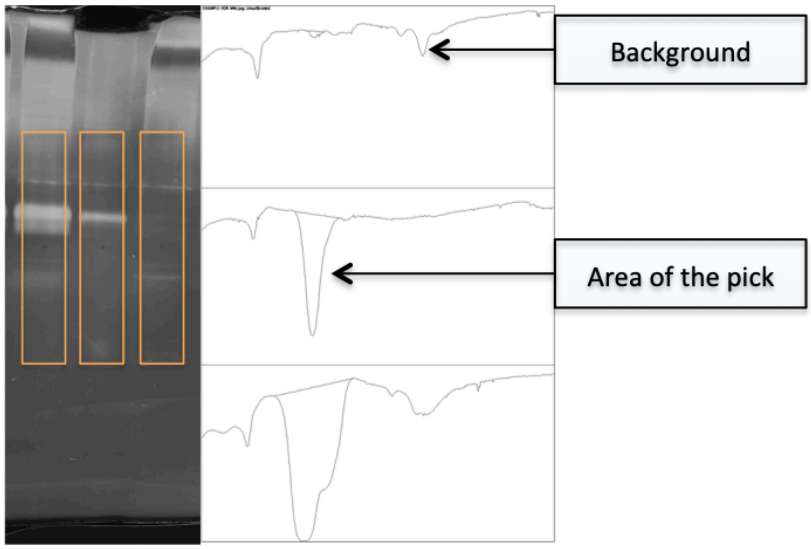


Figure 2.7 Analysis of Zymography in Image J

2.6.2 Western blotting

2.6.2.1 Deglycosylation and acetone precipitation of proteins from conditioned media

The conditioned media used for Zymography was also used for western blotting. The conditioned media was deglycosylated with the chondroitinase ABC and the endo-β-galactosidase. Chondroitin sulphate and dermatan sulphate, which are the components of the proteoglycans, are removed by the chondroitinase ABC. This enzyme does not change the activity on core proteins, keratan and heparan sulphate chains. Endo-β-galactosidase can cleave keratan sulphate. 150 µl of conditioned media were mixed to 49 µl of 4X deglycosylation buffer at pH 7.5 and 0.5 µl of chondroitinase ABC at 20 UN/µl and 0.5 µl of each endo-β-galactosidase at 10 UN/µl. The 4X deglycosylation buffer was prepared with 200 mM of Tris, 100 mM of EDTA and 200 mM sodium acetate. The mixture was incubated overnight at 37°C on a shaker. 1 ml of ice-cold acetone was added to precipitate the proteins and incubated at -20°C for 1 hr. After centrifugation at 13,000 g at 4°C for 30 min

to pellet the precipitated protein, the supernatant was removed allowing the pellet to air-dry for 1 hr.

2.6.2.2 Protein isolation from cultured cells

Cultured cells were washed in 1X PBS and lysed directly using 50-100 µl of radioimmunoprecipitation (RIPA) protein lysis buffer (Sigma), plus protease inhibitor cocktail (Sigma) and phosphatase inhibitor (Sigma) at 10 µl/ml for both. After incubation for 40 min on ice cell were centrifuged at 12,000 g at 4°C for 15 min to pellet the cell debris. The supernatant was then used to quantify the concentration of protein with a Pierce Bicinchoninic Acid (BCA) assay kit (Life technologies). This assay is based on the reduction of Cu^{2+} to Cu^{+} by protein in an alkaline medium forming a light blue complex. The more the sample contain peptides with more than 3 amino acid residues more cupric ions are formed. In a second reaction, the cupric ions react with the bicinchoninic acid forming a purple coloured reaction. The standard curve was prepared with BSA from 0-2 mg/mL and plates were sealed to avoid evaporation and incubated at 37°C for 30 min. The absorbance was measured at 562 nm with a microplate reader.

2.6.2.3 Sample preparation and running the gel

The 1X laemmli buffer was prepared as described in **Table.19** and 50 µl of this buffer was used to resuspend the protein pellet. Samples were boiled for 5 min at 100°C and briefly centrifuged. 37 µl of samples were loaded onto 4-12% Bis-Tris protein precast gels (ThermoFisher). A protein molecular weight marker was used in one well (Biorad) and the tank was filled with 1X MOPS buffer (ThermoFisher) allowing the medium to large protein for

separating. The gel was run for 15 min at 110V then at 160V until the loading buffer reached the bottom of the gel (≈ 55 min).

Table.19. Composition of 1X laemmili buffer

Step	Volume (µl) per sample
4X Laemmli	11.25
β-Mercaptoethanol	1.25
Deglycosylation buffer	37.5

50 ng of active recombinant human proteins (MMP-8 and MMP-9, (R&D systems)) were used as positive control for MMP-8 and MMP-9 respectively. The positive control used for aggrecan cleavage was bovine aggrecan from articular cartilage (Sigma) at 10 µm/ml.

2.6.2.4 Transfer and antibody staining

The gels were removed from the gel tank and the proteins were transferred to a polyvinylidene difluoride (PVDF) membrane (Bio-Rad) using a semi-dry transfer system (Bio-Rad) at 1.3 Amps, 25 V for 7 min. The membranes were transferred to 1X Tris- buffered saline and tween 20 (TBS-T) buffer composed of 0.2 M of Tris and 1.5 M of NaCl and 0.05 % of tween 20 (Sigma). The Ponceau S staining (0.1 % w/w Ponceau S dye and 1 % w/v acetic acid) was used to locate protein bands on membrane as shown in **Figure 2.8**. The membranes were incubated for 30 min with gentle agitation and immediately rinsed with distilled water until the background is clean. The membranes were scanned with Epson V700 Photo scanner using Epsonscan software and washed for 10 min in TBS-T for complete removal of the dye.

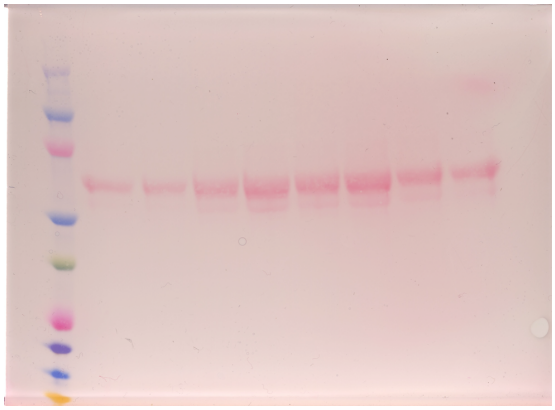


Figure 2.8 PVDF membrane stained with Ponceau S solution to see the protein bands

The membranes were transferred to a blocking solution (5 % of BSA in TBS-T) for 2 hr to prevent non-specific binding. After blocking, the primary antibody (diluted in blocking solution) was added to the membranes and incubated overnight at 4°C on a plate shaker allowing the primary antibody to bind to the protein (**Table.20**). The membranes were then washed four times (15 min each) with 1X TBS-T and incubated with a secondary antibody (diluted in blocking solution) for 1 hr at room temperature (**Table.21**). The secondary antibody, conjugated with HRP, will form a complex with the primary antibody. The membranes were washed three times (15 min each) with 1X TBS-T followed by a final wash in PBS. The membranes were then incubated with an ECL chemoluminescence solution (ThermoFisher) for 1 min. The HRP enzyme oxidizes the substrate present in the chemoluminescence solution (luminol) to a product that emits light that can be captured using a gel doc system (UVITEC).

Table.20. Primary antibodies list abbreviations: all primary antibodies were purchased from Abcam

Antigen (Name)	Host	Type	Source	Concentration
BC-3	Mouse	Monoclonal	Abcam ab3773	1:100
6-B-4	Mouse	Monoclonal	Abcam ab3778	1:100
MMP-8	Rabbit	Monoclonal	Abcam ab81286	1:1,000
MMP-9	Rabbit	Monoclonal	Abcam ab73734	1:1,000
ADAMTS1	Mouse	Monoclonal	Abcam ab236497	1:2,000
COL-1	Mouse	Monoclonal	Abcam ab6308	1:1,000
β-tubulin	Mouse	Monoclonal	Sigma T8328	1:200

Table.21. Secondary antibodies list abbreviations: all secondary antibodies were purchased from ThermoFisher

Target Species	Host	Conjugated	Source	Concentration
Anti-rabbit	Goat	HRP	ThermoFischer 31460	1:20,000
Anti-mouse	Goat	HRP	ThermoFischer 31430	1:10,000

The membranes were stripped for 10-15 min with stripping buffers (ThermoFisher) to dissociate and strip primary and secondary antibodies so the membranes can be re-probed to detect a different protein target. The membranes were washed in TBS-T for 15 min and directly transferred to a fresh blocking solution and continued as described.

The protein intensity was quantified using the same technique as described in the section 2.6.1.5.

2.7 SiRNA for MMP-8 and MMP-9

2.7.1 SiRNA optimization

2.7.1.1 Principles of siRNA

To silence MMP-8 and MMP-9 expression in human osteoclasts

cultured on cartilage, cells were transfected with small interfering (si) RNA. siRNA is small double-stranded RNA (21 nucleotides) that is encapsulated in lipids droplets for their delivery into the cells. The composition of these lipids is similar to the cellar membrane allowing the droplets to merge with the cell membrane and to release the siRNA into the cytoplasm. The endonuclease called Dicer cuts dsRNA into short segments; the strands are often called passenger-strand and guide-strand (**Figure 2.9**). Argonaute degrades one strand and the second bind to the enzyme to be used as a guide strand. This strand is incorporated into a complex known as RNA-Induced Silencing Complexes (RISCs). RISCs use the guide strand to find the mRNA that has a complementary sequence leading to the cleavage and the degradation of the targeted mRNA[191].

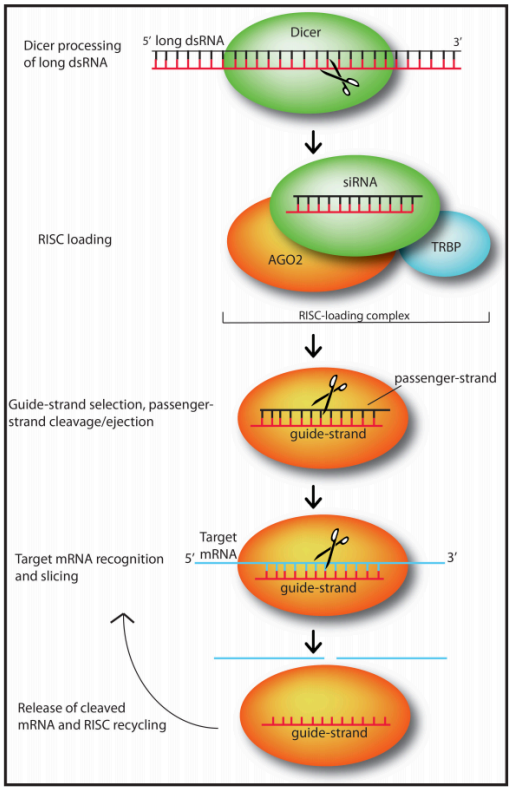


Figure 2.9 The passenger-strand is degraded whereas the guide-strand is used to find the mRNA that has a complementary sequence leading to the cleavage of the mRNA (Dana et al, International journal of biomedical science , 2017)[192]

2.7.1.2 Measurement of mRNA and protein expression

Monocytes were seeded at 1 x 10^6/well in a 24-well plate and cultured for 6 days with complete α-MEM containing M-CSF and RANKL. At day 7 fresh cells were refreshed with 500 µl per well with unsupplemented α-MEM and transfected with and siRNA (Life technologies) against MMP-8, MMP-9 or a non-specific siRNA using lipofectamine RNAiMax (Life technologies). Two siRNA were used to a single target gene (***Table.22***).

Table.22. List of siRNA used for the experiment

Target	siRNA ID	Labels	Sense	Antisense
MMP-8	105332	Si1	GCAACCAGUAUCAGUCUACTT	GUAGACUGAUACUGGUUGCTT
MMP-8	112911	Si2	GCCUUUUUGUCACCUCAAUTT	AUUGAGGUGACAAAAAGGCTT
MMP-9	104072	Si1	GGAUGGGAAGUACUGGCGATT	UCGCCAGUACUUCCCAUCCTT
MMP-9	113182	Si2	CCAAUCUCACCGACAGGCATT	UGCCUGUCGGUGAGAUUGGTT

Briefly, the lipofectamine was diluted in OPTI-MEM medium (Gibco) in a tube and the siRNA was diluted in OPTI-MEM medium in another tube. The two solutions were mixed at a ratio of 1:1 and incubated for 5 min. Finally, the siRNA-lipid complex was added to the cells with a final concentration of siRNA at 25, 50 or 75 nM and l5 µl of lipofectamine per well. After 6 hr, the cells were refreshed with complete α-MEM containing M-CSF and RANKL. RNA was collected 24 hr after transfection to monitor mRNA level and determine the optimal concentration of siRNA to use (**Figure 2.10**).

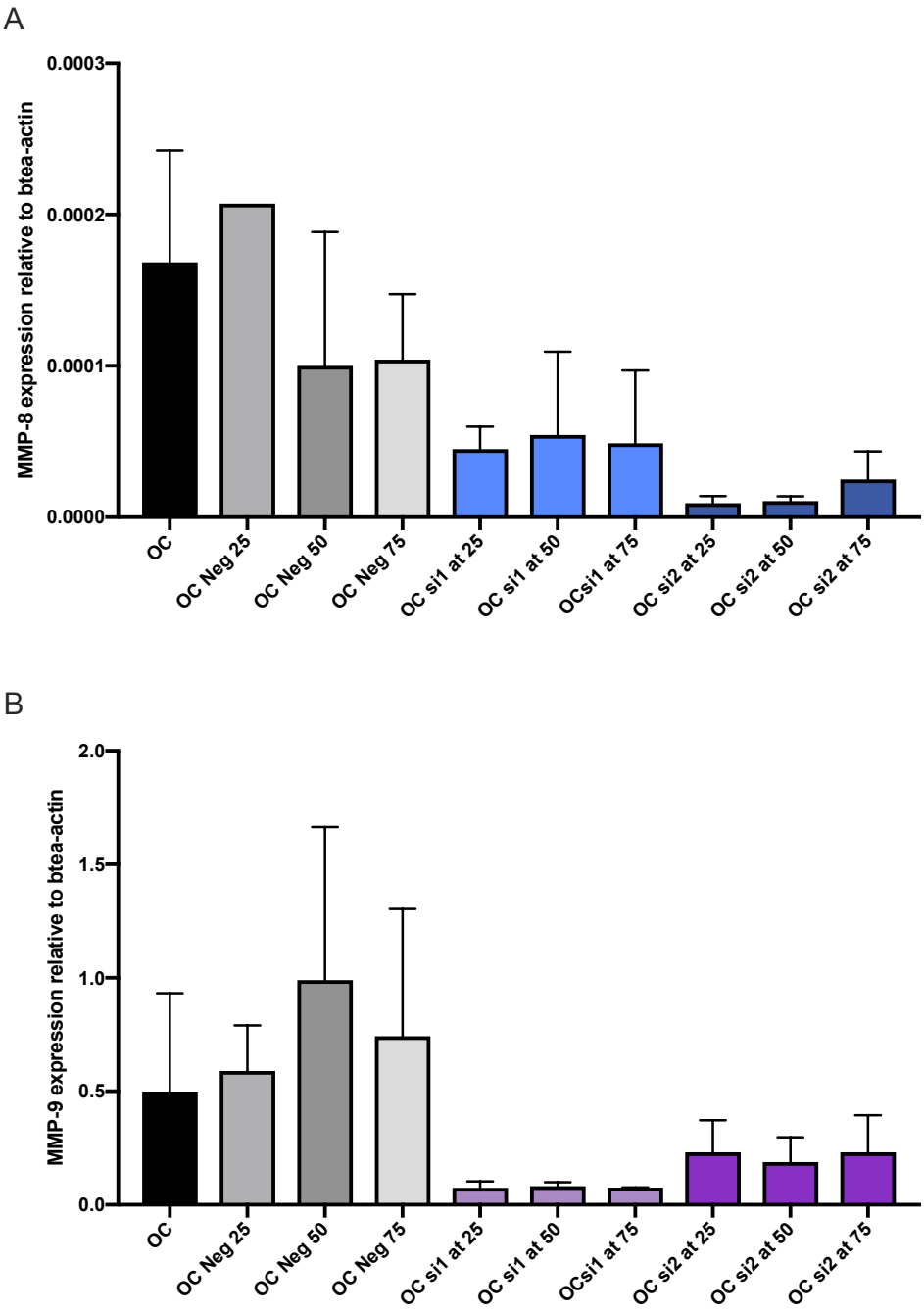


Figure 2.10 Optimization of siRNA, mRNA levels was monitored with 2 osteoclasts preparation. A. OC: osteoclasts MMP-8 expression in presence of MMP-8 siRNA construct 1, construct 2 or siRNA control (sineg) at 25, 50 and 75 nM. B. Similar to A. but MMP-9 expression with MMP-9 siRNA

The final concentration of siRNA used was 25 nM for each siRNA for MMP-8, MMP-9 and the non-specific siRNA. Proteins and conditioned

media were collected at 24, 48 and 72 hr to test the protein level of the targets (**Figure 2.11** and **Figure 2.12**).

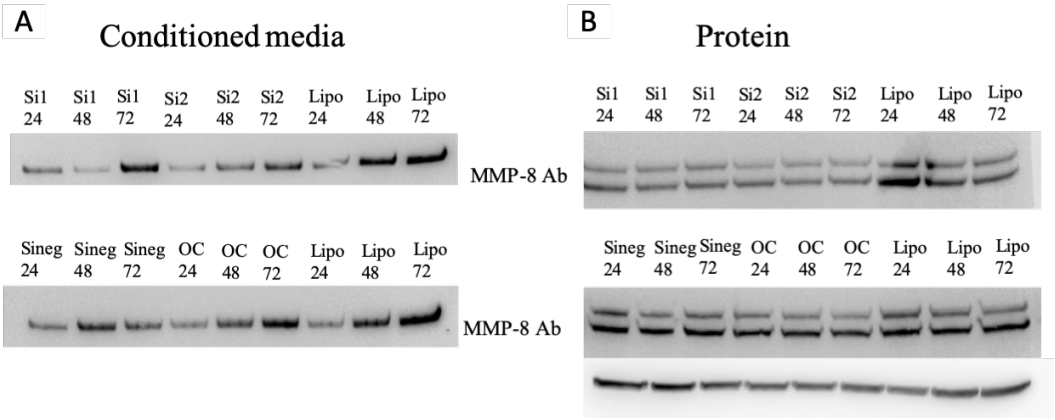


Figure 2.11 Optimization of MMP-8 siRNA, protein levels monitored with 4 osteoclasts preparation in conditioned media (A.) and cells (B.). MMP-8 siRNA construct 1 and 2 at 24, 48 and 72 hours, Lipo: lipofectamine (no siRNA), Sineg: siRNA control and OC: osteoclasts.

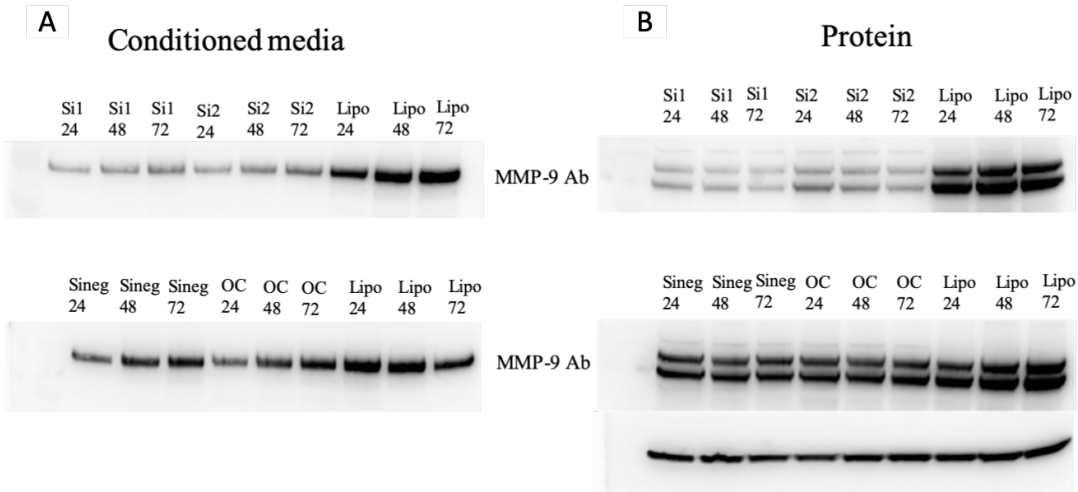


Figure 2.12 Optimization of MMP-9 siRNA, protein levels monitored with 4 osteoclasts preparation in conditioned media (A.) and cells (B.). MMP-9 siRNA construct 1 and 2 at 24, 48 and 72 hours, Lipo: lipofectamine (no siRNA), Sineg: siRNA control and OC: osteoclasts.

2.7.1.3 Protein expression when osteoclasts were cultured on cartilage

Quantification of replicate Westerns showed a reproducible trend to reduce MMP-8 protein levels (p value: 0.0938) in response to the siRNA transfection while MMP-9 was significantly inhibited (**Figure 2.13 A.** and **C.**). Protein levels were visibly reduced by siRNA targeting both MMP-8 (**Figure 2.13 B.**) and MMP-9 (**Figure 2.13 D.**).

The protein expression of MMP-9 in osteoclasts transfected with MMP-8 siRNA was not increased and MMP-8 expression was not increased in osteoclasts transfected with MMP-9 siRNA (**Appendix A.7 A.** and **B.**).

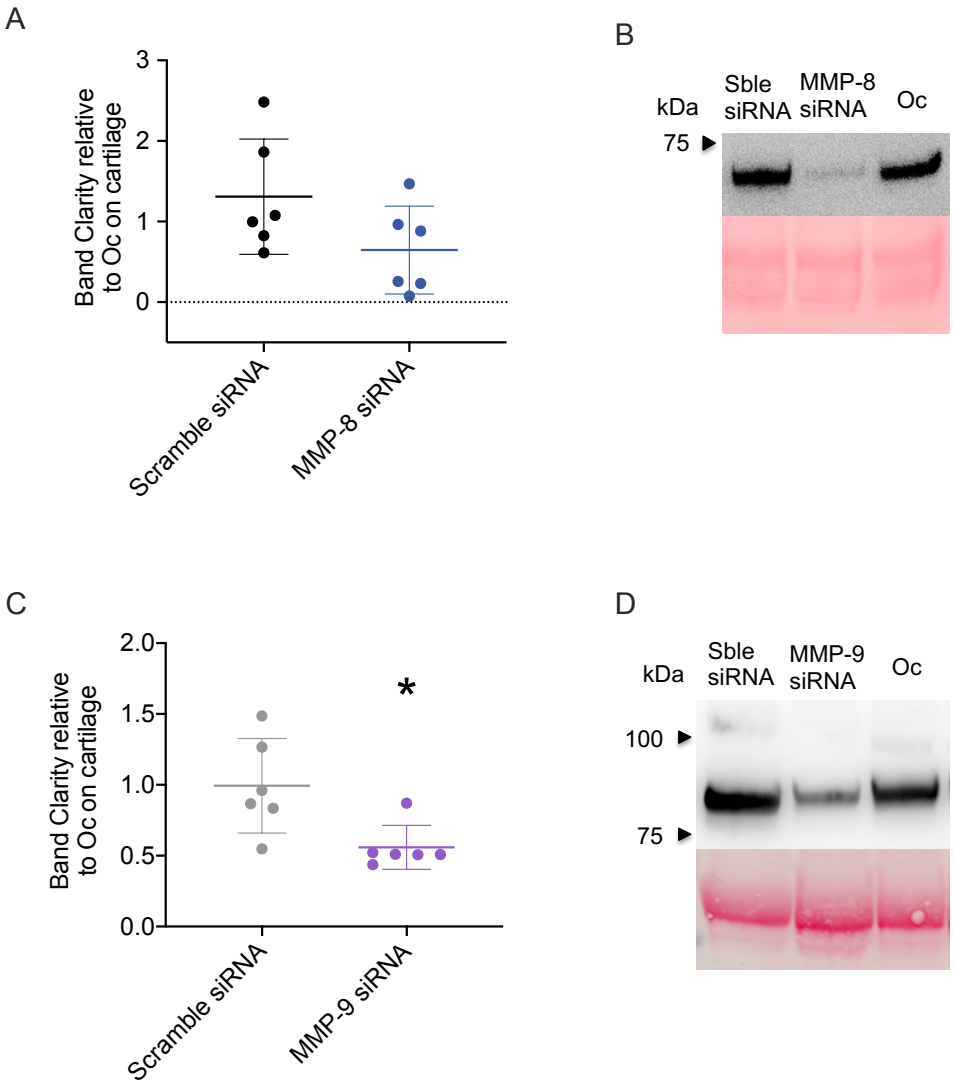


Figure 2.13 Decrease of MMP-8 and MMP-9 protein secreted by osteoclasts on cartilage after transfection of siRNA. Osteoclasts were cultured on acellular cartilage. At day 7 the cells were transfected with a scramble siRNA (control), MMP-8 or MMP-9 siRNA or untransfected and the conditioned media was collected at day 10. **A.** Band clarity of MMP-8 protein expression after transfection with the scrambled control or MMP-8 siRNA. The band clarity is relative to osteoclasts on cartilage (un-transfected cells) **B.** A representative Western Blot of MMP-8 expression. **C.** Similar to **A.** but the cells were transfected with MMP-9 siRNA. **D.** Similar to **B.** showing MMP-9 protein expression. The detection of MMP-8 and MMP-9 protein in osteoclasts transfected with the scramble siRNA compared with non-transfected osteoclasts confirmed the absence of nonspecific effects from the siRNA. Sble siRNA: scramble control siRNA, Oc: osteoclasts. *p<0.05 and n=6

2.8 Statistics

Statistical analysis was performed using GraphPad Prism 8 (GraphPad Software, California, USA). Statistical significance was determined using one-way ANOVA with Dunnett Multiple comparison or Student's T-test. Results were considered significant if *$p<0.05$; **$p<0.01$; ***$p<0.001$ and ****$p<0.0001$. All figures include at least three independent experiments and are plotted as mean ± SD. The number of n corresponds to the number of cartilage donors and/or the number of blood donors. Each experiment was run with triplicate. Similar statistical analysis was performed when the experiment was comparing the fold change.

Chapter 3

OSTEOCLASTS ARE PRESENT IN DISEASED JOINTS AND DEGRADE CARTILAGE *IN VITRO*

INTRODUCTION

3.1 Joint-related pathologies

The proximity of osteoclasts and cartilage is common to many joint-related diseases. This suggests that osteoclasts may have a role in regulating cartilage turnover in joint pathologies.

OA and GCTB patients show histologically visible multinucleated cells degrading cartilage. Knowles et al conducted a phenotypic analysis of these cells showing they expressed osteoclast markers (CD14-, CD51+) and exhibited an osteoclast-like phenotype with strong expression of TRAP, MMP-9 and Cathepsin K[188].

In this chapter, 7 different pathologies are investigated to establish whether osteoclasts are present within cartilage tissue or in cartilage-like tissue of tumours. This list is not exhaustive but does demonstrate the multiple situations where osteoclasts are seen in contact with cartilage. This led us to study the function of osteoclasts in contact with cartilage later in the chapter.

3.1.1 Osteoclasts in osteoarthritis (OA)

The main pathologies of OA are the degradation of the articular cartilage and changes to the subchondral bone, primarily in the hip and knee.

Osteoclasts are being increasingly identified in the subchondral plate in experimental animal models of OA supporting the idea that osteoclasts participate in the pathobiology of the joints.

Alendronate, which is a bone resorption inhibitor, is chondroprotective in a rat model of surgical induction of OA and inhibits the vascular invasion into the calcified cartilage[193]. Treatment with alendronate increased the thickness of the calcified cartilage compared to vehicle treated rats. This observation suggests that alendronate inhibited the resorption of calcified cartilage by osteoclasts[194]. Kadri et al used mice overexpressing Runx2 to increase bone remodelling. A partial meniscectomy was then performed to induce OA. Mice were treated with pamidronate, an osteoclast inhibitor, once a week for six weeks post-surgery. They observed that pamidronate blocked bone resorption and prevented an increase in OA. Immunohistochemistry of cartilage revealed an important decrease of ADAMTS-4 and ADAMTS-5 in the presence of pamidronate. However, cartilage explants from mice cultured *ex vivo* with pamidronate showed no change in proteoglycan release highlighting the presence of a crosstalk between the subchondral bone and cartilage[195]. RANKL, expressed by osteoblastic lineage cells as well as chondrocytes, is essential during osteoclastogenesis. RANKL expression is increased in human OA cartilage compared with normal cartilage, largely due to its expression by hypertrophic chondrocytes. Shimizu et al demonstrated the protective effect of OPG against cartilage destruction in murine OA development. More precisely, OA was surgically induced in mice knockout for OPG and wild-type and the generative changes in the articular cartilage were significantly enhanced in OPG $^{-/-}$ mice. Also, intraarticular injection of human recombinant OPG in wild type mice with OA induced surgically prevented cartilage destruction. The authors proposed that OPG inhibited chondrocyte apoptosis[196], but it is unclear whether OPG affected only

chondrocytes or indirectly through osteoclastic formation and activity via RANK signalling.

Shibakawa et al examined articular cartilage from human knee OA and non-arthritic cadavers. Osteoclasts were found in both conditions in contact with calcified cartilage, however, only OA specimens showed an invasion of osteoclasts into the articular cartilage. Immunohistochemistry showed that the multinucleated cells were positive for osteoclast markers such as VNR and expressed MMP1, MMP3 and MMP13. Therefore, they proposed that osteoclasts degrade cartilage matrix with MMPs[197]. Bertuglia et al suggested that RANKL expression by chondrocytes in the middle and deep zone of cartilage is an important chemo-attractant for osteoclasts from the subchondral bone in equine post-traumatic OA. These osteoclasts expressed high levels of cathepsin K, a powerful collagenase that may participate in the degradation of the bone-cartilage interface[184]. Another study revealed that monocytes isolated from the blood of patients with OA have an enhanced capacity to generate osteoclasts with high resorptive activity and reduced osteoclast apoptosis[198].

3.1.2 Rheumatoid arthritis (RA)

RA is a connective tissue disease associated with bone and cartilage destruction. Proliferating synovial cells infiltrate into the joint tissues to form a pannus. Bone loss in RA is mediated by osteoclasts that are located at the pannus-bone interface. Gravallese et al showed that haematopoietic osteoclast precursors needed to be in contact with bone and/or calcified cartilage to fully differentiate into osteoclasts. They suggested that calcitonin was the essential

marker for late stage differentiation[199]. The osteoclasts formed expressed the typical markers of the osteoclast lineage; TRAP and cathepsin K. Bromley and Woolley identified typical cells with all the characteristics of osteoclasts degrading cartilage in RA[200]. They suggested that the mineralised cartilage is eroded by osteoclasts, which enhances the invasion of the pannus. This occur as the cartilage is directly exposed to cytokines and matrix-degrading enzymes from osteoclasts. Kotake et al isolated multinucleated cells from the synovial lesions of RA patients and showed that they could form bone resorption pits, thus confirming them to be osteoclasts[201].

The microenvironment of the joint in RA is pro-osteoclastogenic; synovial fibroblast-like cells and T cells provide signals for monocytes to differentiate into osteoclasts. *In vitro* cell culture shows that synovial like fibroblasts from patients with RA and T cells from the synovial tissue express high levels of RANKL[202,203]. M-CSF is secreted by synovial fibroblasts, osteoblasts, macrophages and T cells in RA patients[204].

Pro-inflammatory cytokines such as TNF-α, IL-17 and IL-1 are present in RA and known to drive osteoclast formation[205]. TNF-α potentiates the effect of RANKL and induces osteoclast formation which explains the high efficacy of TNF-α-blocking agents in the protection of bone structure in patients with RA[206]. Overexpression of TNF-α enhances formation of osteoclasts, inducing severe osteoporosis and erosive arthritis in mice[207]. Bone erosion was completely blocked, and cartilage damage was partly inhibited after repeated injection of an inhibitor of osteoclast function (Zaledronic acid)[208].

3.1.3 Giant Cell Tumour of Bone (GCTB)

GCTB is characterised by significant local bone destruction, believed to be caused by the many osteoclast-like giant cells within the tumour tissue. These cells express osteoclast markers and ruffled membranes but are often larger and contain more nuclei than normal osteoclasts. Without immediate treatment, GCTB causes bone loss, destruction of the knee joint and invasion of the tumour into surrounding articular subchondral bone and cartilage. Campanacci et al observed that 5 % of GCTB cases extended into the joint[209]. Osteoclast-like giant cells isolated from GCTB and cultured on cartilage are capable of releasing GAG from hyaline cartilage[188].

3.1.4 Osteosarcomas

Osteosarcomas are the most frequent malignant primary bone tumours and are most common between the age of 10-16 or after 40 years. They most frequently appear at the metaphysis of long bones, therefore often located adjacent to joints. Osteosarcomas show an immature bone growth called osteoid. Type I collagen is the main component of the osteoid-extracellular matrix.

Giant cell-rich osteosarcoma is a rare type of osteosarcoma that contains more than 50 % of osteoclast-like giant cells in the tumour and therefore is very aggressive[210,211]. The presence of osteoid is the only way to differentiate it from a GCTB. In 1982, Simon et al reported that 7 cases out of 45 osteosarcomas showed an invasion of articular cartilage by the tumour, and 10 cases penetrated the osteochondral junction without perforating the articular cartilage[212]. Conversely in 2005, Quan et al did an examination of

27 cases of osteosarcoma near synovial joints and they revealed that joint involvement was uncommon, with articular cartilage acting as a relative barrier to tumour invasion. The resistance of cartilage to malignant invasion has been attributed to the expression of various angiogenesis inhibitors in cartilage[213]. In 2013, Wang et al described that 2 out of 9 patients had their knee joint involved with articular surface destruction[214].

3.1.5 Osteochondroma

Osteochondroma is one of the most common benign bone tumours. It is common in children and the growth of the osteochondroma is parallel to the growth of the patient.

It is commonly located at the transition of metaphysis and diaphysis and projects out of the underlying bone. A trapped growth plate emerges from the surface of the bone via a stalk. Endochondral ossification is seen at the cartilage-bone surface with the formation of mature bone trabeculae.

The cartilaginous cap is the site of growth of the bony mass and is composed of the periosteum, hyaline cartilage with chondrocytes and bone. Chondrocytes are often arranged in columns as is normally seen at the cartilage-bone interface. Yamagishi et al reported that osteochondroma from 13 patients expressed high levels of RANKL[215].

3.1.6 Chondroblastoma

Chondroblastoma accounts for less than 1% of all bone tumours and most patients are between 10 and 25 years old. The tumour contains three dominant components: the neoplastic mononuclear cells also called

chondroblast-like cells, multinucleated osteoclast-like giant cells, and chondroid matrix fragments often called chicken wire calcification.

The epiphyseal location shows that articular cartilage can be eroded by the tumour. Only a few cases have shown an involvement of the articular surface in progression of the disease[216]. It has been reported that both RANKL mRNA and protein were present in the tumour cells of chondroblastoma[217]. Osteoclast-like giant cells are possibly the cells from the tumour that are able to extend through the subchondral plate. The multinucleated cells of chondroblastoma are positive for osteoclast specific enzymes such as TRAP and carbonic anhydrase II[164]. Chondroblastoma was previously called calcifying giant cell tumour of bone due to the resemblance to giant cell tumours.

3.1.7 Chondromyxoid fibroma

Chondromyxoid fibroma is a rare, slow-growing tumour of cartilaginous origin. Patients are between 10 and 30 years old and it is more common in men than in women. Giant cells are present especially at the periphery of the lesion and the presence of the myxoid element is decisive to do the diagnosis.

It is mainly located in the metaphysis of long bones and may extend to the epiphyseal line and even abut the articular surface.

The appearance of the tumour can be similar to hyaline cartilage since it displays morphologic features of different stages of chondrogenesis. Chondromyxoid fibromas are lobulated and the centre is hypocellular. The

periphery of the lobule is more cellular with spindle cells, blood vessels and osteoclast-like giant cells.

3.2 Osteoclasts and cartilage

3.2.1 Chondroclasts

In 1966, Schenk et al described multinucleated cells degrading mineralised cartilage during endochondral ossification of growing rats. They defined these as chondroclasts – cells identical to osteoclasts, only with a different substrate[218]. In 1984, Woolley et al described the presence of both osteoclasts and chondroclasts in RA knee joints[200,219]. The chondroclasts where in close contact with non-mineralised and calcified cartilage. To complete the description from Schenk et al, a chondroclast was defined by abundant mitochondria, vacuoles, lysosomes[220,221], poorly developed ruffled borders without actin rings and a decreased TRAP activity[222]. There has been a debate since to determine the proper nomenclature of these cells in the scientific community.

Gravallese et al in 1998 and Knowles et al in 2012 did the final identification of these cells as osteoclasts[188,199]. For the first group the presence of the calcitonin receptor was the major osteoclast marker allowing them to distinguish osteoclasts from other haematopoietic and bone cells. They revealed that multinucleated cells in the inflammatory synovial tissue only expressed the calcitonin receptor when they were in direct contact with calcified cartilage or the subchondral bone. This observation suggests that final differentiation to osteoclasts depends on direct contact with mineralised tissue such as calcified cartilage or bone. Knowles et al conducted a

phenotypic analysis of these cells showing they expressed osteoclast markers (CD14-, CD51+) and exhibited an osteoclast-like phenotype with strong expression of TRAP, MMP-9 and Cathepsin K[188]. However, the mechanism of cartilage degradation by osteoclasts needs to be understood.

3.2.2 Culturing osteoclasts on cartilage

Culturing osteoclasts on cartilage *in vitro* is a challenging technique compared to culturing osteoclasts on dentine and has been little explored. In the literature, osteoclasts are often cultured on osteochondral explants but the effect of osteoclasts on cartilage alone cannot be derived as the cells are interacting with two tissues at the same time and it is complicated to avoid any indirect effect between those tissues (subchondral bone and cartilage).

In 2005, Suzumoto et al cultured mouse osteoclasts on rabbit cartilage, bone and decalcified bone. They found that osteoclasts on decalcified bone were multinucleated with a weak TRAP activity whereas the cells were mononuclear and devoid of TRAP activity when cultured on cartilage[223]. In 2012, Knowles et al cultured human osteoclasts and macrophages on human cartilage pieces. After confirming the immunophenotype of the cells on cartilage (CD14-, CD68+ and CD51+), they showed that osteoclasts were able to degrade the cartilage matrix by release of GAG into the media[188]. In 2018, Lofvall et al cultured human osteoclasts on bovine cartilage, osteochondral junction and cortical bone. As observed by Knowles et al, the presence of osteoclasts on cartilage increased the amount of ECM degradation. However, this paper measured the amount of type II collagen rather than the amount of GAG in the media. Both of them reflect the

degradation of the cartilaginous matrix. Lofvall et al used acidification, cathepsin K and MMP inhibitors to understand how osteoclasts degrade cartilage. According to their finding, and unlike resorption of bone, osteoclasts on cartilage did not use acidification to degrade the ECM[185] (discussed in detail in Chapter 4).

3.3 Objectives

The overarching aims of this chapter were to determine if osteoclasts in contact with articular cartilage could be found in different joint pathologies and were able to degrade cartilage. More specifically, this chapter aimed to:

1. Determine whether osteoclasts are in contact with the articular cartilage in a range of joint pathologies such as inflammatory and non-inflammatory arthritis and bone tumours.

2. Investigate the effects of osteoclasts on cartilage turnover by measuring collagen and aggrecan degradation products. Optimise the techniques required to demonstrate the capacity of osteoclasts to degrade cartilage in vitro. Confirm with another source of osteoclasts whether mature and active osteoclasts are responsible for cartilage degradation.

3. Compare the morphological and functional characteristics of osteoclasts cultured on cartilage with osteoclasts cultured on -dentine.

RESULTS

3.4 Osteoclasts in joint pathologies

The first aim of this chapter was to see if osteoclasts could be found in a range of joint and bone pathologies – non-inflammatory arthritis (OA), inflammatory arthritis (RA) and bone cancer (GCTB, osteosarcoma, osteochondroma, chondroblastoma).

3.4.1 Osteoclasts are observed in the deep zone of OA articular cartilage

Osteochondral sections were obtained from 8 OA knees with macroscopically damaged and undamaged cartilage regions and observed following H&E staining. Patients showed degradation of the superficial zone of articular cartilage. In 6 patients out of 8, osteoclasts were found in contact with the deep zone of cartilage.

The subchondral bone (#) contains osteocytes surrounded by bone matrix. The hyaline cartilage and the mineralised cartilage beneath contain embedded chondrocytes with a round shape and a single nucleus. Osteoclasts were found in contact with mineralised cartilage (**Figure 3.1A.** and **C.**). At higher magnification, the osteoclasts have between 4 and 14 nuclei (**Figure 3.1 B.** and **D.**).

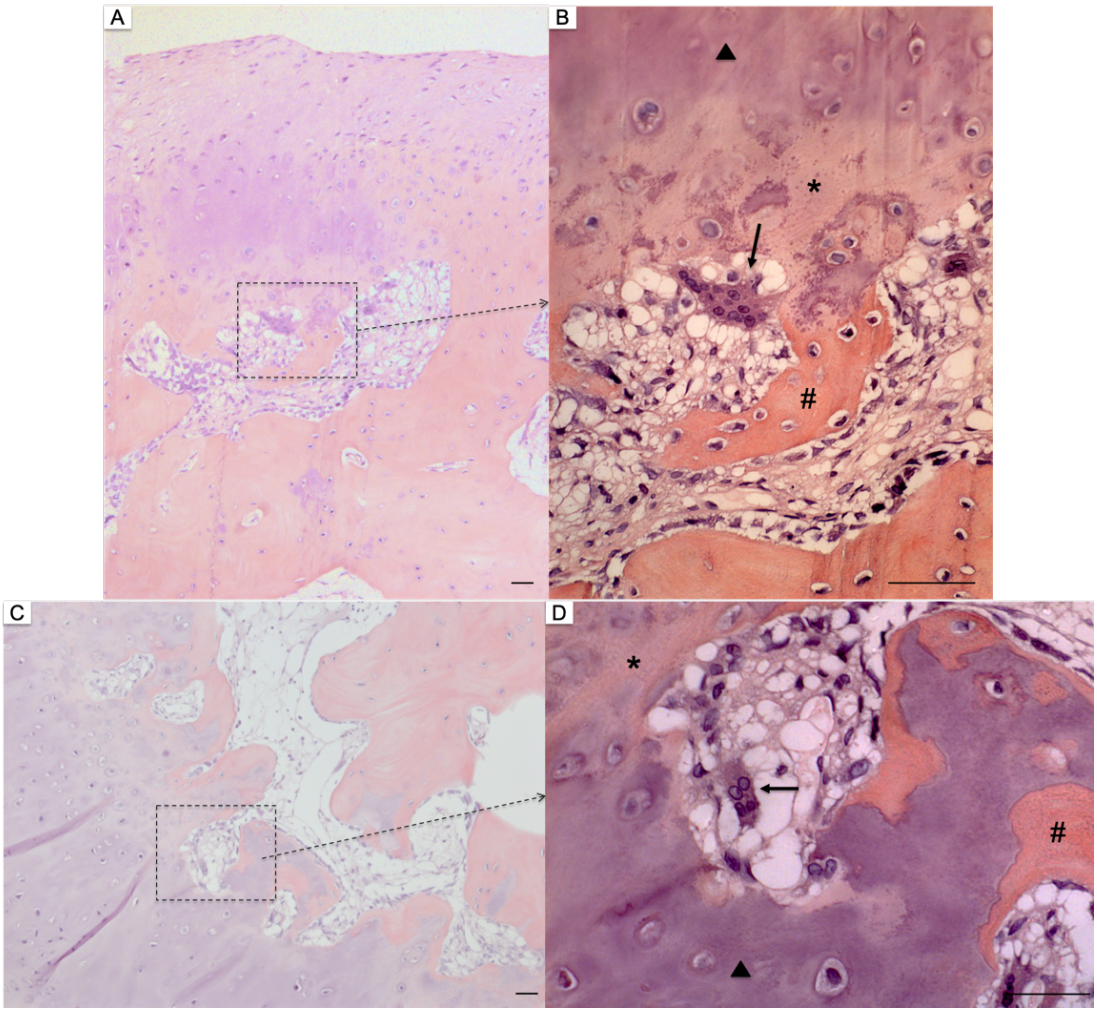


Figure 3.1 H&E staining of a damaged knee joint of OA patient containing osteoclasts. A. Osteochondral tissue of OA patient, the articular cartilage is on the top of bone. Dotted square magnified in **B.**; **C.** Osteochondral tissue from another OA patient. Dotted square magnified in **D.** Osteoclasts (←) resorb subchondral bone (#) and invade mineralized cartilage (*) and unmineralized cartilage (▲). Scale Bar = 100µm.

3.4.2 Osteoclasts are found in the pannus in rheumatoid arthritis (RA)

The hyaline cartilage with chondrocytes was found next to the pannus **Figure 3.2 A.**). The subchondral bone (#) is beneath the mineralised cartilage (*). In contrary to cartilage degradation in OA, the pannus penetrates into the cartilage from the hyaline cartilage in direction of the mineralised cartilage.

This invasion can be seen at low magnification (**Figure 3.2 B.**). Osteoclasts, that are part of the pannus, were seen in contact with mineralised cartilage (Black arrow, **Figure 3.2 C.**). This suggests that osteoclast-mediated degradation allows the pannus to penetrate into the cartilage.

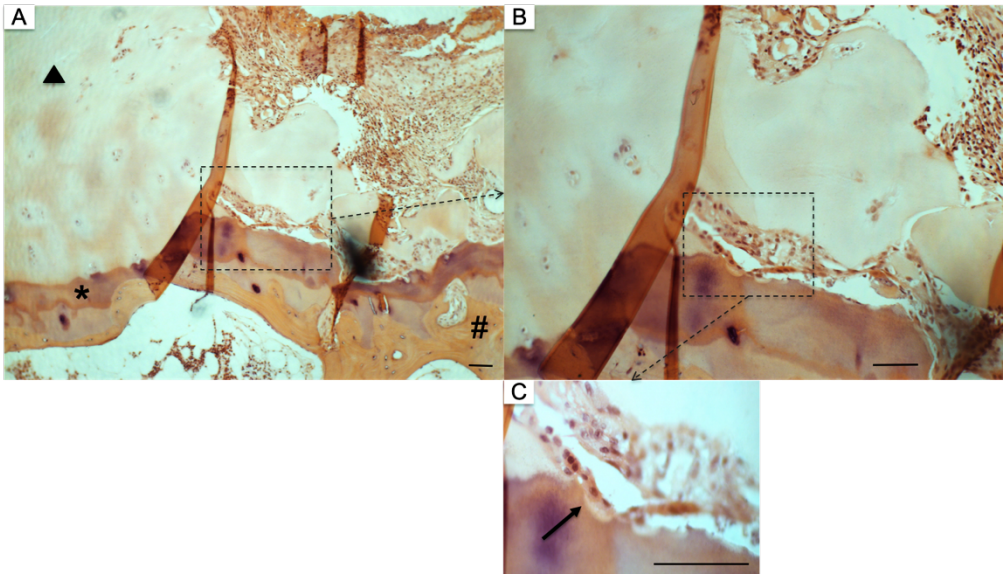


Figure 3.2 H&E staining of RA tissue section. The cells in the pannus penetrate the mineralized cartilage (*) and (▲) unmineralized cartilage. (#) indicate subchondral bone and (←) osteoclasts. **A.** dotted square magnified in **B.** and **B.** dotted square magnified in **C.** Bar = 100µm.

3.4.3 Osteoclasts of Giant Cell Tumour of Bone (GCTB) invade cartilage

Numerous osteoclast-like giant cells were seen in GCTBs that had invaded through the subchondral bone plate and extended to the articular cartilage (**Figure 3.3**). This was seen in all 4 cases analysed. GCTBs are also made up of round mononuclear cells which represent the neoplastic component of the tumour (**Figure 3.3 A.-B.**). The osteoclast-like giant cells were found on the deep surface of unmineralized articular cartilage (**Figure**

3.3 A., **B.** and **D.**) and on the mineralised subchondral cartilage (**Figure 3.3 C.**).

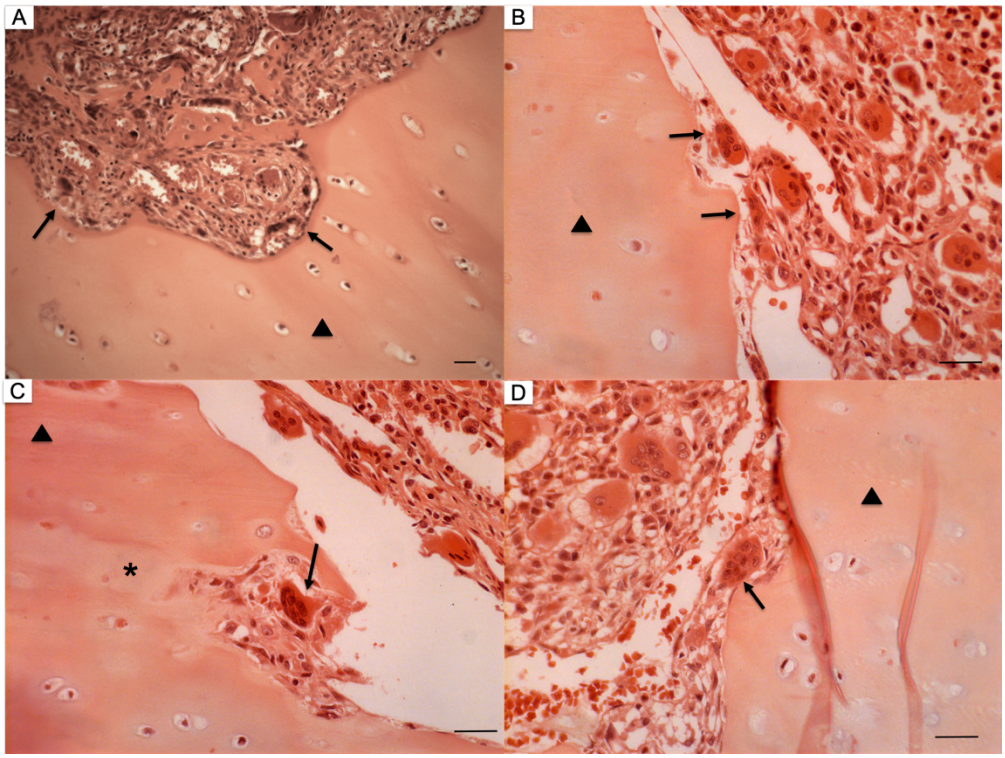


Figure 3.3 H&E staining of GCTB tissue sections. A. and **B.** Osteoclast-like cells (←) invading (▲) unmineralized cartilage. **C.** Osteoclast-like cells (←) invading mineralized cartilage (*). **D.** Additional examples of osteoclasts in contact with cartilage. Bar = 100µm.

3.4.4 Giant cell rich osteosarcoma in proximity with cartilage

Osteoclast-like cells were observed in contact with articular cartilage in giant cell rich osteosarcoma (**Figure 3.4**). Anaplastic stromal cells (red arrow), that are also part of the tumour, are seen above the osteoclasts.

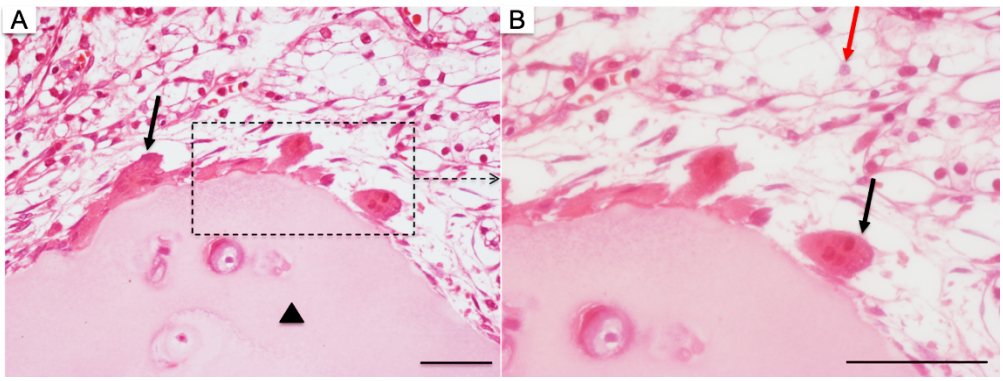


Figure 3.4 H&E staining of giant cell rich osteosarcoma tissue sections extending through the subchondral plate. A. Osteoclast-like cells (←) degrading (▲) unmineralized cartilage and mononuclear cells that are also part of the tumour (←). Dotted square magnified in **B.** Bar = 100 µm.

3.4.5 Osteoclasts were observed at the junction of the cartilage cap and the cancellous bone in osteochondroma

The cartilaginous cap (▲) is located between the periosteum and the cancellous bone (#). The junction of the cartilage with the cancellous bone resembles a normal epiphyseal growth plate; the cartilage becomes calcified and undergoes endochondral ossification with the formation of mature trabecular bone. Osteoclasts in contact with articular cartilage are indicated with a black arrow (**Figure 3.5 C.-D.**). At lower magnification, it is evident that most of the osteoclasts are at the border of the cartilage cap and the cancellous bone. The presence of osteoclasts indicates a site of endochondral ossification (**Figure 3.5 A.-B.**).

Chondrocytes (red arrows) are round with indistinct cytoplasmic borders and small, dark nuclei with perinuclear clearing (**Figure 3.5 B.** and **C.**). In actively growing osteochondromas, the chondrocytes align themselves in closely parallel columns or clusters with increasing size of the lacunar

spaces as they approach the interface with the underlying cancellous bone (**Figure 3.5 A.** and **B.**).

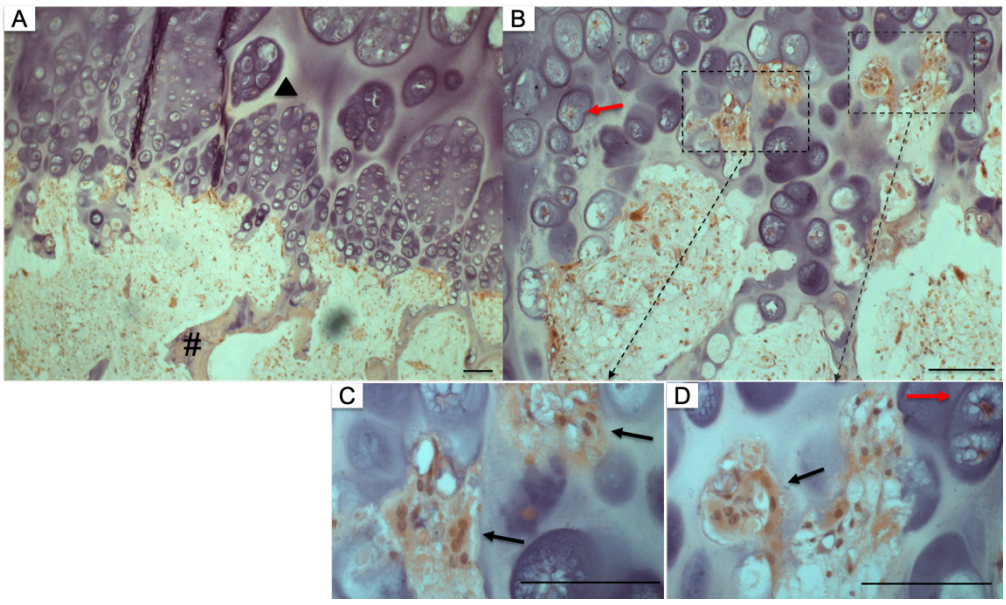


Figure 3.5 Osteochondroma sections stained with H&E. A. The cancellous bone (#) beneath the unmineralized cartilage cap (▲) is visible at low magnification. **B.** Dotted square magnified in **C**. and **D.** Osteoclast-like cells (←) degrading the unmineralized cartilage with chondrocytes (←). Bar = 100µm.

3.4.6 Benign chondroblastoma contains osteoclast-like cells

Benign chondroblastoma showed a mix of chondroid matrix, mononuclear cells with oval nuclei and scattered osteoclast-like cells (indicated with a black arrow, **Figure 3.6**).

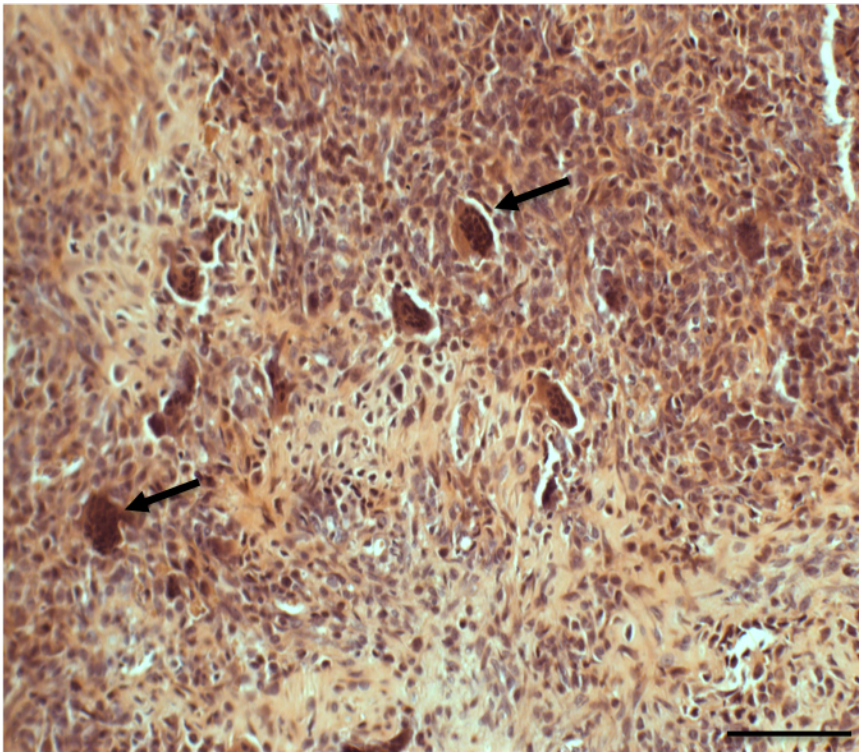


Figure 3.6 H&E tissue section of chondroblastoma with osteoclasts. Osteoclast-like cells (←) Bar = 100μm.

3.4.7 Chondromyxoid fibroma also contains osteoclast-like cells

Chondromyxoid fibroma specimens possessed a cartilaginous tumour with characteristic chondroid lobules resembling mature hyaline cartilage, mesenchymal cells and mononuclear cells as well as osteoclast-like cells (indicated with a black arrow, **Figure 3.7**).

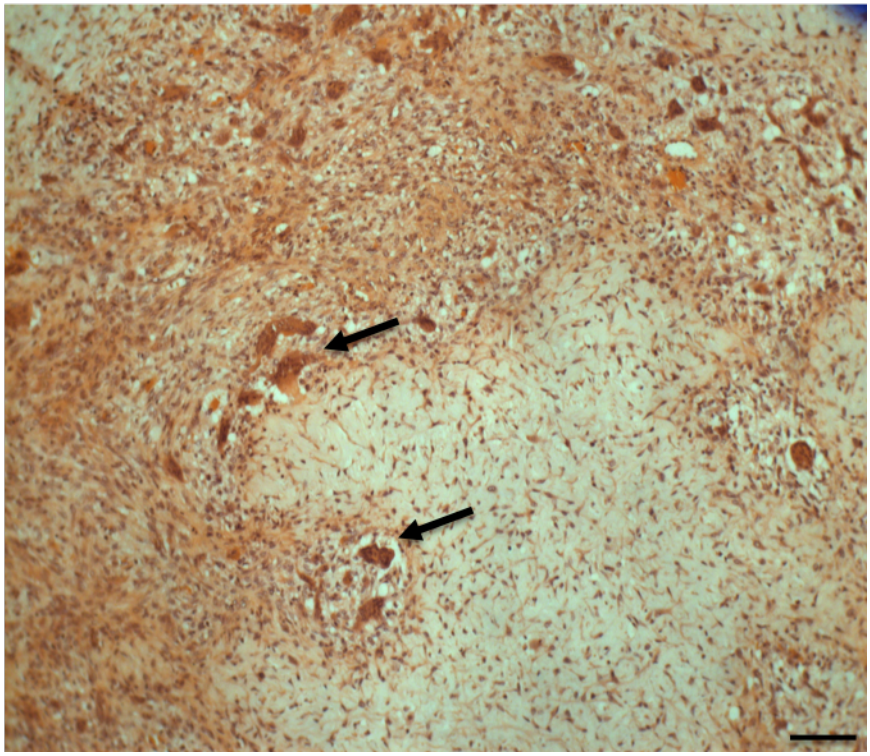


Figure 3.7 Multinucleated osteoclast-like cells in chondromyxoid fibroma with chondroid lobules. Osteoclast-like cells (←) Bar = 100μm

3.5 Development and testing of the osteoclast-cartilage culture system

To determine if osteoclasts could degrade cartilage, a technique similar to the one described in Knowles et al was used. As a positive control, monocytes were differentiated into osteoclasts on dentine for 16 days. To determine an adequate duration for the experiment, osteoclasts' differentiation and resorbing activity were assessed. By day 10 osteoclasts were formed and active; multinucleated cells exhibited major osteoclast characteristics such as the presence of TRAP and vitronectin receptor (VNR) staining (**Figure 3.8 A.**, **B.** and **D.**). The ability to form resorption pits on dentine was used to confirm the activity of osteoclasts (**Figure 3.8 C.** and **E**).

Thus, TRAP and VNR staining and the pit resorption assay show that osteoclastogenesis should be for at least 10 days to measure resorption / digestion activity on dentine. Moreover, after day 16 a drop of the number of osteoclasts was seen suggesting that the experiment should not last for more than 13 days.

To develop and test an *in vitro* osteoclast-cartilage co-culture system, monocytes were differentiated into osteoclasts on cartilage pieces.

The cartilage pieces were either cellular or acellular. More precisely, chondrocytes were maintained active in cellular cartilage whereas acellular cartilage was flash frozen in liquid nitrogen. The cell viability assay confirmed that chondrocytes were metabolically inactive in acellular cartilage compared to cellular cartilage between day 10 and day 13 (**Figure 3.9 A.**).

To investigate the effects of osteoclasts on cartilage, biomarkers of ECM turnover such as collagen and aggrecan degradation were measured for 16 days. Prior to addition of osteoclasts, the basal levels of collagen and aggrecan released in the media were assessed.

Collagen degradation (as measured by hydroxyproline release) highlighted that cellular and acellular cartilage spontaneously released the same amount of collagen. This could be related to the strong mechanical release post-sectioning (**Figure 3.9 B.**). Aggrecan degradation (as measured by GAG release) indicated a strong release by acellular explants at the beginning of the experiment. The difference between cellular and acellular cartilage suggested that this could be related to the flash freezing process (**Figure 3.9 C.**).

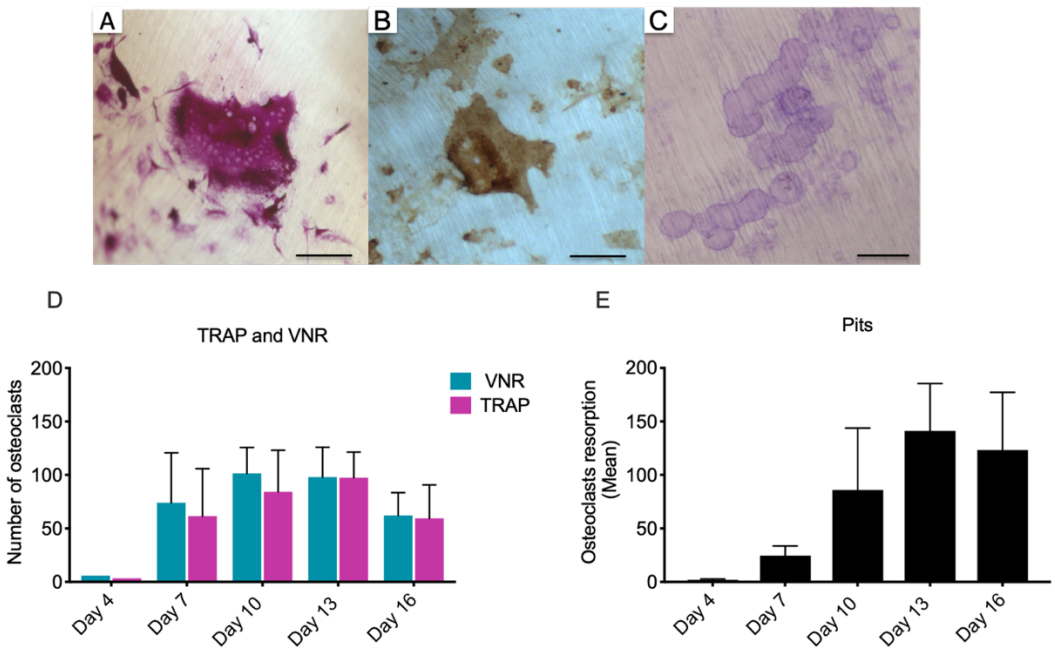


Figure 3.8 Osteoclast characterization on dentine. A. Positive TRAP staining showing large and multinucleated cells after 10 days in culture with M-CSF and RANKL. **B.** These large cells also express CD51/61 (VNR). **C.** Resorption pits produced by active osteoclasts. Bar = 100µm. **D.** Number of osteoclasts positive for TRAP and expressing VNR over time, from day 4 until day 16, n=5. **E.** Total resorbed area by osteoclasts over time, n=5.

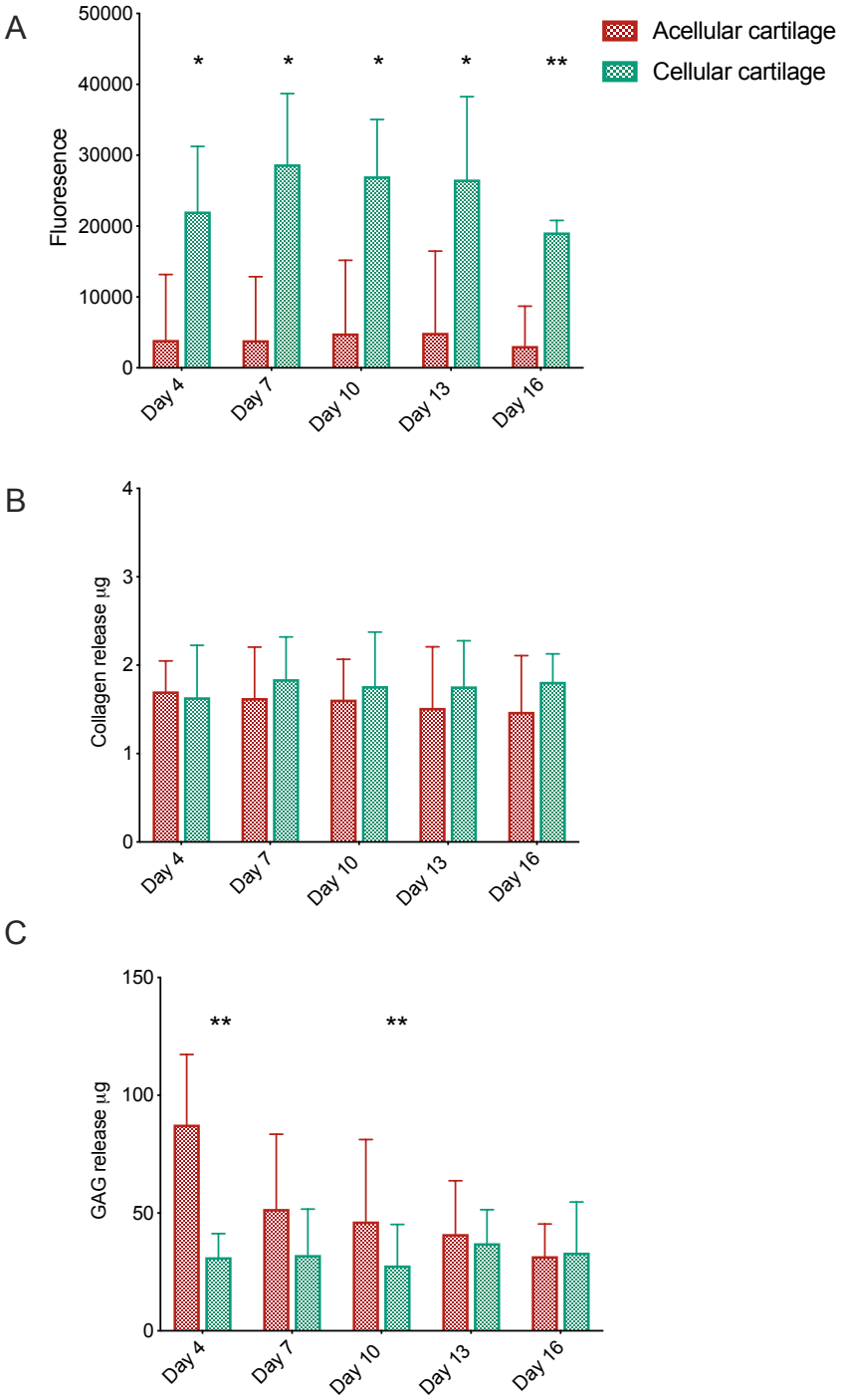


Figure 3.9 Characterization of cartilage explants used for the experiment. A. Cell viability over time tested with alamar blue assay, n=13 **B.** Collagen assay giving the total amount of collagen released in culture media, n=8 **C.** Total amount of GAG released by cellular and acellular cartilage cultured, n=8.

To evaluate the viability of osteoclasts on different substrates, monocytes were seeded on dentine, on cellular or on acellular cartilage and differentiated over 16 days (**Figure 3.10 A.**). The metabolic activity of osteoclast-dentine culture coincides with the formation and activity of osteoclasts seen on dentine (**Figure 3.8 D. and E.**). This experiment suggested that the most appropriate time was between day 7 and day 13 (**Figure 3.10 B.**).

The differentiation of monocytes into osteoclasts takes 10 days therefore, the cells at day 4 and day 7 will not all be osteoclasts. This observation suggested that starting the experiment at day 10 will assure us to mostly have osteoclasts on top of cartilage. Based on osteoclast viability and ECM degradation, and in agreement with osteoclast-dentine cultures, the analysis of osteoclast-cartilage cultures was also chosen to be conducted between day 10 and day 13.

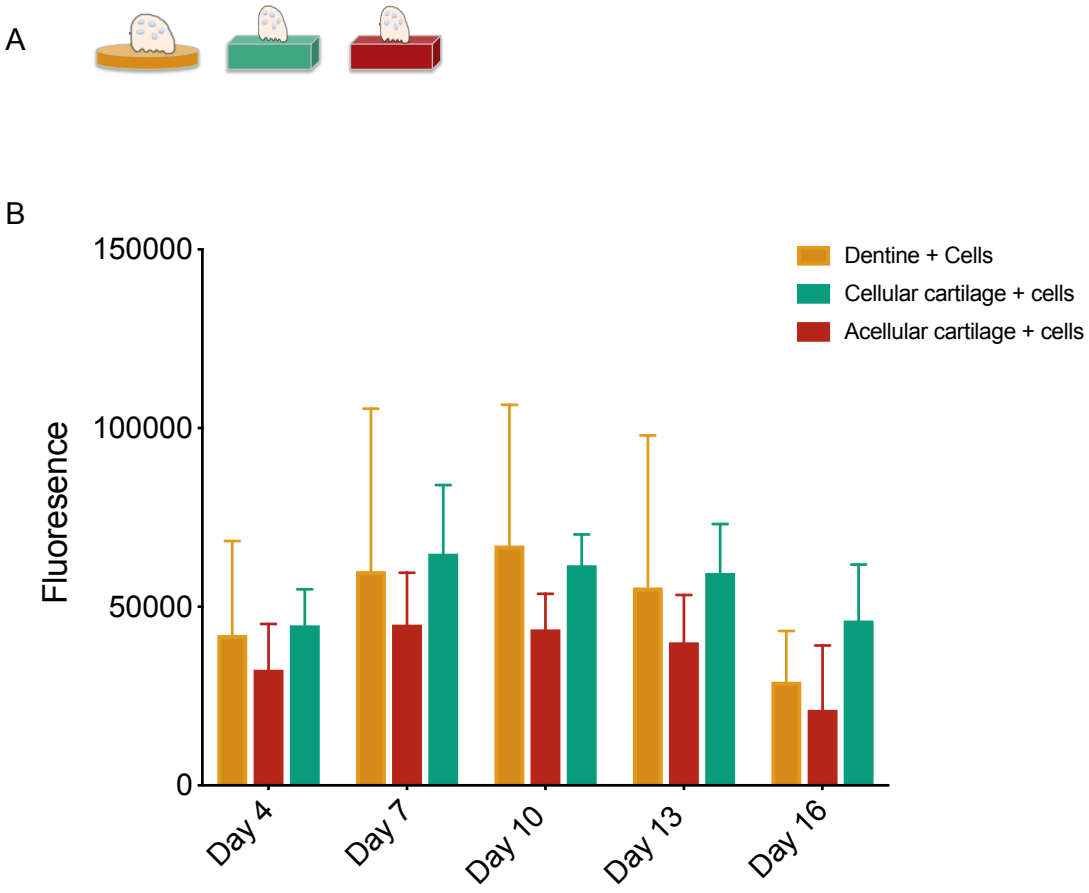


Figure 3.10 Cell viability of monocytes differentiated into osteoclasts on dentine, cellular and acellular cartilage. A. Diagram representing osteoclasts cultured on either dentine, cellular or acellular cartilage. **B.** Cell viability over time tested with alamar blue assay, n=13.

3.5.1 Increase of aggrecan release in osteoclast-acellular cartilage culture

To assess whether osteoclasts could actively degrade cartilage, the release of GAG, which is the major non-collagen component of the cartilage ECM, was measured. The experiment was repeated with 20 blood donors on cartilage samples therefore, n= 20.

The background release of GAG in the culture media declined between day 10 and day 13 (84.17 µg at day 10 and 68.9 µg at day 13, **Figure 3.11 B.**

and **C.** respectively). The average of the total amount of GAG released at day 10 was 97.74 μg in the presence of osteoclasts and 84.17 μg in the control (**Figure 3.11 B.**). In fact, 12 out of 20 osteoclast-cartilage cultures increased the total amount of GAG released at day 10. At day 13, the release of GAG was significantly increased (by 21 %) in the osteoclast-cartilage culture; the average amount was 87.18 μg compared to 68.90 μg for the control (**Figure 3.11 C.**). 15 out of 20 osteoclast preparations degraded the cartilage at day 13. Osteoclasts were therefore actively digesting cartilage and affecting the integrity of the ECM.

A large SD was seen in absence of osteoclasts at day 10 and day 13 reflecting the high inter-individual variability between cartilage donors. And as observed with collagen release and osteoclast activity on dentine, the large SD in GAG release in presence of cells demonstrated the high variability between blood donors (**Figure 3.11 B.** and **C.)**. The fold change of day 13 over day 10 did not show any difference between osteoclasts cultured on cartilage and the control (**Figure 3.11 D.)**.

The release of GAG was monitored from day 4 to day 16 during the optimisation experiments. The blood preparation and the cartilage donors were not the same as used in **Figure 3.11**. A significant increase of GAG release was seen in osteoclast-cartilage culture at day 7, day 10 and day 13 (**Appendix A.1 A.)**. Therefore, this experiment confirmed that osteoclasts were able to degrade proteoglycans**.**

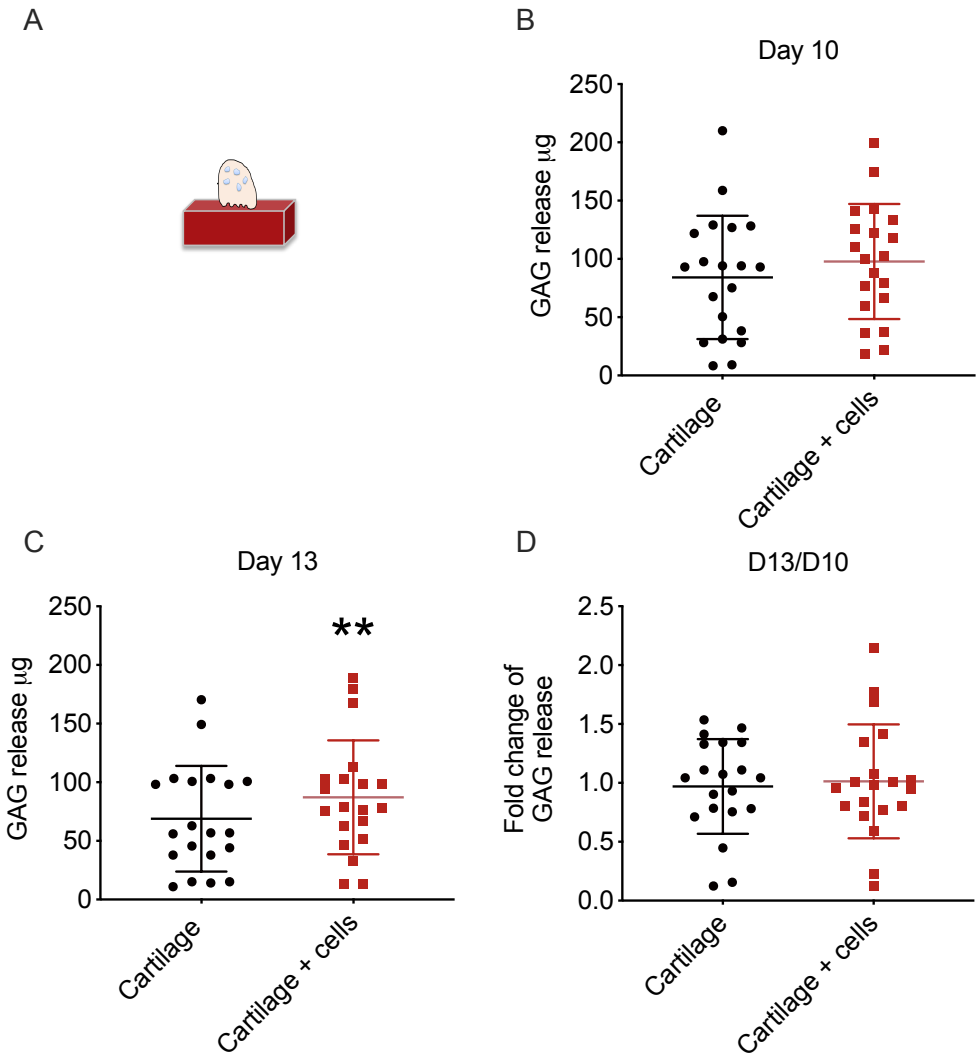


Figure 3.11 GAG release in culture media by osteoclasts on acellular cartilage at day 10, day 13 and over time. **A.** Diagram showing osteoclast on acellular cartilage. **B**. Total GAG released at day 10 by acellular cartilage compared to cartilage with osteoclasts on the surface. **C**. Total GAG released at day 13. **D**. Fold change of D13/D10. ***p*<0.001 and n= 20.

3.5.2 Type II collagen degradation by osteoclasts

To determine whether osteoclasts could degrade type II collagen contained in articular cartilage, the collagen assay was performed with osteoclasts cultured on acellular cartilage (**Figure 3.12**).

On average, 2.40 μg at day 10 and 2.43 μg at day 13 were found in the culture media with cartilage pieces. This revealed that acellular cartilage spontaneously released collagen and the amount were similar overtime. At day 10, the amount of collagen released was on average 3.01 μg in the presence of osteoclasts and 2.40 μg for the control, however the increase was not significant (p=0.074 **Figure 3.12 B.**). The average amount of collagen released in the culture media at day 13 was very similar to day 10; 2.43 μg for cartilage with osteoclasts and 3.06 μg for the control (**Figure 3.12 C.**). The fold change of collagen release between day 13 and day 10 showed that osteoclast activity did not change (**Figure 3.12 D.**)

The release of collagen from day 4 to day 16 was tested during the optimisation experiments. This experiment was also used to verify what has been observed at day 10 and day 13. Surprisingly, the data clearly show that the addition of osteoclasts on acellular cartilage resulted in a significant increase of collagen release from day 7 to day 16 (**Appendix A.1 B.**).

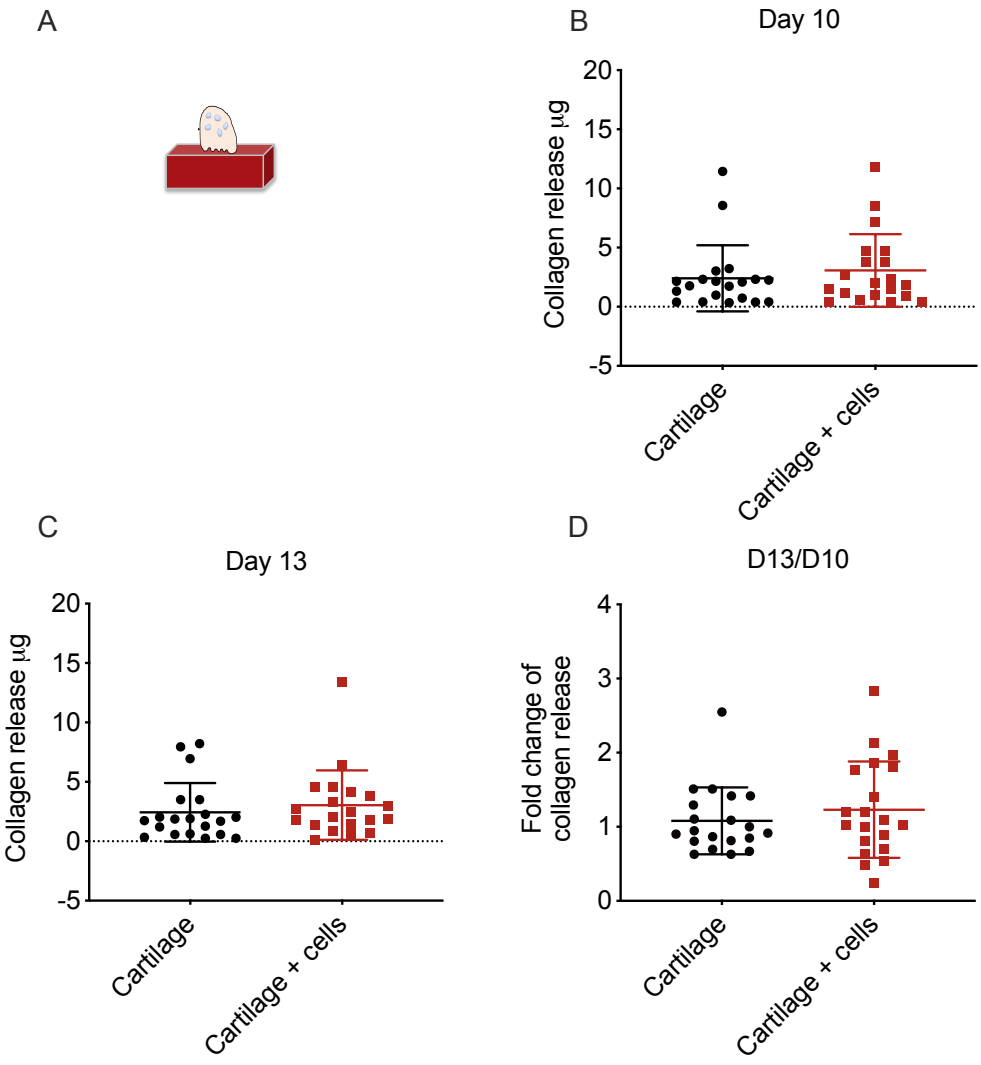


Figure 3.12 Collagen release in culture media in presence of osteoclasts on cartilage. **A.** Diagram showing osteoclast on acellular cartilage. Osteoclasts were cultured with M-CSF and RANKL. **B**. Total collagen released by acellular cartilage compared to cartilage cultured with osteoclasts at the surface. **C**. Similar to **B**. but osteoclasts were cultured for 13 days. **D**. Fold change of D13/D10, n= 20

3.5.3 Bone resorption *in vitro:* collagen release

The resorption of dentine and the biomarkers released have been extensively described before. In this project, the resorption of dentine served mainly as a validation of functional osteoclasts (**Figure 3.13 A.**). The release of the bone resorption biomarker (type I collagen) confirmed that osteoclasts

actively resorbed bone between day 10 and day 13. The GAG release was undetectable when osteoclasts were on dentine.

The presence of osteoclasts on dentines significantly increased the amount of collagen released compared to control at day 10 (**Figure 3.13 B.**) and day 13 (**Figure 3.13 C.**). The amount of collagen released at day 10 was on average 3.71 μg compared to 1.26 μg in the control, which is an increase of 66 % (**Figure 3.13 B.**). At day 13, the presence of osteoclasts increased by 77 % the total amount of collagen released. Precisely, the average of the osteoclast-free control was 1.35 μg collagen released compared to 5.93 μg when osteoclasts were on dentine (**Figure 3.13 C.**). The large increase in SD in collagen release from dentine with osteoclasts compared with the control underlines the high inter-individual variability between blood donors.

To see if osteoclasts increase or decrease their release of collagen over time, the amount of collagen released at day 13 was divided by the release at day 10. This fold change was compared to the fold change of the control. In the presence of osteoclasts, the release at day 13 was 1.7 times higher than day 10. Osteoclasts therefore remain active until day 13 (**Figure 3.13 D.**).

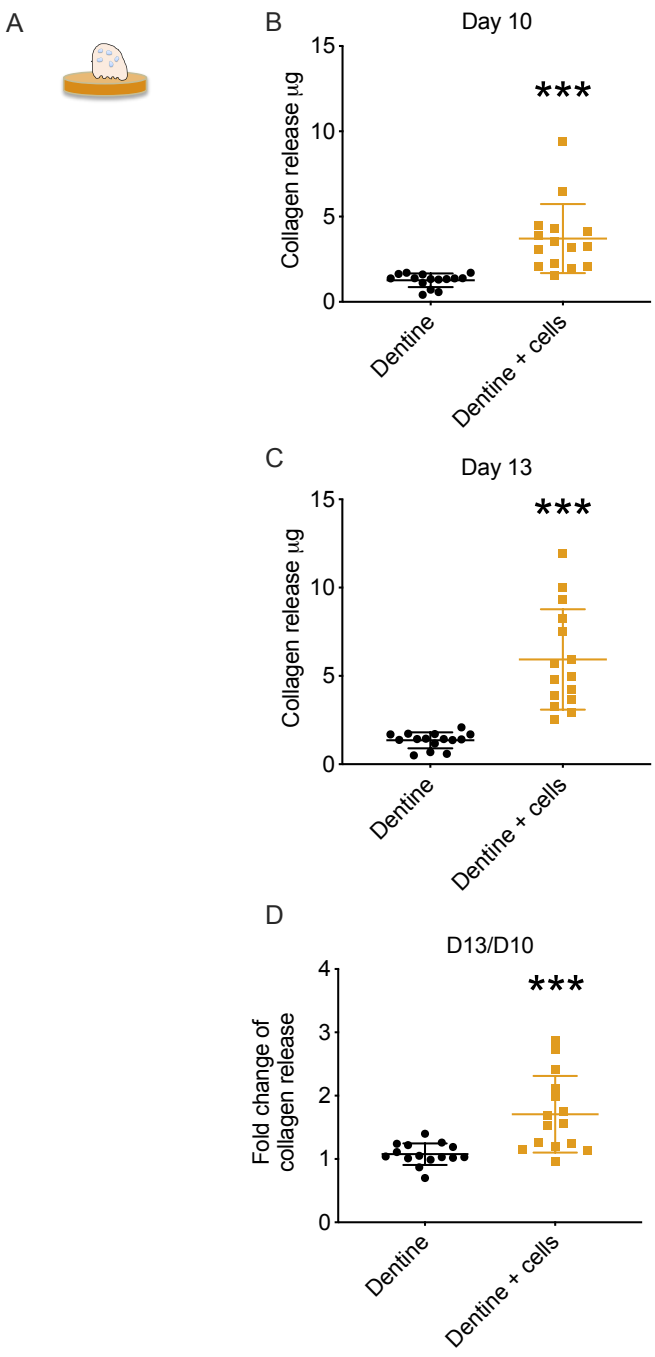


Figure 3.13 Collagen release into culture media by osteoclasts on dentines. **A.** Diagram showing osteoclast on dentine. Osteoclasts were cultured with M-CSF and RANKL on dentine. **B**. Total collagen released at day 10 by osteoclasts cultured on dentine compared to dentine without cells. **C**. Similar to **B**. but osteoclasts were cultured for 13 days. **D**. Fold change of total collagen release at day 13 over total collagen release at day 10. ***p<0.0001 n=16

3.6 Mature and active osteoclasts degrade bone and cartilage

To confirm that osteoclasts are able to degrade cartilage, mature and active osteoclasts isolated from the GCTB were used. Human GCTB-derived osteoclasts were cultured on acellular cartilage or on dentine (as positive control).

As observed with monocytes differentiated into osteoclast, the GAG release was significantly increased in present of active and mature osteoclasts (**Figure 3.14 A.**).

A significant increase of collagen was observed when osteoclasts were cultured on dentine (**Figure 3.14 B.)**. The cells were active on dentine and cartilage, the response was similar to osteoclasts differentiated from monocytes.

The number of replicates was lower than for osteoclasts differentiated from monocytes as the treatment for GCTB is generally successful and therefore few patients require a curettage.

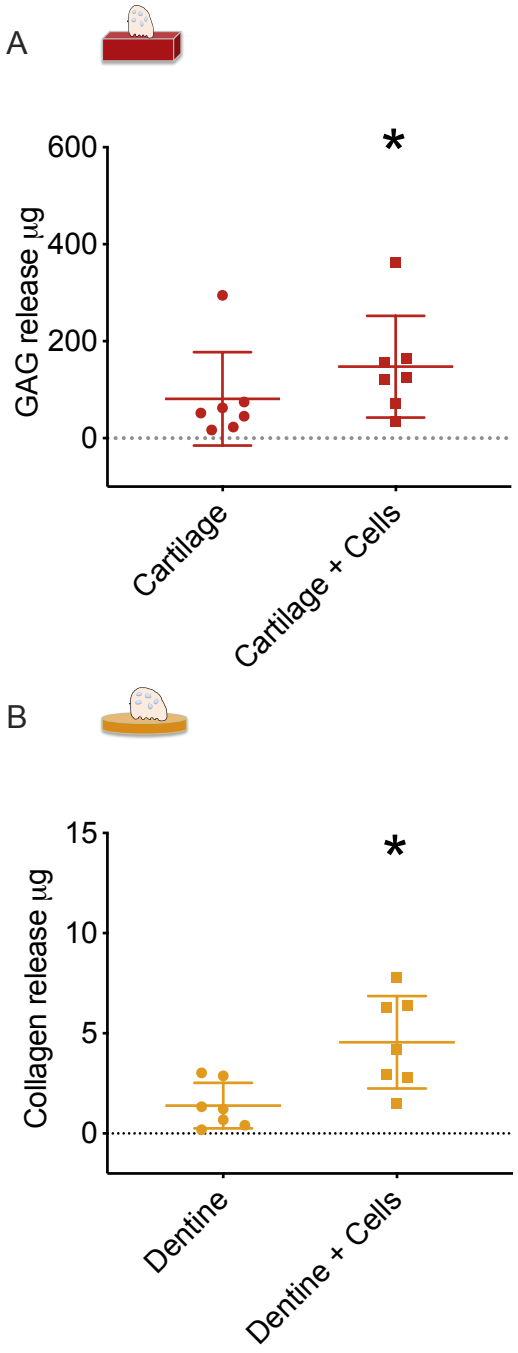


Figure 3.14 Osteoclasts isolated from GCTB cultured on dentine or cartilage. A. GAG released in culture media in presence of osteoclasts on acellular cartilage **B.** Collagen release by osteoclasts cultured on dentine *$p \leq 0.05$, n=7

3.7 Morphological and immunophenotypic characteristics of osteoclast-cartilage

culture compared with osteoclast-dentine culture

3.7.1 Osteoclasts cultured on cartilage do not have a sealing zone

To assess whether osteoclast-cartilage culture showed the same characteristics as osteoclast-dentine culture, an immunofluorescence staining of actin and the nucleus was performed. Non-degrading osteoclasts classically exhibit a podosome belt whereas active osteoclasts are polarised with a sealing zone[224].

Osteoclasts on glass, have a large podosome belt which corresponds to numerous F-actin rings arranged in layers at the cell periphery but is not considered as a sealing zone (**Figure 3.15 A.**).Osteoclasts do not degrade glass therefore they cannot be considered as active cells degrading bone or cartilage.

On dentine the sealing zone is centred and smaller compared to the podosome belt formed on glass (**Figure 3.15 B.**).

Osteoclasts on acellular cartilage did not show the formation of a podosome belt or a sealing zone (**Figure 3.15 C.**).

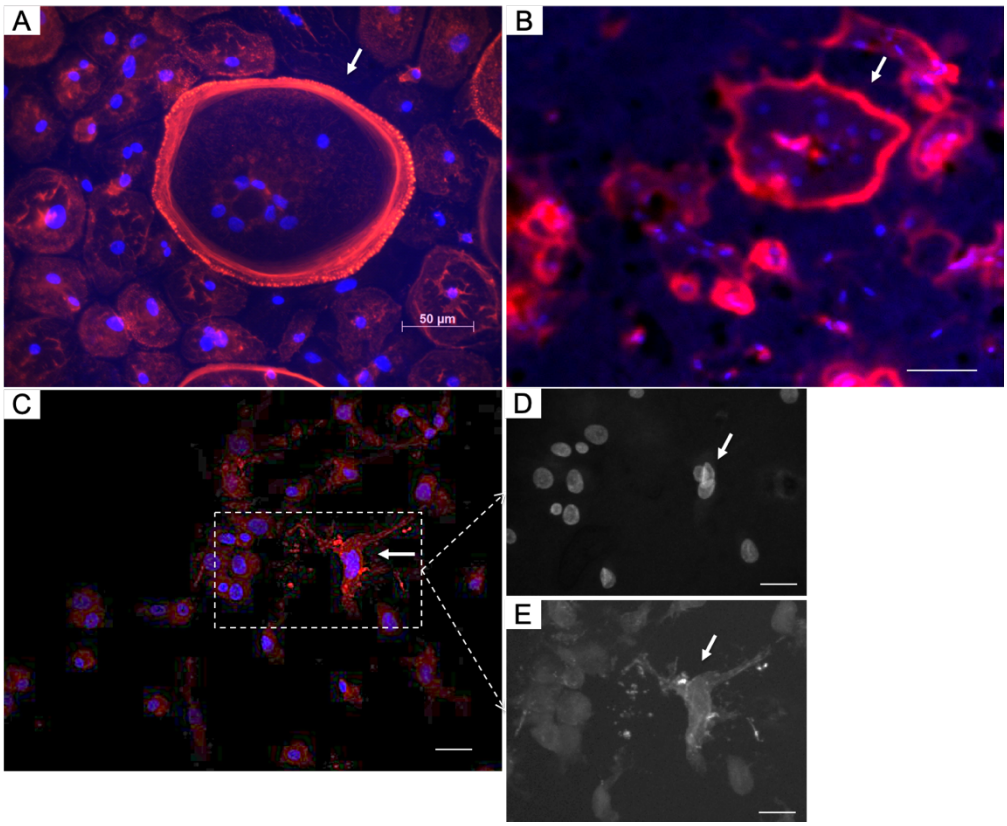


Figure 3.15 Immunofluorescence staining of actin (Phalloidin) and nuclei (DAPI) in osteoclasts on different substrates. **A.** Osteoclasts (white arrow) after 10 days in culture with M-CSF and RANKL on glass coverslips, actin (red) and nuclei (blue). Bar=50µm **B**. Osteoclasts (white arrow) cultured on dentine. **C.** Osteoclasts (white arrow) cultured on cartilage. Dotted square from **C.** in **D.** showing grey scale of the nuclei staining, white arrow indicating an osteoclast with 3 nuclei. **E.** Showing grey scale photo of the phalloidin staining, white arrow pointing the cytoskeleton of an osteoclast. Bar = 100µm

3.7.2 TRAP and VNR positive osteoclasts on articular cartilage

To validate whether monocytes were able to differentiate into osteoclasts on articular cartilage (**Figure 3.16 A.**), the differentiated cells were stained for osteoclast markers (**Figure 3.16 B.-H.**). The large cells were positive for TRAP staining and multinucleated. TRAP activity is regarded as an important cytochemical marker of osteoclasts. The cells cultured on

cartilage were large cells; 50-100 μm in diameter and also expressed the vitronectin receptor.

The similarities of cell morphology and staining between osteoclasts on dentine and on cartilage at day 10 reaffirmed the presence of osteoclasts on cartilage (**Figure 3.8** and **Figure 3.16**). The cell population on cartilage is a mix of osteoclasts and monocytes/macrophages (**Figure 3.16**); monocytes / macrophages are positive for TRAP staining but are not positive for VNR staining.

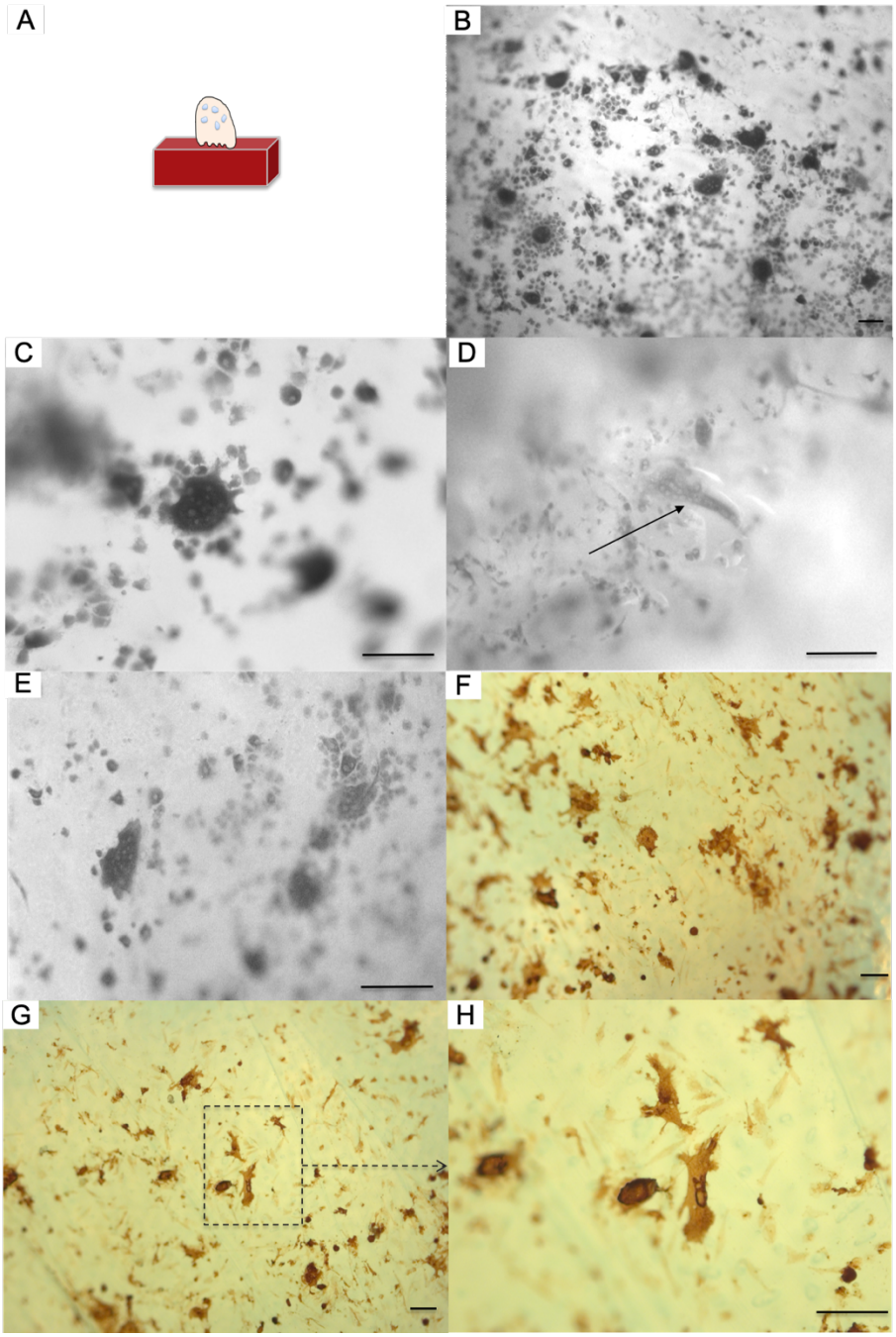


Figure 3.16 Monocytes can differentiate into osteoclasts on cartilage. **A.** Diagram representing osteoclasts cultured on acellular cartilage. **B.** Low magnification of positive TRAP staining showing large and multinucleated cells after 10 days in culture with M-CSF and RANKL on cartilage. **C.-E.** Additional examples of TRAP positive osteoclasts at higher magnification. Black arrow: multinucleated osteoclast. **F.-H.** Osteoclasts expressed CD51/61 (VNR) after 10 days in culture with M-CSF and RANKL. **G.** dotted square magnified in **H.** Bar = 100µm.

3.7.3 Osteoclasts degrading articular cartilage matrix *in vitro*

While dentine could be cut precisely with a diamond saw, the cartilage had to be cut with a scalpel before the experiment so could never provide a flat piece of cartilage, preventing us increasing the magnification. To bypass this issue and to observe the matrix surrounding and under the osteoclasts, osteoclasts-cartilage explants were observed by SEM.

Chondrocytes embedded in the cartilage matrix gave an undulating surface (red arrows in **Figure 3.17 A.** and **B.**) in the absence of osteoclasts. Osteoclasts on cartilage were large (120 μm diameter) and spherical (**Figure 3.17 C.-E.**). The undulating cartilage surface was visibly damaged around the osteoclasts, confirming that osteoclasts are able to degrade cartilage bone matrix (yellow arrows in **Figure 3.17 D.** and **E.**).

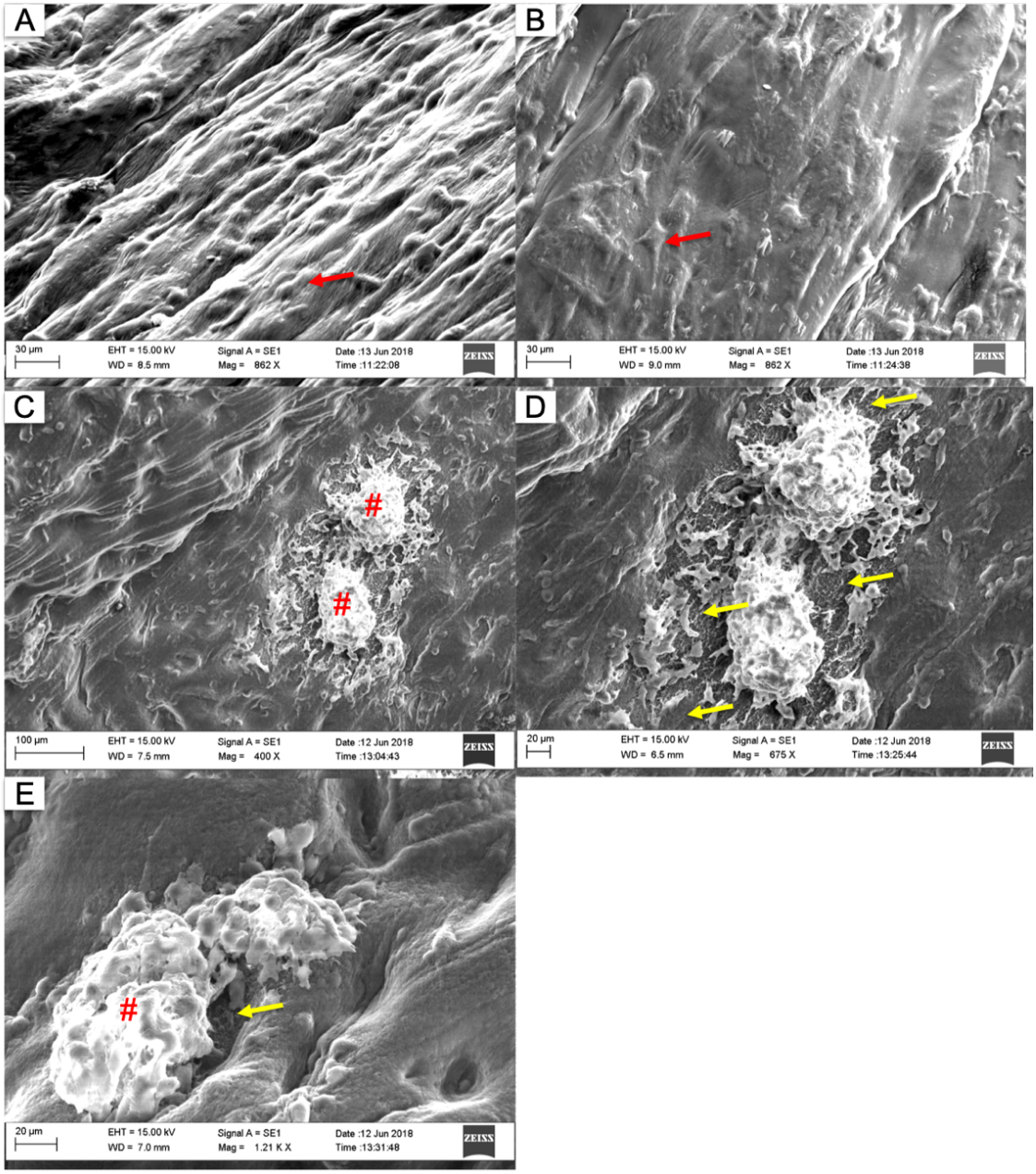


Figure 3.17 SEM images of osteoclasts on cartilage. **A.** and **B.** Acellular cartilage without osteoclasts showing chondrocytes (←) **C.** Osteoclasts (#) cultured on degrading cartilage after 10 days in culture with M-CSF and RANKL. **D.** Higher magnification of **C. D.** and **E.** Additional example of osteoclast (#) degrading the surrounding cartilage matrix (←) at high magnification.

Normally, osteoclasts degrade the bone matrix in the resorption pit formed beneath the cell. Whether osteoclasts form resorption pits to degrade cartilage remains unknown. To examine this question, osteoclasts on cartilage were cross-sectioned (**Figure 3.18 A.**) The pictures **B.**, **C.** and **D.** were taken from the pilot experiment; to find the side on which osteoclasts were, the cartilage was stained for TRAP before being embedded. Tissue sections were then stained for H&E therefore, the double staining of the tissue caused a dark staining of the cells (**Figure 3.18 B.-D.**).

A magnified TRAP-positive osteoclast with 6 perceptible nuclei reasserted the presence of osteoclasts on the surface of cartilage (**Figure 3.18 D.**). Also, the proximity with a monocyte (black arrow) reaffirmed that osteoclasts are large cells (**Figure 3.18 E.**)

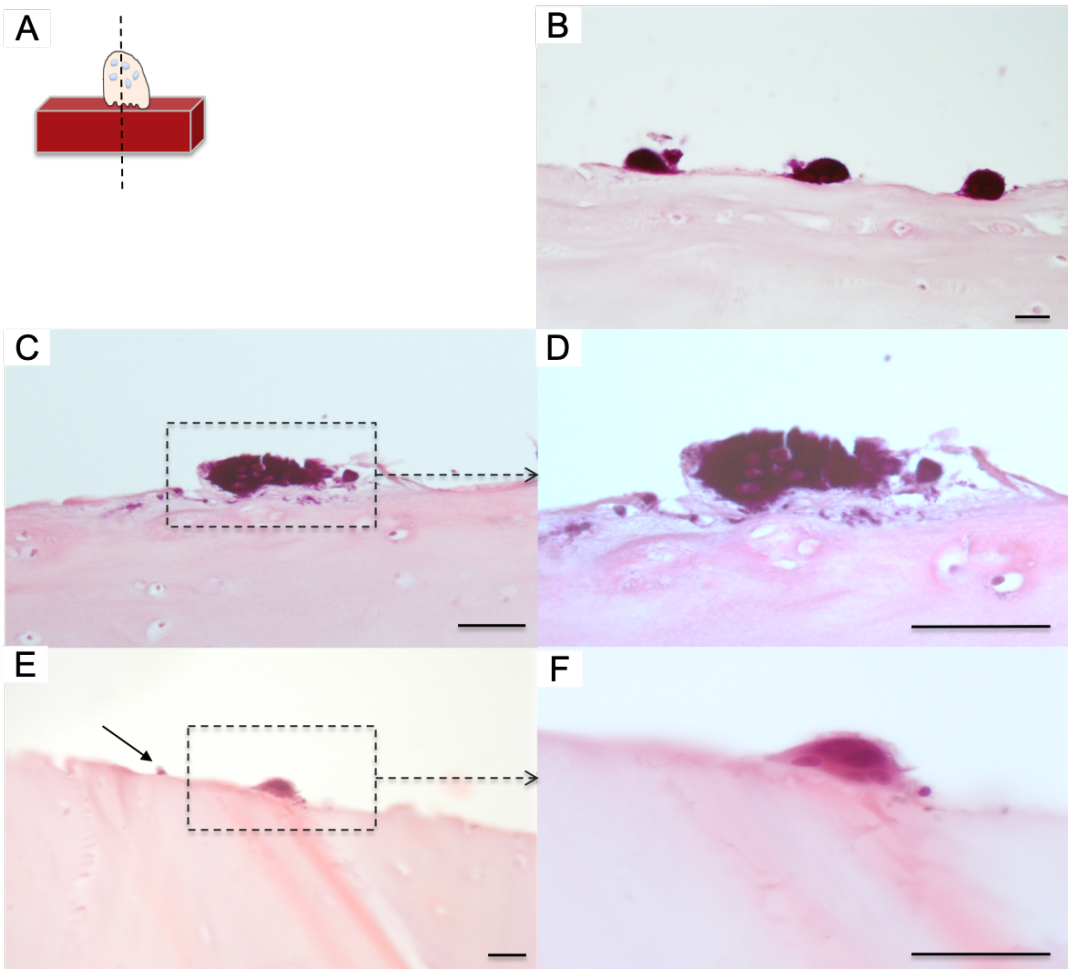


Figure 3.18 Transverse sections of osteoclasts degrading cartilage *in vitro*. A. Diagram showing osteoclasts on cartilage and how samples were sectioned. **B.** Cross-section of osteoclasts degrading cartilage after 10 days in culture with M-CSF and RANKL. **C.-E.** Additional examples of osteoclasts degrading cartilage. **C.** dotted square magnified in **D.** and **E.** Osteoclast on cartilage with a monocyte (←), dotted square magnified in **F.** Bar = 100μm.

3.7.1 Osteoclasts resorbing bone *in vitro*

Osteoclasts on dentine were imaged using SEM to compare their morphology with osteoclasts on cartilage.

Osteoclasts on dentine were readily identified by their large size and broad cytoplasmic extensions (Red circles in **Figure 3.19**). Osteoclasts were

approximatively 100 µm in diameter compared to 13 µm for a monocyte (**Figure 3.19 A.**) Lacunar resorption pits can be occupied by osteoclasts and are located under the cells (**Figure 3.19 B. and C.**). The osteoclasts are observed at the head of a tunnel formed by the resorption of the bone matrix. (**Figure 3.19 A.-D.**; **D.** at lower magnification).

Osteoclasts grown on cartilage did not form a degradation track as seen on dentine (**Figure 3.19**).

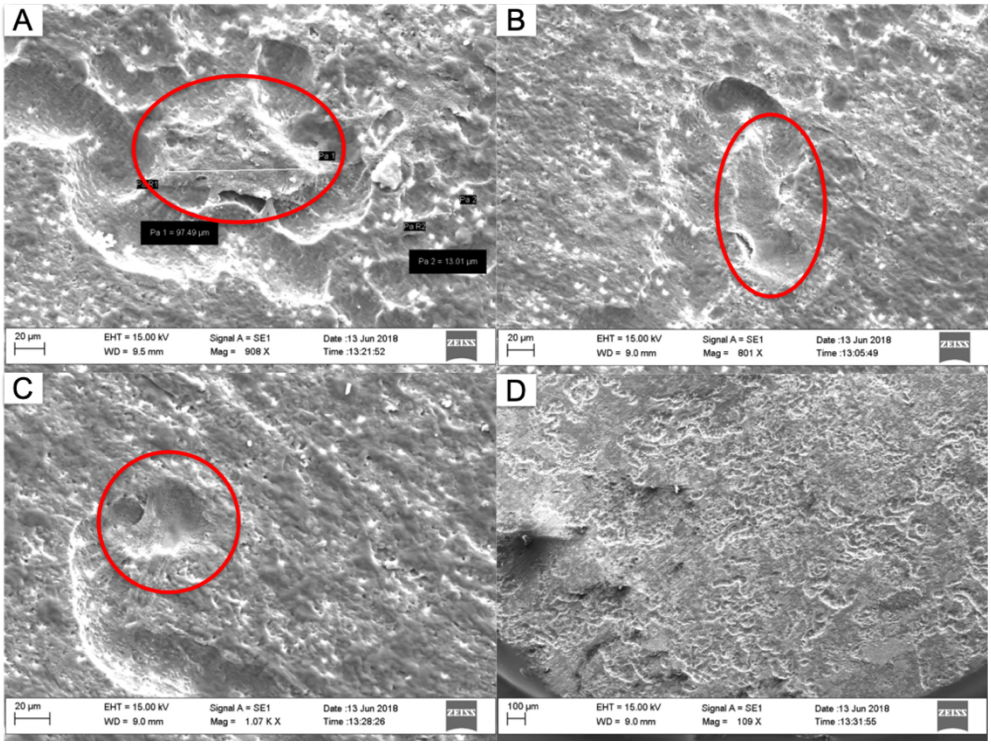


Figure 3.19 SEM images of osteoclasts on dentine. **A.** Osteoclast (red circle) resorbing bone matrix after 10 days in culture with M-CSF and RANKL. **B.** and **C.** Additional examples of resorption pit with flat osteoclasts. **D.** Lower magnification showing the degradation of the bone matrix.

To confirm the presence of resorption pits under osteoclasts cultured on dentine the cells and their substrates were embedded in paraffin, cross-

sectioned and stained with H&E (**Figure 3.20Figure 4.12 A.**). Multinucleated osteoclasts with a resorption pit underneath were recognisable on dentine (**Figure 3.20 B.**). Abandoned regions of resorbed bone matrix were also noticeable (black arrows); highlighting that osteoclasts can migrate to resorb another region of the dentine (**Figure 3.20 B.** and **C.**).

The cartilage beneath the osteoclast did not show the resorption pits seen in dentine where the cell body occupied the space underneath (**Figure 3.18 D.** and **F.**). This difference suggests that osteoclasts do not degrade cartilage matrix in the same way as bone matrix.

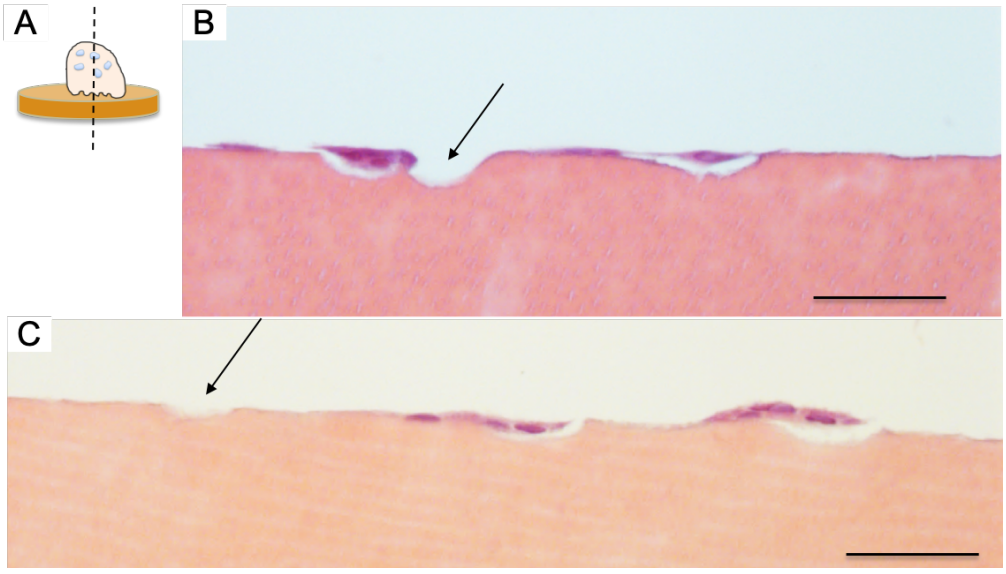


Figure 3.20 H&E transversal section of active osteoclasts on dentine. **A.** Diagram showing osteoclasts on dentine and how samples were sectioned. **B. and C.** Representative cross-sections of osteoclasts degrading dentine after 10 days in culture with M-CSF and RANKL. Bar = 100µm.

3.7.2 The expression of osteoclasts markers varies depending on the substrate

To evaluate the impact of the substrate on gene expression, a RT-qPCR comparing 5 genes (*TRAP, V-ATPase, CA2, CLCN7* and *STAT3*) known to be expressed in active osteoclasts was performed with osteoclasts cultured on dentine and cartilage. Since the morphology of osteoclasts was not the same when osteoclasts were on plastic, we decided to study the gene expression profile of these osteoclasts.

None of the osteoclasts markers have shown a difference however, the expression of TRAP was almost significantly decreased in osteoclast-dentine culture compared to osteoclasts on plastic ($p=0.0879$, **Figure 3.21 A.**).

At the same time, the expression of the two proteolytic enzymes used by osteoclasts to degrade the organic bone matrix; cathepsin K (*CTSK*) and *MMP9* was tested. Surprisingly, the expression of *CTSK* by osteoclast on dentine was significantly decreased compared to osteoclasts on plastic. Comparably, *MMP9* expressed in osteoclasts on dentine and on cartilage were significantly decreased compare to osteoclasts on plastic (**Figure 3.21 B.**). However, no differences were seen between osteoclast-dentine and osteoclast cultured on cartilage for the expression *CTSK* and *MMP9*.

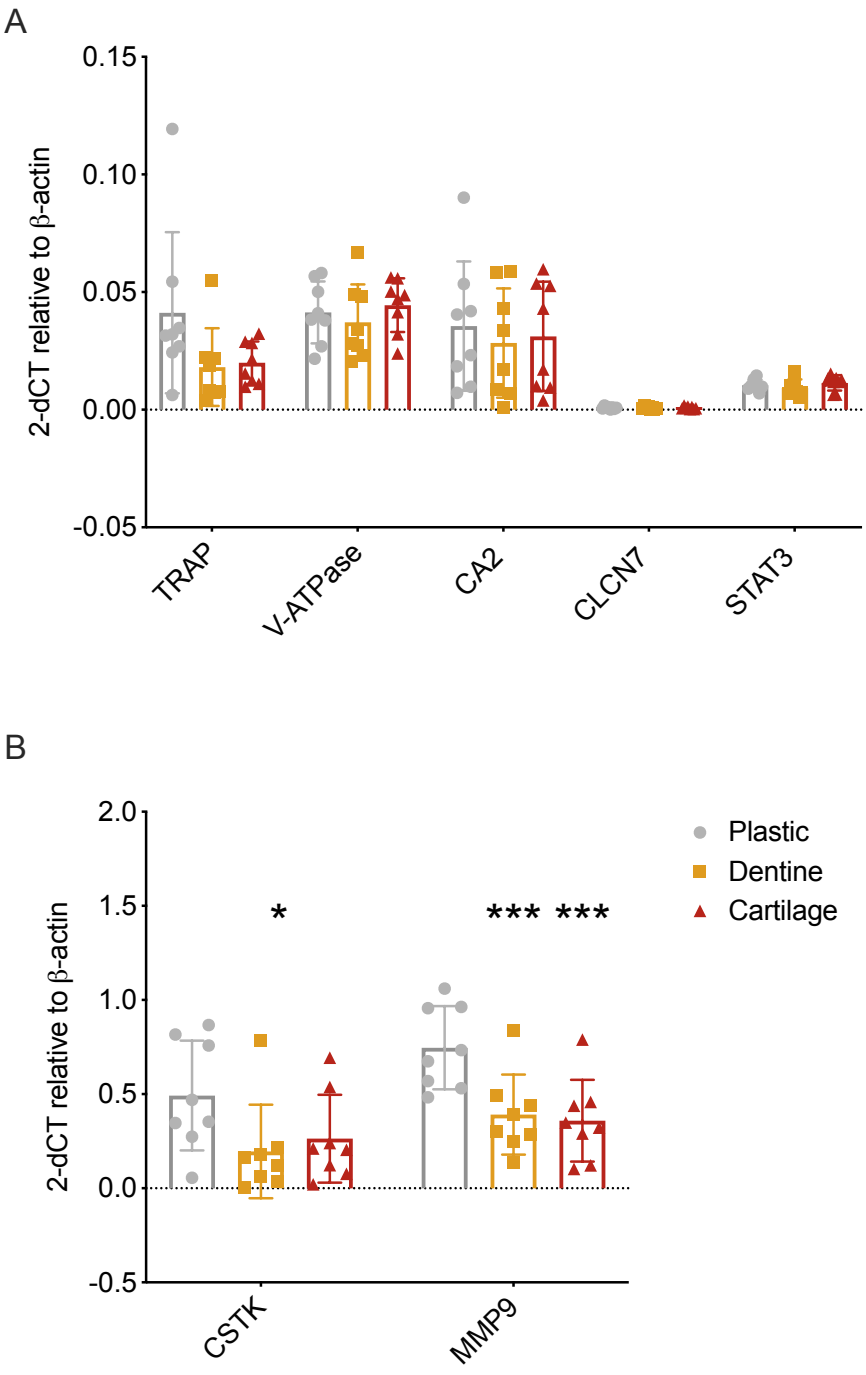


Figure 3.21 RT-qPCR of classical osteoclast genes expressed by osteoclasts on plastic, dentine or cartilage. A. Individual mRNA expression relative to β-actin of osteoclasts cultured on plastic, dentine or cartilage. Osteoclast markers: *CA2*: calcitonin receptor, *STAT3*: Signal Transducer and Activator of Transcription 3 **B.** Two important proteolytic enzymes expressed by osteoclasts to degrade organic bone matrix. Expression relative to β-actin, *CTSK*: Cathepsin K * $p<0.05$, ***$p<0.0001$ for comparison against osteoclasts on plastic n= 8.

DISCUSSION

Osteoclasts in contact with cartilage in many joint diseases suggests they play a direct role in the pathophysiology of the joints. How and why osteoclasts are in contact with cartilage is poorly understood. Once osteoclasts are in proximity with cartilage, they can degrade the ECM as we have shown in this chapter.

Osteoclasts in contact with cartilage were seen in GCTB, osteosarcoma, and osteochondroma and other skeletal tumours with multinucleated osteoclasts were observed such as chondroblastoma and chondromyxoid fibroma. It is considered that osteoclasts confer the aggressiveness of the tumours and therefore only anti-osteolytic drugs inhibit the expansion of the tumour. Osteoclasts expressing high levels of TRAP have previously been seen at the site of tumour infiltration in osteosarcoma[225]. This thesis also confirms previous studies where osteoclasts are present in cartilage of inflammatory (RA) and non-inflammatory (OA) arthritis. Gravallese et al proposed that the space formed by osteoclast-mediated degradation of the cartilage enhances the invasion of the pannus in RA, leaving the cartilage directly exposed to cytokines and matrix-degrading enzymes[202]. Despite the reporting of osteoclasts within cartilage in multiple joint diseases, their role in regulating cartilage turnover and degradation is poorly understood.

Osteoclasts on cartilage had the same morphology to those on dentine; the cells were large, multinucleated and expressed the same markers; TRAP and vitronectin receptor (**Figure 3.22**). A distinct actin sealing zone was

clearly seen when osteoclasts were on dentine. The sealing zone delimits the ruffled border membrane from which osteoclasts secrete protons. To demonstrate that minerals are essential to induce the formation of the sealing zone, Saltel et al cultured osteoclasts on coverslips covered half with apatite and half with glass. Podosomes were observed on the glass whereas the sealing zone was observed on the mineralised surface[226]. The absence of a sealing zone in osteoclasts on cartilage is probably due to differences in the mechanical, physical and chemical properties of acellular cartilage compared to dentine (**Figure 3.22**).

SEM pictures and the cross-section of osteoclast-cartilage culture did not clearly show the presence of a resorption pit, even though evidence of cartilage degradation was evident by SEM. Without a sealing zone, the ruffled border cannot be formed and therefore no resorption pit will be seen.

Chambers et al reported that rabbit osteoclasts formed resorption pits on slices of human femoral cortical bone but not on demineralised bone suggesting that osteoclasts do not polarise in the absence of minerals[227]. In line with this observation, two studies revealed that osteoclasts sitting on cartilage *in vivo* have a less visible ruffled border; in human osteoclasts in RA[27] and young rat osteoclasts degrading cartilage[37]. Therefore, we can suppose that the presence of minerals is necessary to induce the formation of the sealing zone.

Suzumoto et al highlighted that structural differentiation and functions of osteoclasts differed depending on their microenvironment. Mouse bone marrow-derived macrophages were cultured on bone, decalcified bone or

cartilage slices from rabbit. After the differentiation of the cells into osteoclasts, the slices of tissue were observed by SEM and TEM. Osteoclasts cultured on cartilage and decalcified bone did not show a ruffled border[223]. The absence of a ruffled border and a sealing zone suggests that acidification is not necessary to degrade cartilage.

A RT-qPCR for the genes known to be expressed in active osteoclasts were compared with osteoclasts on plastic, dentine and cartilage. The expression of calcitonin receptor (*CA2*) and signal transducer and activator of transcription 3 (*STAT3*) were equally expressed in osteoclasts on any of the substrate. *V-ATPase* and *CLCN7* are the two essential proteins for bone resorption and their gene expression was not different from osteoclast on plastic or on cartilage. These observations revealed that first, osteoclasts formed in each culture condition expressed those genes and that not all the genes expressed by osteoclast depend on the surface. The mechanical properties of the ECM alongside its specific components could influence the structural and functional organization of cells. Saltel et al and this thesis demonstrated the absence of the sealing zone when osteoclasts are on non-physiological surfaces like plastic or glass.

Cathepsin K (*CTSK*) and *MMP9* were significantly decreased in osteoclasts on dentine and osteoclasts on cartilage compared with osteoclasts on plastic (**Figure 3.22**). This highlights the ability of the osteoclasts to modify their gene expression according to the surface on which they are. Cathepsin K and MMP-9 drive the degradation of the organic bone matrix in parallel with the reduction of local pH to remove the minerals. Plastic is not

a physiological substrate for osteoclasts, and it is possible that osteoclasts increased the expression of cathepsin K and MMP-9 to attempt to degrade plastic substrate. But once the cells are on dentine or cartilage the resorption of the organic matrix is successful and higher expression of these proteinases is not necessary. Kleinhans et al have shown that the expression of osteoclast-specific markers was not affected when osteoclasts were cultured on plastic compared to bone[229]. The markers used were cathepsin K and VNR which is an integrin mediating the strong adhesion of the osteoclasts to bone tissue. They found that VNR was stained in osteoclasts on plastic but was not located at the periphery of the cells as seen in osteoclasts on bone. Moreover, the cells cultured on plastic were smaller and did not have a sealing zone. This, in combination with this thesis implies that different substrates influence both the morphology and function of osteoclasts, but it is unknown how osteoclast recognizes bone or cartilage as appropriate for resorption and degradation. The inhibition of vitronectin inhibited *in vivo* and *in vitro* bone resorption[230–232] and Fuller et al have shown the structural rigidity was not enough to induce resorptive behavior. In fact, they demonstrated that VNR was sufficient to induce osteoclasts to form the podosome belt on glass, to secrete enzymes and to form sealing zone and ruffled border on bone[233].

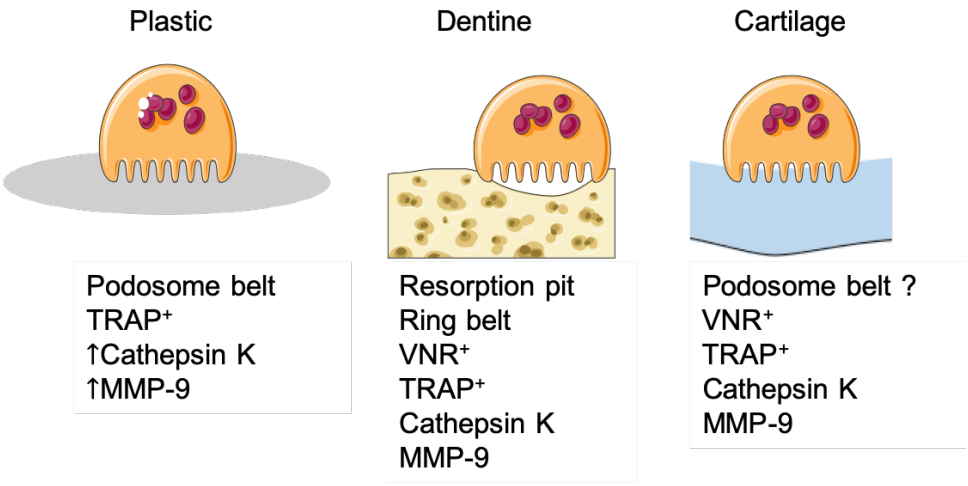


Figure 3.22 Summary of the particularities of osteoclasts cultured on plastic, dentine and cartilage.

As observed by Knowles et al osteoclast-cartilage culture significantly increased the GAG release compared to cartilage alone[188]. Proteoglycans are degraded mostly by MMPs and ADAMTSs. The mechanism by which osteoclasts degrade proteoglycans will be explored in chapters 4 and 5.

In this thesis, the collagen assay was almost significant ($p=0.07$ with $n=20$) while the overtime collagen release showed a significant increase at day 7, day 10 and day 13 ($n=8$). These results revealed that the mechanism of cartilage degradation targeted primarily the proteoglycans but also collagen to a lesser extent. Lofvall et al used another biomarker to measure the collagen degradation when osteoclasts were on articular cartilage. Collagen type II degraded by MMPs (C2M) is a metabolite of MMP-mediated collagen type II degradation. The articular cartilage is composed mainly of type II collagen and large proteoglycans (mainly aggrecan) surrounding the cells. Cartilage contains also type IX and X collagen. Their data clearly showed that the addition of osteoclasts resulted in an increase of C2M release. Considering

their results, it is possible that the technique used in this thesis was not adapted and sensitive enough to detect the collagen. The particularity of the hydroxyproline assay is to detect degradation of any type of collagen hence the assay was selected as it could be used for osteoclasts on dentine or on cartilage.

Studying osteoclasts and cartilage was challenging to optimise and matching the arrival of cartilage tissue and blood was logistically complicated. Osteoclasts were cultured for 13 days and the amount of cartilage tissue from total knee arthroplasty (TKA) was variable. The cartilage tissue removed from the extremity of the bone was cut into pieces. The amount of minerals could not be exactly the same between the cartilage pieces and could therefore modify the resorbing behaviour of osteoclasts. Additionally, the distance between damaged cartilage and where the pieces were taken may vary leading to further variability in osteoclast activity due to accessibility of already damaged ECM. The high inter-individual variability of blood donors and cartilage required many repeats for statistical significance. Imaging osteoclasts on uneven surfaces was also limited as the thickness of specimens meant it was not possible to take high magnification pictures. Developing a new technique to cut and sterilise the cartilage should be considered to decrease the risk of contamination from the surgery. For example, Suzumoto and Lofvall stored the slices in 70 % ethanol after sectioning[185,223]. However, it will be important to confirm that GAG and collagen release are stable by day 10 until day 13 and confirm that 70 % ethanol would penetrate into the cartilage and not affect later the activity of

osteoclasts. The staining of the actin ring could be further optimized according to the substrate on which the cells are cultured. For example, the thickness of the cartilage pieces and the opacity of the dentine were a problem and their autofluorescence limited the staining. Treating the substrates with Sudan Black B after fixation might effectively suppress autofluorescence.

In this chapter, the hydroxyproline assay confirmed that osteoclasts were able to degrade type I collagen present in dentine. Dentine is made from dentinal tubules embedded in a mineralized matrix of type I collagen. However, the degradation of collagen contained in cartilage was not detected accurately. This lack of reproducibility when osteoclasts were cultured on cartilage lead us to cease this assay. ELISA assays for CTX-I and CTX-II could have been used. This assay quantifies the amount of human cross-linked C-telopeptide of type I and type II collagen, respectively. This assay is sensitive but according to the volume of the experiment, it was not cost effective for this project. Lindstrom et al cultured human osteoclasts on slices of osteochondral junction from OA patients, the concentration of CTX-I was increased in the presence of osteoclasts (nM) and CTX-II was also increased but the detection range was in pM[234]. The small amount of type II collagen that Lindstrom detected, the lack of sensitivity of hydroxyproline at low concentrations and its day-to day variability may explain why collagen degradation was difficult to measure. The experiment was run with more than 6 blood donors each time to overcome the experimental variability. Another limitation of the hydroxyproline assay was the detection of other types of

collagen in the samples; it was impossible to know the type of collagen that was detected.

CONCLUSION

Sections of bone and articular tissue from different joint pathologies showed osteoclasts in direct contact with cartilage. The capacity of osteoclasts to differentiate from PBMCs on cartilage has been demonstrated, as well as their ability to degrade cartilage proteoglycans and collagen. It is therefore important to elucidate mechanistically how osteoclasts degrade the ECM of the cartilage. This could have implications for treating a range of joint pathologies with cartilage phenotypes.

Chapter 4

OSTEOCLASTS USE MMPS TO DEGRADE CARTILAGE AND CONTACT WITH THEIR SUBSTRATE IS ESSENTIAL

INTRODUCTION

In this chapter the mechanisms by which osteoclasts degrade cartilage were investigated and compared to those used in bone resorption. Transwell experiments were performed to determine whether the effect of osteoclasts on cartilage degradation was due to direct contact with the substrate or to the release of paracrine factors. Osteoblasts and osteoclasts can communicate with each other through direct cell-cell contact or by the release of cytokines[235]. Osteoblasts can affect osteoclast formation, differentiation and activity through several pathways. Osteoclast and chondrocyte transwell and co-culture were used to investigate if these cells could also interact and modify their functions.

4.1 Acidification by V-ATPase

Bone resorption by osteoclast is often described in two phases; the inorganic degradation which corresponds to the destruction of hydroxyapatite crystals and the organic phase which consists of degrading type I collagen and other bone proteins. Bone resorption is dependent on the ability of osteoclasts to form a sealing zone and a ruffled border where local acidification occurs. More precisely, hydrogen and chloride ions are transported into the lacunae to form hydrochloric acid. The protons are pumped by the V-ATPases across the ruffled border whereas the chloride ions are transported via the chloride channel 7 (CLCN7)[236]. The reduction of the pH in the lacunae resorption pit dissolves the hydroxyapatite crystals releasing the organic matrix.

Bafilomycin, first isolated from bacteria in 1983, is frequently used to inhibit the V-ATPase in osteoclasts *in vitro*. Therefore, protons cannot be transported to the resorption lacunae and in the absence of acidification, the hydroxyapatite minerals are not dissolved[237]. Inhibiting CLCN7 also blocks the resorption of bone[238].

4.2 Cathepsin K

After the solubilisation of the hydroxyapatite crystals, proteolytic enzymes are secreted into the resorption lacuna and are subsequently activated by the low pH. Both cathepsin K and MMPs have been shown to play roles in this process. Cathepsin K can cleave the native triple helix of collagen at multiple sites[239], enabling the triple helix to unwind and become available for degradation by proteinases with gelatinolytic activity. Pycnodysostosis is a rare skeletal dysplasia caused by a mutation in the gene coding for cathepsin K. This disease is characterised by high bone mass and bone abnormalities such as short stature and skull deformities[240]. Cathepsin K deficient osteoclasts can demineralise bone but cannot degrade the type I collagen matrix. Similarly, cathepsin K knockout mice show deficient bone resorption resulting in a strong osteopetrotic phenotype in long bones. In contrast, overexpression of cathepsin K in mice results in accelerated turnover of metaphyseal trabecular bone[241]. E64 is an irreversible and highly selective cysteine protease inhibitor that was first isolated from Aspergillus japonicus in 1978. E64 can inhibit peptidases including papain, cathepsin B, cathepsin L and cathepsin K. E64 is not used clinically since more selective cathepsin

inhibitors have been developed. Neutzky-Wulff et al showed that the inhibition of cathepsin K reduced by 80 % the degradation of type I collagen.

4.3 MMPs

The fact that not all collagenase activity is removed in Pycnodysostosis indicates that other proteinases are able to solubilise bone collagen. Everts et al cultured calvariae and long bone pieces from mouse explants with proteinase inhibitors. MMPs were shown to be essential for the removal of collagen and this removal was a prerequisite for deposition of new matrix in the resorption lacunae[242]. Later the same group suggested that the roles of MMPs differed dependent on whether the osteoclasts were degrading flat or long bones[243]. Furthermore, Neutzky-Wulff et al observed that inhibiting both cathepsin K and MMPs completely abrogated the degradation of type I collagen. The MMP inhibitor used was a broad-spectrum inhibitor called ilomastat, GM6001 or galardin. It is a reversible inhibitor that forms a complex with the critical active-site zinc. Adding only GM6001 significantly reduced type I collagen degradation but did not decrease osteoclast viability or number. The type of MMP involved in bone degradation is not well known but MMP-9 is the most abundant MMP in bone[241].

4.4 Interaction between bone and cartilage

In RA the pannus directly infiltrates joint tissues contributing to loss of articular cartilage and bone. Degradation of cartilage and bone ECM is a

result of the activation of a cascade of molecular pathways which terminates in the production of matrix-degrading enzymes. Therefore, interaction between immune and stromal cells from the pannus, cartilage and bone with each other and the ECM is evident. Proinflammatory cytokines (e.g. TNF-α, IL-1β, IL-17) expressed in RA increase RANKL synthesis by cells of the pannus such as synovial fibroblasts, B and T cells. Kong et al showed that activated T cells regulate bone loss and joint destruction in adjuvant arthritis in the rat. They demonstrated that activated T cells could induce osteoclastogenesis through increased expression and secretion of RANKL. Rats with arthritis had a complete erosion of cartilage and a destruction of underlying bone plate. Rats treated with the RANKL inhibitor, OPG, exhibited minimal loss of cortical bone lesions compared to untreated arthritic bone but surprisingly, OPG also preserved the integrity of cartilage. Therefore, RANKL expressed by T cells can affect cartilage and bone integrity. Whether OPG protects the cartilage indirectly by decreasing the number of osteoclasts or has a direct effect on cartilage maintenance is not clear[152].

RANKL expression has been localised in the extracellular matrix of subchondral bone and cartilage in human OA. Martinez-Calatrava et al showed that in rabbit models of antigen-induced arthritis or meniscectomy-induced OA RANKL expression was higher in OA compared to healthy cartilage and RANKL expressed by chondrocytes diffused from articular cartilage to subchondral bone[244]. Cytokines other than RANKL can diffuse through cartilage; for example, hepatocyte growth factor (HGF) is localised

in the deep zone of articular cartilage, the calcified cartilage and the subchondral bone. However, chondrocytes do not express HGF and Guévremont et al showed that HGF is synthesised by osteoblasts in the subchondral bone with OA. Therefore, this factor diffuses to the cartilage region and can regulate cartilage homeostasis and repair in early OA[245,246]. *In vitro*, small molecules can also perfuse between bone and cartilage (see section 1.6.2.1). Importantly, these experiments highlight the diffusion of RANKL and other factors through the bone-cartilage interface both *in vitro* and *in vivo*.

4.4.1 Communication between osteoblasts and chondrocytes *in vitro*

Cellular communication between chondrocytes and osteoblasts has been observed using a number of *in vitro* systems. In 2005, Sanchez et al performed indirect co-culture of osteoblasts from non-sclerotic or sclerotic zones of subchondral bone with chondrocytes isolated from OA articular cartilage. The sclerotic area is the region just below the cartilage lesion and where subchondral bone is thickening. Osteoblasts from the sclerotic zone decreased chondrocyte expression and secretion of aggrecan and increased gene expression of *MMP3* and *MMP13*, suggesting that local factors secreted by osteoblasts initiate matrix degradation and matrix mineralisation[247]. In a second paper, they demonstrated that osteoblasts from sclerotic bone decreased chondrocyte *SOX9* and *COL2A1* gene expression but increased the mRNA level of osteoblast stimulating factor 1 (*OSTF1*). These data indicate that osteoblast-chondrocyte interactions can induce hypertrophic differentiation of chondrocytes[248].

4.4.2 Communication of monocytes and macrophages with chondrocytes

The intensity of macrophage infiltration into synovium is correlated with the progression of RA, therefore monocytes and macrophages are thought to play an important role in inflammatory joint disease. Interaction between macrophages and chondrocytes has been revealed by Dreier et al in a coculture experiment. Human macrophages were overlayed with agarose gel containing human chondrocytes. The conditioned medium from cocultured chondrocytes contained increased active MMP-1, MMP-3 and MMP-9 compared to monoculture of chondrocytes or macrophages. The inactive form of MMP-9 was detected by gelatin zymography in monoculture of macrophages however, chondrocytes were necessary for MMP-9 activation. Monocultured monocytes also produced the inactive form of MMP-9 which was activated in presence of chondrocytes. The presence of monocytes also increased the expression of MMP-1 and MMP-3 in chondrocytes. These observations highlight the possible interaction between chondrocytes and both macrophages and monocytes[249].

4.4.3 Communication between osteoclasts and chondrocytes

Interaction between osteoclasts and chondrocytes has been less studied than the interaction of chondrocytes with other types of cells. In fact, only a few publications have shown that co-culture of chondrocytes could induce the differentiation of spleen cells or bone marrow cells into osteoclasts[250,251]. Usui et al proposed that hypertrophic chondrocytes may regulate osteoclastogenesis through BMP-induced RANKL expression. In their

experiment, they co-cultured murine chondrocytes with spleen cells and observed that chondrocytes induced the formation of osteoclasts. Addition of BMP-2 in their co-culture increased the number of osteoclasts formed and monocultures of chondrocytes responded to BMP2 by increasing the expression of RANKL[252]. Vitamin D_3 has also been shown to stimulate chondrocytes to produce RANKL[253]. The precise role of RANKL and RANK signalling by chondrocytes during endochondral ossification remains poorly understood. On the other hand, it is well known that chondrocytes produce both OPG and RANKL in OA[184,254] and RA[244], which affects the formation and the activity of osteoclasts. To understand the effect of osteoclasts on cartilage it is important to characterise whether osteoclasts interact with chondrocytes, and if so, how this affects osteoclast activity. The nature of the communication (cell-cell contact or paracrine factors) might be relevant for multiple joint diseases where chondrocytes and/or osteoclasts are involved.

4.5 Objectives

Following the findings of chapter 3, it became evident that finding the mechanism(s) involved in osteoclasts' cartilage degradation was important. To more closely mirror physiological conditions, experiments were also performed on cellular cartilage. Explants of cartilage collected after surgery were maintained in the cell culture incubator before use. The presence of live chondrocytes in cellular cartilage allowed investigation of the possible interactions between osteoclasts and chondrocytes.

More specifically, this chapter aimed to:

1. Determine whether cartilage degradation by osteoclasts is modified by the presence of live chondrocytes. We hypothesised that the presence of chondrocytes in cartilage might change osteoclast behaviour.

2. Identify the key proteinases responsible for osteoclast-driven degradation of cartilage. It was hypothesised that osteoclasts degrading cartilage might use similar mechanisms to those used in bone resorption.

3. Investigate whether the effect of osteoclasts on cartilage digestion is due to direct contact with the substrate or to the release of paracrine factors by osteoclasts. Osteoclasts resorb bone onto which they are tightly sealed therefore, we hypothesised that contact with cartilage is essential for cartilage degradation.

4. Understand whether chondrocytes affect the formation and activity of osteoclasts through direct or indirect interactions. It was hypothesised that chondrocytes could affect osteoclast resorption and degradation of bone or cartilage.

RESULTS

4.6 Osteoclasts degrade cellular cartilage

In these experiments, acellular cartilage corresponds to cartilage that has been flash frozen in liquid nitrogen, making the chondrocytes metabolically inactive. Cellular cartilage represents cartilage pieces containing active chondrocytes; the cartilage was briefly kept in media in tissue culture until the experiment.

To establish if chondrocytes affect osteoclast-driven cartilage degradation, monocytes were differentiated into osteoclasts on cellular cartilage (**Figure 4.1A. and Figure 4.2 A.**) and GAG and hydroxyproline release was measured.

4.6.1 Osteoclast-driven proteoglycan degradation is increased on cellular compared to acellular cartilage explants

. GAG release from cellular cartilage was significantly increased by osteoclasts at day 10 (50 % increase; 91.22 μg compared to 46.02 μg, **Figure 4.1 B.**). At day 13, the GAG release was 32.6 % increased, with 116.94 μg GAG released in the presence of osteoclasts compared to 78.83 μg in the control (**Figure 4.1 C.**). Osteoclasts were therefore active on cellular cartilage and modified the integrity of the ECM.

The basal (in the absence of osteoclasts) release of GAG by articular cartilage tends to increase overtime; from 46.02 μg to 78.83 μg. The fold change of day 13 over day 10 did not show any difference between osteoclasts cultured on cartilage and the osteoclast-free control (**Figure 4.1 D.**), suggesting that osteoclasts are equally active with respect to GAG release at both timepoints

At day 10, basal release of GAG was lower in cellular cartilage compared to acellular cartilage, suggesting that the presence of live chondrocytes inhibited the degradation of proteoglycans (46.02 μg compared to 84.17 μg in acellular cartilage, **Figure 4.1 B. and Figure 3.11 B.**). Additionally, 31.65 μg more GAG was released from cellular than acellular cartilage in the presence of osteoclasts at day 10 (**Figure 4.1 B. and Figure 3.11 B.**). At day 13, GAG release from cellular cartilage was 19.83 μg more than acellular cartilage with osteoclasts (**Figure 4.1 C. and Figure 3.11 C.**). However, it is not possible to ascertain whether chondrocytes were increasing GAG release by osteoclasts or vice versa.

As mentioned in Section 3.5.1, the GAG release by osteoclasts cultured on cellular cartilage was measured from day 4 until day 16 (**Appendix A.3 A.**), although the blood preparations and the cartilage donors were not the same as used in **Figure 4.1**. These two experiments confirmed that GAG release was significantly increased at day 10. GAG release was also significantly increased at day 4 and day 7 suggesting that monocytes / macrophages were able to degrade cartilage and this increase was amplified by the presence of chondrocytes. However, it was not possible to ascertain

whether chondrocytes are increasing GAG release by osteoclasts or vice versa (**Appendix A.1 A.** and **Appendix A.3 A**).

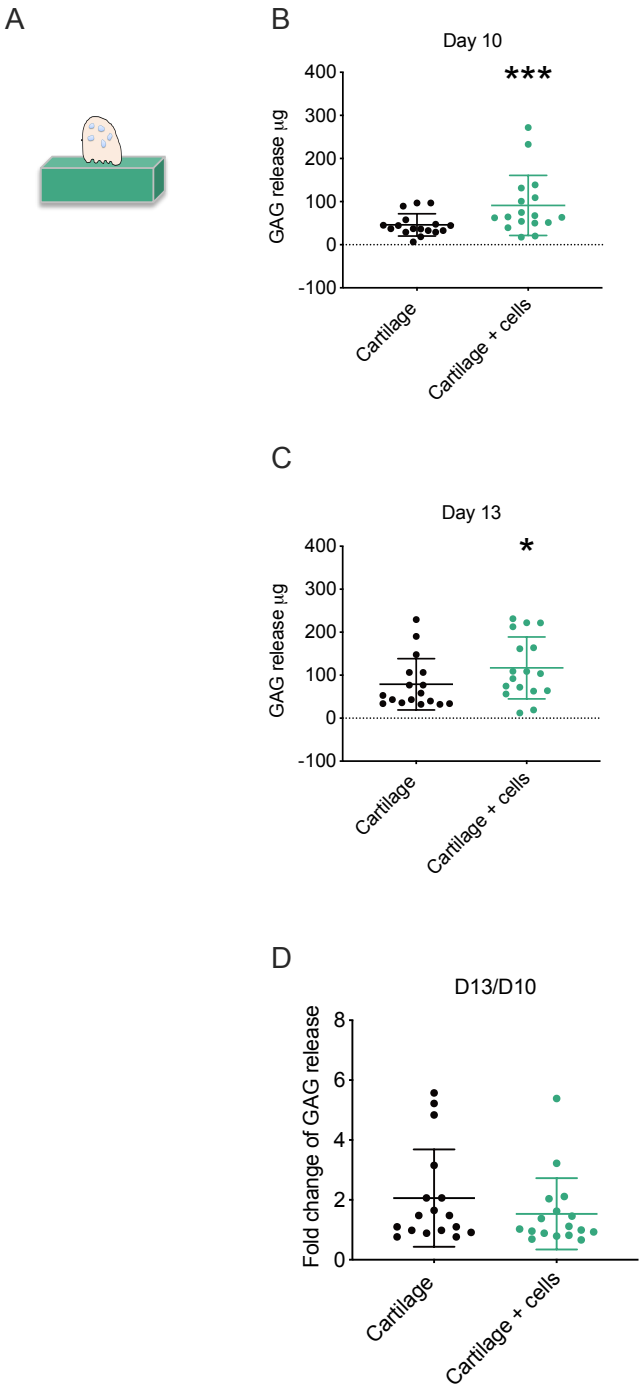


Figure 4.1 GAG release in the presence of osteoclasts on cellular cartilage. **A.** Diagram showing osteoclast on cellular cartilage. **B**. GAG release by cellular cartilage without osteoclasts compared to cellular cartilage cultured with osteoclasts on the surface. Osteoclasts were cultured

for 10 days with M-CSF and RANKL. **C**. Similar to **B**. but osteoclasts were cultured until day 13. **D**. Fold change of D13/D10. *$p \leq 0.05$ and ** $p \leq 0.001$, n=17

4.6.2 Live chondrocytes do not increase collagen degradation by osteoclasts

To determine whether chondrocytes could encourage osteoclasts to degrade collagen from cartilage, the conditioned media of osteoclasts cultured on cellular cartilage was used for the hydroxyproline assay (**Figure 4.2 A.**). The presence of chondrocytes did not change the ability of osteoclasts to degrade collagen contained in the cartilaginous ECM.

At day 10, the amount of collagen released was on average 2.76 μg in the presence of osteoclasts and 2.08 μg for the control, however the increase was not significant (**Figure 4.2 B.**). At day 13, the amount of collagen released was almost equal; 2.52 μg for cartilage with osteoclasts and 2.53 μg for the control (**Figure 4.2 C.**). In addition to basal GAG release, cartilage pieces spontaneously released collagen; 2.08 μg at day 10 and 2.53 μg at day 13.

The lack of fold change of collagen release at day 13 over day 10 showed that the ability of osteoclasts to release collagen did not change over time (**Figure 4.2 D.**)

The difference of collagen release between osteoclast-cartilage culture and cartilage alone was similar on cellular and acellular cartilage (0.68 μg in acellular cartilage and 0.66 μg in cellular cartilage at day 10, **Figure 3.12 B.** and **Figure 4.2 B**). The basal level of collagen degradation was higher but not

significant in acellular cartilage compared to cellular cartilage; 2.40 μg in acellular and 2.08 μg in cellular cartilage.

As for the proteoglycan, collagen degradation from cellular cartilage in the presence and absence of osteoclasts was assessed from day 4 until day 16. This experiment was also used to verify what was observed at day 10 and day 13 in **Figure 4.2**. No significant differences in hydroxyproline release were seen at any time point, whereas it was significantly increased when osteoclasts were cultured on acellular cartilage (**Appendix A.1 B.** and **Appendix A.3 B.**).

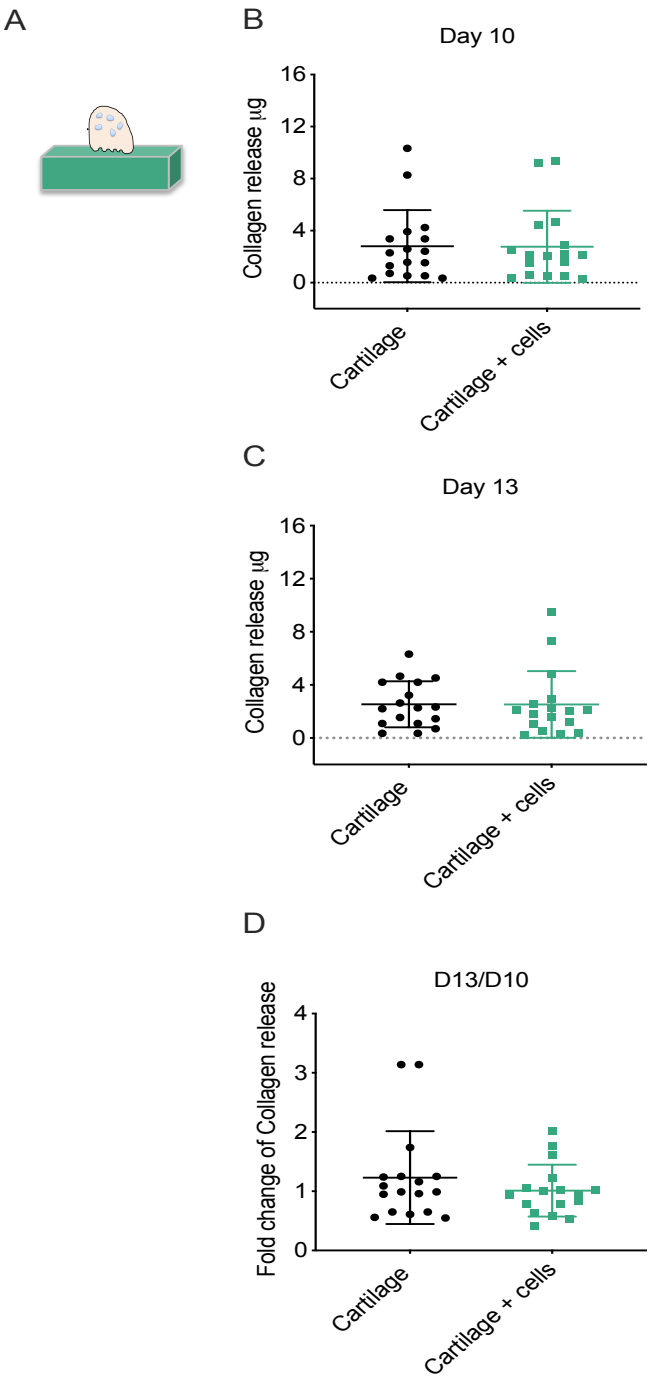


Figure 4.2 Collagen release in culture media in the presence of osteoclasts on cartilage. **A.** Diagram showing osteoclast on cellular cartilage. **B**. Collagen release by cellular cartilage without osteoclasts compared to cartilage with osteoclasts cultured at the surface. Cartilage and osteoclasts were cultured for 10 days with M-CSF and RANKL. **C**. Similar to **B**. but osteoclasts were cultured until day 13. **D**. Fold change of D13/D10, n=17

4.7 Use of inhibitors to find the mechanism of degradation used by osteoclasts

It was hypothesised that osteoclasts degrading cartilage use similar mechanisms that are used in bone resorption. Osteoclasts degrade the inorganic bone matrix via acidification and cathepsin K, while MMPs degrade the organic phase. Osteoclasts were cultured on acellular or cellular cartilage in the presence of an acidification inhibitor (Bafilomycin), a cathepsin K inhibitor (E64) or an MMP inhibitors (GM6001). Osteoclasts cultured on dentine were used as a comparator. The degradation products GAG and hydroxyproline were quantified to determine the key proteinases responsible for osteoclast-driven degradation of cartilage.

4.7.1 Acidification is not required for cartilage digestion

GAG release from cartilage by osteoclasts was not changed in the presence of bafilomycin (**Figure 4.3 A.-C.**), suggesting that cartilage is degraded independently of acidification.

As expected, bafilomycin blocked osteoclast resorption of dentine at day 10 and day 13 as assessed by pit formation (**Figure 4.3 D.-F.**) and by the amount of collagen released (**Figure 4.3 G.-I.**). These results support that acidification of the lacuna is an essential step for bone resorption.

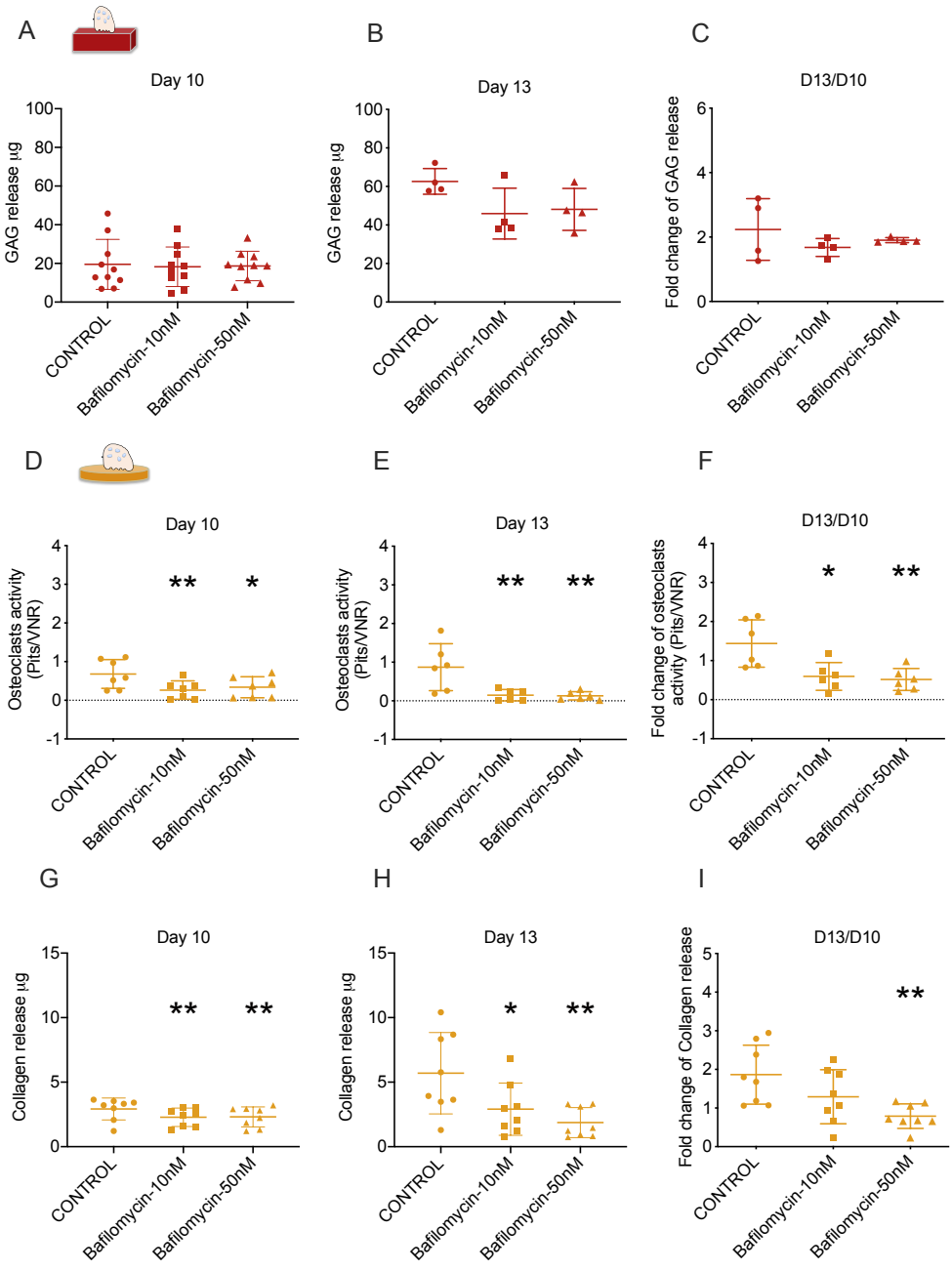


Figure 4.3 Osteoclasts cultured on dentine and cartilage in presence of bafilomycin. A.-C. Osteoclasts cultured on acellular cartilage **A.** GAG release at day 10. **B.** GAG release at day 13. **C.** Fold change of GAG release. **D.-I.** Osteoclasts were cultured on dentine **D.** Osteoclast pit formation at day 10. **E.** Osteoclast pit formation at day 13. **F.** Fold change of osteoclast pit formation. **G.** Collagen release at day 10. **H.** Collagen release at day 13. **I.** Fold change of collagen release. *$p \leq 0.05$ and **$p \leq 0.01$

4.7.2 Cathepsin K is not required for proteoglycan degradation

Osteoclasts cultured on acellular cartilage in the presence of E64 did not change the amount of GAG released compared to the control (**Figure 4.4 A.-C.**), suggesting that cartilage is degraded independently of cathepsin K.

E64 significantly decreased osteoclast pit formation at day 13 (**Figure 4.4 E.**) and the amount of collagen released was also significantly decreased at day 13 compared to the control (**Figure 4.4 G.-I.**) confirming what has been described in the literature.

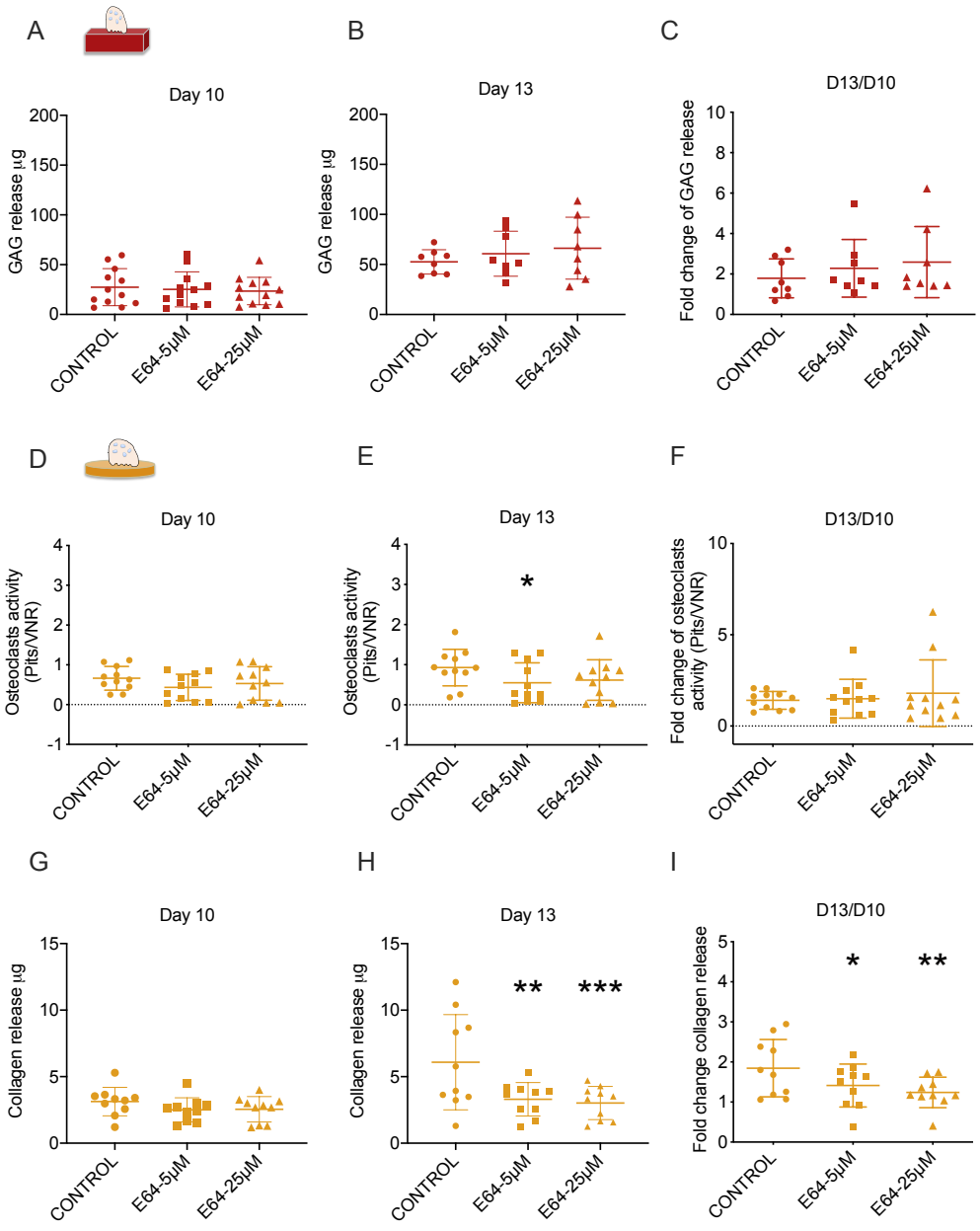


Figure 4.4 Osteoclasts cultured on dentine and cartilage in presence of cathepsin K inhibitor. A.-C. Osteoclasts cultured on acellular cartilage **A.** GAG release at day 10. **B.** GAG release at day 13. **C.** Fold change of GAG release. **D.-I.** Osteoclasts were cultured on dentine **D.** Osteoclast pit formation at day 10. **E.** Osteoclast pit formation at day 13. **F.** Fold change of osteoclast pit formation. **G.** Collagen release at day 10. **H.** Collagen release at day 13. **I.** Fold change of collagen release. *$p \leq 0.05$, **$p \leq 0.01$ and ***$p \leq 0.001$

4.7.3 Osteoclasts use MMPs to degrade cartilage

Importantly, inhibition of osteoclast MMP activity with the MMP inhibitor GM6001 significantly reduced GAG release from cartilage at day 10 (**Figure 4.5 A.**) and at day 13 (**Figure 4.5 B.** and **C.).** GAG release decreased by 26 % at day 10 and 43 % at day 13 in the presence of 50 μM GM6001. This indicates that osteoclasts use MMPs to degrade cartilage and release proteoglycans.

GM6001 reduced osteoclast pit formation on dentine at day 10 (**Figure 4.5 D.-F.**) but did not change the amount of collagen released by osteoclasts cultured on dentine at any time (**Figure 4.5 G.-I.**).

To make sure that the effects observed were due to the presence of osteoclasts, acellular cartilage without osteoclasts was cultured in the presence of GM6001, E64 or bafilomycin (**Appendix A.2**). No significant difference was seen suggesting that only osteoclasts were inhibited, and any difference seen was due to their inhibition.

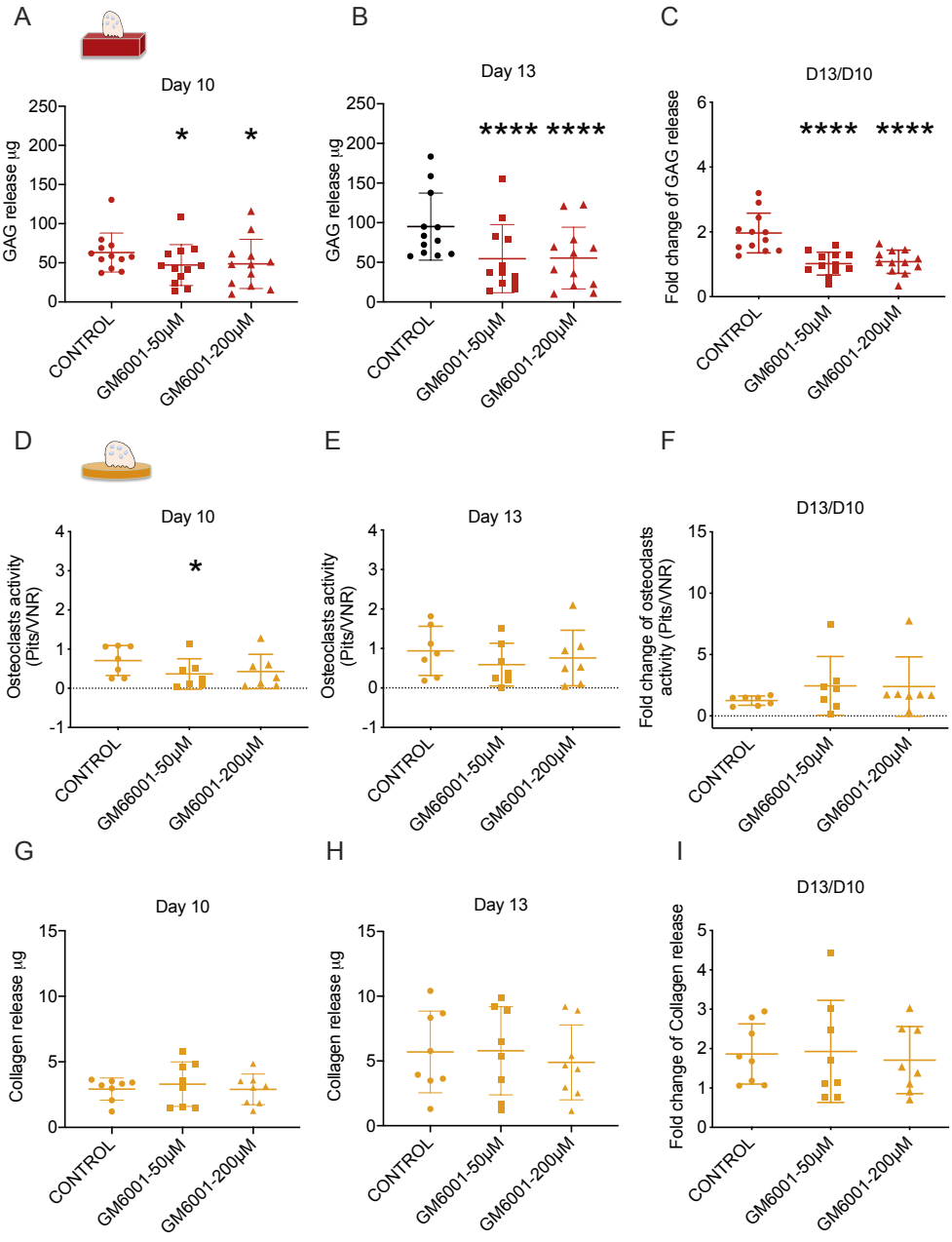


Figure 4.5 Osteoclasts cultured on dentine and cartilage in presence of MMP inhibitor. A.-C. Osteoclasts cultured on acellular cartilage **A.** GAG release at day 10. **B.** GAG release at day 13. **C.** Fold change of GAG release. **D.-I.** Osteoclasts were cultured on dentine **D.** Osteoclast pit formation at day 10. **E.** Osteoclast pit formation at day 13. **F.** Fold change of osteoclast pit formation. **G.** Collagen release at day 10. **H.** Collagen release at day 13. **I.** Fold change of collagen release. *$p \leq 0.05$ and ****$p \leq 0.0001$

4.7.4 Osteoclasts also degrade cellular cartilage via MMPs

Osteoclasts cultured on cellular cartilage in the presence of bafilomycin did not decrease the amount of GAG released at day 10 or day 13, although a significant decrease was evident over time at the higher concentration (**Figure 4.6 A.-C.**).

The inhibition of cathepsin K did not change the amount of GAG released into the culture media (**Figure 4.6 D.-F.**).

In the same way as for the osteoclasts cultured on acellular cartilage, GM6001 significantly decreased the amount of GAG released at day 10 and at day 13 when osteoclasts were cultured on cellular cartilage (**Figure 4.6 G.-I.**). At 50 μM of GM6001 the GAG release was decreased by 37 % at day 10 and 58 % at day 13.

At 50 μM GM6001, GAG release by osteoclasts cultured on acellular cartilage at day 10 was decreased by 26 % and it was decreased by 37 % when osteoclasts were cultured on cellular cartilage (**Figure 4.5 A. and Figure 4.6 G**.). At day 13, the GAG release was 43 % decreased in acellular and 58% decreased in cellular cartilage in the presence of osteoclasts **(Figure 4.5 B. and Figure 4.6 H.**). Therefore, at both timepoints the cellular cartilage with osteoclasts is inhibited more than acellular cartilage, suggesting that not only osteoclasts are inhibited by GM6001. To determine if this was due to inhibiting the MMP activity of the chondrocytes, the osteoclasts or both, cellular and acellular cartilage explants without osteoclasts were cultured in the presence of GM6001 (**Appendix A.2 and Appendix A.4**). A significant

decrease of GAG release was seen in cellular cartilage, suggesting that active chondrocytes also release MMPs that degrade cartilage.

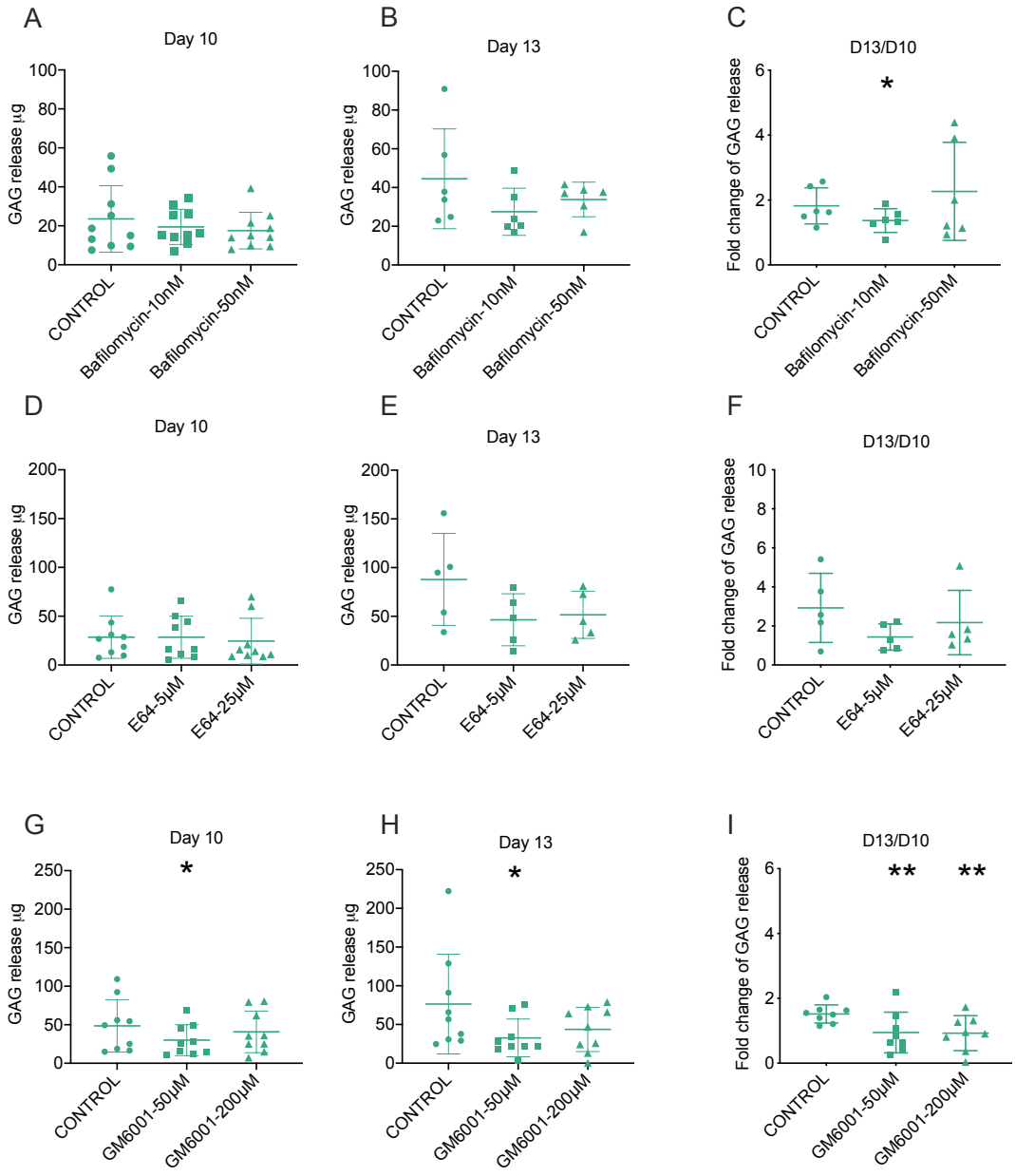


Figure 4.6 Osteoclasts cultured on cellular cartilage in the presence of inhibitors. A. GAG release in the presence of bafilomycin at day 10. **B.** GAG release in the presence of bafilomycin at day 13. **C.** Fold change of GAG release with bafilomycin. **D.** GAG release in the presence of E64 at day 10. **E.** GAG release in the presence of E64 at day 13. **F.** Fold change of GAG release with E64. **G.** GAG release in the presence of GM6001 at day 10. **H.** GAG release in the presence of GM6001 at day 13. **I.** Fold change of GAG release with GM6001. *$p \leq 0.05$, **$p \leq 0.01$

4.7.5 Similar trend with mature and active osteoclasts and inhibitors

Due to the small number of samples available, none of the inhibitors significantly modified the amount of GAG released when GCTB-derived osteoclasts were cultured on acellular cartilage (**Figure 4.7 A., C.** and **E.**). However, there was a trend towards decreased GAG release in the presence of GM6001 at 50 μM (p=0.0962) (**Figure 4.7 E.**).

Only bafilomycin significantly decreased collagen release when osteoclasts from GCTB were cultured on dentine (**Figure 4.7 B., D.** and **F.**).

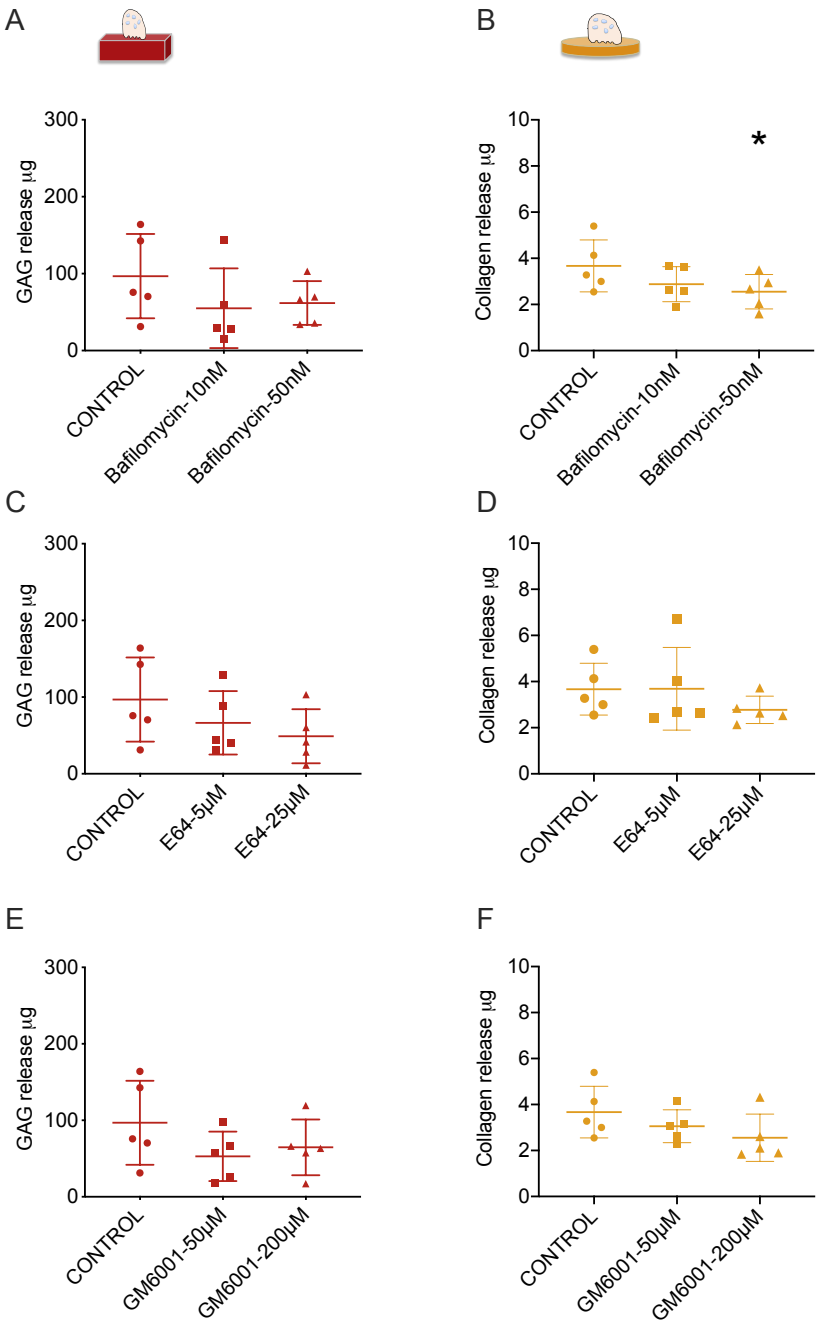


Figure 4.7 GCTB-derived osteoclasts cultured on dentine and cartilage in presence of inhibitors. A., C. and E. Osteoclasts were cultured on acellular cartilage. **B., D. and F.** Osteoclasts were cultured on dentine. **A.** GAG release in presence of bafilomycin. **C.** GAG release in presence of E64. **E.** GAG release in presence of GM6001. **B.** Collagen release in presence of bafilomycin. **D.** Collagen release in presence of E64. **F.** Collagen release in presence of GM6001. *$p \leq 0.05$, n=5

4.8 Direct contact between osteoclasts and cartilage is necessary for GAG release

It is essential that osteoclasts are tightly sealed to the bone surface that they are resorbing but it is unknown if direct contact is also required when osteoclasts degrade cartilage. To investigate whether contact between osteoclasts and cartilage is essential, or whether osteoclasts could release paracrine factors, a transwell experiment was used to separate cartilage from osteoclasts *in vitro*. Pieces of cartilage were placed in the transwell and the osteoclasts were cultured on plastic or dentine at the bottom of the well. GAG and hydroxyproline assays were performed to assess the degradation of proteoglycan and collagen.

Osteoclasts cultured on plastic did not release any paracrine factors able to degrade proteoglycans present in acellular or cellular cartilage (**Figure 4.8 A.** and **B.** respectively). Direct contact between osteoclasts and their resorbing surface appears to be essential to degrade proteoglycans.

The same experiment was performed when osteoclasts were on their 'natural' (bone) substrate, dentine (**Figure 4.8 C.** and **D.)**. In the absence of osteoclasts, there was a 30 % decrease of GAG release from acellular cartilage (87.48 μg on average) compared to cellular cartilage (61.3 μg., **Figure 4.8 C.** and **D.**) confirming that chondrocytes protect the integrity of the ECM.

The amount of GAG released from cellular cartilage was significantly decreased, by 47 %, when osteoclasts were cultured on dentine with cellular

cartilage in the transwell above (**Figure 4.8 D.**). The only difference between **Figure 4.8 C.** and **D.** is whether acellular or cellular cartilage was used. This suggests that osteoclasts resorbing bone were able to increase the protective activity of chondrocytes and reduce the degradation of the ECM, whereas osteoclasts cultured away from their natural substrate (plastic) could not (**Figure 4.8 A. and B.**).

This strengthened the idea that contact between osteoclasts and cartilage is necessary for proteoglycan degradation and indicated that bone-active osteoclasts secrete factors that amplify the protective response of chondrocytes.

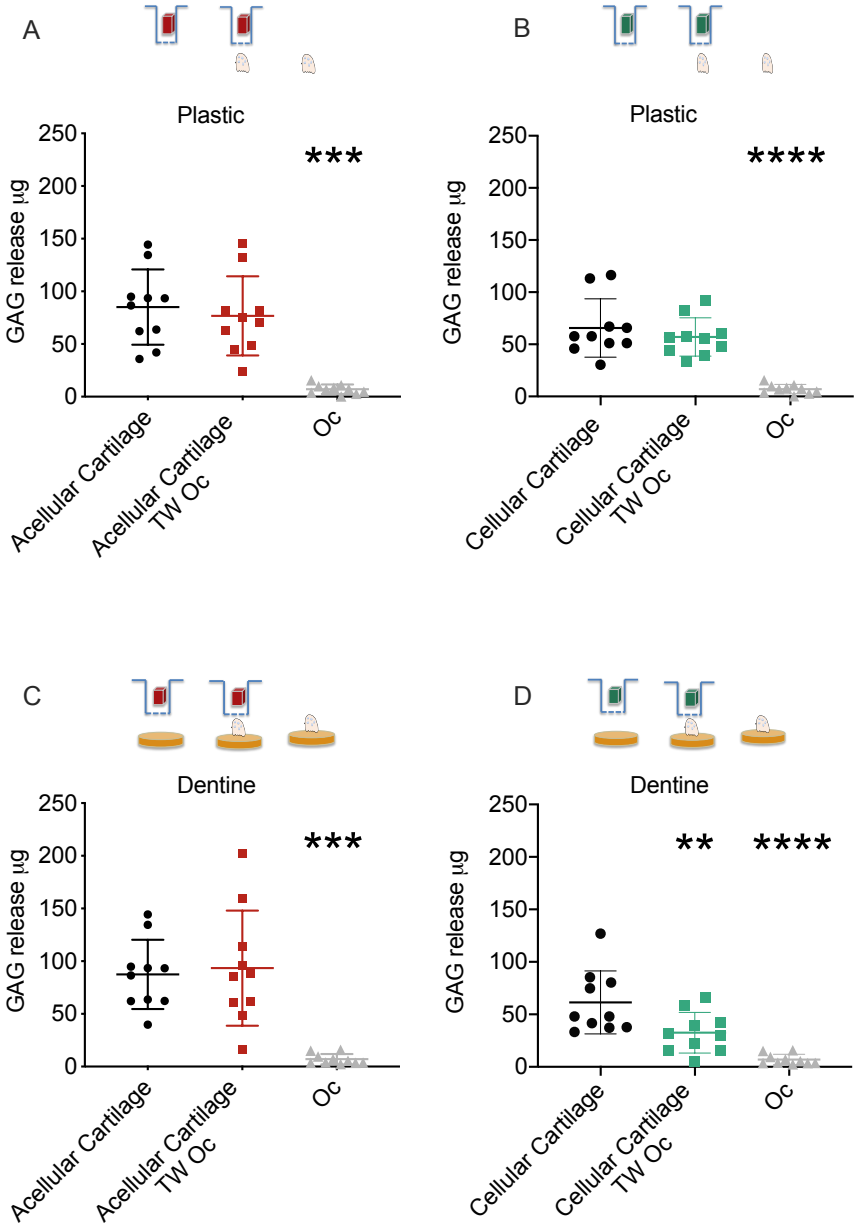


Figure 4.8 Osteoclasts cultured on plastic or on dentine with pieces of cartilage in the transwell. Cartilage: cartilage is placed in the transwell, without cells at the bottom. Cartilage TW Oc: cartilage is placed in the transwell, osteoclasts were cultured at the bottom on plastic or dentine. Oc: osteoclasts cultured at the bottom on plastic or dentine. **A.** Osteoclasts cultured on plastic and the cartilage was acellular. **B.** Osteoclasts cultured on plastic and the cartilage was cellular. **C.** Osteoclasts cultured on dentine and the cartilage was acellular. **D.** Osteoclasts cultured on dentine and the cartilage was cellular. Significance compared to acellular or cellular cartilage without osteoclasts $**p \leq 0.01$, $***p \leq 0.001$ and $****p \leq 0.000$, n=10

4.9 The interaction between osteoclasts and chondrocytes exists and is modified according to the surface on which osteoclasts are cultured

4.9.1 Osteoclasts interact with chondrocytes to stimulate collagen release from cartilage

To determine whether paracrine factors released by osteoclasts could degrade the collagen of the cartilage matrix, osteoclasts were cultured on plastic and pieces of cartilage were placed in the transwell above (**Figure 4.9**). As the hydroxyproline assay is not specific to one type of collagen, osteoclasts were cultured only on plastic (not dentine), ensuring that cartilage was the only possible source of collagen detected in the media.

In the absence of osteoclasts, there was no difference between collagen release by acellular cartilage (1.48 μg on average) compared to cellular cartilage (1.51 μg., **Figure 4.9 A.** and **B.**).

Unexpectedly, the amount of collagen released into the media was significantly increased (by 57 %) when osteoclasts were cultured with cellular cartilage in the transwell compared to cartilage alone (**Figure 4.9 B.**). The only difference between **Figure 4.9 A.** and **B.** is whether acellular or cellular cartilage was used. Osteoclasts were able to affect the activity of chondrocytes by increasing the degradation of the ECM by chondrocytes.

It is again becoming evident that crosstalk between osteoclasts and chondrocytes is likely to exist.

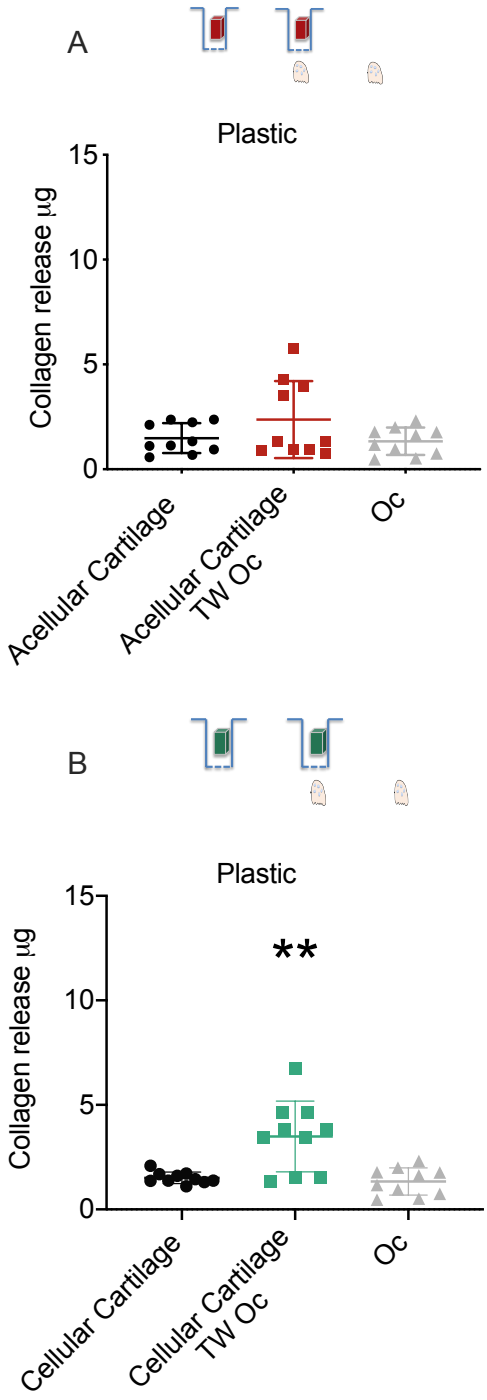


Figure 4.9 Presence of paracrine factors modifying chondrocyte activity in the ECM. Cartilage: cartilage is placed in the transwell, without cells at the bottom. Cartilage TW Oc: cartilage is placed in the transwell, osteoclasts were cultured at the bottom on plastic. Oc: osteoclasts cultured at the bottom

on plastic. **A.** Collagen release from acellular cartilage after 10 days of culture with M-CSF and RANKL. **B.** Same experiment as A. with cellular cartilage pieces. Significance compared to acellular or cellular cartilage without osteoclasts $**p \leq 0.01$and n=10

4.9.2 Direct co-culture of osteoclasts and chondrocytes on coverslips

To further investigate the interactions between osteoclasts and chondrocytes, direct and indirect co-culture were used. Initially, morphological staining of a mixed co-culture of osteoclasts and chondrocytes was assessed.

Coverslips seeded with either monocytes alone or monocytes and chondrocytes were cultured for 10 days with M-SCF and RANKL, after which the cytoskeleton and nuclei were stained by immunofluorescence. Multi-nucleated cells with a peripheral ring belt were easily identifiable in monoculture and co-culture as osteoclasts (**Figure 4.10 A.** and **B.**). Chondrocytes were mononucleated and smaller, with a fusiform shape (**Figure 4.10 B.**).

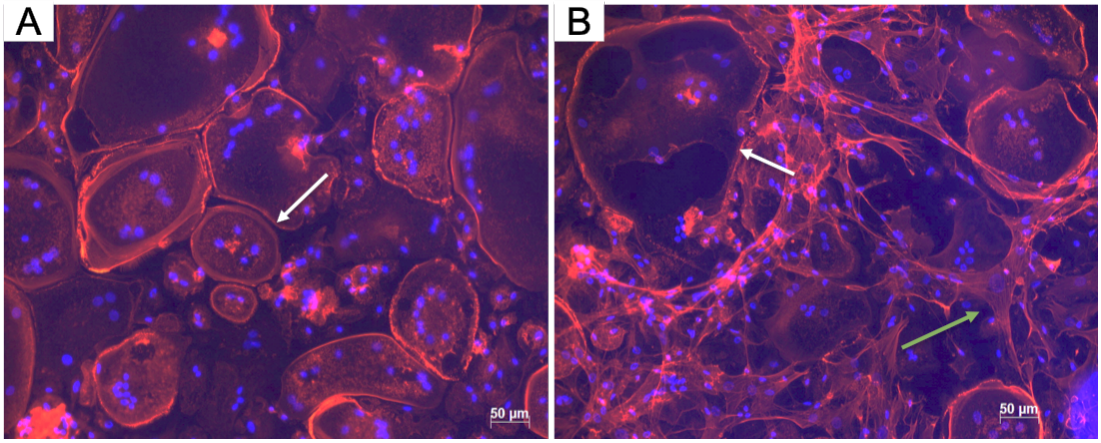


Figure 4.10 Actin cytoskeleton and nuclear staining of osteoclasts and chondrocytes. **A.** Monocytes differentiated into osteoclasts (white arrow)

after 10 days in culture with M-CSF and RANKL on coverslips. **B.** Monocytes differentiated into osteoclasts (white arrow) and chondrocytes (green arrow) co-cultured for 10 days with M-CSF and RANKL on coverslips.

Cells from the same conditions were also stained for TRAP to confirm the presence of osteoclasts. Visually, the number of osteoclasts appeared to increase in the presence of chondrocytes (**Figure 4.11 A.** and **B.**). However, there was actually no difference in the total number of multi-nucleated osteoclasts (cells with >3 nuclei) formed (**Figure 4.11 C.**), although the number of large osteoclasts (>10 nuclei) was significantly increased when osteoclasts and chondrocytes were co-cultured (**Figure 4.11 D.**). This suggests that chondrocytes release factors that increase the formation of large osteoclasts.

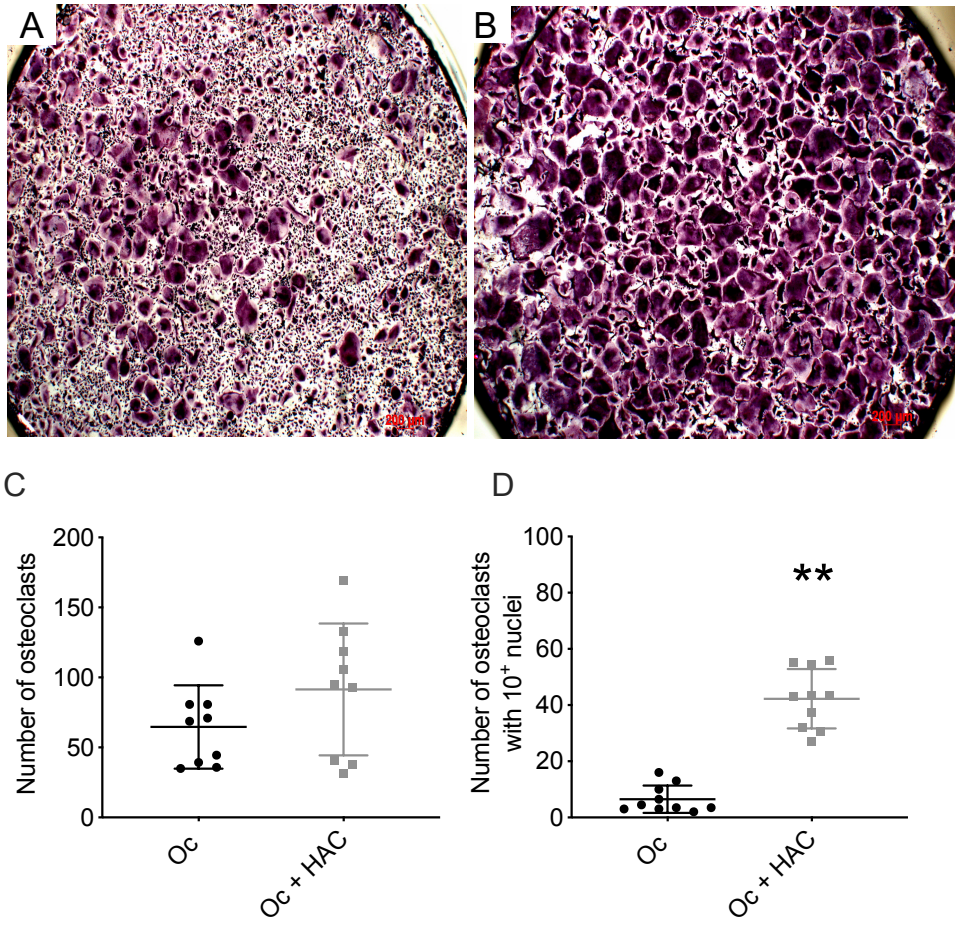


Figure 4.11 Co-culture of osteoclasts and chondrocytes on coverslips. A. Monocytes differentiated into osteoclasts for 10 days with M-CSF and RANKL. **B.** Monocytes and chondrocytes cultured for 10 days with M-CSF and RANKL. **C.** Number of TRAP-positive cells with 3 or more nuclei, n=9. Oc: osteoclasts and Oc +HAC: co-culture of osteoclasts and chondrocytes. **D.** Number of TRAP positive cells with more than 10 nuclei. ****$p \leq 0.0001$and n=10

4.9.3 Effect of chondrocytes on the morphology and resorption activity of osteoclasts differentiated on dentine

The GAG and collagen release experiments in **section 4.8** and **4.9.1** highlighted that osteoclast activity varies by substrate. To further understand the role that substrate plays, the impact of chondrocytes on osteoclast formation and activity was compared on dentine. As well as using direct co-

culture, an indirect co-culture experiment was performed to determine if contact between osteoclasts and chondrocytes is necessary.

In contrast to the previous experiment on glass coverslips, the number of osteoclasts formed on dentines by monocytes co-cultured with chondrocytes appeared to be decreased compared with monoculture (**Figure 4.12 A.** and **B.**).

To determine if a paracrine factor could affect osteoclast behaviour, indirect co-culture was performed with osteoclasts on dentine cultured with chondrocytes in a transwell above. Resorption pits were counted and the cells on dentine were stained for TRAP and VNR. The number of osteoclasts was also significantly decreased when chondrocytes were in the transwell, suggesting chondrocytes release a paracrine factor that reduces the formation of osteoclasts on dentine. However, osteoclast activity was not decreased by this paracrine factor (**Figure 4.12 C., D.** and **E.**).

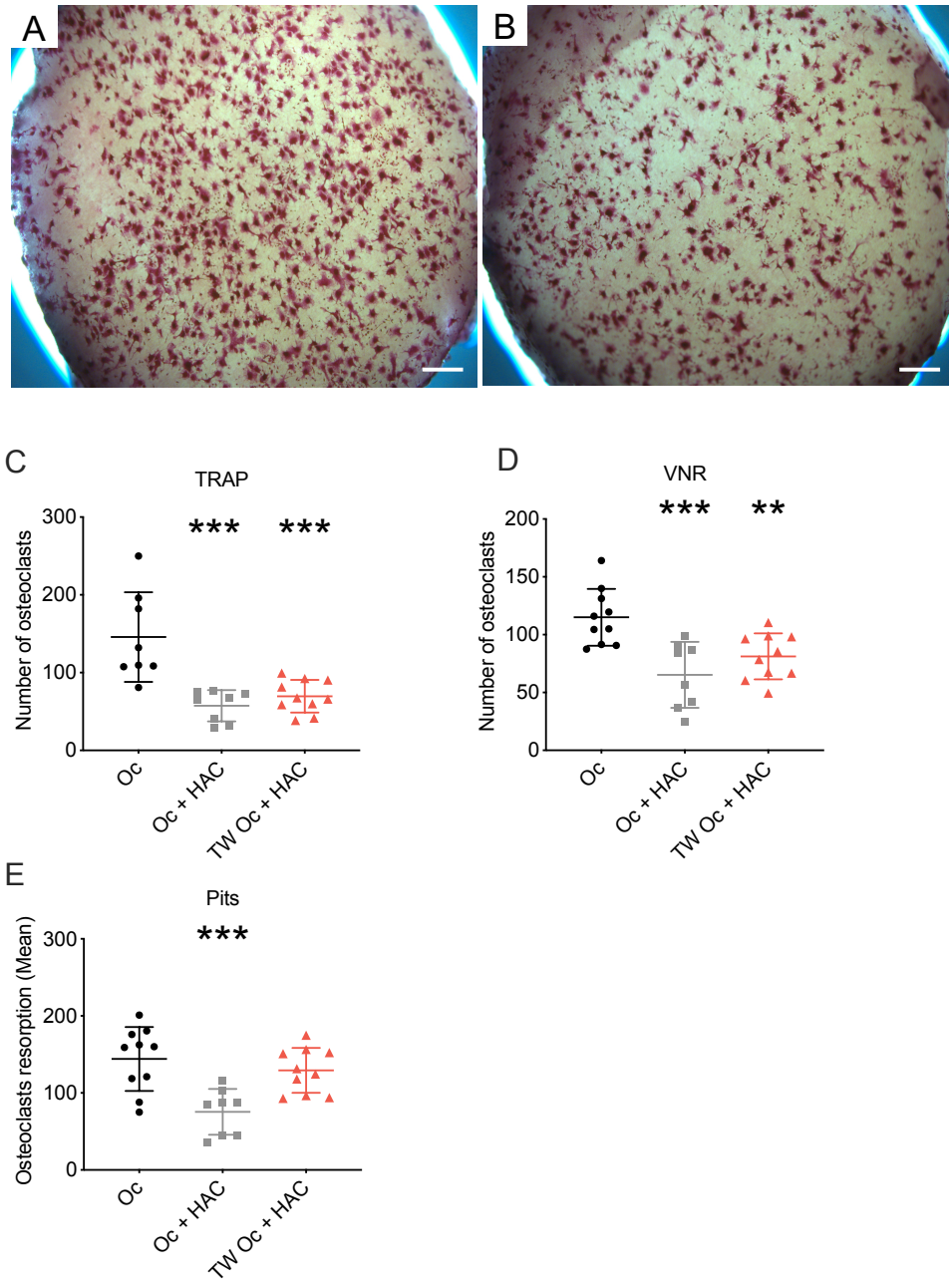


Figure 4.12 Osteoclasts cultured with or without chondrocytes on dentine. A. Monocytes cultured for 10 days with M-CSF and RANKL on dentine. **B.** Osteoclasts and chondrocytes cultured for 10 days with M-CSF and RANKL on dentine. **C.** TRAP positive cells counted, Oc: Osteoclasts, Oc + HAC: co-culture of osteoclasts and chondrocytes and TW Oc + HAC: osteoclasts were on dentine and chondrocytes were in the transwell. **D.** VNR-positive cells. **E.** Osteoclast resorption (pits area per osteoclast). $^{**}p \leq 0.01$ and $^{***}p \leq 0.001$, n=8

4.9.4 Expression levels of OPG and RANKL by chondrocytes change when they are cultured on plastic or dentine

It is possible that chondrocytes express cytokines that will inhibit formation of bone-associated osteoclasts. OPG and RANKL are the most well-known cytokines that regulate osteoclast differentiation and activity. OPG is a soluble decoy receptor for RANKL, competing with RANK for RANKL binding.

In order to determine expression levels of *OPG* and *RANKL* in chondrocytes, we used RT-qPCR to measure mRNA levels in chondrocytes co-cultured with osteoclasts on plastic and chondrocytes co-cultured with osteoclasts on dentine. The relative expression of *OPG* was 21 times higher when the co-culture was on dentine compared to plastic (**Figure 4.13 A.**). Chondrocytes were the source of these cytokine mRNAs since osteoclasts do not express *OPG* and *RANKL*. Indeed, RT-qPCR of chondrocytes and osteoclasts monoculture have confirmed that chondrocytes were the main source of *OPG* and *RANK*L (**Appendix A.5**). Potentially, the paracrine factors secreted specifically by osteoclasts actively resorbing dentine, induced a response in chondrocytes resulting in an increase in expression of *OPG*.

There was no significant difference in the expression of *RANKL* (**Figure 4.13 B.**). Therefore, the ratio of *RANKL* / *OPG* was significantly decreased (**Figure 4.13 C.**).

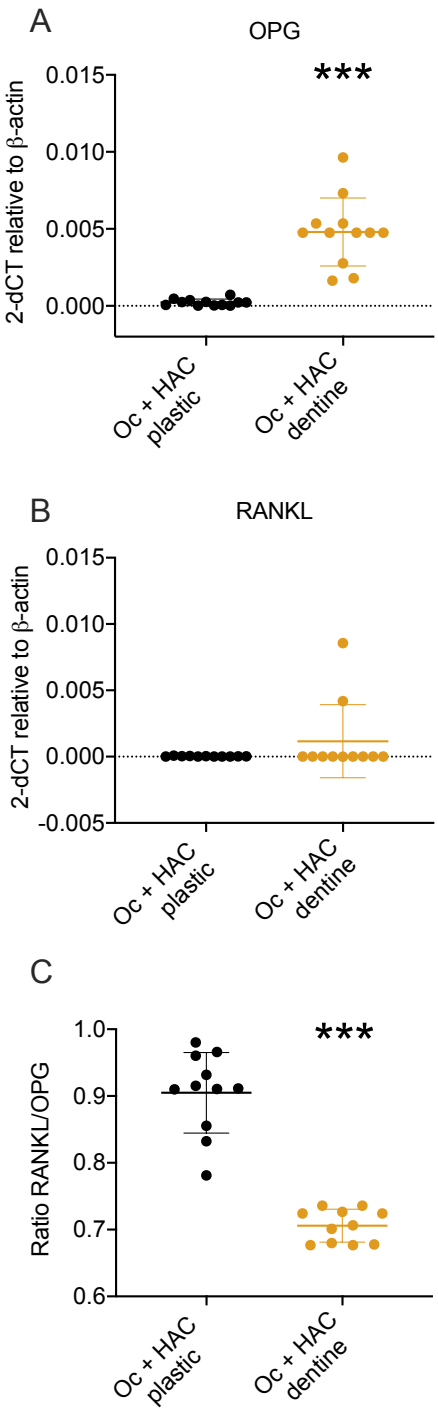


Figure 4.13 Expression levels of OPG and RANKL. **A.** *OPG* expression relative to β-actin in co-culture of osteoclasts and chondrocytes on different substrates. **B.** *RANKL* expression relative to β-actin in co-culture of osteoclasts and chondrocytes on different substrates. **C.** Ratio of *RANKL* / *OPG*. ***$p \leq 0.001$ and n=11

DISCUSSION

The aim of this chapter was to determine which proteinases are involved in cartilage degradation and whether osteoclasts could secrete paracrine factors to degrade cartilage. During the course of these experiments, it became evident that the substrate on which osteoclasts are grown and the interaction between osteoclasts and chondrocytes should also be investigated.

The first objective of this chapter was to better reproduce physiological conditions by conducting the experiments from chapter 3 with cellular cartilage instead of acellular cartilage. The metabolically active chondrocytes in cellular cartilage have the potential to modify the interaction between osteoclasts and the cartilage ECM. Osteoclasts on cellular cartilage were able to release proteoglycan as seen in Chapter 3 on acellular cartilage but the presence of osteoclasts on cellular cartilage did not change the collagen release.

A significant increase of aggrecan release showed that osteoclasts can degrade cartilage containing active chondrocytes. Quantification of GAG release at day 4, day 7 day 10, day 13 and day 16 revealed a significant increase at day 4 and day 7. The cells seeded at day 1 were monocytes and differentiated into osteoclasts over 10 days therefore, the cells present at day 4 and day 7 are a mix of monocytes, macrophages and immature osteoclasts. The capacity of monocytes and macrophages to degrade cartilage is supported by previous studies including that by Knowles et al[188], who showed that human monocytes seeded on human acellular cartilage and cultured in

presence of M-CSF for 4 days significantly increase the amount of GAG released into the media compare to cartilage alone. In this thesis, later time points at day 10 and day 13 were used to make sure that the GAG and hydroxyproline assays reflected predominantly osteoclast activity, rather than monocytes and macrophages. Dreier et al have also shown that chondrocytes, monocytes and macrophages mutually induce alteration in their activities. They observed that human macrophages cocultured with human chondrocytes induced new protease activities (MMP-9 and MMP-1) in the media compared to the monocultures. In parallel, a coculture of monocytes and chondrocytes reduced aggrecan and collagen II protein expression and increased aggrecan degradation[249]. This interaction is also supported by our results where live chondrocytes induce differences in osteoclasts-driven degradation.

This is the first time that cartilage degradation by osteoclasts has been compared on cellular and acellular cartilage. GAG release was higher when osteoclasts were cultured on cellular cartilage versus acellular cartilage suggesting either that chondrocytes amplify the degradative effect of osteoclasts or that osteoclasts cause increased cartilage degradation by chondrocytes. The amount of collagen released when osteoclasts were cultured on cellular cartilage was almost the same as cellular cartilage alone. However, collagen release from acellular cartilage was increased by osteoclasts (Chapter 3). The reduction in osteoclast-induced GAG and collagen release from cellular compared to acellular cartilage suggests that chondrocytes in cellular cartilage may have a role in the protection of the

ECM. It might be also possible that this was also due to structural damage caused by flash freezing and subsequent thawing. Given the variability between blood donors and the limited sensitivity of this assay it has been decided to use the collagen assay only when osteoclast was cultured on dentine.

The second objective of this chapter was to find the key proteinases responsible for osteoclast-driven degradation of cartilage. It was hypothesised that osteoclasts degrading cartilage might use similar mechanisms to those used in bone resorption. Therefore, inhibitors blocking organic and inorganic bone matrix degradation were used. More precisely, V-ATPase inhibitor, cathepsin K inhibitor and a broad MMPs inhibitor were used with osteoclasts cultured on cartilage compared to osteoclasts on cartilage untreated. Osteoclast-driven GAG release from acellular and cellular cartilage required MMPs, whereas acidification and cathepsin K activity were not necessary. Mature and active osteoclasts isolated from GCTB confirmed that osteoclasts actively degrade cartilage (see chapter 3 section 4.7.5) and suggested that this was also MMP-dependent, although this second experiment did not reach statistical significance.

Osteoclast-driven degradation of acellular cartilage GAG was reduced by the MMP inhibitor GM6001, but not by inhibition of V-ATPases or cathepsin K, suggesting that cartilage degradation is MMP-dependent. A publication has shown that cathepsin K inhibitors can block the degradation of cartilage by osteoclasts; Lofvall et al postulated that osteoclasts use MMP-mediated and cysteine protease-mediated resorption to degrade calcified

cartilage[185]. They used the same inhibitors for cathepsin K and MMPs that were used in this thesis. Osteoclasts were placed on cortical bone, acellular articular cartilage and acellular osteochondral junction. As observed in osteoclast-dentine culture with bafilomycin in this thesis, blocking the V-ATPase significantly reduced the amount of type I collagen released from cortical bone[185]. The inhibition of type I collagen release by Bafilomycin was greater when osteoclasts were on cortical bone compared to the osteochondral junction. The degree of inhibition of degradation caused by V-ATPase inhibitors might reflect the degree of mineralisation of the substrate. Therefore, their culture highlighted the low level of minerals in the calcified cartilage compared to the cortical bone. As observed in our experiment, E64 also significantly reduced the amount of type I collagen released into the media when osteoclasts were cultured on bone or on dentine.

Differing from our results, Lofvall et al showed that GM6001 significantly decreased the amount of type I collagen released when osteoclasts were cultured on cortical bone and on osteochondral junction[185]. MMP inhibition appeared to have a stronger effect on osteochondral junction CTX-I release than on cortical bone CTX-I release. It is possible that reduced mineralisation in the osteochondral junction facilitated the function of MMPs. Henriksen et al demonstrated that MMPs are the predominant proteases on a decalcified matrix; osteoclasts cultured on calcified bone in the presence of GM6001 did not reduce the amount of type I collagen, only when osteoclasts were cultured on decalcified bone was a significant reduction in CTX-I

seen[239]. The results obtained in this thesis are in agreement with Henriksen et al; GM6001 affects degradation of unmineralized but not mineralised matrix.

Henriksen et al also described that the effect of cathepsin K inhibition on decalcified bone was not as clear as it was on calcified bone[239]. In this thesis, the addition of cathepsin K on cartilage did not change the amount of GAG released whereas a significant decrease of collagen release was seen in osteoclasts-dentine culture. Lofvall et al observed a significant decrease of CTX-I release when osteoclasts were cultured on osteochondral junction explants in the presence of E64[185]. Cathepsin K is active at low pH and the minerals in calcified cartilage are degraded by the acidification process of the osteoclasts. Therefore, the presence of minerals ensures acidification and thus the activation of cathepsin K. Kafienah et al demonstrated that human recombinant cathepsin K was able to cleave human and bovine type II collagen. The optimal activity of cathepsin K against native type II collagen was between pH 5.0 and 5.5 and between pH 4.0 and 7.0 against denatured collagen[255]. Nevertheless, it is important to note that their experiment was not performed with cells or with matrix in native form but with the recombinant human cathepsin K mixed with collagen and that the presence of denatured type II collagen was detected by western blot but never quantified with CTX-II or hydroxyproline assay. Similarly to our experiment, Lofvall et al observed that cathepsin K was not involved in articular cartilage degradation. Using hydroxyproline or CTX-II assays would provide confirmation of no effect of cathepsin K on cartilage degradation in our experimental system.

In this thesis only GM6001 significantly decreased the amount of GAG released from cartilage. Lofvall et al showed a trend to completely abrogate the release of type II collagen by osteoclasts cultured on acellular articular cartilage with the same inhibitor. Their experiment suggested that osteoclasts degrade type II collagen in articular cartilage via MMPs but do not degrade aggrecans. GAG release was not quantified in their experiment. Our findings and their results agree that osteoclasts use MMPs to degrade cartilage, despite differences in the resorption products that were detected. They also used GM6001 with osteoclasts cultured on osteochondral junction and degradation of type I collagen and C2M (a biomarker to measure an MMP-generated neo-epitope of type II collagen) were significantly decreased, suggesting that MMPs are able to degrade the collagen present in both bone and articular cartilage. This result supports this thesis in highlighting the capability of osteoclasts to degrade different substrates i.e. bone, calcified cartilage and articular cartilage, via MMPs. Unfortunately, the lack of sensitivity of the hydroxyproline assay did not allow us to assess the collagen release of osteoclast-cartilage culture in the presence of inhibitors.

This thesis also shows that osteoclasts on cellular cartilage require MMPs to degrade the ECM. The degree of inhibition of osteoclast-mediated cartilage degradation by GM6001 was higher in cellular cartilage, suggesting that chondrocyte activity also drives MMP-dependent GAG release. This is supported by that observation that cellular, but not acellular, cartilage explants without osteoclasts also showed a significant decrease of GAG release in the presence of GM6001. Brown et al used multiple inhibitors of MMPs on

bovine articular and nasal cartilage to show that proteoglycan breakdown stimulated by IL-1, TNF or retinoic acid required MMPs[256]. The experiments in this chapter use GM6001 which is broad spectrum MMP inhibitor and therefore cannot determine which type of MMP is involved in this process.

Surprisingly, in the absence of osteoclasts on cellular cartilage, bafilomycin significantly decreased the amount of GAG released at day 10. This decrease was not seen with acellular cartilage. Hence, it is possible that V-ATPase activity drive the response of chondrocytes to bafilomycin. Yocum et al observed that monolayers of chondrocytes and cartilage explants stimulated by IL-1 significantly decreased the proteoglycan degradation in the presence of this inhibitor[257]. They suggested that bafilomycin induces a disruption of the acidification of lysosomes preventing the cytokine stimulated proteoglycan degradation[257,258]. It is possible that live chondrocytes, which are known to amplify the degradation of proteoglycans, have been inhibited by the bafilomycin.

The third objective was to investigate whether osteoclast-driven cartilage degradation was due to direct contact with the substrate or to the release of paracrine factors by osteoclasts. Experiments with osteoclasts grown on plastic beneath pieces of cellular or acellular cartilage in a transwell insert were performed to determine if being in contact with cartilage was essential for osteoclasts to degrade this substrate. No differences of GAG release were seen when the experiment was performed with acellular or cellular cartilage. These observations suggested that the contact between osteoclasts and cartilage was necessary for the proteoglycan degradation and osteoclasts on

plastic did not release paracrine factors that were able to degrade the cartilage ECM.

To investigate whether actively resorbing osteoclasts within bone are able to release paracrine factors to degrade cartilage, the same experiment has been performed with osteoclasts resorbing dentine instead of being on plastic. No differences of GAG release were seen when the experiment was performed with acellular cartilage. Active bone-resorbing osteoclasts may however affect chondrocytes embedded in the cartilage ECM; a significant decrease of GAG release was observed when compared with the 'no osteoclasts' control in cultures with cellular cartilage. The results were in agreement with the level of GAG release obtained when osteoclasts were in contact with cartilage. This suggested a protective response from the chondrocytes in response to the presence of the products released during bone resorption by osteoclasts and/or to the release of paracrine factors by these osteoclasts (**Figure 4.14 B.**).

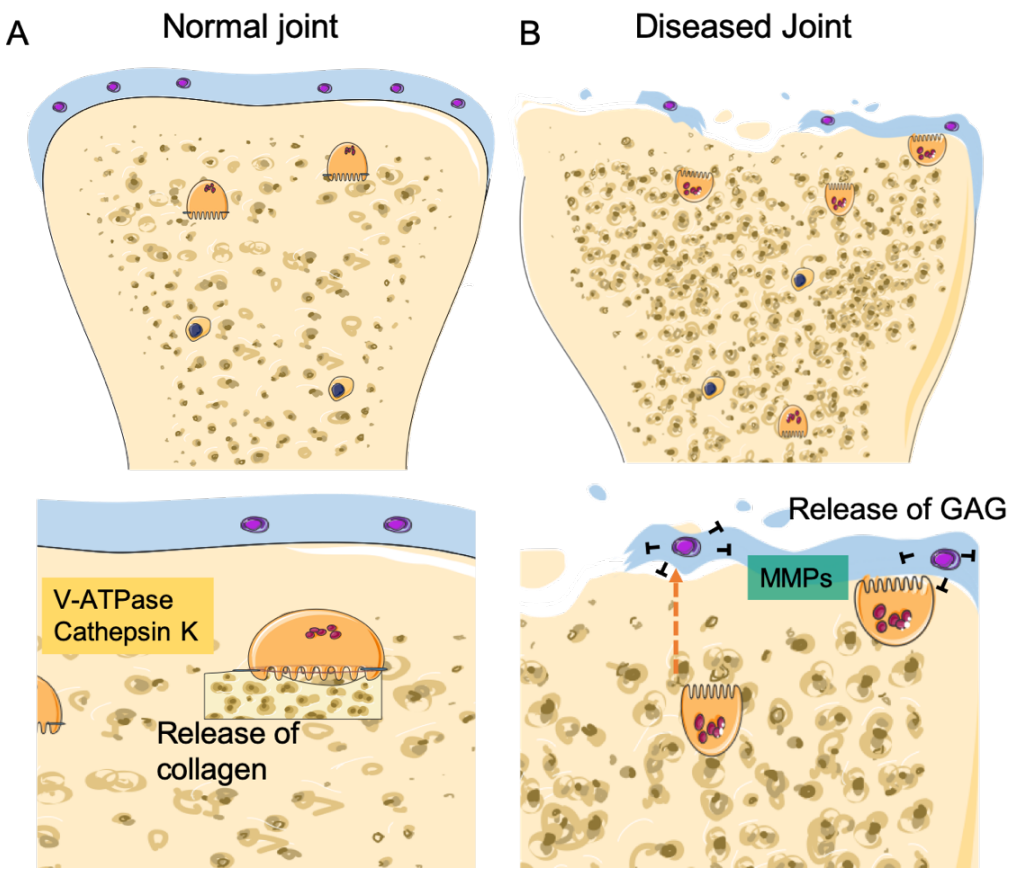


Figure 4.14 Schematic representation of the results of Chapter 4. A. In the normal joint bone homeostasis is maintained by a balance between bone resorption by osteoclasts and bone formation by osteoblasts. Osteoclasts in the subchondral bone degrade minerals via acidification and cathepsin K degrades bone matrix. Osteoclasts resorbing bone enhance chondrocyte behavior to protect their ECM. **B.** Osteoclasts in contact with cartilage use MMPs to degrade cartilage. Chondrocytes amplify the degradative effect of osteoclasts or osteoclasts increase cartilage degradation by chondrocytes. Osteoclasts degrading bone release paracrine factors or bone degradation products that induce a chondroprotection of the GAG release.

In parallel to the quantification of GAG released in the media, the amount of collagen was measured via the hydroxyproline assay. Unfortunately, it was not possible to culture osteoclasts on dentine and assess collagen release from cartilage, since the type I collagen release from dentine would also be detected by the hydroxyproline assay, making it impossible to determine specific effects on type II collagen release from cartilage.

Therefore, the collagen assay was performed with osteoclasts cultured on plastic. When cellular, but not acellular cartilage explants were in the transwell a significant increase of collagen seen. This may suggest that osteoclasts release a paracrine factor that could degrade type II collagen. However, this is unlikely for two reasons; osteoclasts directly in contact with cellular cartilage did not degrade type II collagen and osteoclasts cultured on plastic with acellular cartilage in the transwell did not induce an increase in collagen release. Therefore, it is most probable that osteoclasts grown on plastic release a paracrine factor that can alter the behaviour of chondrocytes that in response degrade type II collagen via the release of proteinases or induce the loss of the chondrocyte protective effect.

To further investigate whether chondrocytes degrade collagen of the ECM in response to active bone-resorbing osteoclasts, CTX-I and CTX-II assays could be performed on osteoclasts on dentine with pieces of cartilage in the transwell. The type I collagen present in the media would come from the resorption of the dentine and type II collagen would be from the degradation of cartilage. If type II collagen release was observed in cultures with cellular cartilage, this could be due to a paracrine factor secreted from osteoclasts on dentine that either directly degrades the type II collagen or induces the chondrocytes to degrade the matrix via e.g. MMPs and ADAMTSs. Doing the same experiment with acellular cartilage will help us to distinguish these hypotheses. If type II collagen release is increased in cultures with acellular cartilage it will mean that osteoclasts can directly degrades the type II collagen It is possible that the proposed CTXI / CTXII

experiment would reveal that bone-resorbing osteoclasts do not degrade collagen from cartilage. This would suggest that collagen degradation is unique to osteoclasts present away from their normal (bone) substrate, making it particularly relevant to disease conditions when osteoclasts are directly in contact with cartilage. This chapter shows that osteoclast activity is highly dependent on the substrate that the osteoclasts were on. Osteoclasts on plastic do not release factors that affect cartilage GAG release, but they do produce factors that increase collagen release from cellular cartilage (ie inhibit the protective effect of chondrocytes on the ECM), whereas osteoclasts on dentine enhance the chondrocyte protective effect on proteoglycan.

Finally, the last objective of this chapter was to understand whether chondrocytes affect the formation and activity of osteoclasts on plastic and dentine through direct or indirect interactions. It has been shown that an interaction between osteoclasts and chondrocytes is possible and this interaction is not the same when the cells were on plastic or on dentine. Finally, chondrocytes cultured on dentine decreased osteoclasts formation and activity.

Direct co-culture of osteoclasts and chondrocytes on plastic showed increased formation of large osteoclasts, potentially due to changes in gene expression of *RANKL* / *OPG* ratio in the chondrocytes. Conversely, direct and indirect co-culture of osteoclasts and chondrocytes on dentine decreased formation of osteoclasts, potentially due to a reduced *RANKL* / *OPG* ratio. This is in agreement with the results from the cartilage transwell experiments in this thesis: when osteoclasts are on dentine chondrocyte-osteoclast

interactions inhibit joint damage, whereas when osteoclasts are away from their natural substrate chondrocyte-osteoclast interactions promote joint damage. Martínez-Calatrava et al observed that co-cultures of human chondrocytes with PBMCs produced RANKL and induced osteoclast differentiation[244]. This experiment was conducted on plastic[244] and is in agreement with results of this thesis. Bone marrow stromal cells and osteoblasts are thought to be the major players in regulating osteoclast differentiation and activity through expressing RANKL and OPG cytokines. OPG is a soluble decoy receptor to RANKL, competing with RANK for RANKL binding. The absence of interaction between RANK and RANKL inhibits osteoclast differentiation and function. RANKL has been localised in the middle and deep zone of articular cartilage and correlated to the degeneration of cartilage in OA and the presence of osteoclasts[244]. Bertuglia et al suggested that chondrocytes may have a role in recruiting osteoclasts from the subchondral bone to the calcified cartilage[184]. This thesis suggests that expression of RANKL / OPG by chondrocytes could be at least part of the mechanism by which chondrocytes recruit osteoclasts and / or how chondrocytes modulate their activity (**Figure 4.15**). Moreover, *in vivo*, OPG is likely to also affect other bone cells via its interaction with RANKL and previous work has shown it can decrease the apoptosis of osteoclasts[259] and chondrocytes[196] via its second ligand; TNF apoptosis related inducing ligand (TRAIL).

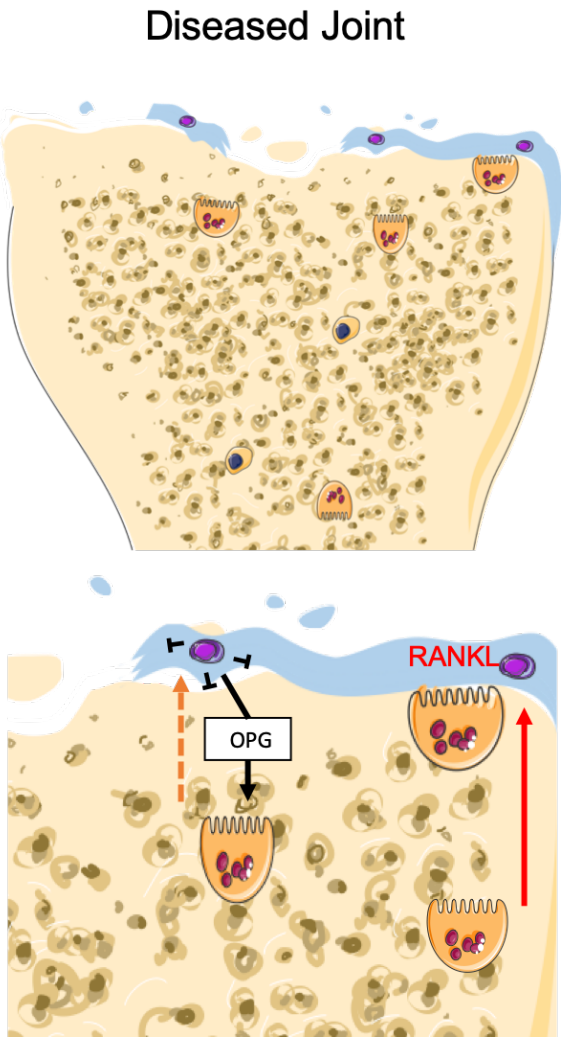


Figure 4.15 Schematic representation of the results of Chapter 4. Osteoclasts degrading subchondral bone release paracrine factors and/or the products resulting from bone matrix degradation alter chondrocytes activity regarding the maintenance of the ECM integrity. Chondrocytes secrete OPG as part of chondroprotection. In disease this is over-ridden by increased RANKL production: from the literature, chondrocytes in OA and RA express RANKL [184,244] which is a chemoattractant for osteoclasts and might explain how osteoclasts leave their normal bone substrate.

In summary, when osteoclasts are in their 'normal' bone environment paracrine factors produce during bone degradation help to maintain the protective effect of chondrocytes on the cartilage ECM. At the same time, chondrocytes express OPG that keep the osteoclasts in distance from the

cartilage. Once the osteoclasts leave their normal bone substrate (e.g. to invade cartilage in disease) the interaction between chondrocytes and osteoclasts may instead shift to activate osteoclasts towards cartilage degradation (via MMPs) and prevent chondrocyte protection of its ECM. In OA, the neo-vascularisation of the subchondral bone might encourage the formation of osteoclasts next to the mineralised cartilage. The presence of microcracks could facilitate the diffusion of local factors such as RANKL that increase the recruitment, formation and activation of osteoclasts. At the same time, osteoclasts located in the bone-cartilage interface produce factors such as MMPs (when they are in direct contact with cartilage) that degrade the surrounding cartilaginous matrix.

This chapter adds to the data in chapter 3 that osteoclasts formation and activity were highly dependent on the substrate that the osteoclasts were on. In chapter 3 the morphology and the expression profile of osteoclasts markers (by RT-qPCR) was shown to be different when they were cultured on plastic compare to dentine and cartilage. In chapter 4, it was shown that osteoclasts on plastic do not release factors that affect cartilage GAG release, but they produce factors that increase collagen release from cellular cartilage. It is possible that osteoclasts on plastic attempted to degrade their substrates and released factors in the media that *in vivo* would be released in the resorption lacuna. Therefore, secreted factors such as cathepsin K and proteinases are released in the media and drive the degradation of the cellular cartilage. Another explanation could be that paracrine factors secreted by osteoclasts altered the behaviour of chondrocytes that in response degraded type II

collagen. Co-culture experiments in this chapter shows increased formation of large osteoclasts on plastic, potentially due to an increased RANKL / OPG ratio in the chondrocytes. Plastic is not a natural substrate for osteoclasts and therefore osteoclasts may not be truly active, however further investigation regarding the differences between substrates is necessary.

CONCLUSION

Osteoclasts can degrade cartilage whether chondrocytes are metabolically active or inactive. The use of GM6001 revealed that osteoclasts degrade cartilage via MMPs, causing release of proteoglycans. The contact between osteoclasts and the cartilage is essential to this process. Conversely, osteoclasts on plastic were able to modify the release of collagen by changing chondrocytes activity via secretion of paracrine factors. The ability of osteoclasts to interact with chondrocytes has been shown *in vitro*. When chondrocytes are active osteoclasts may modify their behaviour depending on the substrate to which the osteoclasts are attached (which is protective on dentine and catabolic on glass / plastic). Similarly, direct and indirect co-culture of chondrocytes and osteoclasts revealed the ability of chondrocytes to affect osteoclasts formation and activity potentially via the expression of *OPG*.

Chapter 5

OSTEOCLASTS SECRETE MMP-8 AND MMP-9 TO DEGRADE CARTILAGE

INTRODUCTION

The morphological characteristics of osteoclasts cultured on cartilage and their expression of the protein markers of osteoclasts was shown in Chapter 3. The ability of osteoclasts to degrade proteoglycans was also demonstrated in this chapter. In chapter 4 the use of the inhibitor GM6001 showed that the MMP family is primarily responsible for cartilage degradation by osteoclasts. The primary objective of this chapter is to identify the key candidate(s) driving osteoclast-mediated MMP-dependent cartilage degradation. Following up on the observation that substrate critically regulates osteoclast function (see Chapter 4), the second aim is to compare how substrate affects osteoclast gene expression. As GM6001 is a broad spectrum MMP inhibitor, the specific MMPs involved in cartilage degradation by osteoclasts remain unknown. In this introduction, the MMPs and ADAMTSs that could be involved in osteoclast-driven degradation of the cartilage extracellular matrix will be discussed. The TIMPs are endogenous MMP inhibitors that have been used in this chapter to allow us to determine the subtype of MMPs involved in cartilage degradation. To reveal the key candidates responsible for cartilage degradation by osteoclasts gene expression profiling by RT-qPCR and RNA sequencing was carried out. By comparing gene expression profiles of osteoclasts on different substrates; plastic, dentine and cartilage and the impact of the substrate on gene expression has been determined. Since GM6001 did not completely abrogate the degradation of proteoglycans, it is possible that MMP independent

degradation does occur. Gene expression and western blot were therefore used to investigate the whether any proteinases from the ADAMTS family was also involved in cartilage degradation.

5.1 MMPs

MMPs are classified into 6 subgroups; collagenases, gelatinases, stromelysins, matrilysins, membrane-type MMPs and other non-classified MMPs. Except the membrane-type MMPs that are anchored to the plasma membrane, other MMPs are soluble and therefore secreted as extracellular protein. MMPs have been shown to regulate osteoclast recruitment, coupling of bone resorption and formation, osteoblast survival and angiogenesis.

5.1.1 Collagenases

The triple-helical domains of intact collagen type I, II and III are resistant to digestion by most proteases. Collagenases orchestrate the first cleavage of the collagen fibres allowing other MMPs to degrade the unwounded collagen. The collagenases-1, -2 and -3 are respectively called MMP-1, MMP-8 and MMP-13. They can cleave collagen at a single and specific location; glycine-leucine or glycine-isoleucine. MMP-1 and MMP-8 show 72 % homology in amino acid sequence but differ in substrate specificity. MMP-1, also called interstitial or fibroblast collagenase, is highly present in the synovial fluid of patients suffering from joint injuries and osteoarthritis. MMP-1 degrades, preferentially, collagen type III and is mainly found in the superficial zone of osteoarthritic articular cartilage where type III collagen is present[260,261]. MMP-1 is also highly abundant in the

synovial fluid of rheumatoid arthritis patients, correlating with inflammatory activity.

MMP-8 degrades collagen type I, II and III with a preference for type I and it can also degrade aggrecan. MMP-8 cleaves preferentially aggrecan at the MMP site but it also has the ability to cleave aggrecan at the same site as aggrecanase cleaves; (Glu^{373}-Ala^{374}) in the interglobular domain of aggrecan[262,263]. For this reason, Fosang et al. and Cole et al. suggested that MMP-8 might be the unidentified aggrecanase[264,265] but aggrecanase enzymes are in fact part of the ADAMTS family.

MMP-8 was previously called neutrophil collagenase or polymorphonuclear leukocyte collagenase since it was thought that neutrophils were the only cells producing it[266,267]. Fosang et al and Arner et al demonstrated the ability of MMP-8 to degrade aggrecan[265,268]. One year later, the expression of MMP-8 was undetected in normal human articular chondrocytes collected from 6 cadavers and found to be upregulated in 12 patients with OA[269] suggesting the role of MMP8 in pathology. The same group tested the MMP response of porcine chondrocytes to cytokines and retinoic acid, they found that mRNA level of MMP8 increased only when chondrocytes were treated with TNF-α. Conversely, Cole et al observed that MMP-8 protein and mRNA were present in 13 human cadavers chondrocytes and it was up-regulated in following treatment with IL-1β to mimic the initiation and progression of OA[264].

Cartilage degeneration was monitored over time in a transgenic Del1 mouse model of OA. These mice harbored a 15 amino acid deletion in the type II collagen chain predisposing the animals to early onset OA. mRNA

levels of MMP8 were identical between the control and OA mice and after 2 months MMP8 expression increased with aging in both groups[270]. MMP-8 expression was detected in cultured rheumatoid synovial fibroblasts from RA patients and was upregulated in the presence of TNF-α[271]. It is now well known that various other types of cells also express *MMP8* including stem cells[272], endothelial cells[273], smooth muscle cells[274], chondrocytes[264], eosinophils[275] and macrophages[276]. Other studies have shown that MMP-8 is involved in pathological conditions such as atherosclerosis[272,277], acute hepatitis[278], acute lung injury[267] and cancers[279].

MMP-13 is the most efficient to degrade collagen type II and gelatin compared to MMP-8 and MMP-1 which are mainly found in the superficial zone of the articular cartilage in osteoarthritis but MMP-13 can be found in deep and superficial layers[280]. Cartilage degradation with a joint pathology similar to OA is observed in transgenic mice that express constitutively active human MMP-13 in hyaline cartilage[281]. Conversely, MMP-13-null mice exhibited cartilage protected from degradation in the surgically induced OA model[282]. MMP-13 is the predominant MMP expressed by chondrocytes and, although it preferentially degrades type II collagen, it can also degrade other types of collagen such as I, III, VII and X as well as gelatin and aggrecan.

The gelatinase A (MMP-2) and the membrane type 1 MMP (MMP-14) have a collagenolytic activity, but they belong to other subgroups due to their domain compositions.

5.1.2 Gelatinases

Gelatin is a poor substrate for collagenases suggesting that another group of proteases is able to degrade gelatin. Harris et al. were the first to observe this enzyme in explant culture of rheumatoid synovial fibroblasts[283,284]. Sellers et al. observed that rabbit bones in culture produce collagenase and a metalloproteinase that was able to degrade gelatin, suggesting the name of gelatinase[285]. There are two gelatinases: MMP-2 known as gelatinase A and MMP-9 known as gelatinase B. The domain structure is similar to the collagenases except for the three repeats of a type 2 fibronectin in their catalytic domains allowing them to bind to their substrate. MMP-2 also cleaves type IV collagen and preferentially degrades denatured collagen and aggrecan at the MMPs common site. It is also able to cleave type I, II and III collagens. Gelatinases plays an important role in the growth and metastasis of tumours[286]. MMP-2 activates other MMPs such as proMMP-9 and proMMP-13. MMP-2 is important in angiogenesis; it can regulate the degradation of newly formed vessels by the release of cytokines and growth factors. Mutations in human MMP-2 resulting in the absence of the active enzyme are linked to a form of multicentric osteolysis and arthritis called vanishing bone syndrome. This disorder is characterised by a progressive bone loss and joint destruction causing skeletal deformities and functional impairment[287]. Mice lacking MMP-2 showed disrupted skeletal delay and skull deformities due to intramembranous ossification defects[288].

MMP-9 is part of the multi-domain enzyme family with many functions in biology and pathology. MMP-9 was originally identified as a human leukocyte gelatinase with the ability to degrade type V collagen. The linker

domain of MMP-9 is 64 amino acids long and is highly O-glycosylated. This domain was previously called the collagen V-like domain because it was thought to be responsible for the specificity of MMP-9 for type V collagen. A deletion in the O-glycosylated domain reduces the efficiency of degradation of large gelatinous substrates and disrupts endogenous inhibition by TIMPs[289].

MMP-9 is mostly active during embryonic development during angiogenesis in the growth plate and apoptosis of hypertrophic chondrocytes[290]. Due to its role in angiogenesis, MMP-9 is also highly expressed during wound healing[282]. Ahrens et al demonstrated that in RA the levels of MMP-9 were elevated in serum and joint synovial fluid and this increase was correlated with disease progression and severity[291]. MMP-9 is also increased in OA suggesting a potential role in cartilage destruction[292].

5.1.3 Membrane-type MMPs

Most MT-MMPs are anchored by a single-pass transmembrane domain followed by an intracellular cytoplasmic tail that is considered to be important for the localisation of the enzyme at the cell surface[293]. This family can be divided into two subgroups; the type I transmembrane proteins including MMP-14 (or MT1-MMP), MMP-15, MMP-16 and MMP-24 and the glycosylphosphatidylinositol-anchored proteins including MMP-17 and MMP-25. All these MMPs are activated intracellularly and the active enzymes are expressed at the cell surface. MMP-14 null mice show skeletal abnormalities during post-natal development and die within 3 weeks[294,295]. MMP-14 can cleave collagen type I, II and III in a similar way to collagenases

and is also capable of cleavage of many membrane-anchored proteins such as E-cadherin, integrins and several cell surface proteins. MMP-14 is a major activator of pro-MMP-2, a trimeric complex of TIMP2-pro-MMP-2 and MMP-14 leading to the removal of the propeptide from pro-MMP-2. Other MT-MMPs are highly expressed in cancer cells, for example MMP-15, also called MT2-MMP, is over-expressed in breast cancer[286].

5.2 ADAMTS

ADAMTS-1, ADAMTS-4 and ADAMTS-5 are the only three aggrecanases that can cleave aggrecan at four sites in the GAG-rich region of proteoglycan in addition to the interglobular domain. ADAMTS-8 and ADAMTS-9 can also cleave aggrecan but show much lower activity than ADAMTS-4 and ADAMTS-5.

5.2.1 ADAMTS-1

ADAMTS-1 is expressed in human cartilage and synovium and has been shown to cleave proteoglycans such as aggrecan and versican[78]. Chockalingam et al shown, in rats with surgically induced OA, that the degradation of aggrecan was significantly reduced by using an inhibitor which binds to the zinc of only ADAMTS-4 and ADAMTS-5. Therefore, the interest in ADAMTS-1 was lost in favour of ADAMTS-4 and ADAMTS-5 as targets for novel OA therapies.

5.2.2 ADAMTS-4 and ADAMTS-5

Murine inflammatory arthritis models are induced using an antigen or collagen injected into the knee joint whilst OA models generally utilise

surgical joint destabilisation. In inflammatory and non-inflammatory models of arthritis ADAMTS-5 null mice are protected from cartilage aggrecan loss and cartilage erosion[296,297]. Genetically modified mice with a mutation that renders the interglobular domain (IGD) of aggrecan resistant to aggrecanase but that retain a chondroitin sulphate rich domain that is susceptible to cleavage provide an opportunity to analyse the contribution of IGD cleavage to cartilage pathology *in vivo*. Aggrecan loss and cartilage erosion were significantly decreased in surgically induced OA mice and a model of inflammatory arthritis[298]. Despite the fact that only one site of aggrecanase is located in the IGD, it appears that this site is critically involved in cartilage pathology[298].

In humans, ADAMTS-4 is induced by pro-inflammatory cytokines in the OA synovium and cartilage whereas ADAMTS-5 is constitutively present[299]. Experiments have demonstrated that ADAMTS-4 plays a significant role in aggrecanolysis *in vitro;* using siRNA for ADAMTS-4 attenuated the degradation of aggrecan in cytokine-stimulated normal cartilage[300]. Neutralising antibodies against ADAMTS-4 and ADAMTS-5 in pig chondrocytes or bovine cartilage have a 90 % reduction in aggrecanase activity in cytokine-stimulated normal cartilage [301,302].

5.2.3 Other ADAMTSs

ADAMTS-2, ADAMTS-3 and ADAMTS-14 are responsible for removing the N-terminal pro-peptide of pro-collagen enabling collagen fibril formation[303]. Their expression is increased in human OA cartilage, but this may reflect an attempted repair response by osteoarthritic chondrocytes[303].

Any inhibitor for OA therapy should not abolish the activity of these three enzymes since their expression is important for cartilage homeostasis and repair[78].

5.3 Cleavage of aggrecan by MMPs and ADAMTSs

There is a consensus on the ability of the majority of MMPs to cleave aggrecans at a specific site: Asn[341]~Phe[342] *in vivo* and *in vitro*[55,262,265,304–306] (

Figure 5.1). Additional MMP-sensitive sites have also been reported: next to G2 within the interglobular domain (IGD) (Asp[441]~[442]Leu) [304,306]and between G2 and G3 before the keratan sulphate enrichment region (Gly[666]~[667]Ile)[307]. MMP-1, MMP-7 and MMP-8 can cleave aggrecan at Asp[441]~[442]Leu. More sites have also been reported within the chondroitin sulphate region indicating that MMP-1, MMP-3, MMP-7, MMP-8 and MMP-12 can degrade aggrecan at multiple sites[263,308]. It is interesting that four different metalloproteinases (Gelatinase, collagenase, Stromelysin and matrylisin) with different substrate specificities can all cleave at the same site in the IGD.

MMP-derived aggrecan fragments can be detected *in vivo* in normal cartilage and in synovial fluid from normal, osteoarthritis and knee-injured patients[61]. However, the contribution of MMP cleavage in the IGD of aggrecan, generating fragments in knee cartilage from injured and OA subjects, is low compared with fragments produced by aggrecanase cleavage in the IGD. Struglics et al. suggested that MMPs are mainly

involved in aggrecan turnover in healthy joints and might have a less-active role in aggrecan degradation during knee injury and OA[309]. Little et al. and Van Meurs et al. showed that aggrecan-degrading MMPs were active only at later stages of cartilage catabolism when ECM degradation had already occurred[308,310,311]. In 2012, a study assessed the cleavage efficiency of MMPs relative to aggrecanases and their contribution to aggrecan proteolysis *in vitro*. Durigova et al. found that the cleavage efficiency was relatively low compared to aggrecanase. This might explain the minor contribution of MMPs to aggrecan catabolism *in vivo*[263]. MMP-8 preferentially cleaves aggrecan at the MMP site ($Asn^{341}\sim^{342}Phe$) but it also has the ability to cleave aggrecan at the same site as aggrecanase cleaves ($Glu^{373}\sim^{374}Ala$) within the IGD[263]. However, this cleavage is only visible when high concentrations of human MMP-8 are used indicating that this is not a preferred cleavage site[262,265,312]. Buttner et al also suggested that MMP-14 can also cleave aggrecan at the aggrecanase site[313].

$Glu^{373}\sim^{374}Ala$ is the main aggrecanase sensitive site where ADAMTS-4 and ADAMTS-5 cleave the aggrecan core protein[56] (

Figure 5.1). There are four other aggrecanase cleavage sites situated in the GAG rich region of aggrecan molecules between the globular domains G2 and G3 within the chondroitin sulphate region. These sites include $Glu^{1545}\sim^{1546}Gly$, $Glu^{1714}\sim^{1715}Gly$, $Glu^{1819}\sim^{1820}Ala$ and $Glu^{1919}\sim^{1920}Leu$ [314–316]. More fragments can be found in human articular cartilage extracts suggesting that there are probably multiple and complex catalytic processes contributing to the net loss of aggrecan from cartilage[305,317]. However, it is

important to keep in mind that cleavage sites shown *in vitro* do not necessarily also occur *in vivo*. ADAMTS-1 preferentially cleaves aggrecan at $Glu^{1919}\sim^{1920}Leu$ in the chondroitin sulphate region[77,318]. There is increasing evidence showing that the IGD is a key site for the attack of aggrecan by proteinases. Cleavage in this region is important as it releases a major proteoglycan fragment from the G1 domain with binds to the aggregates. The hypothesis for aggrecan degradation is that ADAMTSs and MMPs cleave first the chondroitin sulphate rich domain which liberate parts of aggrecans and then the MMPs cleave their favoured site in the IGD that is more accessible[316]. Another exception to the rules for aggrecan neoepitope specificity is that ADAMTS-1 and ADAMTS-4 can cleave at the MMP site ($Asn^{341}\sim^{342}Phe$)[319].

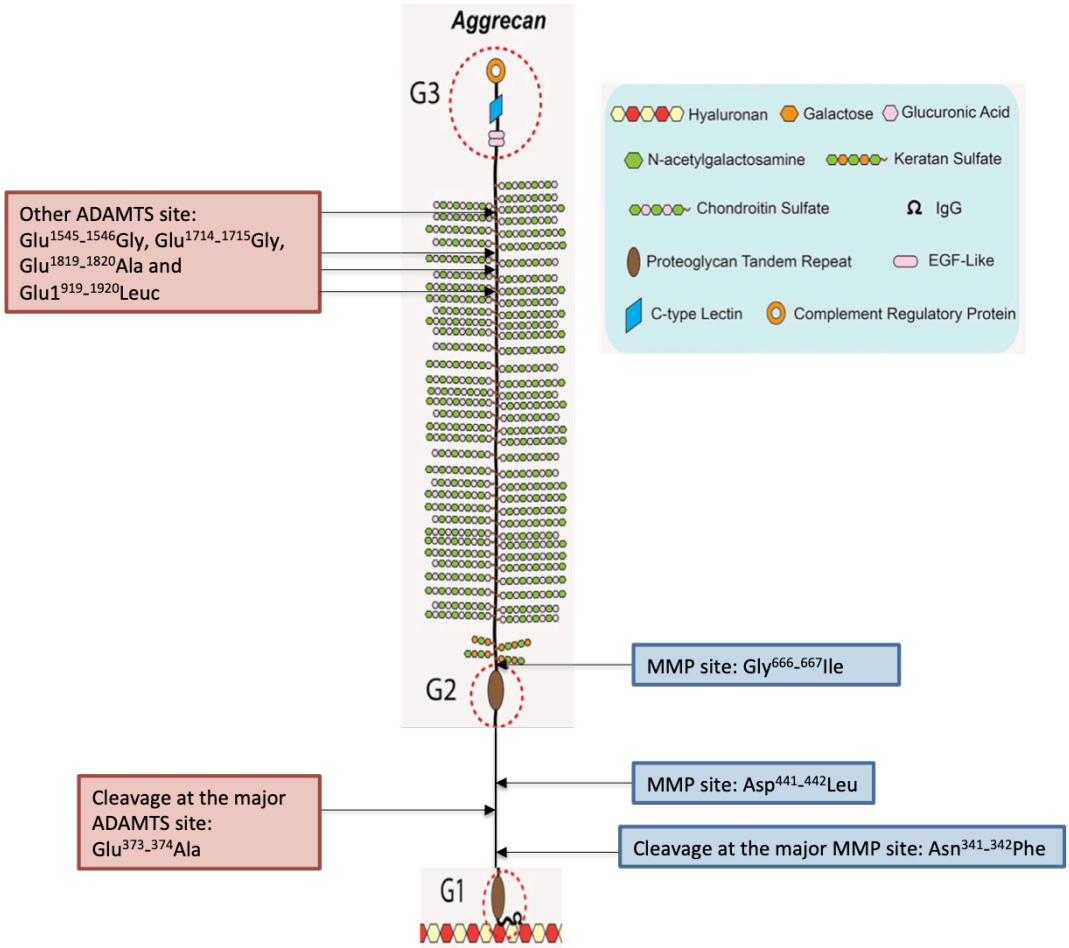


Figure 5.1 Aggrecanase (in red) and MMP (in blue) cleavage sites found within aggrecans.

5.4 TIMPs

TIMPs are the endogenous inhibitors of MMPs, ADAMs and ADAMTSs. The specificity of the inhibition varies, for example TIMP-1 inhibits all MMPs except MT-MMPs and also inhibits ADAM-10 activity. *Timp1* null mice exhibit significant learning and memory impairment which is not thought to be related to direct actions of TIMP-1 on memory but linked to the effect of abnormal ECM turnover on neuron development[90]. Other *Timp1* null mouse studies identified alterations in reproduction and steroid-

genesis, implicating a role for TIMP-1 in regulating the murine reproductive cycle[320]. TIMP-1 is an important regulator of cell growth, differentiation and apoptosis suggesting that TIMPs behave as a cytokine regulating directly downstream pathways.

TIMP-2 inhibits all MMPs including MT-MMPs and is important in the cell-surface activation of pro-MMP-2. A complex is formed between pro-MMP-2, TIMP-2 and MT1-MMP (MMP-14) to cleave the pro-domain of the zymogen. *TIMP-2* null mice confirmed that TIMP-2 is required for pro-MMP-2 activation *in vivo* and *in vitro*. It is important to note that exogenous addition of TIMP-2 could restore activation of pro-MMP-2 *in vitro*[92].

Disruption of the balance between the production of MMPs and ADAMTS and their inhibition may result in diseases associated with disorganised ECM turnover in tissue remodelling, arthritis and cancer. Despite the increase of TIMP expression, proteolytic degradation of the articular cartilage still occurs in diseased joints, suggesting an imbalance between MMP and TIMP activity in favour of MMPs[90].

It is well known that the microenvironment *in vivo* influences cell behaviour and should be considered in *in vitro* experiments. For example, the mechanics and the biochemical characteristics of the bone tissue is important *in vivo* to regulate cellular activity. Cytokines secreted by osteoblasts or osteocytes are important to regulate osteoclast activity[150]. In this thesis, the possible influence of the substrate (the surface on which osteoclasts are cultured) on osteoclast activity has been highlighted – and reflects difference in the cartilage and bone environment where osteoclasts are found *in vivo*. Indeed, in chapter 3 the organization of the cytoskeleton was shown to be

different on glass, dentine and cartilage. A RT-qPCR for the genes known to be expressed in active osteoclasts: *CA2, CLCN7, STAT3, V-ATPase, CSTK* and *MMP9* were compared in osteoclasts on plastic, dentine and cartilage. The significant increase of *CTSK* and *MMP9* in osteoclasts on plastic revealed the importance of the surface and highlighted the necessity to look deeper into expression profile. In chapter 4, the release of paracrine factors enabling degradation of cartilage explants in transwells, was not the same when osteoclasts were cultured on plastic or on dentine. This implies that different substrates influence both the morphology and function of osteoclasts. Differences in gene expression in osteoclasts cultured on plastic, dentine and cartilage has never been characterised and will be a focus of the current chapter.

5.5 Objectives

The overall objective of this chapter was to identify the key candidate(s) driving osteoclast-mediated MMP-dependent cartilage degradation. Following the observation that substrate critically regulates osteoclast function (see Chapter 4), the second aim of this chapter was to compare how substrate affects osteoclast gene expression.

More precisely, this chapter aimed to

1. Determine whether the MMPs involved in cartilage degradation by osteoclasts were membrane type MMPs or soluble MMPs.
2. Use RNAseq to further identify the specific MMPs that drive degradation on different substrates.

3. Elucidate whether gene expression differences exist between osteoclasts cultured on plastic, dentine or cartilage using RNA sequencing.
4. Confirm the expression and activity of MMPs identified in aims 1 and 2 and their effects on cartilage degradation. It was hypothesised that siRNA for MMP8 and MMP9 would decrease the amount of proteoglycan degraded.

RESULTS

5.1 *MMP8* and *MMP9* are the key candidates responsible for cartilage degradation

5.1.1 Osteoclasts degrade cartilage via soluble MMPs

It was shown in chapter 4 that osteoclasts degrade cartilage matrix via MMPs, however as the broad-spectrum MMP inhibitor GM6001was used, it did not provide information on the specific MMPs responsible. To establish whether the MMPs responsible for cartilage degradation are soluble or membrane-bound inhibition by TIMPs was utilised. To refine our knowledge on the key candidate(s) further RT-qPCR and then RNAseq were performed to compare the expression profile of osteoclasts on dentine with osteoclasts on cartilage.

TIMPs are the endogenous inhibitors of MMPs. TIMP-1 inhibits all MMPs except membrane-anchored MT-MMPs. To determine if the MMPs

involved in cartilage degradation were soluble or membrane type MMPs, osteoclasts on cartilage were cultured with recombinant TIMP1 protein and effects on GAG release were assessed. The total GAG release was significantly decreased in the presence of TIMP1 suggesting that the MMPs responsible for cartilage degradation were soluble proteins (**Figure 5.2 A.**). The same experiment was performed without osteoclasts to confirm that the inhibited MMPs were produced by the osteoclasts and no differences in GAG release were seen (**Appendix A.6 A.**).

To confirm that MMP14, the major MT-MMP in cartilage, was not involved in cartilage degradation by osteoclasts, a blocking antibody against MMP-14 was used. The presence of the blocking antibody did not alter osteoclast-driven GAG release from cartilage supporting our hypothesis that soluble MMPs mediate degradation of cartilage by osteoclasts (**Figure 5.2 B.**) however, it is important to note that possibly, another MT-MMP might be involved. To complement this experiment, osteoclast-free cartilage explants were cultured in presence of the anti-MMP14 neutralising antibody and no changes in GAG release were seen (**Appendix A.6 B.**)

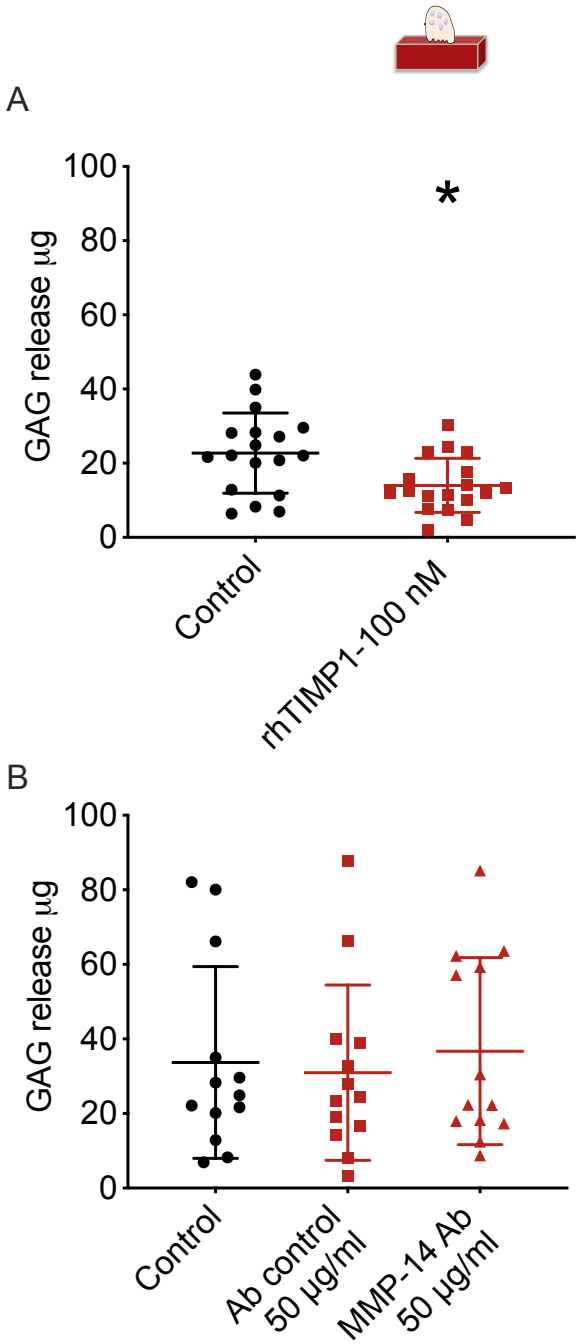


Figure 5.2 Soluble MMPs are involved in cartilage degradation. Osteoclasts were cultured for 10 days on acellular cartilage. **A.** Total GAG release by osteoclasts cultured on cartilage without or with recombinant human TIMP1 and n=18. **B.** Total GAG release by osteoclasts on cartilage with monoclonal anti-MMP14 neutralising antibody or negative control antibody against intracellular desmin. *p<0.05 and n=13.

To narrow down which soluble MMPs could be involved in cartilage degradation the expression level of multiple MMPs (*MMP1, MMP2, MMP3, MMP7, MMP9, MMP12, MMP13*) was explored by RT-qPCR in osteoclasts cultured on dentine or cartilage (**Figure 5.3**). Since MMP-14 is known to be expressed in osteoclasts, its expression level has also been tested. The ability of ADAMTS-1, ADAMTS-4 and ADAMTS-5 to cleave cartilage is well known. To investigate if they are expressed in osteoclasts during cartilage degradation, a RT-qPCR was also performed for those 3 genes.

The basal levels of *MMP9* expression were high in osteoclasts on dentine and on cartilage (**Figure 5.3**). MMP-9 is one of the two proteolytic enzymes used by osteoclasts to degrade the organic bone matrix.

Conversely, *MMP12* was significantly downregulated in osteoclast-cartilage culture compared to osteoclast-dentine culture (**Figure 5.3**).

Among the three ADAMTSs tested only *ADAMTS-1* was detected in osteoclasts on dentine and cartilage, showing a trend to increase (not significant, $p<0.105$) when osteoclasts were on cartilage.

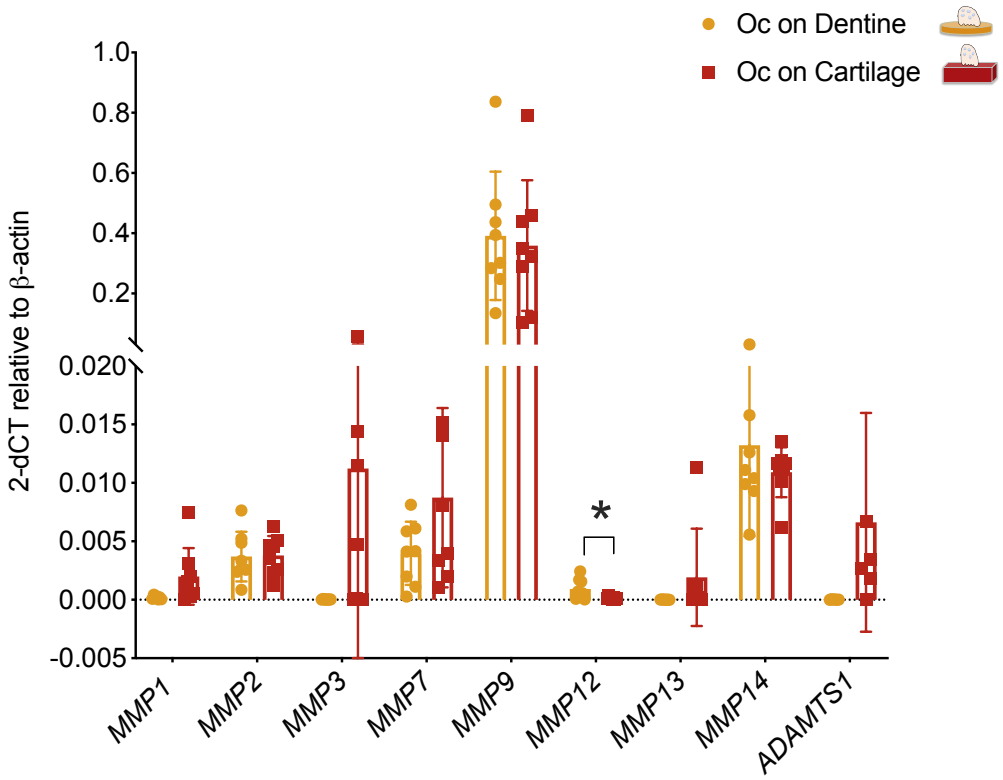


Figure 5.3 mRNA expression of MMPs in osteoclasts cultured on dentine and acellular cartilage. Gene expression relative to β-actin expressed in osteoclasts cultured on same substrate. * $p<0.05$ for comparison against osteoclasts on dentine and n=8.

5.1.2 RNA sequencing and its validation

It became evident that RNAseq should be used to interrogate if there were any other matrix degrading genes involved in cartilage degradation. The RNA sequencing experiment was performed with osteoclasts from 8 different blood donors cultured on plastic, dentine and cartilage. Initially, we focussed on comparing gene expression on the natural substrates; dentine and cartilage. The comparison of osteoclasts on plastic, dentine and cartilage will be discussed later on.

A stringent criterion was applied to determine the effects of differentially expressed genes where only those with level of expression such that p <0.05

and fold change was >1 were pursued further. Forty-one genes were differentially expressed in osteoclast-dentine culture compared with osteoclast-cartilage culture with a p value <0.05 (**Figure 5.4**).

The gene Epstein-Barr Virus Induced 3 (*EBI3*) was the most up-regulated (fold change: 3.63) in osteoclasts on dentine compared to osteoclasts on cartilage (**Figure 5.4** and **Figure 5.5** A.)

However, *MMP8* showed the greatest fold upregulation in osteoclasts on cartilage compared to osteoclasts on dentine. More precisely, the expression of *MMP8* was 8.89 times higher in osteoclasts on cartilage compared to osteoclasts on dentine. (**Figure 5.4** and **Figure 5.5 B.**).

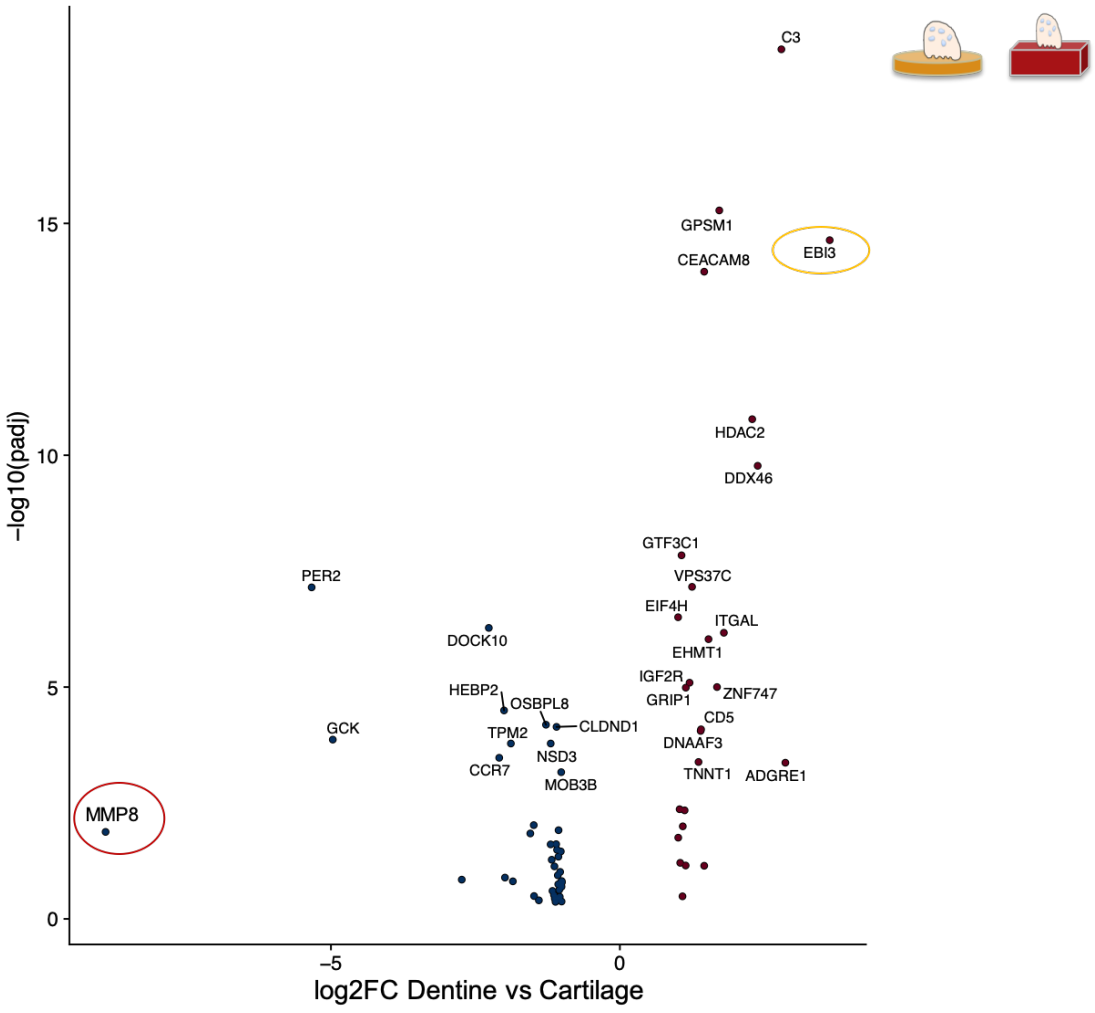


Figure 5.4 Volcano plot highlighting significantly different genes between osteoclasts on dentine and cartilage. red dot: osteoclasts dentine: and blue dot: osteoclasts on cartilage. Red circle shows the most numerically upregulated gene in osteoclast-cartilage culture. Yellow circle: showing the most numerically upregulated gene in osteoclast-dentine culture LFC: Log fold change and padj: p value adjusted

A

Gene	LFC	padj
EBI3	3.63120961	2.30E-15
ADGRE1	2.86388812	4.28E-04
C3	2.79503503	1.76E-19
DDX46	2.38487209	1.69E-10
HDAC2	2.2903217	1.67E-11
ITGAL	1.79970299	6.74E-07
GPSM1	1.72040895	5.25E-16
ZNF747	1.68091764	1.00E-05
EHMT1	1.53405134	9.27E-07
CEACAM8	1.45933975	1.10E-14
CD5	1.40490144	8.16E-05
DNAAF3	1.39791084	8.83E-05
TNNT1	1.36103603	4.13E-04
VPS37C	1.24908955	6.89E-08
IGF2R	1.20606078	8.05E-06

B

Gene	LFC	padj
MMP8	8.89993669	1.33E-02
PER2	5.33387028	7.07E-08
GCK	4.96826831	1.36E-04
DOCK10	2.26797421	5.30E-07
CCR7	2.0880772	3.35E-04
HEBP2	2.00439463	3.19E-05
TPM2	1.8862969	1.65E-04
STAG3	1.54982285	1.44E-02
H2AFY	1.49036968	9.50E-03
OSBPL8	1.27888291	6.49E-05
DIRAS1	1.19834275	2.47E-02
NSD3	1.19698843	1.65E-04
GATS	1.10256273	2.45E-02
CLDND1	1.09619631	7.22E-05
LGI2	1.08712524	3.24E-02

Figure 5.5 The top 15 over-expressed genes. A. In osteoclast cultured on dentine **B.** In osteoclast cultured on cartilage Green: The most numerically upregulated and red the least increased. LFC: Log fold change and padj: p value adjusted.

To confirm that *MMP8* was upregulated in osteoclasts cultured on cartilage, RT-qPCR was performed (**Figure 5.6 A.)**.

Two other genes up-regulated (Leucine-rich repeat glioma-inactivated family member 2 (*LGI2*) and down-regulated (the integrin subunit alpha L (*ITGAL*) on cartilage versus dentine were selected as additional controls (**Figure 5.6 B.** and **C.**).

According to the high expression of *MMP9* (by RT-qPCR) and *MMP8* (by RNAseq) in osteoclasts-cartilage culture, it was hypothesised that MMP-8 and MMP-9 were involved in cartilage matrix degradation.

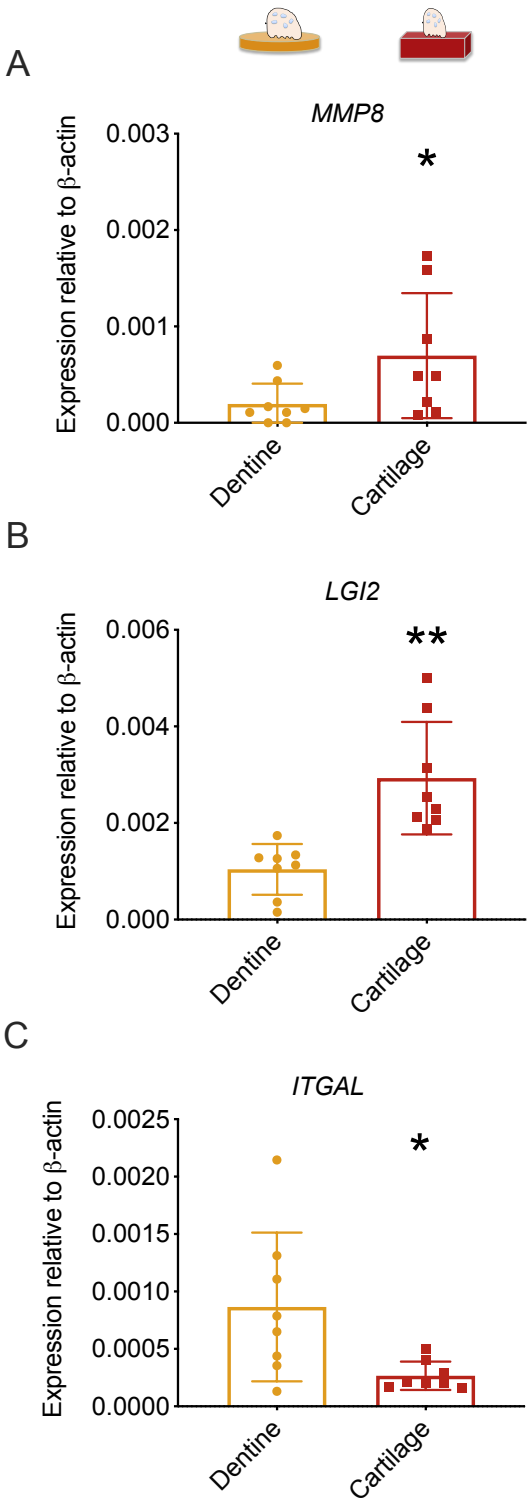


Figure 5.6 RT-qPCR validating gene expression differences between osteoclasts on dentine and osteoclasts on cartilage.A. Expression of MMP-8 relative to β-actin. **B.** Expression of LGI2 relative to β-actin. **C.** Expression of ITGAL relative to β-actin. * $p<0.05$, ** $p<0.001$ and n= 8.

5.2 Effect of substrate on osteoclast gene expression

In chapter 3 it was shown that if osteoclasts were cultured on cartilage or plastic, the sealing zone and therefore the resorption pit were not systematically present. In addition to this, the substrate also changed osteoclast activity as demonstrated in chapter 4.

Now, to further interrogates the effect of substrate on osteoclast activity, the expression of osteoclast markers on each substrate was compared by RNAseq. More specifically, osteoclasts on plastic (and therefore unable to digest the surface) were compared with osteoclasts resorbing bone (dentine) and degrading acellular cartilage.

Principal Component Analysis revealed distinct gene expression responses dependent on the surface on which osteoclasts were cultured (**Figure 5.7**). Distinct gene expression profiles were seen between osteoclasts cultured on plastic, dentine and cartilage. It important to notice that 3 preparations of osteoclasts cultured on cartilage appeared to be very similar to osteoclasts cultured on plastic.

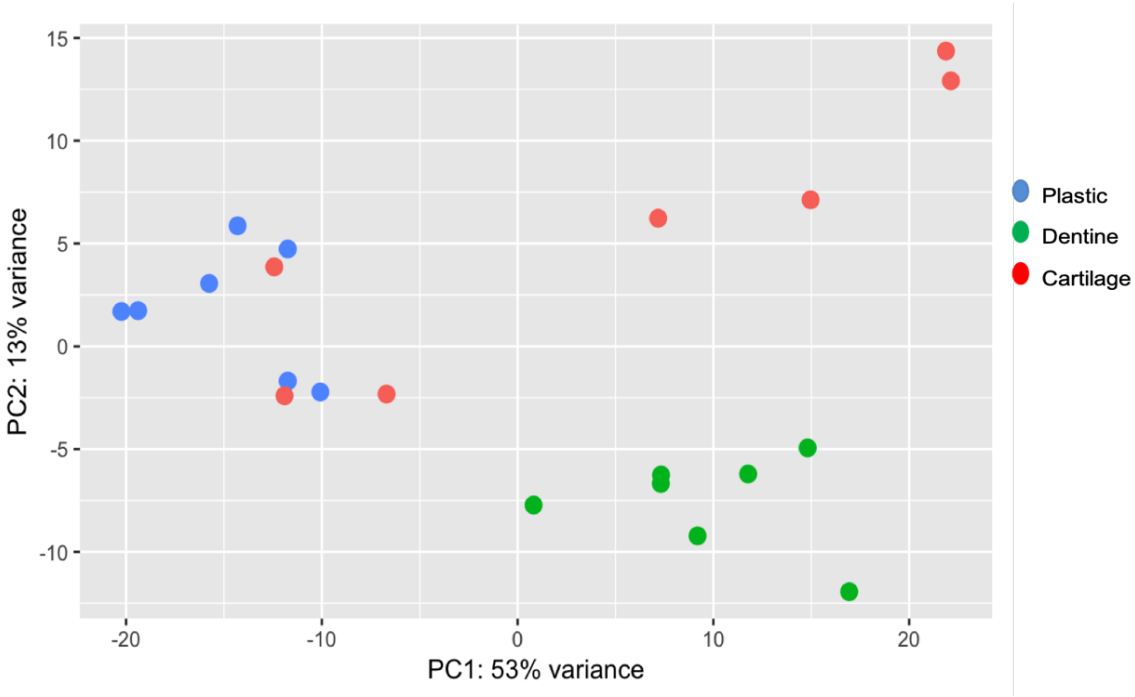


Figure 5.7 Principal Component Analysis (PCA) plot of osteoclasts on cartilage, dentine and plastic (no substrate). Blue: osteoclasts cultured on plastic, green: osteoclast-dentine culture and red: osteoclast-cartilage culture.

5.2.1 Gene expression differences between osteoclasts cultured on plastic and osteoclasts cultured on dentine

Two hundred and thirty-six genes were differentially expressed between osteoclast-plastic culture compared with osteoclast-dentine culture with a p value <0.05 (**Figure 5.8**).

The gene Nicotinamide Riboside Kinase 2 (*NMRK2*) was the most up-regulated (fold change: 4.23) in osteoclasts on plastic compared to osteoclasts on dentine (**Figure 5.8** and **Figure 5.9** A.). On the contrary, the Adhesion G Protein-Coupled Receptor E1 *(ADGRE1*) showed the greatest upregulation (fold change: 5.51) in osteoclasts on dentine.

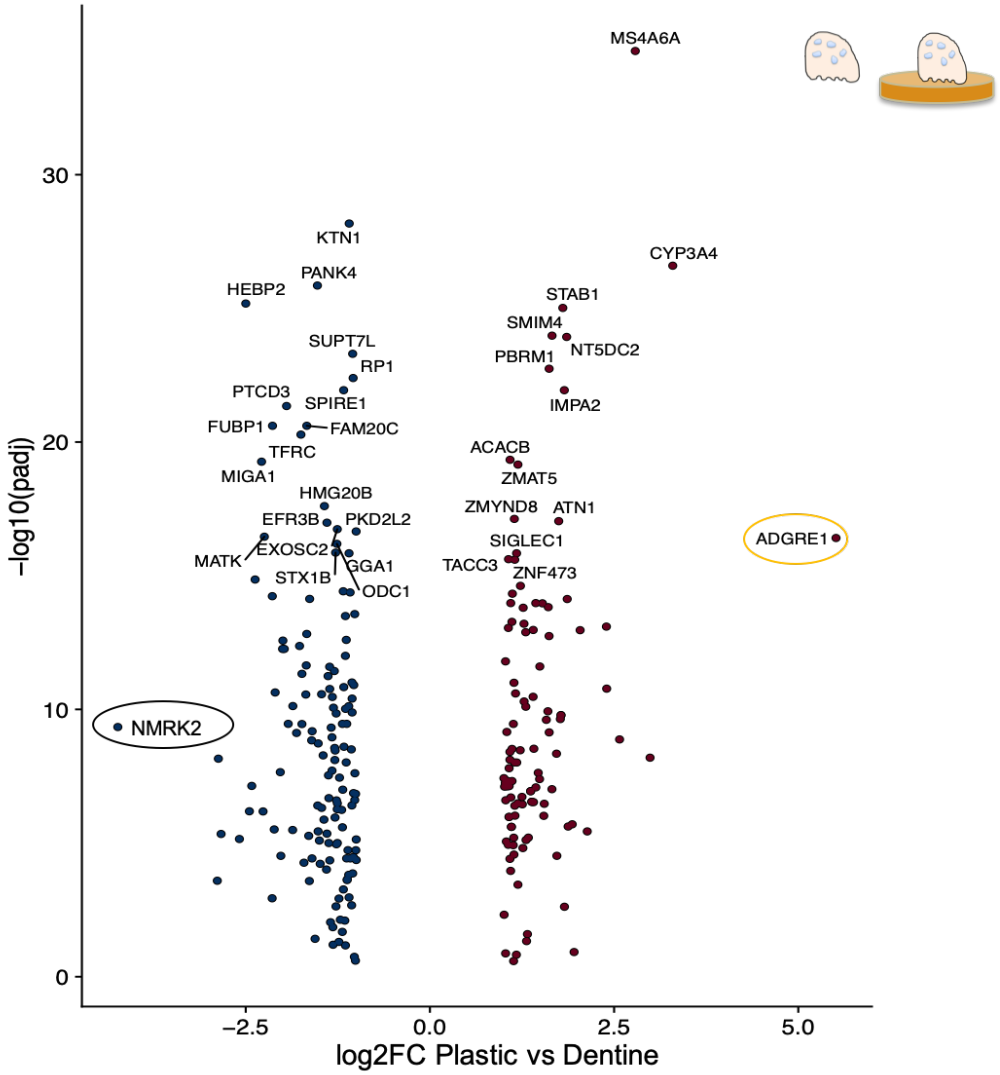


Figure 5.8 Volcano plot highlighting significantly different genes between osteoclasts on plastic and osteoclasts on dentine. Blue dot: osteoclasts on plastic, red dot: osteoclasts on cartilage. Gene labelling when p value<0.01. Black circle showing the most numerically upregulated in each type of osteoclasts. LFC: Log fold change and padj: p value adjusted

A

Gene	LFC	padj
NMRK2	4.23621881	4.57E-10
DSP	2.88584858	2.57E-04
GIPC3	2.87139362	6.99E-09
TNFSF14	2.83457051	4.58E-06
CPSF7	2.58582054	7.06E-06
HEBP2	2.49963	6.60E-26
SZT2	2.45051919	6.48E-07
CCR7	2.41830062	7.30E-08
USP33	2.37283218	1.39E-15
MIGA1	2.28504569	5.44E-20
PROK1	2.26487298	6.57E-07
MATK	2.24730745	3.48E-17
MARCH4	2.14135144	1.17E-03
RETREG1	2.13940706	5.84E-15
FUBP1	2.13673255	2.47E-21

B

Gene	LFC	padj
ADGRE1	5.51186386	3.89E-17
CYP3A4	3.2957877	2.54E-27
CD38	2.98789111	6.42E-09
MS4A6A	2.787449	2.36E-35
F13A1	2.57425334	1.33E-09
C3	2.39920713	1.68E-11
BOK	2.39533179	8.02E-14
SRCIN1	2.1355287	3.67E-06
IFNLR1	2.03885578	1.09E-13
CCDC152	1.93148553	1.99E-06
SELENOP	1.8757286	2.41E-06
GLIS3	1.86354949	7.45E-15
NT5DC2	1.85604332	1.17E-24
PRPSAP1	1.82595954	2.42E-03
IMPA2	1.82423285	1.15E-22

Figure 5.9 The top 15 over-expressed genes. A. Osteoclast cultured on plastic. **B.** Osteoclast cultured on dentine Green: The most numerically upregulated and red the least increased. LFC: Log fold change and padj: p value adjusted.

5.2.2 Gene expression differences between osteoclasts cultured on plastic and osteoclasts cultured on cartilage

One hundred and twenty-nine genes were differentially expressed between osteoclast-plastic culture and osteoclast-cartilage culture with a p value <0.05 and a fold change >1 (**Figure 5.10**).

The gene sialic acid binding Ig like lectin 10 (*SIGLEC10*) was the most up-regulated (fold change: 2.72) in osteoclasts on plastic compared to osteoclasts on cartilage (**Figure 5.10** and **Figure 5.11** A.).

On the contrary, the glucokinase (*GCK*) gene showed the greatest upregulation (fold change 3.83) in osteoclasts on cartilage.

Despite a p value at 0.0703 it is important to note that *MMP8* was 6.66 times higher in osteoclasts on cartilage compared to osteoclasts on plastic (red circle, **Figure 5.10**).

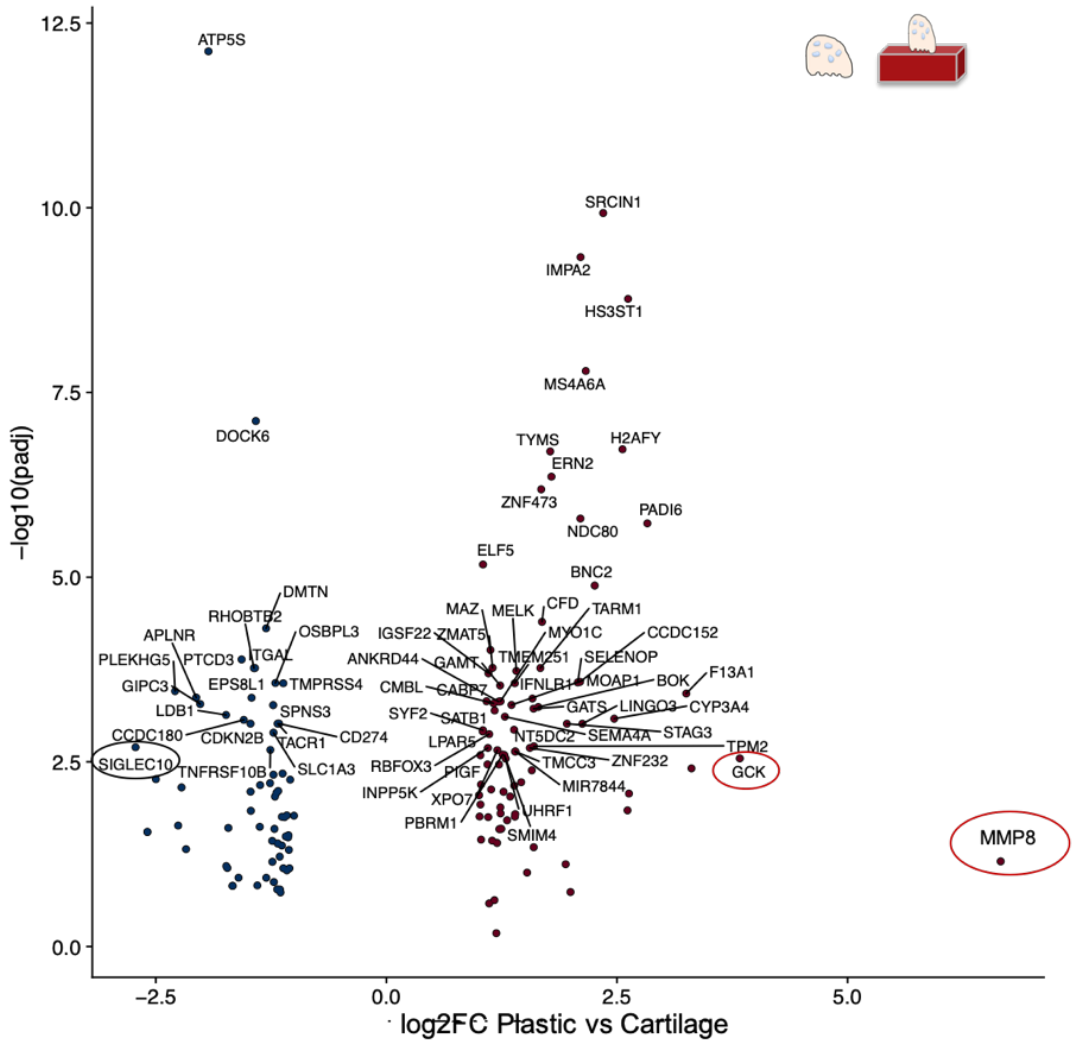


Figure 5.10 Volcano plot highlighting significantly different genes between osteoclasts on plastic and on cartilage. Blue dot: osteoclasts on plastic, red dot: osteoclasts on cartilage. Gene labelling when p value<0.01. The most numerically upregulated genes in osteoclasts on plastic are in black and on cartilage are in red. LFC: Log fold change and padj: p value adjusted

A

Gene	LFC	padj
SIGLEC10	2.72050756	2.01E-03
ZNF707	2.59161613	2.81E-02
DSP	2.49973287	5.43E-03
PLEKHG5	2.29168757	3.49E-04
NMRK2	2.25836457	2.30E-02
TNFSF14	2.22153177	7.02E-03
DPP10	2.17253816	4.81E-02
APLNR	2.06311675	4.26E-04
GIPC3	2.01922592	5.22E-04
ATP5S	1.9297862	7.63E-13
LDB1	1.73888018	7.34E-04
SZT2	1.71457433	2.48E-02
PTCD3	1.57027079	1.30E-04
CCDC180	1.54667483	8.55E-04
CDKN2B	1.47395559	9.62E-04

B

Gene	LFC	padj
GCK	3.83197084	2.84E-03
PRPSAP1	3.30787474	3.88E-03
F13A1	3.25111329	3.76E-04
PADI6	2.82958779	1.87E-06
ADGRE1	2.62977957	8.50E-03
HS3ST1	2.62029925	1.71E-09
PER2	2.61425419	1.43E-02
H2AFY	2.55978365	1.86E-07
CYP3A4	2.47007875	8.24E-04
SRCIN1	2.350571	1.18E-10
BNC2	2.25824161	1.30E-05
MS4A6A	2.16155334	1.62E-08
LINGO3	2.12441548	9.65E-04
IMPA2	2.10504092	4.66E-10
NDC80	2.10336742	1.61E-06

Figure 5.11 The top 15 over-expressed genes. A. In osteoclast cultured on plastic. **B.** In osteoclast-cartilage culture. Green: The most numerically upregulated and red the least increased. LFC: Log fold change and padj: p value adjusted.

5.2.3 Analysis of the protein expression and activity of secreted MMP-8 and MMP-9 using Western blot and gelatin zymography

Based on *MMP8* and *MMP9* mRNA level in osteoclasts degrading cartilage, the expression and activity of these genes was assessed at the protein level using Western blot and gelatin zymography. The amount and activity of MMP-8 and MMP-9 protein secreted by osteoclasts cultured on cartilage was compared to those cultured on dentine to extend these studies on how substrate alters the mechanism of ECM degradation.

Western blots were performed to confirm the presence of the MMP-8 and MMP-9 proteins. The active form of MMP-8 was detected in the conditioned media of osteoclasts cultured on cartilage and in smaller amounts in conditioned media of cartilage alone (**Figure 5.12 A.**). Similarly, the active form and pro-form of MMP-9 were present predominantly in the conditioned media of osteoclasts on cartilage (**Figure 5.13 A.**).

Gelatin zymography confirmed the presence of active MMP-8 (**Figure 5.12 B.** and **C.)** and MMP-9 (**Figure 5.13 B.** and **C.**) in the conditioned media of osteoclasts cultured on cartilage. The relative band clarity represents the activity of the protein. In the absence of osteoclasts (with cartilage alone), both MMP-8 and MMP-9 activity was almost absent.

This suggests that osteoclasts cultured on cartilage can secrete active MMP-8 and MMP-9.

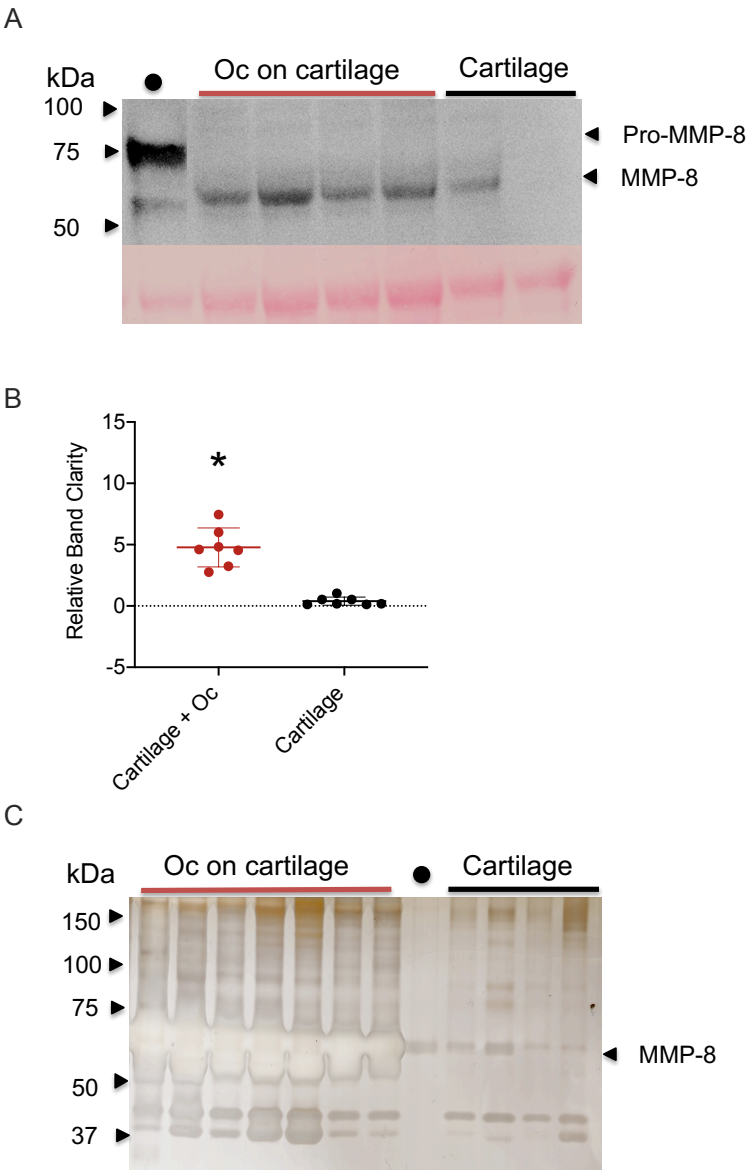


Figure 5.12 MMP-8 is secreted by osteoclasts on cartilage and actively degrades gelatin. A. Western blot showing MMP-8 expression in conditioned media of osteoclasts on cartilage (Oc on cartilage) and cartilage alone. The first lane corresponds to the recombinant MMP-8 protein (•: purified recombinant 50 ng), which was mostly present in the pro-enzyme form at 75 kDa rather than the active form at 65 kDa. Ponceau staining was used as a loading control. **B.** Gelatin zymography analysis of MMP-8. The intensity of the band representing the active form of MMP-8 was normalised to the corresponding recombinant protein for MMP-8 **C.** Representative zymography of MMP-8 found in the conditioned media of osteoclasts on cartilage compared to recombinant protein and cartilage alone. * $p<0.05$ and n=7

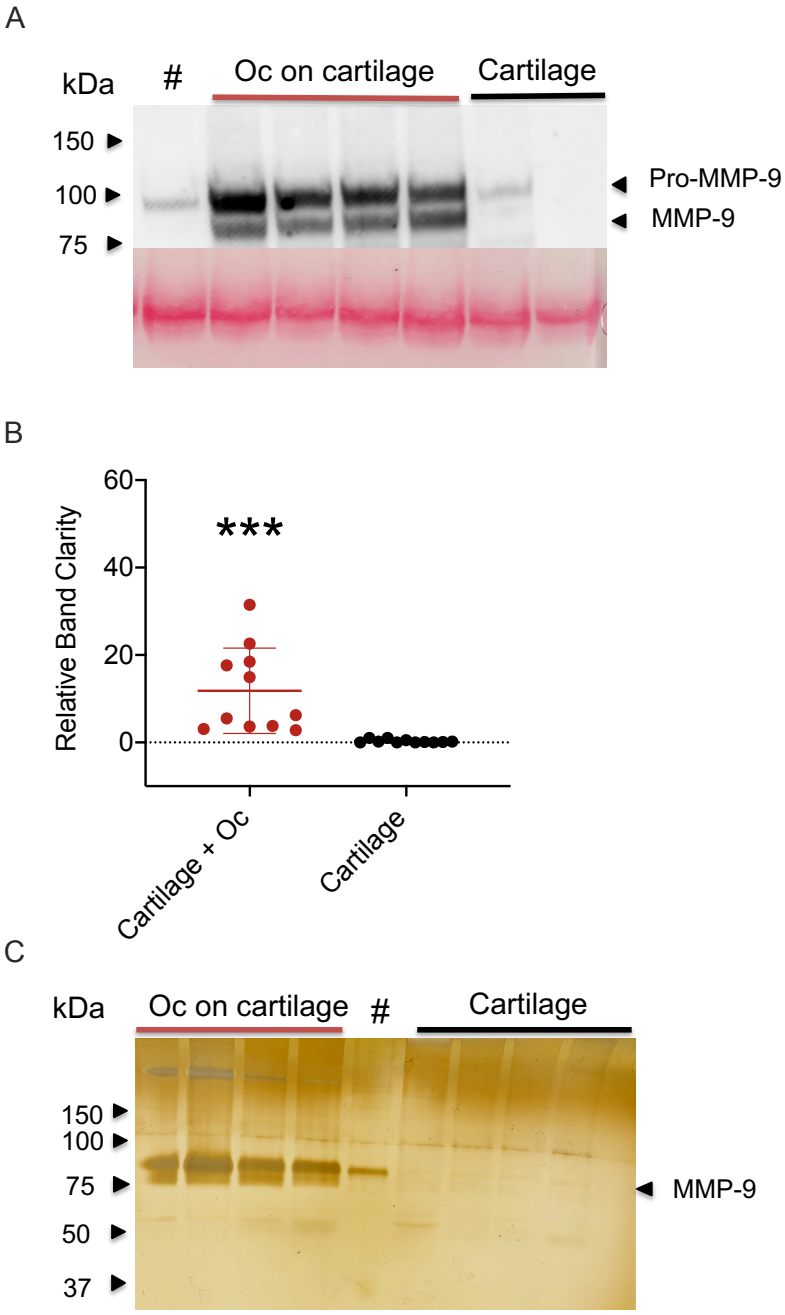


Figure 5.13 Expression of the protein MMP-9 by osteoclasts on cartilage and its gelatinase activity. A. Western blot showing MMP-9 expression in conditioned media of osteoclasts on cartilage (Oc on cartilage) and cartilage alone, #: purified recombinant human MMP-9 at 50 ng. The pro-active form can be seen at 92 kDa and the pro-form at 82kDa. Ponceau staining was used as a loading control. **B.** Gelatin zymography analysis of MMP-9, the intensity of the band was normalised to the corresponding recombinant protein for MMP-9. **C.** Representative zymography showing MMP-9 activity in conditioned media of osteoclasts on cartilage and compared with recombinant protein MMP-9 and cartilage alone. ***p<0.0001 and n=7

5.2.4 MMP-8 and MMP-9 contribute to cartilage degradation by osteoclasts

To study the role of MMP-8 and MMP-9 in cartilage degradation, osteoclasts cultured on acellular cartilage were transfected with *MMP8*, *MMP9* or scrambled control siRNA. The specificity and efficacy of siRNAs on osteoclasts were confirmed by RT-qPCR and Western blot as described in Chapter 2 section 2.7.1.2 and 2.7.1.3.

To determine the involvement of MMP-8 and MMP-9 in cartilage degradation, the amount of GAG was measured in culture media when osteoclasts had been treated with the siRNAs. Knockdown of both MMP-8 and MMP-9 in osteoclasts significantly reduced GAG release from cartilage explants (**Figure 5.14 A.** and **B)**. The transfection of the osteoclasts with the control siRNA did not change the amount of GAG released into the media (**Figure 5.14 A.** and **B)**.In the absence of osteoclasts, no differences in GAG release were seen following siRNA treatment (**Figure 5.14 C.** and **D.**). These results confirm that the inhibition of osteoclasts' expression of MMP-8 and MMP-9 was the only reason for the significant decreases in GAG release.

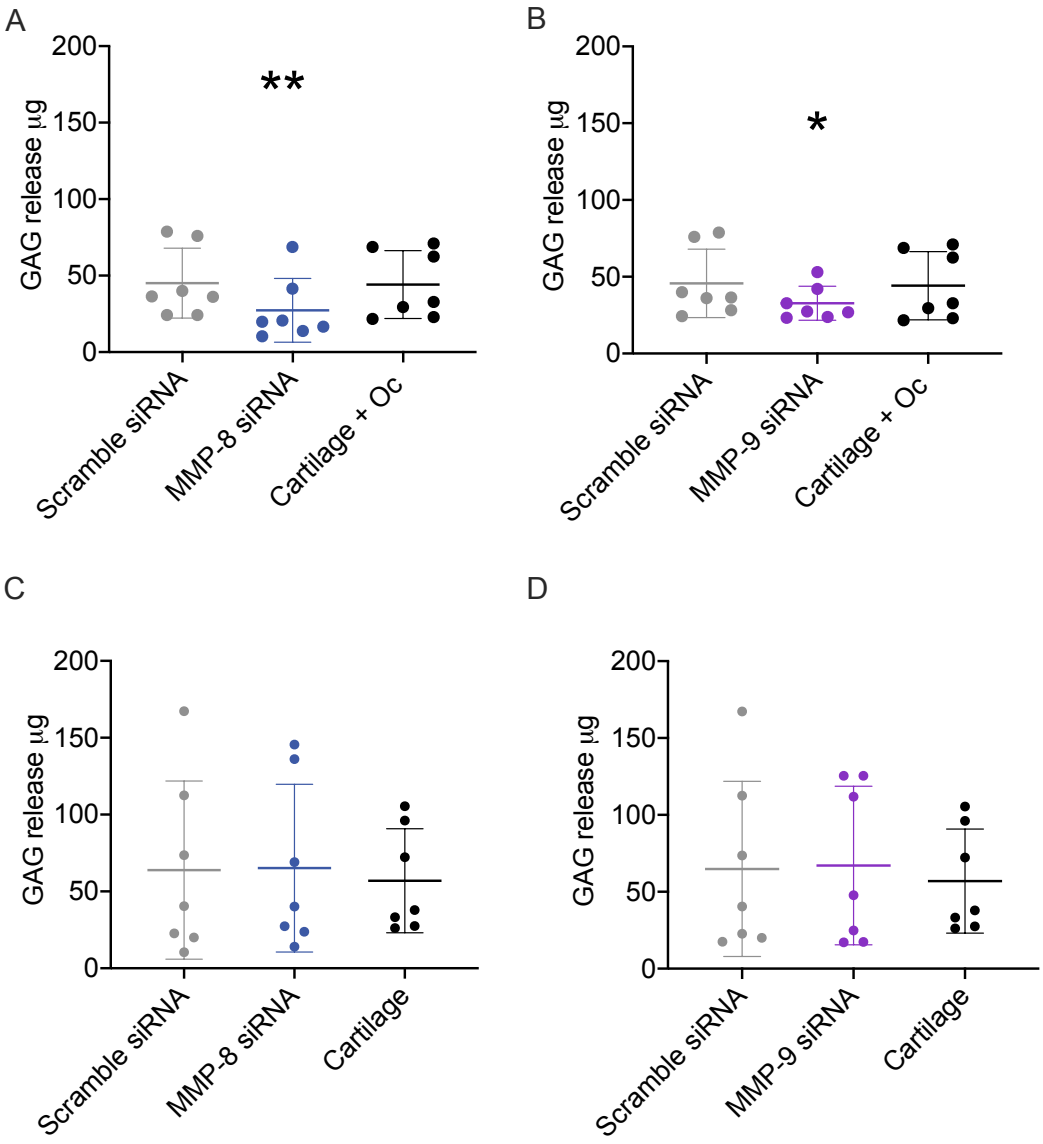


Figure 5.14 Osteoclasts cultured on acellular cartilage use MMP-8 and MMP-9 to degrade the ECM. Osteoclasts were cultured on acellular cartilage for 10 days. At day 7 the cells were transfected with a scrambled siRNA (control), MMP-8 or MMP-9 siRNA **A.** Total amount of GAG released into the media after treatment with MMP-8 siRNA. **B.** Similar to **A.** but the cells were transfected with MMP-9 siRNA. **C.** Similar to **A.** but without osteoclasts on the surface of the cartilage pieces and **D.** Absence of osteoclasts on the surface of the cartilage pieces transfected with MMP-9 siRNA. * $p<0.05$, ** $p<0.001$ and n=7

5.2.5 MMP-8 cleaves aggrecan at MMP and aggrecanase cleavage sites.

Detection of the fragments of aggrecan produced by the cleavage activity of MMP-8 and MMP-9 was used to confirm their role in cartilage matrix degradation. Most of the MMPs cleave aggrecan at the site $Asn^{341}\sim^{342}Phe$, while ADAMTSs found in cartilage (ADAMTS-1, ADAMTS-4 and ADAMTS-5) can cleave aggrecan between the residues $Glu^{373}\sim^{374}Ala$. MMP-8 is the only MMP able to cleave aggrecan at the same site as these aggrecanases.

The antibody BC-3 specifically recognises the cleaved site by aggrecanase at $Glu^{373}\sim^{374}Ala$. Hence, detection by Western blot of these fragments of aggrecan would reveal that ADAMTSs and/or MMP-8 are responsible for at least some of the cleavage. A Western blot was performed with the conditioned media of osteoclasts on cartilage and that of cartilage without osteoclasts. The detection of the $Glu^{373}\sim^{374}Ala$ cleaved site was greater when osteoclasts were cultured on cartilage compared to cartilage alone, although this was not statistically significant (**Figure 5.15 A.** and **B.)**.

As observed in section 5.11, only *ADAMTS-1* mRNA was expressed by osteoclasts on cartilage. To understand whether MMP-8 alone was responsible for aggrecan cleavage at that specific site, the protein expression of ADAMTS-1 was assessed in osteoclasts grown on cartilage compared to cartilage alone by Western blot (**Figure 5.16 A.** and **B**). ADAMTS-1 protein was expressed by osteoclasts; the aggrecanase activity detected by BC-3 could therefore be due to ADAMTS-1 and/or MMP-8.

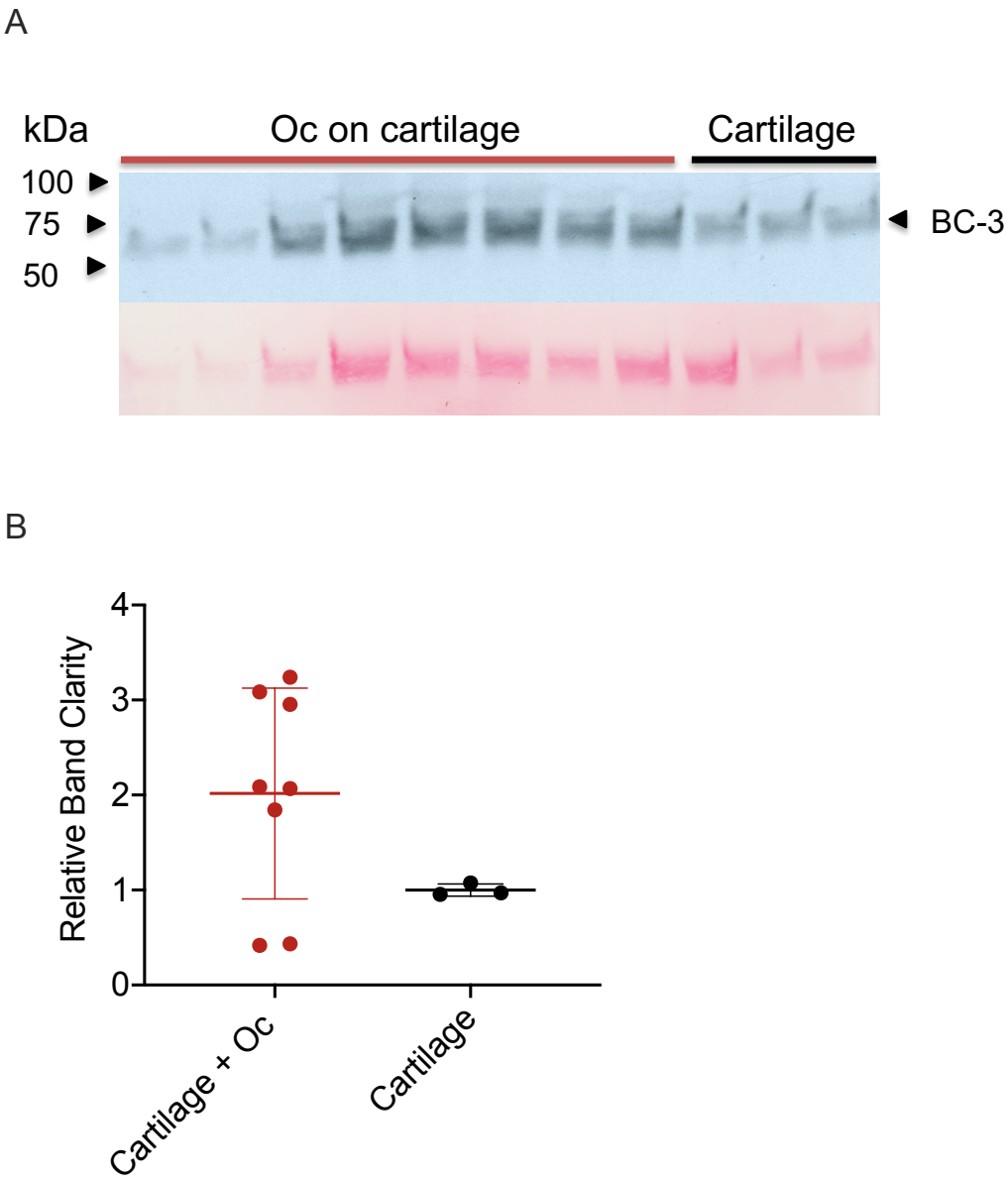


Figure 5.15 Osteoclasts degrade the ECM via the aggrecanase cleavage site Glu^{373}~^{374}Ala. A. Osteoclasts cultured on cartilage were compared to cartilage without cells. Conditioned media was analyzed for aggrecan fragments by BC-3 Western Blot analysis. Ponceau staining was used as a loading control. **B.** Band clarity of BC-3 protein expression, Oc: osteoclasts.

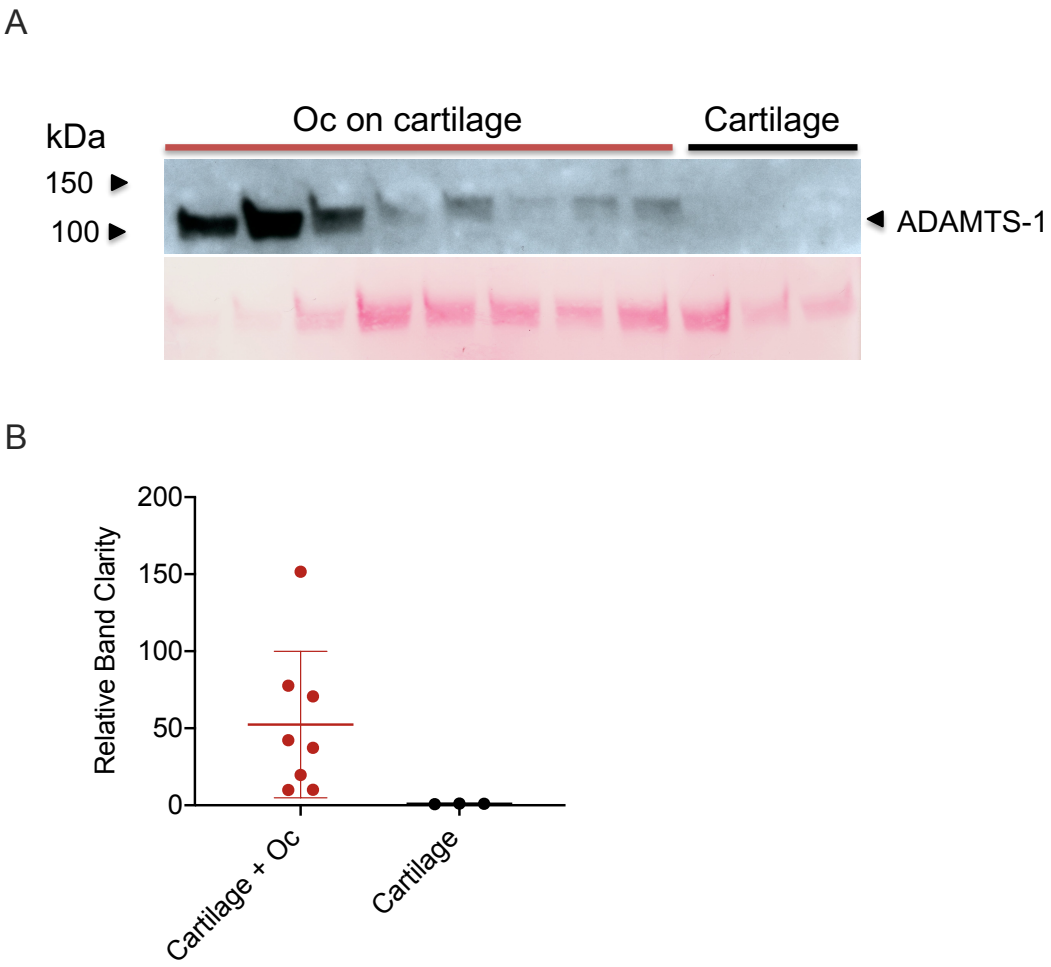


Figure 5.16 Protein expression of ADAMTS-1 in osteoclasts A. Osteoclasts were cultured on cartilage and compared to cartilage without cells. Conditioned media was analyzed for ADAMTS-1 by Western Blot analysis. Ponceau staining was used as a loading control. **B.** Band clarity of ADAMTS-1 protein expression Oc: osteoclasts.

5.2.6 MMP-8 and MMP-9 are expressed by osteoclasts in contact with cartilage *in vivo*

Tissue sections from OA patients were stained by immunohistochemistry to evaluate the presence of MMP-8 and MMP-9 in osteoclasts in contact with cartilage *in vivo*.

Multinucleated osteoclast-like cells in contact with cartilage expressed MMP-8 (**Figure 5.17 A.** and **B.**) and MMP-9 protein (**Figure 5.18 A.-D.**).

The majority of the osteoclasts positive for MMP-8 and MMP-9 were located between the articular cartilage and the subchondral bone. Chondrocytes surrounded by the ECM were slightly positive for MMP-8 and MMP-9 (red arrows).

The negative control confirmed the specificity of the staining (**Figure 5.17 C**. and **Figure 5.18 E.** and **F.**).

These images support our findings in our *in vitro* experiments, suggesting that osteoclasts may degrade cartilage *in vivo* via MMP-8 and MMP-9.

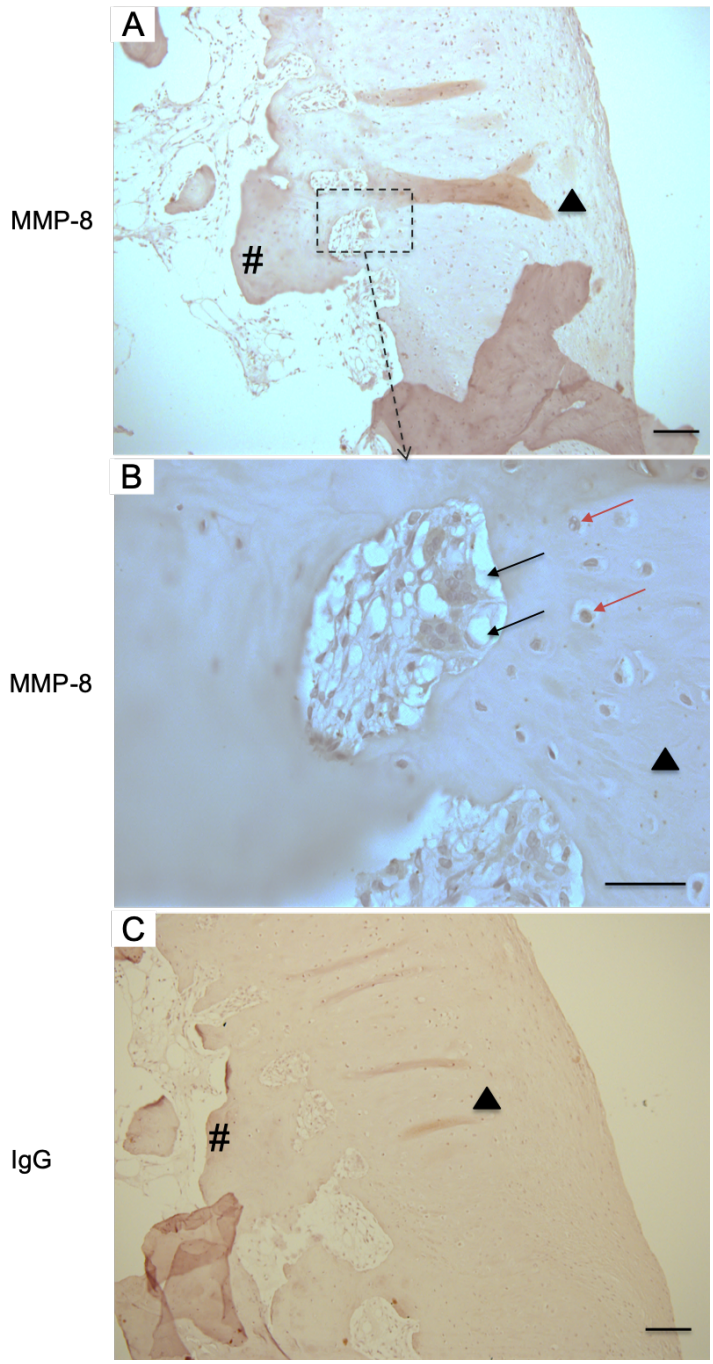


Figure 5.17 MMP-8 immunohistochemistry in OA tissue. MMP-8 was detected by immunohistochemistry and counterstained with hematoxylin and eosin. **A.** and **B.** Brown color indicates positive staining. **A.** dotted square magnified in **B.** and **C.** Mouse IgG used as a negative control. (▲) designates the cartilage, (#) indicates the subchondral bone, (←) osteoclasts and (←) chondrocytes. Bar = 100μm.

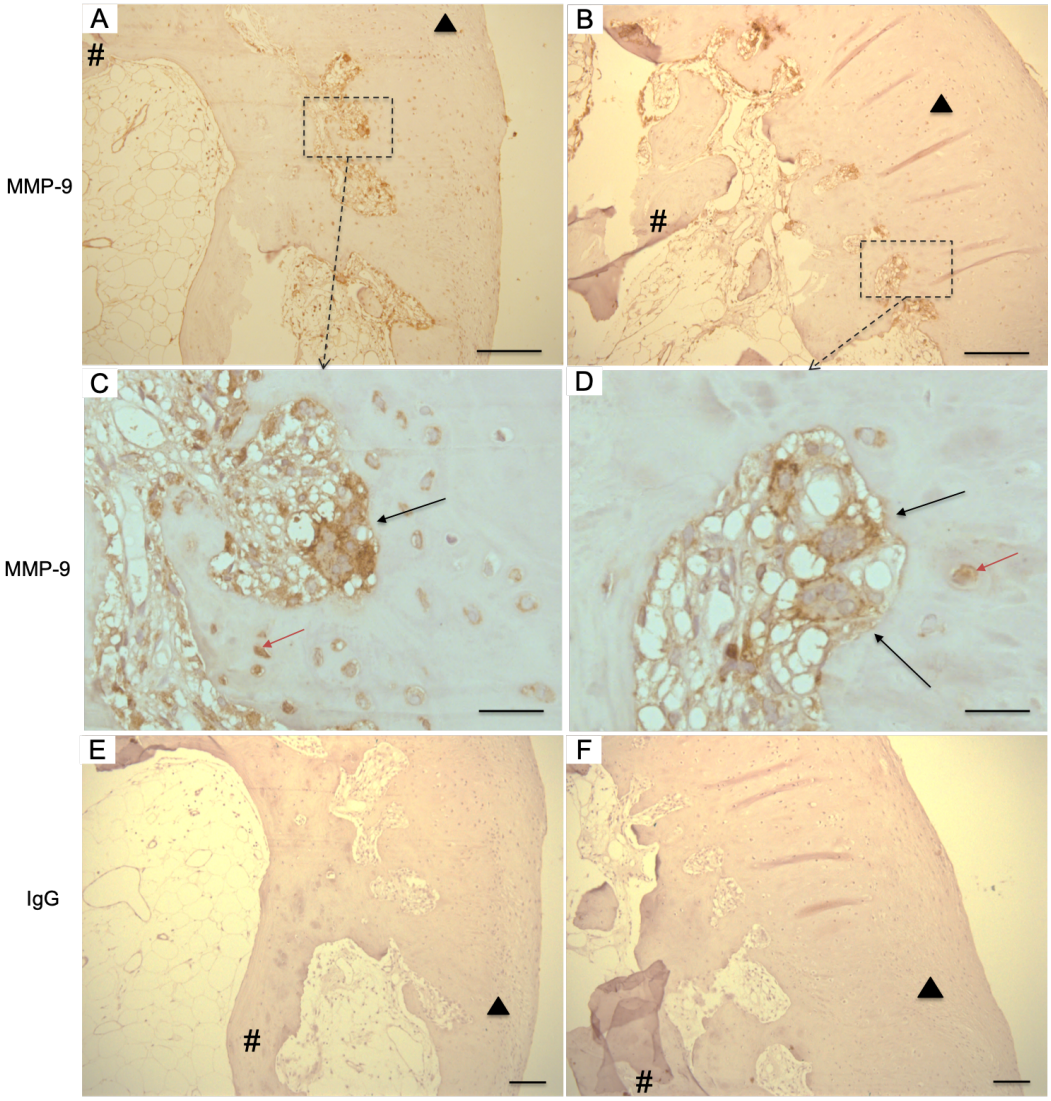


Figure 5.18 MMP-9 immunohistochemistry in OA tissue. MMP-9 was detected by immunohistochemistry and counterstained with hematoxylin and eosin. Brown color indicates positive staining, A. and B. dotted square magnified in C. and D., respectively. E. and F. mouse IgG served as a negative control. (▲) designates the cartilage, (#) indicates the subchondral bone, (←) osteoclasts and (←) chondrocytes. Bar = 100µm.

DISCUSSION

Following on from the chapter 4 result that broad inhibition of MMPs prevents osteoclast-mediated degradation of cartilage, this chapter used inhibitors blocking soluble MMPs and an antibody blocking MMP-14 to narrow down the type of MMP involved. It was shown that osteoclasts secreted soluble MMPs to degrade cartilage. To help determine exactly which MMP(s) were involved, RT-qPCR and bulk RNA sequencing were performed to compare gene expression of osteoclasts cultured on different substrates. To find out the key candidate(s) responsible for cartilage degradation, gene expression of osteoclasts cultured on cartilage was compared to those cultured on dentine. *MMP9* was highly expressed by osteoclasts on dentine and on cartilage. The RNA sequencing revealed that *MMP8* was also upregulated in osteoclasts on cartilage compared with osteoclasts on dentine. MMP-8 and MMP-9 protein expression was confirmed by Western blot and gelatin zymography revealed activity of both enzymes. Osteoclast-cartilage cultures transfected with either *MMP8* or *MMP9* siRNA significantly decreased GAG release from cartilage explants. Finally, the presence of MMP-8 and MMP-9 in OA patient tissue confirmed that osteoclasts in contact with cartilage express these two soluble MMPs. It was observed in chapter 3 section 3.7.2 that osteoclast marker gene expression changed according to the surface. A broad analysis using RNA sequencing highlighted that osteoclasts on cartilage or dentine had more similarities than with osteoclasts on plastic.

MMPs can be grouped into soluble and membrane anchored MMPs. Membrane type MMPs are MMP-14, MMP-15, MMP-16, MMP-17, MMP-24 and MMP-26 and all the other MMPs are soluble[321]. The recombinant protein TIMP1 inhibits the soluble MMPs but not the membrane-type MMPs. The addition of TIMP1 to cultures of osteoclasts on cartilage decreased release of GAG. TIMP1 irreversibly inactivates most of the MMPs (MMP-1, MMP-2, MMP-3, MMP-7, MMP-8, MMP-9, MMP-11, MMP-12, MMP-13 and MMP-16). MMP-14 is the predominantly expressed MT-MMP in osteoclasts[241]. In support of the result with TIMP1, blocking MMP-14 activity did not affect GAG release from osteoclasts cultured on cartilage. This suggests that osteoclasts use soluble MMPs to degrade cartilage. Neither inhibitor affected GAG release when there were no osteoclasts on the cartilage surface, confirming that it was the osteoclasts that secreted the MMPs causing cartilage degradation. It was not possible to use TIMP2 since this protein is required for activation of MMP-2 through association with MMP-14. More precisely, the inhibition of MMP-14 by TIMP2 could be masked by the activation of MMP-2 that could degrade proteoglycan.

Since the discovery of MMP-13 in rat long bone, more than six MMPs have been reported in bone tissue and utilisation of MMP inhibitors on bone blocks the solubilisation of collagen. Knockout mice and human genetic diseases have highlighted the importance of MMP-2, MMP-9 and MMP-14 for skeletal development but also revealed the importance of understanding the role of MMPs in a broader context than bone matrix solubilisation[321,322]. In osteoclasts there is a consensus that MMP-9 and MMP-14 are expressed, but

there are discrepancies for the other MMPs due to the variability of MMP expression and the critical role of MMP for solubilisation of bone matrix has not been identified. In order to obtain clearer insight about the expression of MMPs by osteoclasts, osteoclasts resorbing bone (dentine) and osteoclasts degrading cartilage were compared using RT-qPCR. *MMP14* was one of the most highly expressed MMPs in osteoclasts but the work in this thesis reveals it does not mediate osteoclast-driven GAG release from cartilage. As suggested in the literature, *MMP9* was highly expressed in osteoclasts on dentine and also on cartilage. Xue et al suppressed MMP-9 with siRNA or a specific MMP-9 inhibitor in human RA synovial fibroblasts. In the presence of OA cartilage explants the amount of GAG released was significantly decreased compared to the control, showing that synovial fibroblasts secrete MMP-9 to degrade cartilage[323] and demonstrating its ability to cleave proteoglycans. In this thesis, it has been shown for the first time that osteoclasts cultured on cartilage express *MMP9*. Therefore, this MMP appears to be one of the key candidates responsible for cartilage matrix degradation. Nevertheless, it is important to keep in mind that RT-qPCR was used only for the MMP-related genes that are known to be expressed either in osteoclasts or damaged cartilage. It was therefore necessary to consider another technique to broaden our field of vision.

RNAseq was performed with osteoclasts cultured on either dentine or cartilage. This was done as these matrices most closely mimic the natural surroundings of osteoclasts found in bone or cartilage and so facilitate extrapolation of the results to the *in vivo* situation. Osteoclasts cultured on

plastic are commonly used in tissue culture but, as observed in chapter 3, the morphology and the expression of osteoclast markers changes according to the surface. Therefore, to further investigate the effect of the substrate on gene expression, osteoclasts were also cultured on plastic (no substrate). Briefly the genes significantly upregulated will be discussed.

The gene Adhesion G Protein-Coupled Receptor E1 (*ADGRE1*) was most significantly upregulated in osteoclasts cultured on dentine compared to both osteoclasts on plastic and on cartilage. This gene is known to be expressed in macrophages and osteoclasts, but the function is still unclear. In mice, it has been used as a marker for cells of the mononuclear phagocyte lineage[324]. Epstein Barr virus induced 3 (*EBI3*) was the gene the most numerically overexpressed in osteoclast-dentine culture compared to osteoclast-cartilage culture. EBI3 is also known as IL-27 subunit beta and can be part of the IL-35 structure. Both of these cytokines have shown an ability to inhibit human osteoclastogenesis from monocytes induced by RANKL[325]. An osteoclast-derived complement component 3 (*C3*) was also up-regulated in osteoclasts on dentine compared to osteoclast-cartilage culture. Co-culture of osteoblasts and osteoclasts has previously shown that C3 mediates the coupling of bone resorption to bone formation, more precisely, osteoclasts secreted this protein that could induce osteoblast differentiation[326]. These genes may reflect the presence of a negative regulatory feedback loop contributing to decrease osteoclast activity and induce bone formation.

The comparison of osteoclast-cartilage culture with osteoclasts on dentine or plastic highlighted an up-regulation of the glucokinase (*GCK*) gene

and *MMP8*. GCK is part of a complex formed during the formation and activation of osteoclasts via activation of the NF-κB and JNK pathways. More precisely, these pathways involved the binding of TNF-α to the TNF-receptor 1 (*TNFR1*) suggesting that osteoclasts cultured on cartilage are exposed to TNF-α which regulate osteoclastogenesis independently from RANKL and M-CSF[327]. MMP-8 belongs to the collagenase subfamily of MMPs. It can cleave the triple helix structure of native collagen, initiating the first step of collagen degradation. The expression and secretion of MMP-8 by osteoclasts has never been shown before. The expression and secretion of MMPs is regulated by various pro-inflammatory cytokines such as IL-1β and TNF-α[269,322]. It has also been shown that MMP8 plays a role in hematopoietic stem cell mobilisation and interaction with osteoblasts[328], possibly contributing to osteoclast activation. This suggest that MMP-8 could also regulate activation of osteoclasts on certain substrates as well as degrading cartilage.

When the osteoclasts were cultured on plastic the sialic acid binding immunoglobulin-like lectin-10 (*SIGLEC-10*) gene was the most significantly upregulated compare to osteoclasts on cartilage. SIGLEC-10 is up-regulated in mature osteoclasts but for a long time this gene was considered to be expressed mostly in B cells and dendritic cells[329]. Bone resorbing osteoclasts express the Siglec-15 receptor on their plasma membrane and using blocking antibodies against SIGLEC-15, to inhibit osteoclast differentiation, has been considered as a novel bone loss therapeutic strategy[330,331] The gene TNF superfamily member 14 (*TNFSF14*) was also upregulated in osteoclasts on plastic compared to osteoclasts cultured on dentine or cartilage. Also known

as the **L**ymphotoxins exhibiting **I**nducible expression and competing with herpes simplex virus **G**lycoprotein D for **H**erpesvirus entry mediator, a receptor expressed by **T** lymphocytes, LIGHT is a member of the TNF superfamily that is expressed by lymphocytes, monocytes and granulocytes. Edwards et al showed that TNSF14 promotes RANKL-dependant osteoclast formation and can directly regulate osteogenesis[332] and Hemingway and al have shown that LIGHT can induce osteoclastogenesis independently of RANKL and is not inhibited by OPG[333]. The upregulation of *LIGHT* and *SIGLEC-10* suggest that osteoclasts on plastics do not have feedback on their formation and activity or since osteoclasts on plastic are not active, genes involved in osteoclastogenesis increase their expression.

The RNA sequencing revealed that osteoclasts gene expression is modified according to the substrate they are on, suggesting their ability to sense and respond to different surfaces by adapting their gene expression profile. This adaptive ability was also suggested by the morphological and immunological differences described in chapter 3. Despite these adaptations, on all surfaces these cells are large, multinucleated cells that express classic osteoclast markers such as VNR, TRAP and CTSK.

To confirm MMP-8 and MMP-9 as the key candidate soluble MMPs responsible for cartilage degradation by osteoclasts, we investigated the protein expression and activity in osteoclasts cultured on cartilage. After *MMP8* or *MMP9* knock-down by siRNA, the amount of GAG release into the media of osteoclasts cultured on cartilage was significantly decreased. This

suggests that MMP-8 and MMP-9 are both key mediators of osteoclast-driven cartilage degradation.

As discussed in chapter 3, it was complicated to detect the products of collagen degradation, therefore, it was not tested in these siRNA experiments but using a more sensitive collagen assay such as CTX-II could be an option. Since the objective of this thesis was to identify the key candidates involved in cartilage degradation osteoclasts transfected with siRNA cultured on dentine were not tested. Since the level of expression of MMP-9 was the same when osteoclasts were cultured on dentine or cartilage, a difference in collagen degradation on dentine could be expected. Conversely, MMP8 was only upregulated when osteoclasts were on cartilage, suggesting that collagen degradation on dentine would not be affected by MMP8 siRNA in osteoclasts.

To confirm the observations made *in vitro*, MMP-8 and MMP-9 were stained in tissue sections from OA patients and it was observed that osteoclasts in contact with articular cartilage were positive for MMP-8 and MMP-9, confirming their ability to produce and secrete those MMPs *in vivo*.

Most MMPs cleave aggrecan at the site $Asn^{341}\sim^{342}Phe$, the presence of the fragments cleaved at this location by MMP-9 and MMP-8 has not been investigated in this thesis because of lack of time and the difficulties to obtain this antibody. Fragments of aggrecan formed by another cleavage (between residues $Glu^{373}\sim^{374}Ala$) have been identified in the synovial fluid of patients with OA[334], inflammatory joint disease[335] and in the media from cartilage explants and chondrocytes stimulated with IL-1[57] or retinoic acid[336]. Therefore, the proteinases responsible of this cleavage may play an important

role in cartilage degradation. ADAMTSs (ADAMTS-1, ADAMTS-4 and ADAMTS-5) were considered to be the aggrecanases cleaving aggrecan at the $Glu^{373}\sim^{374}Ala$ site. In this chapter, it was shown that only *ADAMTS-1* expression was increased (not significantly) in osteoclast-cartilage cultures and fragments of aggrecan cleaved at $Glu^{373}\sim^{374}Ala$ were detected in osteoclast-cartilage cultures. MMP-8 is one of the only MMPs able to cleave aggrecans at the same site as aggrecanases[265], although ADAMTS-1 protein was detected in the conditioned media of osteoclast-cartilage cultures. According to the RNAseq revealing the upregulation of *MMP8* and the literature suggesting that ADAMTS-1 preferentially cleave aggrecan at another site, it is possible that MMP-8 is responsible for this cleavage. Reducing the expression of ADAMTS-1 using a specific inhibitor or a siRNA would help us to answer to this question.

CONCLUSION

In this chapter it has been demonstrated that MMP-8 and MMP-9 are expressed and secreted by osteoclasts cultured on cartilage and can drive cartilage proteoglycan degradation. This chapter also highlights the importance of substrate in regulating osteoclast phenotype, with distinct gene expression signatures detected between osteoclasts cultured on dentine and cartilage.

Chapter 6

Summary, Limitations and Future directions

SUMMARY

Osteoclasts are large multinucleated cells responsible for bone resorption. The bone matrix is primarily composed of hydroxyapatite crystals, type I collagen and bone proteins (such as osteocalcin, osteopontin and bone sialoprotein). The degradation of bone matrix by osteoclasts is based on acidification that dissolves the minerals and then breakdown of the organic bone matrix which is performed by cathepsin K and MMP-9. Osteoclasts can also degrade calcified cartilage during endochondral ossification[337]. Furthermore, osteoclasts in contact with cartilage have been observed in rheumatoid arthritis[200] but the mechanism by which osteoclasts degrade calcified and uncalcified cartilage remains unknown. The overreaching aim of this thesis was to determine how osteoclasts drive cartilage degradation in diseased joints. The other aims of this thesis were first to investigate whether the effects of osteoclasts on cartilage are due to direct degradation or the release of paracrine factors and secondly, to characterise how osteoclasts and chondrocytes interact (**Figure 6.1)**. Controlling the activity of osteoclasts would present an attractive target for further research and might represent an interesting perspective for treating a range of joint pathologies with cartilage degradation phenotypes.

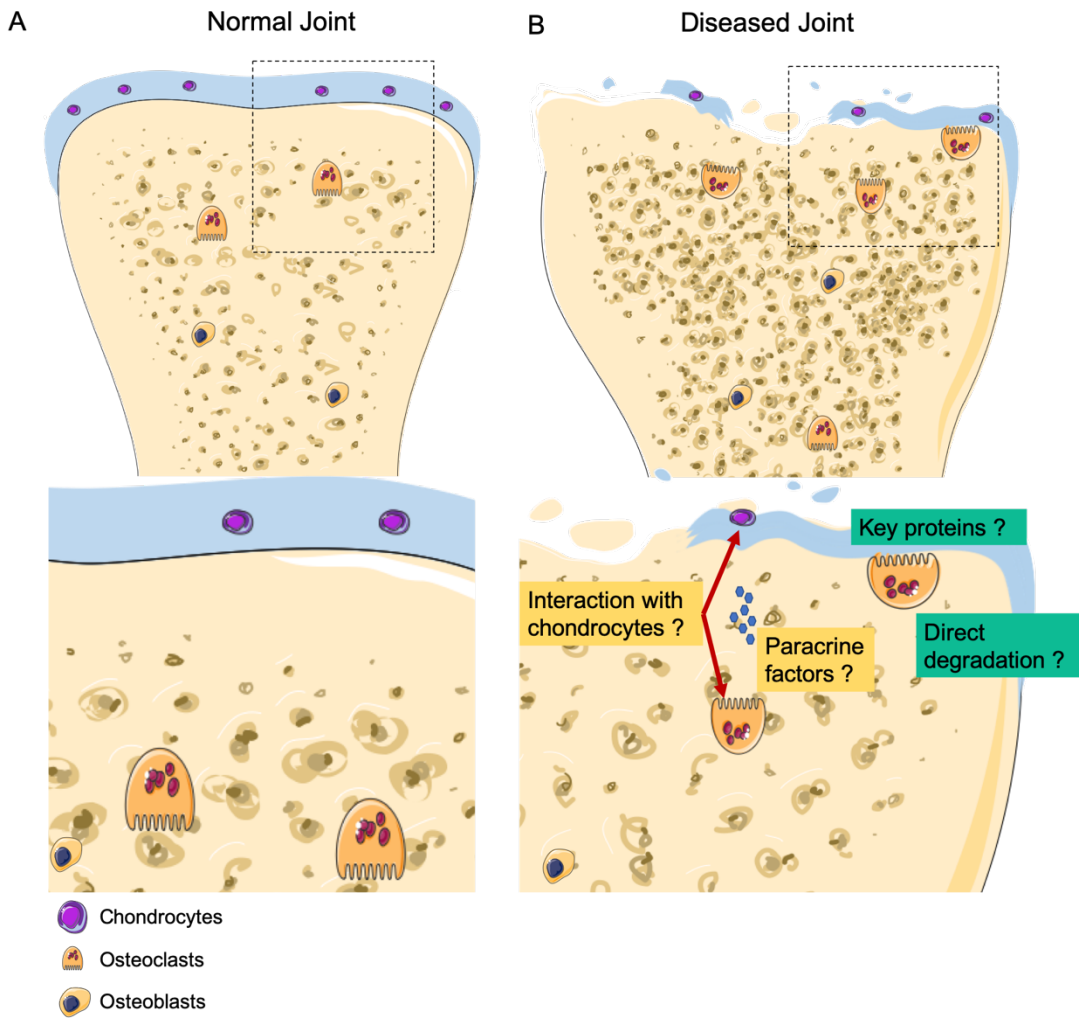


Figure 6.1 Diagram representing the hypothesis of this thesis. A. Osteoclasts help to maintain bone homeostasis with osteoblasts in the bone, chondrocytes are present in cartilage where they maintain cartilage ECM and function. **B.** In disease osteoclasts can degrade bone and are in contact with cartilage leading to cartilage ECM degradation.

6.1 Osteoclasts degrade cartilage via MMP-8 and MMP-9

6.1.1 Osteoclasts are in contact with cartilage in diseased joints

In chapter 3, osteoclasts were observed in proximity to cartilage in inflammatory arthritis (RA), non-inflammatory arthritis (OA) and other joint diseases such as GCTB, osteosarcoma, osteochondroma, chondroblastoma and chondromyxoid fibroma. These observations suggest that osteoclasts might play a direct role in the pathophysiology of the joints.

6.1.2 Osteoclast cultured on cartilage degrade the cartilage ECM

How and why osteoclasts are in contact with cartilage in different joint pathologies is poorly understood. The chapter 3 confirmed that monocyte-derived osteoclasts are found on cartilage explants and can degrade proteoglycans *ex vivo.*[188] In this thesis, the culture of osteoclasts on cartilage explants has been used as described in Knowles et al. and the quantification of the degradation products were in agreement with their final results. In continuation of this project, this thesis investigated in depth the mechanisms involved in the degradation of proteoglycans by osteoclasts.

After confirmation that the cells on the cartilage explants had the morphological and immunophenotypic characteristics of an osteoclast, different techniques were used to characterise how these osteoclasts degrade the surrounding matrix. SEM and cross-sectional H&E staining revealed that osteoclasts on cartilage had a more rounded three-dimensional profile and did

not form resorption pits, in contrast to osteoclasts on dentine. Suzomoto et al. demonstrated the absence of a ruffled border and a sealing zone suggesting that acidification is not necessary to degrade cartilage[223]. Additionally, the cytoskeleton of osteoclasts on cartilage did not form a sealing zone, whereas osteoclasts on dentine did. These results are in agreement with Saltel et al demonstrating the importance of the presence of minerals to form a sealing zone[226]. Finally, the products of cartilage degradation were measured; proteoglycan and, more variably, collagen release into the media was increased in the presence of osteoclasts. As observed by Knowles et al osteoclast-cartilage culture significantly increased the GAG release compared to cartilage alone. Therefore, chapter 3 confirmed that monocytes seeded on cartilage can differentiate into osteoclasts and those osteoclasts are able to degrade the proteoglycans and collagen found in cartilage. Mature and active osteoclasts isolated from GCTB were used to confirm that osteoclasts are able to degrade cartilage. Lofvall et al used another biomarker (Collagen type II degraded by MMPs (C2M)) to measure the collagen degradation when osteoclasts were on articular cartilage. Their data clearly showed that the addition of osteoclasts resulted in an increase of C2M release.

6.1.3 Osteoclasts express MMP-8 and MMP-9 that are the key candidates responsible for proteoglycan degradation from cartilage

In chapter 4, inhibitors of osteoclast bone degradation were used to determine whether osteoclast-mediated degradation of cartilage uses the same broad mechanism(s) as for bone resorption. Briefly, the inhibitors used targeted V-ATPase and cathepsin K, as well as the MMPs. The cessation of

cartilage proteoglycan release following treatment with the pan-MMP inhibitor GM6001 revealed that osteoclasts use MMPs to degrade proteoglycans and this has not previously been identified (**Figure 6.2**). To confirm the efficiency of the inhibitors, osteoclasts on dentine were treated with the same inhibitors and at the same concentration. It confirmed that bone degradation by osteoclasts is dependent on acidification and cathepsin K. Neutzky-Wulff et al cultured osteoclasts on bone slices and showed that the inhibition of cathepsin K reduced by 80 % the degradation of type I collagen by osteoclasts on bone. Only a modest reduction was seen in presence of GM6001 only at high concentration. However, inhibiting at the same time cathepsin K and MMPs completely abrogated the degradation of type I collagen[189]. Similarly and differing from our results, GM6001 significantly decreased the amount of type I collagen released when osteoclasts were cultured on cortical bone or on osteochondral junction. In the same idea, Henriksen et al demonstrated that MMPs are the predominant proteases on a decalcified matrix; osteoclasts cultured on calcified bone in the presence of GM6001 did not reduce the amount of type I collagen, only when osteoclasts were cultured on decalcified bone a significant reduction in CTX-I was seen[239].

In chapter 5, use of the endogenous inhibitor of soluble MMPs, TIMP1, and a blocking antibody against the main MT-MMP expressed in osteoclasts, determined that soluble MMPs, rather than membrane-bound MMPs, drive the degradation of cartilage by osteoclasts. Finally, to elucidate the key candidate MMPs, RNA sequencing and RT-qPCR were used to compare gene

expression in osteoclasts cultured on cartilage with osteoclasts cultured on dentine. This experiment revealed that expression of *MMP8* mRNA and protein were upregulated in osteoclasts cultured on cartilage. MMP-9, one of the main proteinases responsible for bone matrix degradation, was also very highly expressed in osteoclasts cultured on both cartilage and dentine. The degradation of proteoglycans from cartilage by osteoclasts was significantly decreased when expression of either *MMP8* or *MMP9* was silenced with siRNA, which validated the involvement of these two proteins in cartilage degradation. Staining of MMP-8 and MMP-9 in OA patient tissue sections confirmed that osteoclasts in contact with cartilage express these two proteins (**Figure 6.2**). This is the first description of the specific MMPs responsible for osteoclast degradation of cartilage as well as the first time that the gene expression profile of osteoclasts has been compared when they are in contact with their two primary natural substrates.

Most of the studies differentiating osteoclasts have been performed on tissue culture plastic or glass surfaces and have therefore failed to address the critical role played by bone substrate in osteoclast differentiation, polarization and activation[338,339]. There is only few publications were osteoclasts actively resorbing bone received more attention that osteoclasts on plastic[340,341342]. Crotti et al shown that attachment of osteoclast precursors to the bone surface via Annexin A8 is essential in the terminal differentiation and activation of osteoclasts[341]. In another publication the same group demonstrated that bone regulates numerous signalling pathways by attachment to the substrate via the integrin β 3. Findings about osteoclasts degrading bone are critical for a full

understanding of osteoclast differentiation and identification of therapeutic targets[342].

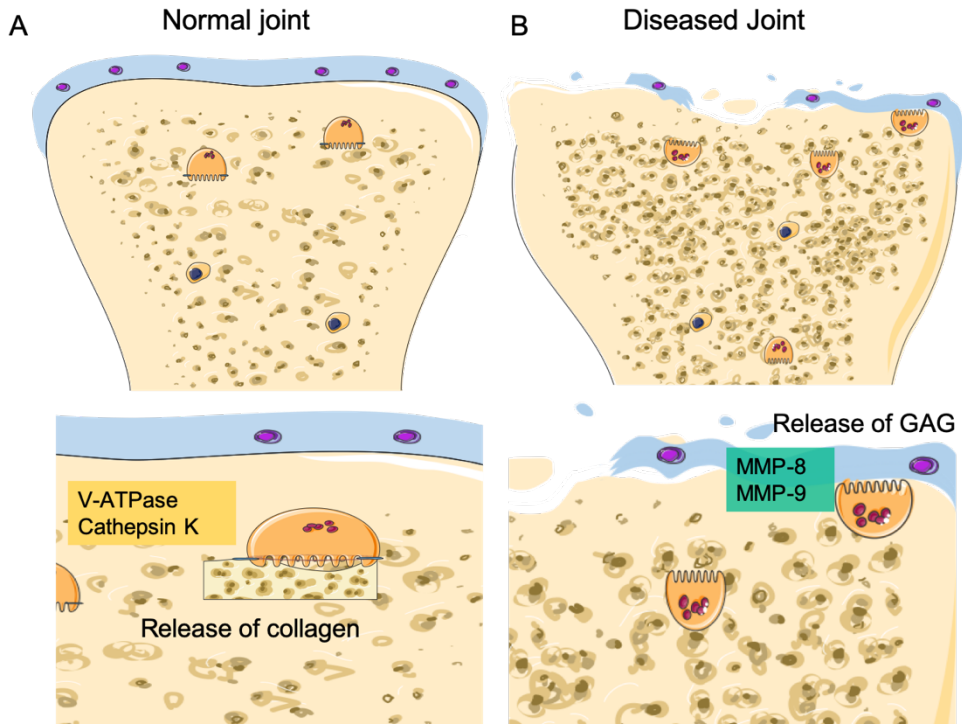


Figure 6.2 Summary of findings: Identification of the key proteins driving osteoclast-mediated cartilage degradation disease. A. In the normal joint, active osteoclasts on bone (dentine) degrade type I collagen as part of normal bone turnover. V-ATPase and cathepsin K are necessary for bone matrix degradation**. B.** Osteoclasts degrade cartilage via MMP-8 and MMP-9 when they are in contact with cartilage in diseased joints.

6.2 Osteoclast can affect the integrity of cartilage also via paracrine factors

6.2.1 Decrease in proteoglycan release by chondrocytes in response to paracrine factors

To simulate whether osteoclasts in the subchondral bone can release paracrine factors that could degrade cartilage, osteoclasts cultured on dentine were placed beneath a transwell containing cartilage. These osteoclasts produced factors that inhibited GAG release from cellular, but not acellular, cartilage. This inhibitory paracrine effect was not seen with osteoclasts cultured on plastic and was opposite to the observations of increased degradation made when osteoclasts were directly in contact with cartilage. This suggests that chondrocytes embedded in the cartilage ECM have a chondro-protective response to paracrine factors secreted by bone-resident osteoclasts. However, when osteoclasts are in contact with cartilage the chondroprotective response of chondrocytes may be outweighed by the activity of osteoclasts. And osteoclasts cultured on cartilage but not on their native bone substrate produce factors that drive cartilage degradation. This amplified protective effect of chondrocytes on the ECM underlines the ability of osteoclasts to exert a paracrine effect on non-bone tissue (**Figure 6.3**). Whether this is to activate mechanisms of degradation or to inhibit protective mechanisms is currently unknown.

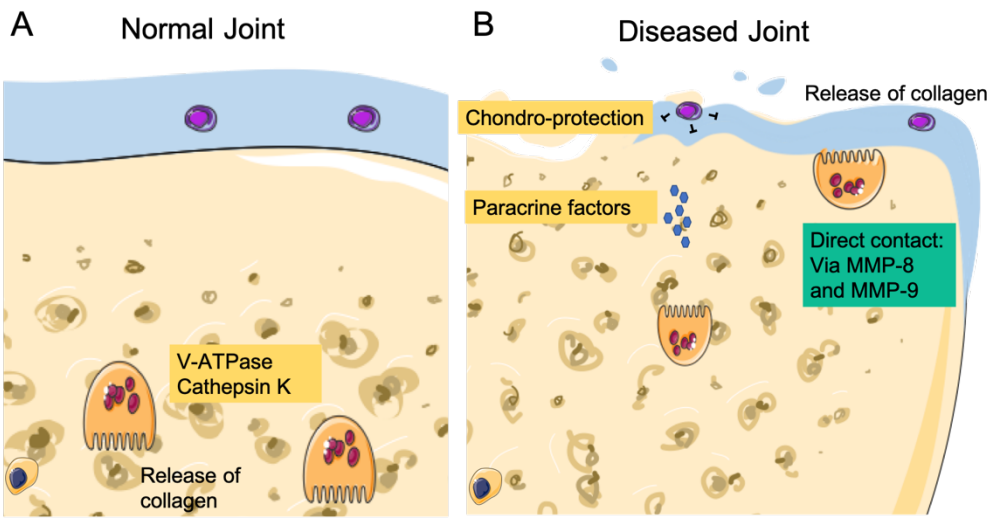


Figure 6.3 Summary of the results of Aim 2: to determine whether the effects of osteoclasts on cartilage degradation are due to direct degradation, the release of paracrine factors or interaction with chondrocytes. A. In normal joints **B.** In diseased joints, the GAG release was significantly decreased when cartilage explant in the cuvette were cultured with osteoclasts degrading dentine underneath. Therefore, factors secreted by osteoclasts induce a response of chondrocytes. Osteoclasts in contact with cartilage degrade proteoglycan (directly) and potentially collagen (directly and indirectly) from cartilage in diseased joints.

Inhibition of osteoclasts located in the subchondral bone decrease the destruction of cartilage in OA[187,343]. Funck-Brentano et al used human bone explants cultured alone or with estradiol or pamidronate (anti-resorptive agents) and transferred the supernatants to cartilage explants[187]. They observed a reduction of aggrecan cleavage and cartilage proteoglycan release indicating that bone-secreted soluble factors that are involved in regulating cartilage catabolism. Blocking of OPG in the bone culture medium transferred into cartilage cultures increased aggrecanase activity suggesting that OPG has a protective effect on cartilage catabolism[187]. The addition of the anti-resorptive agents targeting osteoclasts increased the ratio OPG/RANKL but OPG and RANKL is not produced by osteoclasts,

therefore, other cells present in the bone explants might be responsible. In this thesis, coculture of osteoclasts and chondrocytes embedded in the matrix revealed the presence of paracrine factors. It is possible that in response to paracrine factors produced by osteoclasts, chondrocytes modify the expression of TIMPs. For example; interactions between GAGs and TIMP-3 suggest that this may improve TIMP-3 inhibitory properties against MMPs[344].

6.2.2 Paracrine factors released by osteoclasts increase collagen degradation from cartilage

The collagen assay for the same transwell experiments (cartilage in the transwell, osteoclasts on dentine beneath) could not be performed for logistical reasons, as discussed previously. Osteoclasts on plastic were used as the best alternative substrate and had no paracrine effect on GAG release from acellular cartilage in transwell inserts but induced a paracrine increase in the release of collagen from cellular cartilage. This effect was not seen with acellular cartilage and whether it would happen when osteoclasts are actively degrading bone is unknown.

The ability of osteoclasts to secrete paracrine factors having a direct effect on bone formation has already been demonstrated[345]; for example, sphingosine-1-phosphate is upregulated in mature osteoclasts compared with preosteoclasts and induces osteoblast precursor recruitment and stimulates bone formation through increased activation of Wnt/BMP pathways[346]. However, the ability of osteoclasts to interact with chondrocytes is less described.

6.2.3 Chondrocytes affect osteoclasts formation and activity *in vitro* via OPG and RANKL

In 1993, Taylor et al co-cultured bone marrow cells or spleen cells with a clonal chondrogenic cell line (C5.18) on bone slices to illustrate the ability of chondrocytes to induce the formation of active osteoclasts[250]. The formation of $TRAP^+$ and active osteoclasts from bone marrow and C5.18 cells was shown and conversely, the coculture of spleen cells and C5.18 had small colonies of mononuclear $TRAP^+$ cells without resorbing activity on bone slices. Taylor et al observed that bone marrow cells were also positive for alkaline phosphatase leading them to postulate that bone marrow cells contains factors that are necessary for osteoclasts formation[250]. In this thesis, mixed co-culture and transwell co-culture of osteoclasts and chondrocytes were used to better understand how osteoclasts and chondrocytes interact. The unique aspect tested in this thesis was the formation and activity of osteoclasts directly or indirectly co-cultured with chondrocytes on plastic and dentine. It has shown that chondrocytes cultured *in vitro*, via increased *OPG* expression, can down-regulate osteoclast formation and activity on dentine.

It has been reported that osteoclastogenesis is increased by chondrocytes *in vivo*[252,253]. Wang et al investigated the role of chondrocyte produced OPG on osteoclast formation during post-natal growth. Using a transgenic mouse expressing OPG only under the promoter of type II collagen, they observed that chondrocytes overexpressing OPG increased the mass of the trabecular bone located in proximity to the joint. The formation of osteoclasts on plastic was reduced when spleen cells were co-cultured with chondrocytes from the transgenic mice[251]. This demonstrates that

chondrocytes in contact with spleen cells express *OPG* as seen in this thesis. In another publication, the same group investigated the regulation of osteoclastogenesis via β-catenin signalling in chondrocytes. The severe bone loss observed in β-catenin knockout mice was restored by treatment with human recombinant OPG. This experiment demonstrated that, *in vivo*, β-catenin signalling regulates OPG expression in chondrocytes during postnatal growth[347]. Kwan Tat et al showed that the *OPG* mRNA level was 1,000-fold higher than the *RANKL* mRNA level in OA and normal chondrocytes[254]. Similarly, in this thesis, the expression profile of *OPG* and *RANKL* in co-culture of osteoclasts and OA chondrocytes has been investigated and *OPG* expression level was higher than RANKL. Also, no differences in *OPG* mRNA level were seen between OA or normal cartilage[254]. They found that only the mRNA level of *RANKL* was significantly increased in OA compared with normal cartilage, meaning that the *RANKL* / *OPG* ratio is increased in OA, so enabling an increase in osteoclastogenesis and osteoclast activity. The addition of exogenous RANKL had no effect on the OA chondrocytes, nevertheless, the addition of OPG induced gene and protein expression of MMP-13 and PAR-2 which are two catabolic factors involved in the degradation of OA cartilage [348]. Nevertheless, Martinez-Calatrava et al and Bertuglia et al have respectively shown that human chondrocytes in RA and horse chondrocytes in OA express and secrete RANKL, which might explain the migration of osteoclasts in the diseased tissue[184,244].

Chondroprotection and degradation of cartilage by chondrocytes may be partly controlled by Wnt/β-catenin signalling[349]. Both *RANKL* and *OPG*

expression can be controlled by Wnt/β-catenin and loss of β-catenin leads to a decrease in OPG expression. Indeed, canonical and non-canonical pathways of Wnt/β-catenin are involved in the development of joint pathologies and can affect bone and cartilage[350]. It has also been suggested that activation of Wnt/B-catenin signalling leads to loss of a stable chondrocyte phenotype and destruction of cartilage tissues[351,352]. The contradictory results between animal models and/or within human tissue highlight the complexity of the pathways involved in diseased joints.

In summary, the data in this thesis suggests that osteoclasts in their 'normal' bone environment protect cartilage and help maintain the protective effect of chondrocytes on the cartilage ECM. In diseased joints, osteoclasts leave their normal bone substrate and invade cartilage, for example by following the secretion of RANKL by chondrocytes[184,244,353,354]. The interaction between chondrocytes and osteoclasts shifts to activate osteoclast cartilage degradation via MMP-8 and MMP-9 and to prevent chondrocyte protection of its ECM.

6.3 Osteoclasts activity is altered by substrate they are cultured on

This thesis demonstrates morphological, phenotypic and gene expression differences between osteoclasts cultured on plastic, dentine and cartilage, highlighting the extraordinary ability of osteoclasts to adapt their activities according to the surface on which they are on (**Figure 6.4**). The lack

of *in vivo* or *in situ* studies allowing the characterisation of osteoclasts degrading different tissue underlines the need for more research on this topic. The different pathologies described in Chapter 3 have different environments that can potentially affect osteoclast behaviour. For example, the inflammatory tissue in RA induce the formation and the activation of osteoclasts[104]. Understanding how osteoclasts adapt and modify their activity in these environments could lead to new therapeutic approaches.

In 2019, Romeo et al demonstrated that in the murine metaphysis during endochondral ossification, osteoclasts could be found either at the bone and cartilage interface or at the trabecular bone surface. Through immunofluorescent staining they observed that osteoclasts located at the bone-cartilage interface were positive for TRAP and vitronectin (integrin-β3), but these osteoclasts were smaller with a lower expression of cathepsin K than osteoclasts on trabecular bone[355]. Similarly, osteoclasts cultured on cartilage were positive for TRAP and vitronectin staining as shown in Chapter 3. The addition of inhibitors revealed that osteoclasts use cathepsin K to degrade dentine but not cartilage (Chapter 4). Also, they observed that osteoclasts located at the bone-cartilage interface were closely associated with blood vessels expressing high levels of CD31. Therefore, they postulated that vessel-associated osteoclasts (VAO) should be named differently to bone-associated osteoclasts (BAO) in the metaphysis[355].

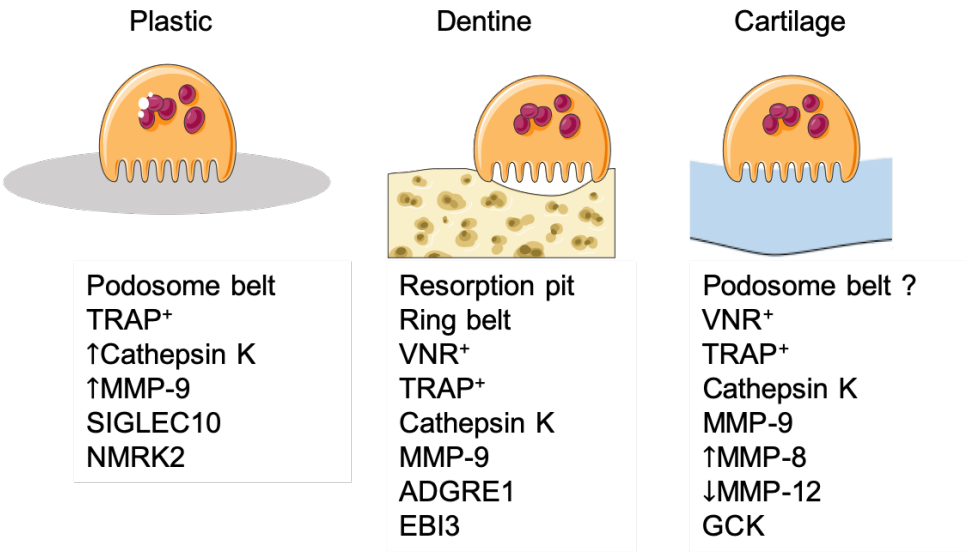


Figure 6.4 Summary of Aim 4: to characterise the differences between osteoclasts cultured on plastic, dentine and cartilage. Understanding how osteoclasts degrade cartilage is not only important for pathologies but is fundamental to skeletal physiology during processes such as endochondral ossification.

6.4 Further exploration into mechanisms of cartilage degradation by osteoclasts

6.4.1 Further validation that osteoclasts are responsible for cartilage degradation

Adding OPG at day 9 of cell culture and measuring proteoglycan and collagen release would be an additional method to confirm that osteoclasts are responsible for cartilage degradation. However, it is important to consider that more than one factor is involved, for example; chondrocytes express OPG and RANKL, as mentioned in section 6.2.

To confirm that osteoclasts are able to degrade cartilage, mature and active osteoclasts isolated from GCTB were used in this thesis. Nevertheless, the osteoclasts isolated from the GCTB contained other cells from the tumour. In parallel to these primary cells, using an osteoclast cell line was considered for validation. For example, the RAW 264.7 murine macrophage cell line is an abundant source of RANKL-sensitive osteoclast precursors[356]. This cell line has a wide availability and is easy to transfect however, the osteoclasts formed rarely resorb bone. For this reason, this approach was not attempted.

6.4.2 Expression and secretion of MMP-8 and MMP-9

Tissue sections from OA patients were stained for MMP-8 and MMP-9 and confirmed their expression in osteoclasts in contact with cartilage in OA. Tissue section of joints from murine models with OA could also be stained for MMP-8 and MMP-9 to help validate our findings. Performing an ELISA to quantify the amount of MMP-8 and MMP-9 protein would enable quantification of the amount of protein present in the conditioned media of osteoclast-cartilage co-cultures.

6.4.3 What is the role of osteoclasts in collagen degradation from cartilage?

Whilst this thesis has demonstrated that osteoclasts secrete MMP-8 and MMP-9 to degrade cartilage and release GAG, there is much more work that needs to be done to further elucidate the entire mechanism. Indeed, this thesis has identified the MMPs responsible for proteoglycan degradation, but it is possible that other proteinases are responsible for the more variably observed collagen degradation. Experimentally the hydroxyproline assay was used to quantify collagen degradation, but as mentioned in chapter 3 this assay is not specific for any type of collagen. Using CTX-II ELISAs would allow us to quantify the amount of type II collagen released and to compare it with the type I collagen resorbed in bone. Lofvall et al suggested that collagen was significantly degraded by osteoclasts cultured on cartilage, therefore using another collagen assay might help to corroborate this finding. They also observed a decrease of collagen release when an inhibitor of cathepsin K was used[185]. Having a more sensitive and specific assay would allow us to study

the role of cathepsin K and /or other proteinases involved in collagen degradation.

6.4.4 Do osteoclasts use an MMP independent mechanism to degrade collagen?

Under a collaboration with Prof James Gallagher at the University of Liverpool, mass spectrometry for proteomics is currently underway to identify the compounds released into the media in osteoclast-on-cartilage culture compared with cartilage alone. Mass spectrometry has been widely used in biology as an indispensable tool for proteomics research[357]. Hydroxyproline has been detected by mass spectrometry and more precisely, hydroxyproline was found in the condition media of osteoclast-cartilage culture but not in cartilage alone. Excitingly, this difference was only seen when osteoclasts were cultured on acellular cartilage corroborating the observations made with the hydroxyproline assay. Briefly, in this thesis, a significant increase of collagen release was seen only when osteoclasts were cultured on acellular cartilage from day 4 until day 13 **(Appendix A.1** and **Appendix A.3)**. Unfortunately, the presence of other markers such as aggrecan is still unknown since the analysis of this experiment is not finished.

6.5 Do osteoclasts in normal joints behave the same as in diseased joints?

6.5.1 Are MMP-8 and MMP-9 present in other diseased joints?

Obtaining tissue sections from the full range of pathologies in which osteoclasts are seen in contact with cartilage would help to confirm whether the same MMPs are potentially relevant across different diseases. Tissue section of joints from murine models of relevant pathologies could be stained for MMP-8 and MMP-9 to help to validate our findings.

6.5.2 Cartilage degradation in normal joints?

The explants of cartilage in this thesis were taken from patients with OA undergoing TKA at the Nuffield Orthopaedic Hospital. Performing the same experiments with healthy cartilage would allow us to see if osteoclasts degrade only cartilage from diseased joints or also from normal joints. However, obtaining cartilage from a cadaver is difficult. An alternative would be to use porcine or bovine cartilage, although human tissue is more relevant to characterise the mechanism. Human and animal cartilage have similarities in cartilage structure, but the biomechanical properties are not the same[358]. Athanasiou et al compared the thickness of articular cartilage from human and other animal species and concluded that human exhibited the thickest cartilage[359]. They also observed that the size of the animal does not correlate with stiffness. Taylor et al showed that human cartilage was the least

permeable[360]. Also, the age of skeletal maturity varies between species and might affect the experiments and human cartilage can provide a large amount of tissue[358]. Nevertheless, animal tissue is more accessible than human tissue and it would ease the experimental constraints.

This thesis found that both osteoclasts differentiated from PBMC and osteoclasts isolated from GCTB were able to degrade cartilage from OA patients. Using osteoclasts isolated from GCTB on normal cartilage may provide a means by which this tumour can invade the cartilaginous tissue.

6.5.3 Developing a model system *in vitro* to understand the importance of the substrate for osteoclast formation and activity

Another technique that warrants more investigation is whether coating tissue culture plates with a gel of collagen type I or collagen type II could mimic organic bone matrix and cartilage matrix respectively. Ultimately, to imitate cartilage matrix aggrecan could be embedded with type II collagen. This technique would enable control of the composition of the ECM formed and give the option to add minerals to the mixture. During this thesis, monocytes were seeded on plates coated with collagen type I or collagen type I mixed with bovine aggrecan. TRAP staining and examination of the morphology of the cells confirmed the presence of osteoclasts, however the experiments quantifying collagen and proteoglycan degradation were not conclusive (**Appendix A.8**). Adding minerals such as hydroapatite or calcium phosphate, as described in Saltel et al[226], would provide a full control of the composition of the matrix helping us to understand the mechanisms of degradation, as well as the genes and proteins that change in osteoclasts

according to their substrates. Staining the cytoskeleton of the cells on different types of coated plate would help to determine in which conditions the actin ring and the sealing zone are formed. It is essential to consider the cell culture substrate when analysing the cellular and molecular mechanisms regulating osteoclast differentiation and activation *in vitro*[342]. Secondly, such research might be relevant for elaborating new therapeutic approaches against osteoclast-related diseases such as pycnodysostosis or osteopetrosis.

6.6 Interaction between osteoclasts and chondrocytes

6.6.1 Is direct contact between chondrocytes and osteoclasts important for the regulation of their formation and activity?

In this thesis, chondrocytes were isolated from OA patients and increased *OPG* expression was observed in direct co-culture with osteoclasts on dentine over direct co-culture on plastic. The basal level of *OPG* and *RANKL* expression by chondrocytes was therefore 'mixed' with that expressed by osteoclasts. However, monocultures have shown that osteoclasts do not express *OPG* and *RANKL* whereas monocultures of chondrocytes expressed *OPG* and *RANL* (**Appendix A.5**).

Therefore, it was hypothesised that chondrocytes on dentine increase their expression of *OPG* in response to factors secreted by active osteoclasts (**Figure 6.3**). Studying gene expression of a monoculture of chondrocytes exposed to the conditioned media of osteoclasts cultured on dentine could

answer to this hypothesis that OPG is upregulated. Additionally, performing RT-qPCR with osteoclasts and chondrocytes in indirect co-culture will indicate whether direct contact is important for this response.

Doing RNA sequencing of chondrocyte monoculture and comparing it with chondrocytes cultured in a transwell with osteoclasts on dentine would help us to characterise the pathways involved. This sequencing would be compared with monocultures of osteoclasts and chondrocytes.

6.6.2 Will the same thing happen between healthy chondrocytes and osteoclasts?

This thesis found that chondrocytes inhibited osteoclast formation and activity when the co-culture was on bone and increased osteoclast formation when the co-culture was on plastic. Better understanding of the mechanisms involved will enable us to enhance our knowledge of the interaction between chondrocytes and osteoclasts. The chondrocytes used for this thesis were obtained from TKA for knee OA operations and used until passage 3. Healthy and OA chondrocytes have the tendency to rapidly dedifferentiate into a fibroblast-like phenotype after passage 2[361]. As suggested for cartilage explants, the co-culture experiments with osteoclasts and chondrocytes should also be performed with chondrocytes isolated from normal joints. Studying the interaction between normal chondrocytes and osteoclasts and ultimately comparing the results with diseased chondrocytes and osteoclasts would help to determine how chondrocytes influence osteoclasts' cartilage turnover in health and disease. In healthy cartilage it can be expected that the

contact between osteoclasts and chondrocytes is not seen highlighting the possible importance of paracrine factors.

Comparing RNA sequencing of chondrocyte monoculture from healthy and diseased chondrocytes (OA and RA for example) with co-culture of osteoclasts on dentine and chondrocytes in a transwell would help us to characterise the pathways regulating osteoclasts formation and activity.

6.6.3 Can chondrocytes induce osteoclast formation via RANKL secretion?

In the literature, it has been suggested that the expression of RANKL by chondrocytes might attract osteoclasts[184,244]. RANKL is also an important cytokine during osteoclastogenesis. It has been observed that the monocytes present in the synovial pannus differentiate into osteoclasts when they are in contact with bone or cartilage[199]. The ability of chondrocytes to differentiate monocytes into osteoclasts via RANKL expression should also be tested. For example, monocytes could be seeded on cartilage explants or with isolated chondrocytes with only exogenous M-CSF but not RANKL added to the culture media. In this thesis, monocytes have been seeded with chondrocytes on a coverslip and stained for TRAP. The number of osteoclasts was increase when monocytes were in co-culture with chondrocytes (**Appendix A.9**). For reasons of time, these experiments have not been continued. The addition of OPG will help us to confirm that the factor RANKL is responsible of osteoclasts formation.

6.7 Can other cells degrade cartilage?

In this thesis osteoclasts were differentiated from monocytes; thus, as full differentiation of all cells is never established, the osteoclast cultures were never a pure population but a mix of monocytes / macrophages and osteoclasts. To make sure that the population was composed of mature osteoclasts, the experiments were performed between day 9 and day 13 of differentiation. However, images of osteoclasts cultured on cartilage show this mix of cell types and Knowles et al demonstrated that monocytes / macrophages are able to degrade cartilage[188]. Monocytes and macrophages are found in direct contact with cartilage in RA[362]. Moreover, in this thesis, the presence of chondrocytes in cellular cartilage amplified the amount of GAG released at day 4 and day 7 by monocytes / macrophages (**Appendix A.1 A.** and **Appendix A.3 A.**). Therefore, monocytes and / or macrophages can interact with chondrocytes and / or affect the behaviour of chondrocytes to increase degradation of the ECM. Understanding by which mechanisms monocytes and macrophages degrade cartilage would enlarge our understanding even if this is away from the osteoclast field and it would open more perspectives for treatment against cartilage degradation. Similarly to what has been performed in this thesis, monocytes could be seeded on cartilage but only in presence of M-CSF and gene and protein expression would be characterised in the prism of MMP-8 and MMP-9.

6.8 Is the presence of blood vessels important for osteoclasts invasion and activity?

Capillaries are the main source of oxygen, nutrients and other factors that are indispensable for appropriate cellular function of osteoclasts in bone[116,363]. Normal cartilage is avascular but the presence of blood vessels invading the cartilage is essential during endochondral ossification[364]. The hypoxic environment is regulated by hypoxia inducible factor (HIF-1α). The role of HIF-1α in the maintenance of cartilage homeostasis is more and more studied especially in diseased joints[365,366]. Hypertrophic chondrocytes release vascular endothelial growth factor (VEGF) to attract blood vessels, meaning that progression of joint pathologies such as OA, RA and cancer is accompanied by the penetration of capillaries into the cartilage[100,367]. Experimentally, the amount of collagen and GAG released by osteoclasts cultured on cartilage in normoxic or in hypoxic conditions should be measured. The hypoxic condition corresponds to normal cartilage without blood vessels and normoxic condition will illustrate the invasion of blood vessels.

Romeo et al demonstrated that the endothelial cells of capillaries in the growth plate express high level of RANKL regulating the number of vascular-associated osteoclasts (VAO). They also found that these endothelial cells are able to digest cartilage matrix via MMP-9 expression and suggested that the VAO did not participate in growth plate resorption[355]. More precisely,

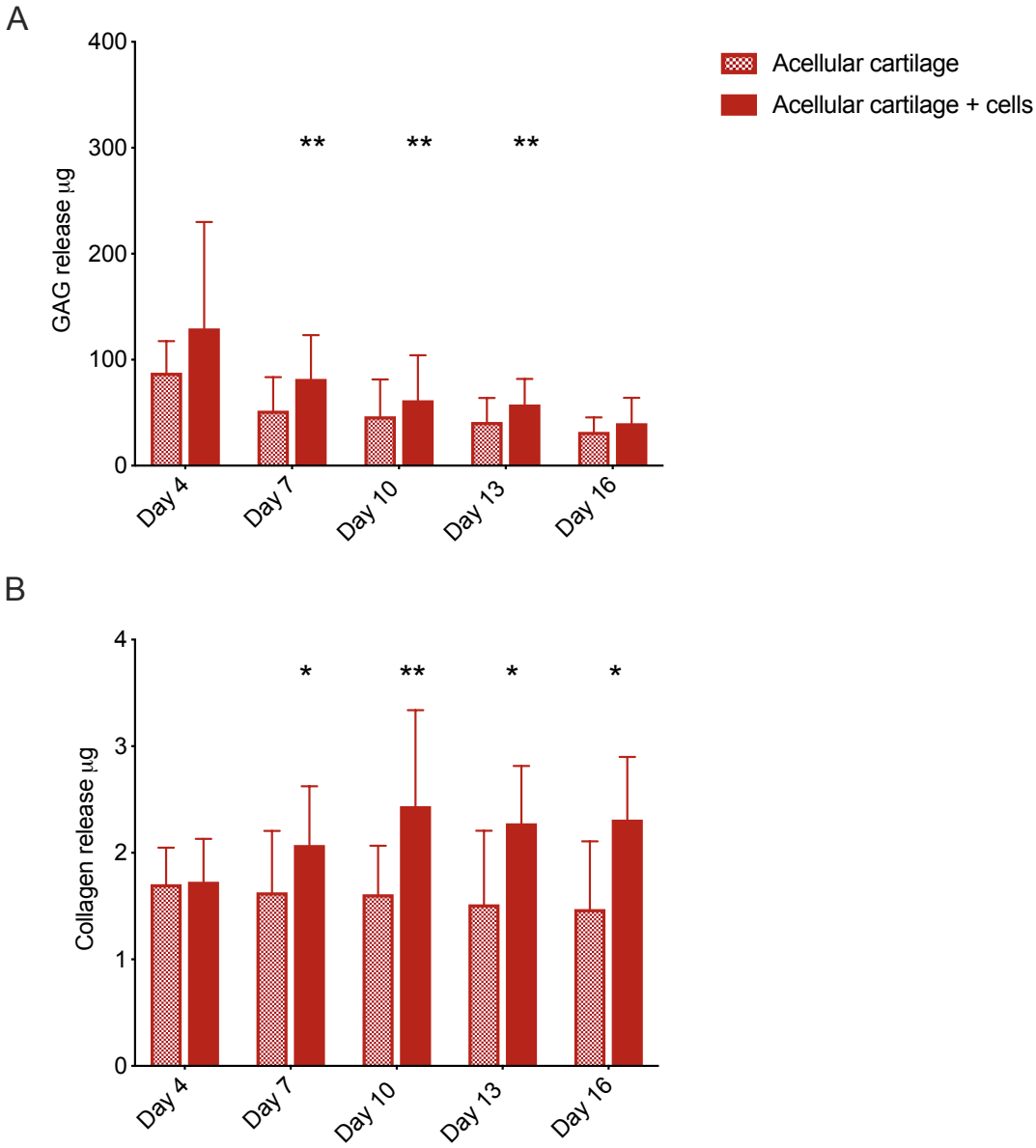
injection of alendronate twice a week for 4 weeks resulted in an increase of the bone mass and a reduction of the number of osteoclasts without affecting the size of the growth plate. However, Vu et al showed that MMP-9 expression did not co-localise with the endothelial marker CD31. More precisely, 3-week-old mice wild type and MMP-9 null mice were positively stained for CD31 in the metatarsal growth plate. Transplantation experiments with irradiated MMP-9-deficient mice confirmed that MMP-9 activity was from a haematopoietic origin rather than an endothelial cell origin[290].

Investigating whether cartilage degradation by osteoclasts and angiogenesis are coupled would be relevant to understand the importance of blood vessels. Staining multiple diseased joints for osteoclasts and CD31 markers would help us to understand if there is any relation between those cells. Co-culture of osteoclasts and endothelial cells on cartilage could be performed and the degradation products should be compared with osteoclasts on cartilage.

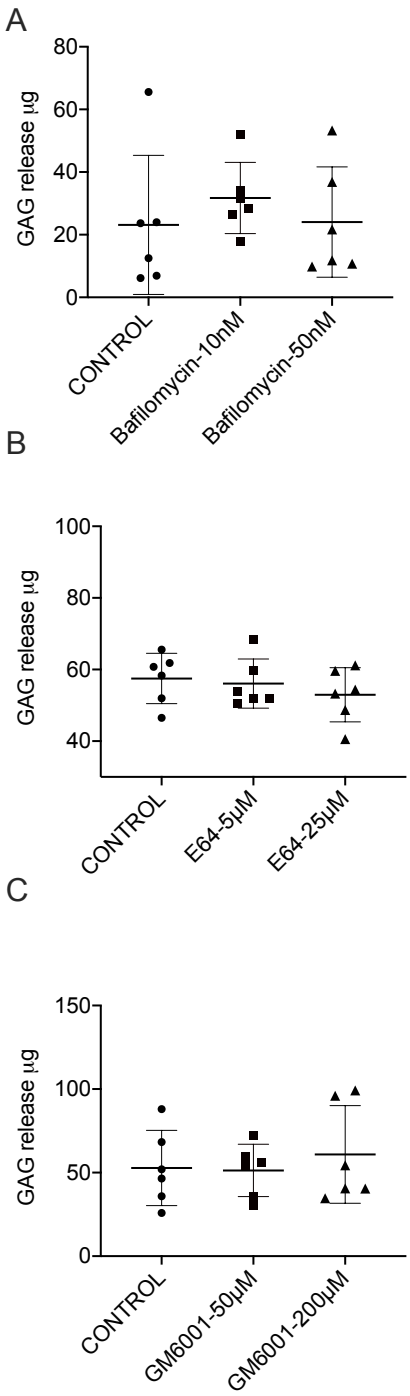
SUMMARY STATEMENT

This thesis supports the hypothesis that osteoclasts can perform proteolysis-driven cartilage degradation and has demonstrated that MMP-8 and MMP-9 are involved in this process. The results presented in this thesis provide new insights into the complexity of interactions between bone and cartilage, and more precisely between osteoclasts and chondrocytes, in a variety of pathological joint conditions. Controlling the activity of osteoclasts would present an attractive aim for further research and might represent a novel avenue for targeting diseases characterized by cartilage loss.

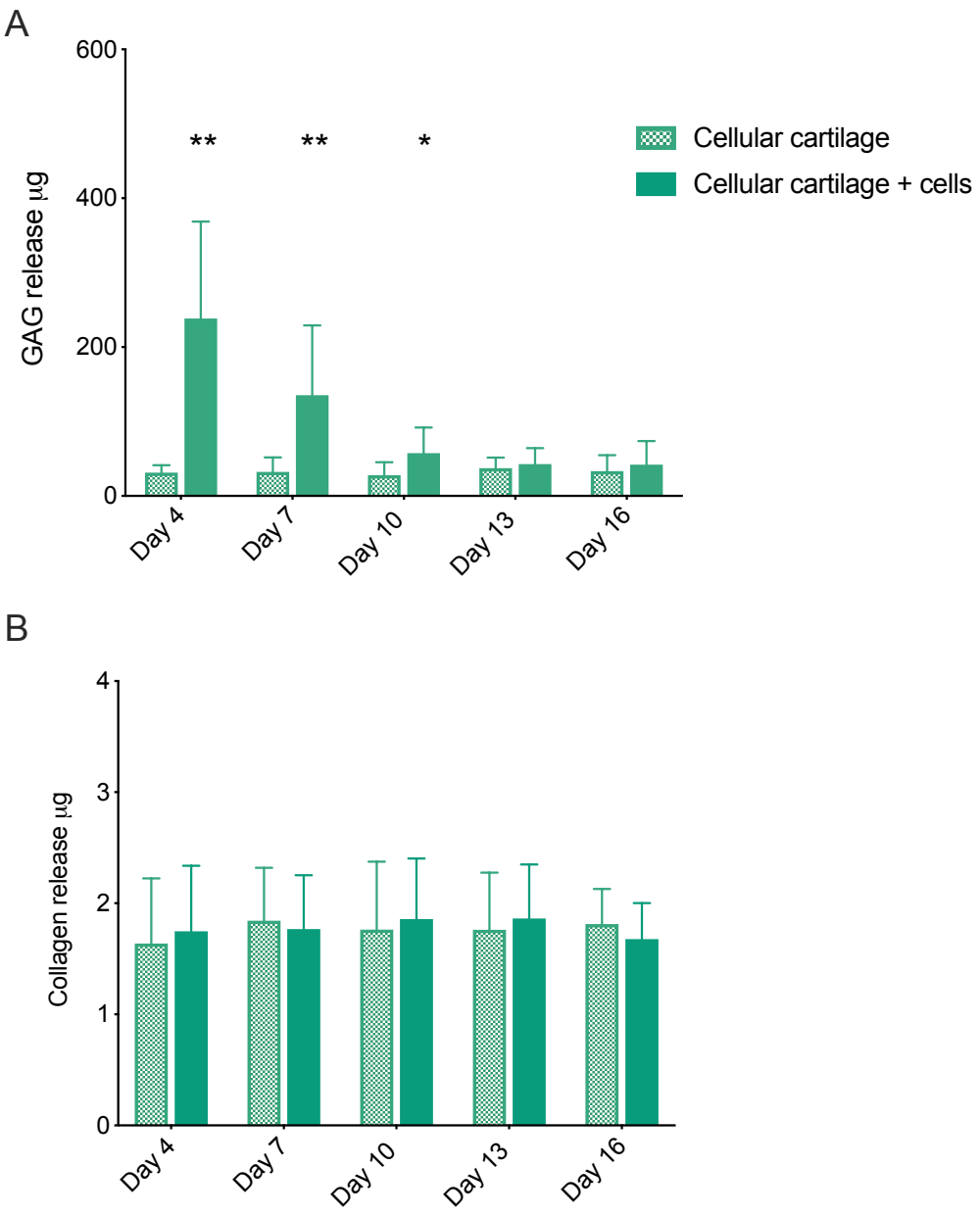
Appendix



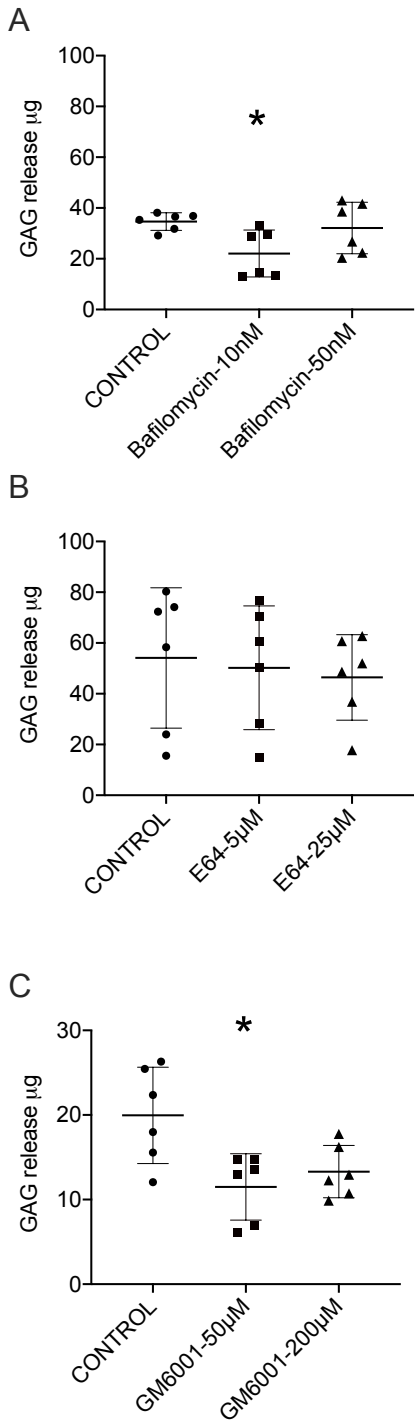
Appendix A.1 Collagen assay giving the total amount of collagen released in culture media. A. GAG release of acellular cartilage explants compared to osteoclasts-acellular cartilage culture. **B.** Collagen release of acellular cartilage explants compared to osteoclasts-acellular cartilage culture, *$p \leq 0.05$ and ** $p \leq 0.001$, n=8.



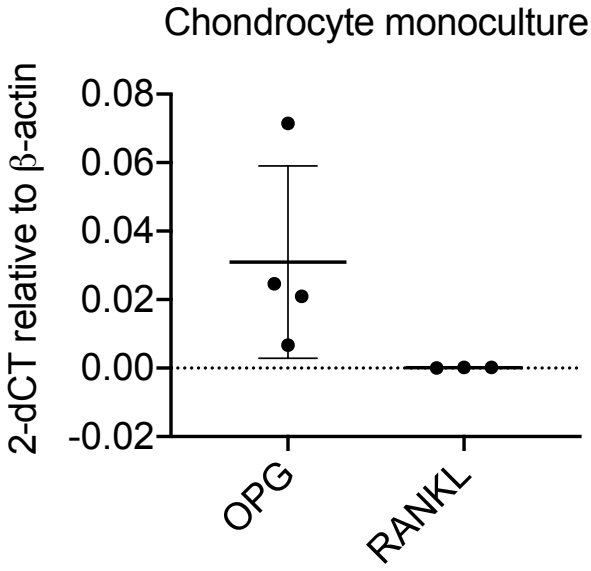
Appendix A.2 Acellular cartilage cultured in the presence of inhibitors. **A.** GAG release in the presence of bafilomycin at day 10. **B.** GAG release in the presence of E64 at day 10. **C.** GAG release in the presence of GM6001 at day 10 and n=6



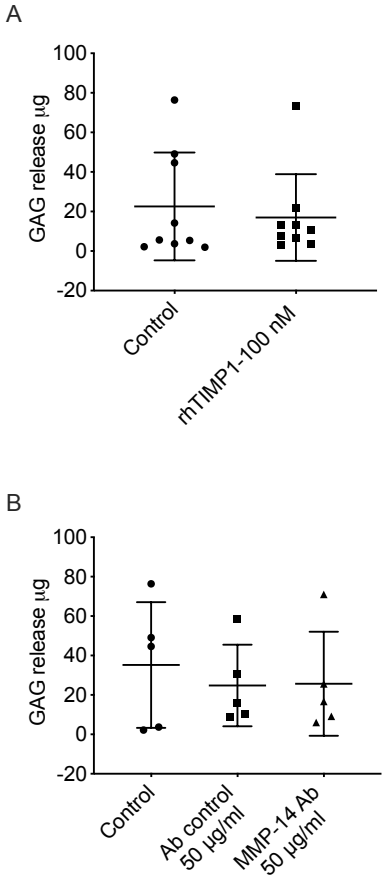
Appendix A.3 Total amount of GAG released by cellular and acellular cartilage cultured with or without cells. A. GAG release of cellular cartilage explants compared to osteoclasts-cellular cartilage culture. **B.** Collagen release of cellular cartilage explants compared to osteoclasts-cellular cartilage culture, *$p \leq 0.05$ and ** $p \leq 0.001$, n=8.



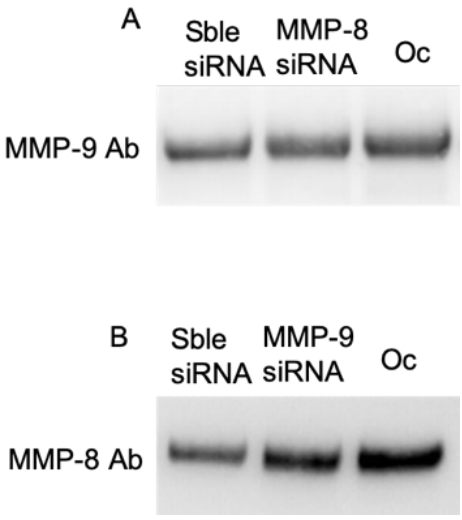
Appendix A.4 Cellular cartilage cultured in the presence of inhibitors. GAG release in the presence of bafilomycin at day 10. **B.** GAG release in the presence of E64 at day 10. **C.** GAG release in the presence of GM6001 at day 10. *$p \leq 0.05$, n=6



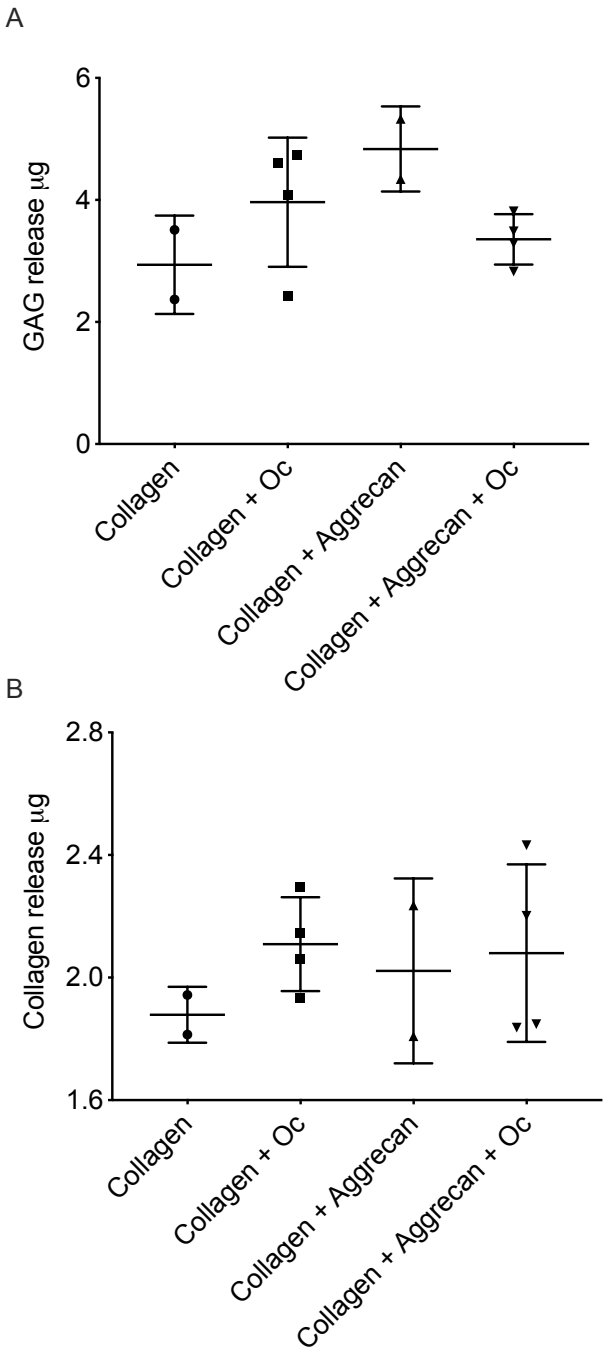
Appendix A.5 Expression levels of OPG and RANKL. *OPG* and *RANKL* expression relative to β-actin in chondrocytes monoculture on plastic



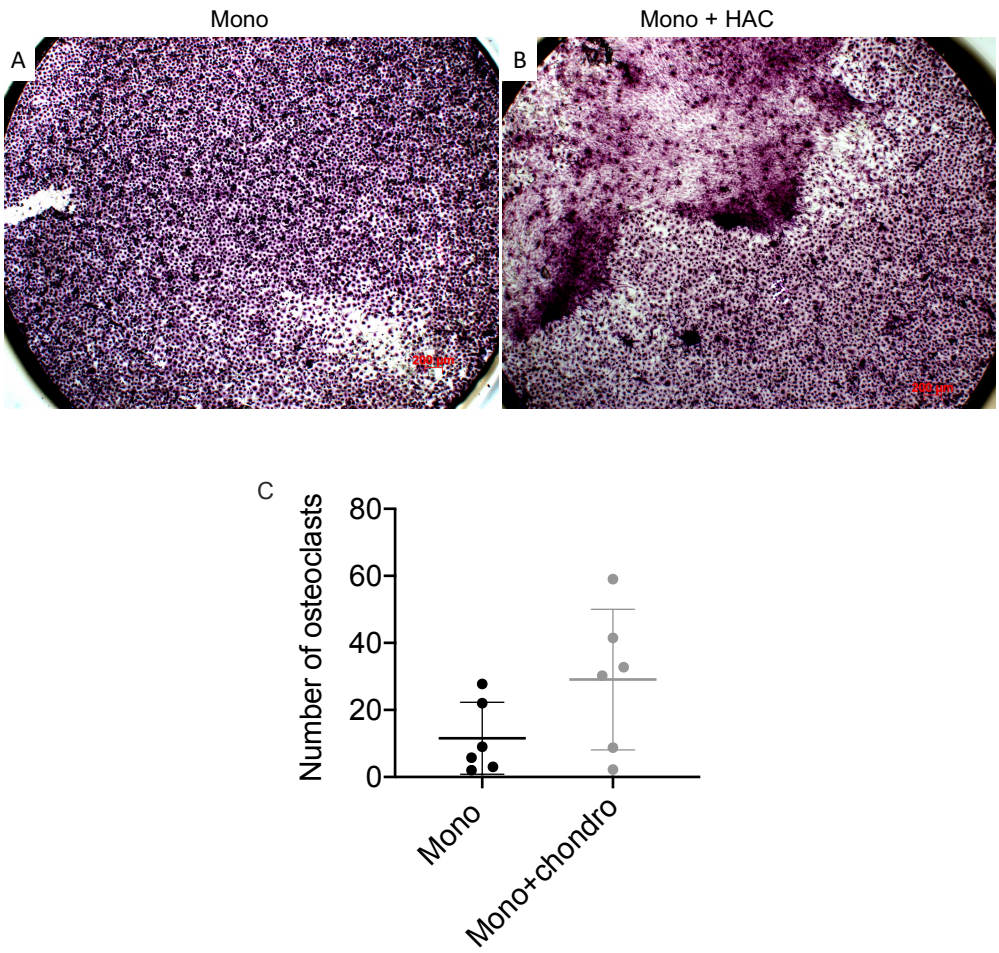
Appendix A.6 Soluble MMPs and MT1-MMP are not released by cartilage. A. Total amount of GAG released by cartilage without or with recombinant human TIMP1. **C.** Cartilage with monoclonal inhibitory antibody against human MMP-14 or negative control antibody fragment and n=5



Appendix A.7 No compensation effect when cells were transfected with MMP-8 and MMP-9 siRNAs. Cells cultured on cartilage were transfected at day 7 and the conditioned media was collected at day 10.



Appendix A.8 GAG and collagen release by osteoclasts on coated plate. Tissue culture plate were coated with either type I collagen or type I collagen and aggrecans. **A**. GAG released in presence or absence of osteoclasts on coated plate. **B.** Quantification of collagen degraded by osteoclasts and n=2 or n=4



Appendix A.9 Co-culture of monocytes and chondrocytes on coverslips. **A.** Monocytes cultured on coverslips for 10 days. **B.** Monocytes and chondrocytes cultured for 10 days. **C.** Number of TRAP-positive cells with 3 or more nuclei. Mono: monocytes and Mono + HAC: co-culture of monocytes and chondrocytes. P value= 0.093 and n=6.

Declaration of authorship

I affirm that all the work presented in this thesis is the result of my own work unless otherwise stated and does not constitute part of any other thesis. The work herein described was carried out while I was a graduate student of the Nuffield Department of Musculoskeletal Sciences working at the Botnar Research Centre under the supervision of Dr Helen Knowles and Dr Sarah Snelling.

Quitterie Larrouture

Presentations

2018 – EuSARC 2018 – The Biology of Sarcoma
Larrouture QL, Gibbons M, Athanasou NA. Snelling SJB, Knowles HJ Can osteoclasts degrade cartilage in sarcoma?

2018 – British Orthopaedic Oncology Society. Larrouture QL, Knowles HJ, Snelling SJB, Gibbons M, Athanasou NA. Osteoclasts are multinucleated cells that degrade cartilage, as well as bone

Posters

2018 – BRS Annual Meeting Larrouture QL, Snelling SJB, Knowles HJ Osteoclasts are multinucleated cells that degrade cartilage, as well as bone

2019 – ASBMR Larrouture QL, Snelling SJB, Knowles HJ. Osteoclasts are multinucleated cells that degrade cartilage, as well as bone

Prizes

John Spivey Research Prize

Word count

49 774 words

REFERENCES

1. J. Gordon Betts, Peter Desaix, Eddie Johnson, Jody E. Johnson, Oksana Korol. James A. Wise, M. W. and K. A. Y. Chapter 9. Joints. in *Anatomy and physiology* (ed. openstax college) 54–61 (2014).
2. Chang, I.-R. & Martin, A. *Anatomy, Cartilage*. *StatPearls* (StatPearls Publishing, 2019).
3. Mahmoud TAMER, T. & Mahmoud Tamer, T. Hyaluronan and synovial joint: function, distribution and healing. (2013). doi:10.2478/intox-2013-0019
4. Mandl, P., Benis, S., Patonay, L. & Balint, P. V. *The Normal Joint*.
5. Sophia Fox, A. J., Bedi, A. & Rodeo, S. A. The basic science of articular cartilage: structure, composition, and function. *Sports Health* **1**, 461–468 (2009).
6. Yin, J., Xia, Y. & Lu, M. Concentration Profiles of Collagen and Proteoglycan in Articular Cartilage by Fourier Transform Infrared Imaging and Principal Component Regression. (2011). doi:10.1016/j.saa.2011.12.002
7. Eyre, D. R. The collagens of articular cartilage. *Semin Arthritis Rheum* **21**, 2–11 (1991).
8. Umlauf, D., Frank, S., Pap, T. & Bertrand, J. Cartilage biology, pathology, and repair. *Cell Mol Life Sci* **67**, 4197–4211 (2010).
9. Akkiraju, H. & Nohe, A. Role of Chondrocytes in Cartilage Formation, Progression of Osteoarthritis and Cartilage Regeneration. *J Dev Biol* **3**, 177–192 (2015).
10. Loeser, R. F. Integrins and chondrocyte–matrix interactions in articular cartilage. *Matrix Biol.* **39**, 11–16 (2014).
11. Singh, P. & Schwarzbauer, J. E. Fibronectin and stem cell differentiation - lessons from chondrogenesis. *J Cell Sci* **125**, 3703–3712 (2012).
12. Goldring, M. B. Chondrogenesis, chondrocyte differentiation, and articular cartilage metabolism in health and osteoarthritis. *Ther Adv Musculoskelet Dis* **4**, 269–285 (2012).
13. Yamashita, S. *et al.* Sox9 directly promotes Bapx1 gene expression to repress Runx2 in chondrocytes. *Exp Cell Res* **315**, 2231–2240 (2009).
14. Chen, F. H., Rousche, K. T. & Tuan, R. S. Technology Insight: adult stem cells in cartilage regeneration and tissue engineering. *REVIEW* doi:10.1038/ncprheum0216
15. Shoulders, M. D. & Raines, R. T. COLLAGEN STRUCTURE AND STABILITY. doi:10.1146/annurev.biochem.77.032207.120833

16. Muiznieks, L. D. & Keeley, F. W. Molecular assembly and mechanical properties of the extracellular matrix: A fibrous protein perspective ☆. *BBA - Mol. Basis Dis.* **1832**, 866–875 (2013).

17. Knupp, C. & Squire, J. M. Molecular packing in network-forming collagens. *ScientificWorldJournal* **3**, 558–577 (2003).

18. Gelse, K., Pöschl, E. & Aigner, T. Collagens-structure, function, and biosynthesis. doi:10.1016/j.addr.2003.08.002

19. Responte, D. J., Natoli, R. M. & Athanasiou, K. A. Collagens of Articular Cartilage: Structure, Function, and Importance in Tissue Engineering. *Crit. Rev. Biomed. Eng.* (2012). doi:10.1615/critrevbiomedeng.v35.i5.20

20. Thomas, J. T. *et al.* Cartilage collagens: strategies for the study of their organisation and expression in the extracellular matrix. *Ann. Rheum. Dis.* **53**, 488–496 (1994).

21. Kiani, C., Chen, L., Wu, Y. J., Yee, A. J. & Yang, B. B. Structure and function of aggrecan. *Cell Res* **12**, 19–32 (2002).

22. Pomin, V. H. & Mulloy, B. pharmaceuticals Editorial Glycosaminoglycans and Proteoglycans. (2018). doi:10.3390/ph11010027

23. Rodriguez, E. & Roughley, P. Link protein can retard the degradation of hyaluronan in proteoglycan aggregates. doi:10.1016/j.joca.2006.02.008

24. Doege, K. J., Sasaki, M., Kimura, T. & Yamada, Y. Complete coding sequence and deduced primary structure of the human cartilage large aggregating proteoglycan, aggrecan. Human-specific repeats, and additional alternatively spliced forms. *J. Biol. Chem.* (1991).

25. Iozzo, R. V & Schaefer, L. Proteoglycan form and function: A comprehensive nomenclature of proteoglycans. *Matrix Biol* **42**, 11–55 (2015).

26. Zheng, J., Luo, W. & Tanzer, M. L. Aggrecan synthesis and secretion. A paradigm for molecular and cellular coordination of multiglobular protein folding and intracellular trafficking. *J. Biol. Chem.* (1998). doi:10.1074/jbc.273.21.12999

27. Aspberg, A. The Different Roles of Aggrecan Interaction Domains. *J. Histochem. Cytochem.* (2012). doi:10.1369/0022155412464376

28. Frantz, C., Stewart, K. M. & Weaver, V. M. The extracellular matrix at a glance. *J. Cell Sci.* **123**, 4195–4200 (2010).

29. Roughley, P. J. Articular cartilage and changes in arthritis: noncollagenous proteins and proteoglycans in the extracellular matrix of cartilage. *Arthritis Res* **3**, 342–347 (2001).

30. Chevalier, X. Fibronectin, cartilage, and osteoarthritis. *Semin. Arthritis Rheum.* **22**, 307–318 (1993).

31. Lin, Z., Willers, C., Xu, J. & Zheng, M. H. The chondrocyte: biology and clinical application. *Tissue Eng* **12**, 1971–1984 (2006).

32. Yang, X. *et al. TGF-/Smad3 Signals Repress Chondrocyte Hypertrophic Differentiation and Are Required for Maintaining Articular Cartilage*. *The Journal of Cell Biology* **153**, (2001).

33. Kim, B.-S., Yu, D.-A. & Han, J. *Stimulation of Chondrogenic Differentiation of Mesenchymal Stem Cells*. *International Journal of Stem Cells* **5**, (2012).

34. Mariani, E., Pulsatelli, L. & Facchini, A. Signaling pathways in cartilage repair. *Int J Mol Sci* **15**, 8667–8698 (2014).

35. Goldring, M. B., Tsuchimochi, K. & Ijiri, K. The control of chondrogenesis. *Journal of Cellular Biochemistry* (2006). doi:10.1002/jcb.20652

36. Mandl, E. W. *et al.* Fibroblast growth factor-2 in serum-free medium is a potent mitogen and reduces dedifferentiation of human ear chondrocytes in monolayer culture. *Matrix Biol.* (2004). doi:10.1016/j.matbio.2004.06.004

37. Martin, I. *et al.* Enhanced cartilage tissue engineering by sequential exposure of chondrocytes to FGF-2 during 2D expansion and BMP-2 during 3D cultivation. *J. Cell. Biochem.* (2001). doi:10.1002/jcb.1203

38. Fukumoto, T. *et al.* Combined effects of insulin-like growth factor-1 and transforming growth factor-β1 on periosteal mesenchymal cells during chondrogenesis in vitro. *Osteoarthr. Cartil.* (2003). doi:10.1053/joca.2002.0869

39. Yaeger, P. C. *et al.* Synergistic action of transforming growth factor-β and insulin-like growth factor-I induces expression of type II collagen and aggrecan genes in adult human articular chondrocytes. *Exp. Cell Res.* (1997). doi:10.1006/excr.1997.3781

40. Maldonado, M. & Nam, J. The Role of Changes in Extracellular Matrix of Cartilage in the Presence of Inflammation on the Pathology of Osteoarthritis. *Biomed Res. Int.* **2013**, (2013).

41. Thomas, L. REVERSIBLE COLLAPSE OF RABBIT EARS AFTER INTRAVENOUS PAPAIN, AND PREVENTION OF RECOVERY BY CORTISONE*. (2019). doi:10.1084/jem.104.2.245

42. Fell, R. B. & Thomas, A. L. *COMPARISON OF THE EFFECTS OF PAPAIN AND VITAMIN A ON CARTILAGE II. T H E EFFECTS ON ORGAN CULTLrREs OF EMBRYONIC SKELETAL T~SSVE*.

43. Lucy, J. A., Dingle, J. T. & Fell, H. B. Studies on the mode of action of excess of vitamin A. 2. A possible role of intracellular proteases in the degradation of cartilage matrix. *Biochem. J.* (2015). doi:10.1042/bj0790500

44. FELL, H. & DINGLE, J. Studies on the mode of action of excess of vitamin A. 6. Lysosomal protease and the degradation of cartilage

matrix. *Biochem. J.* (2015). doi:10.1042/bj0870403

45. Sapolsky, A. I., Altman, R. D., Woessner, J. F. & Howell, D. S. The action of cathepsin D in human articular cartilage on proteoglycans. *J. Clin. Invest.* (1973). doi:10.1172/JCI107224

46. Roman, M. *et al. Assesment of synovial fluid pH in osteoarthritis of the HIP and knee*. *Revista de Chimie -Bucharest- Original Edition-* **68**, (2017).

47. Cummings, N. A. & Nordby, G. L. *Measurement of Synovial Fluid pH in Normal and Arthritic Knees*.

48. Dingle, J. T., Barrett, A. J. & Weston, P. D. Cathepsin D. Characteristics of immunoinhibition and the confirmation of a role in cartilage breakdown. *Biochem. J.* (2015). doi:10.1042/bj1230001

49. Sapolsky, A. I., Howell, D. S. & Woessner, J. F. Neutral proteases and cathepsin D in human articular cartilage. *J. Clin. Invest.* (1974). doi:10.1172/JCI107641

50. Woessner, J. F. Purification of cathepsin D from cartilage and uterus and its action on the protein-polysaccharide complex of cartilage. *J. Biol. Chem.* (1973).

51. Troeberg, L. & Nagase, H. Proteases involved in cartilage matrix degradation in osteoarthritis. (2010). doi:10.1016/j.bbapap.2011.06.020

52. Sapolsky, A. I., Keism, H., Howell, D. S. & Woessner, J. F. *Metalloproteases of Human Articular Cartilage that Digest Cartilage Proteoglycan at Neutral and Acid pH*.

53. Ehrlich, M. G. *et al. Collagenase and Collagenase Inhibitors in Osteoarthritic and Normal Human Cartilage*.

54. Galloway, W. A. *et al.* Purification and characterization of a rabbit bone metalloproteinase that degrades proteoglycan and other connective-tissue components. *Biochem. J.* (2015). doi:10.1042/bj2090741

55. Fosang, A. J., Neame, P. J., Hardingham, T. E., Murphy, G. & Hamilton, J. A. Cleavage of cartilage proteoglycan between G1 and G2 domains by stromelysins. *J. Biol. Chem.* (1991).

56. Sandy, J. D., Neame, P. J., Boynton, R. E. & Flannery, C. R. Catabolism of aggrecan in cartilage explants: Identification of a major cleavage site within the interglobular domain. *J. Biol. Chem.* (1991).

57. Lark, M. W. *et al.* Cell-mediated catabolism of aggrecan: Evidence that cleavage at the 'aggrecanase' site (Glu373-Ala374) is a primary event in proteolysis of the interglobular domain. *J. Biol. Chem.* (1995). doi:10.1074/jbc.270.6.2550

58. Hughes, C. E., Little, C. B., Büttner, F. H., Bartnik, E. & Caterson, B. Differential expression of aggrecanase and matrix metalloproteinase activity in chondrocytes isolated from bovine and porcine articular

cartilage. *J. Biol. Chem.* (1998). doi:10.1074/jbc.273.46.30576

59. Tortorella, M. D. *et al.* Purification and cloning of aggrecanase-1: A member of the ADAMTS family of proteins. *Science (80-.).* (1999). doi:10.1126/science.284.5420.1664

60. Mort, J. S. & Billington, C. J. *Articular cartilage and changes in arthritis Matrix degradation*. (2001).

61. Troeberg, L. & Nagase, H. Proteases involved in cartilage matrix degradation in osteoarthritis. *Biochim Biophys Acta* **1824**, 133–145 (2012).

62. JEROME GROSS ANSD CHARLES M. LAPIERE. COLLAGENOLYTIC ACTIVITY IN AMPHIBIAN TISSUES: A TISSUE CULTURE ASSAY*. *Biochim. Biophys. Acta* **48**, 1014–1022 (1962).

63. Nagase, H., Visse, R. & Murphy, G. Structure and function of matrix metalloproteinases and TIMPs. *Cardiovascular Research* (2006). doi:10.1016/j.cardiores.2005.12.002

64. Cui, N. *et al.* Biochemical and Biological Attributes of Matrix Metalloproteinases HHS Public Access Author manuscript. *Prog Mol Biol Transl Sci* **147**, 1–73 (2017).

65. Ra, H.-J. & Parks, W. C. Control of matrix metalloproteinase catalytic activity. *Matrix Biol.* **26**, 587–596 (2007).

66. Jablonska-Trypuc, A., Matejczyk, M. & Rosochacki, S. Matrix metalloproteinases (MMPs), the main extracellular matrix (ECM) enzymes in collagen degradation, as a target for anticancer drugs. *J Enzym. Inhib Med Chem* **31**, 177–183 (2016).

67. Li, L. & Li, H. Role of microRNA-mediated MMP regulation in the treatment and diagnosis of malignant tumors. *Cancer Biology and Therapy* **14**, 796–805 (2013).

68. Cawston, T. E. & Young, D. A. Proteinases involved in matrix turnover during cartilage and bone breakdown. *Cell Tissue Res* **339**, 221–235 (2010).

69. Nabeshima, K., Inoue, T., Shimao, Y. & Sameshima, T. Matrix metalloproteinases in tumor invasion: Role for cell migration. *Pathol. Int.* **52**, 255–264 (2002).

70. Rundhaug, J. E. Matrix metalloproteinases and angiogenesis. *J. Cell. Mol. Med.* **9**, 267–285 (2005).

71. Tallant, C., Marrero, A. & Gomis-Rüth, F. X. Matrix metalloproteinases: Fold and function of their catalytic domains. *Biochim. Biophys. Acta - Mol. Cell Res.* **1803**, 20–28 (2010).

72. Lynch, C. C. *et al.* MMP-7 promotes prostate cancer-induced osteolysis via the solubilization of RANKL. *Cancer Cell* **7**, 485–496 (2005).

73. Okadasq, Y., Nagasest, H. & Harris, E. D. S. *A Metalloproteinase from Human Rheumatoid Synovial Fibroblasts that Digests Connective Tissue Matrix Components PURIFICATION AND CHARACTERIZATION*. THE JOURNAL 8 Val* **261**, (1986).

74. Fadda, S., Abolkheir, E., Afifi, R. & Gamal, M. Serum matrix metalloproteinase-3 in rheumatoid arthritis patients: Correlation with disease activity and joint destruction. *Egypt. Rheumatol.* (2016). doi:10.1016/j.ejr.2016.01.001

75. Wilson, C. L. *et al.* Regulation of Intestinal α-Defensin Activation by the Metalloproteinase Matrilysin in Innate Host Defense. *Science (80-.).* **286**, 113 LP – 117 (1999).

76. Park, H. I. *et al.* Identification and Characterization of Human Endometase (Matrix Metalloproteinase-26) from Endometrial Tumor. *J. Biol. Chem.* **275**, 20540–20544 (2000).

77. Kuno, K. *et al.* ADAMTS-1 cleaves a cartilage proteoglycan, aggrecan. *FEBS Lett* **478**, 241–245 (2000).

78. Yang, C. Y., Chanalaris, A. & Troeberg, L. ADAMTS and ADAM metalloproteinases in osteoarthritis - looking beyond the 'usual suspects'. *Osteoarthr. Cartil.* **25**, 1000–1009 (2017).

79. Edwards, D. R., Handsley, M. M. & Pennington, C. J. The ADAM metalloproteinases. *Mol. Aspects Med.* **29**, 258–289 (2008).

80. Chubinskaya, S., Mikhail, R., Deutsch, A. & Tindal, M. H. ADAM-10 Protein Is Present in Human Articular Cartilage Primarily in the Membrane-bound Form and Is Upregulated in Osteoarthritis and in Response to IL-1α in Bovine Nasal Cartilage. *J. Histochem. Cytochem.* **49**, 1165–1176 (2001).

81. Millichip, M. I., Dallas, D. J., Wu, E., Dale, S. & McKie, N. The Metallo-Disintegrin ADAM10 (MADM) from Bovine Kidney Has Type IV Collagenase Activityin Vitro. *Biochem. Biophys. Res. Commun.* **245**, 594–598 (1998).

82. Bauer, E. A., Stricklin, G. P., Jeffrey, J. J. & Eisen, A. Z. Collagenase production by human skin fibroblasts. *Biochem. Biophys. Res. Commun.* **64**, 232–240 (1975).

83. Woolley, D. E., Roberts, D. R. & Evanson, J. M. Inhibition of human collagenase activity by a small molecular weight serum protein. *Biochem. Biophys. Res. Commun.* (1975). doi:10.1016/0006-291X(75)90573-2

84. Kuettner, K. E., Hiti, J., Eisenstein, R. & Harper, E. Collagenase inhibition by cationic proteins derived from cartilage and aorta. *Biochem. Biophys. Res. Commun.* (1976). doi:10.1016/0006-291X(76)90956-6

85. Murphy, G., Cartwright, E. C., Sellers, A. & Reynolds, J. J. The detection and characterization of collagenase inhibitors from rabbit tissues in culture. *BBA - Enzymol.* (1977). doi:10.1016/0005-

2744(77)90080-8

86. Vater, C. A., Mainardi, C. L. & Harris, E. D. Inhibitor of human collagenase from cultures of human tendon. *J. Biol. Chem.* (1979).

87. Welgus, H. G. *et al.* A specific inhibitor of vertebrate collagenase produced by human skin fibroblasts. *J. Biol. Chem.* (1979).

88. Cawston, T. E., Galloway, W. A., Mercer, E., Murphy, G. & Reynolds, J. J. Purification of rabbit bone inhibitor of collagenase. *Biochem. J.* **195**, 159–165 (1981).

89. Murphy, G. *et al.* The N-terminal domain of tissue inhibitor of metalloproteinases retains metalloproteinase inhibitory activity. *Biochemistry* (2005). doi:10.1021/bi00247a001

90. Brew, K. & Nagase, H. The tissue inhibitors of metalloproteinases (TIMPs): an ancient family with structural and functional diversity. *Biochim Biophys Acta* **1803**, 55–71 (2010).

91. Arpino, V., Brock, M. & Gill, S. E. The role of TIMPs in regulation of extracellular matrix proteolysis. *Matrix Biol.* **44–46**, 247–254 (2015).

92. Jaworski, D. M., Soloway, P., Caterina, J. & Falls, W. A. Tissue inhibitor of metalloproteinase-2 (TIMP-2)-deficient mice display motor deficits. *J. Neurobiol.* (2006). doi:10.1002/neu.20205

93. Sahebjam, S., Khokha, R. & Mort, J. S. Increased collagen and aggrecan degradation with age in the joints of Timp3-/- mice. *Arthritis Rheum.* (2007). doi:10.1002/art.22427

94. Morris, K. J., Cs-Szabo, G. & Cole, A. A. Characterization of TIMP-3 in human articular talar cartilage. *Connect. Tissue Res.* (2010). doi:10.3109/03008201003686958

95. Black, R. A. *et al.* A14 INJECTED TIMP-3 PROTECTS CARTILAGE IN A RAT MENISCAL TEAR MODEL. *Osteoarthr. Cartil.* (2007). doi:10.1016/s1063-4584(07)60467-1

96. Gill, S. E., Pape, M. C., Khokha, R., Watson, A. J. & Leco, K. J. A null mutation for TissueInhibitor ofMetalloproteinases-3 (Timp-3) impairs murine bronchiole branching morphogenesis. *Dev. Biol.* **261**, 313–323 (2003).

97. Hernandez-Barrantes, S., Shimura, Y., Soloway, P. D., Sang, Q. A. & Fridman, R. Differential Roles of TIMP-4 and TIMP-2 in Pro-MMP-2 Activation by MT1-MMP. *Biochem. Biophys. Res. Commun.* **281**, 126–130 (2001).

98. Koskivirta, I. *et al.* Mice with tissue inhibitor of metalloproteinases 4 (Timp4) deletion succumb to induced myocardial infarction but not to cardiac pressure overload. *J. Biol. Chem.* (2010). doi:10.1074/jbc.M110.136820

99. Sakamuri, S. S. V. P. *et al.* Absence of Tissue Inhibitor of Metalloproteinase-4 (TIMP4) ameliorates high fat diet-induced obesity in mice due to defective lipid absorption. *Sci. Rep.* **7**, 6210

(2017).

100. Krishnan, Y. & Grodzinsky, A. J. Cartilage diseases. *Matrix Biol.* **71**–**72**, 51–69 (2018).

101. Goldring, M. B. The role of the chondrocyte in osteoarthritis. *Arthritis Rheum* **43**, 1916–1926 (2000).

102. Simon, L. S. Osteoarthritis: A review. *Clin. Cornerstone* **2**, 26–37 (1999).

103. Smolen, J. S. *et al.* Rheumatoid arthritis. *Nat. Rev. Dis. Prim.* **4**, 18001 (2018).

104. Schett, G. Cells of the synovium in rheumatoid arthritis. Osteoclasts. *Arthritis Res Ther* **9**, 203 (2007).

105. Huber, L. C. *et al.* Synovial fibroblasts: key players in rheumatoid arthritis. *Rheumatol.* **45**, 669–675 (2006).

106. Posner, A. S. The mineral of bone. *Clin Orthop Relat Res* 87–99 (1985).

107. Clarke, B. Normal bone anatomy and physiology. *Clin J Am Soc Nephrol* **3 Suppl 3**, S131-9 (2008).

108. Lamoureux, F., Baud'huin, M., Duplomb, L., Heymann, D. & Rédini, F. Proteoglycans: Key partners in bone cell biology. *BioEssays* (2007). doi:10.1002/bies.20612

109. Yanagishita, M. Function of proteoglycans in the extracellular matrix. *Pathology International* (1993). doi:10.1111/j.1440-1827.1993.tb02569.x

110. Stock, S. R. The Mineral-Collagen Interface in Bone. doi:10.1007/s00223-015-9984-6

111. Puzas, J. E. Site-specific Mineralized Matrix Formation by Osteoblasts. in *Bone Formation* 71–78 (Springer London, 2004). doi:10.1007/978-1-4471-3777-1_4

112. Olsen, B. R., Reginato, A. M. & Wang, W. *BONE DEVELOPMENT*. *Annu. Rev. Cell Dev. Biol* **16**, (2000).

113. Bukka, P., McKee, M. D. & Karaplis, A. C. Molecular Regulation of Osteoblast Differentiation. in *Bone Formation* **vol 1**, 1–17 (Springer London, 2004).

114. Yang, Y. Skeletal morphogenesis during embryonic development. *Crit Rev Eukaryot Gene Expr* **19**, 197–218 (2009).

115. Baron, R. *Anatomy and Ultrastructure of Bone – Histogenesis, Growth and Remodeling*. *Endotext* (MDText.com, Inc., 2000).

116. Carter, D. R. & Beaupre, G. S. Endochondral Growth and Ossification. in *Skeletal Function and Form* 106–137 (Cambridge University Press, 2000). doi:10.1017/CBO9780511574993.006

117. Carter, D. R. & Beaupre, G. S. Skeletal Tissue Histomorphology and

Mechanics. in *Skeletal Function and Form* 31–52 (Cambridge University Press, 2000). doi:10.1017/CBO9780511574993.003

118. Betts, J. G. *et al. Anatomy & Physiology -OpenStax*. *OpenStax Resources* (2013). doi:10.1017/CBO9781107415324.004

119. Florencio-Silva, R., Sasso, G. R., Sasso-Cerri, E., Simoes, M. J. & Cerri, P. S. Biology of Bone Tissue: Structure, Function, and Factors That Influence Bone Cells. *Biomed Res Int* **2015**, 421746 (2015).

120. Blair, H. C. *et al.* Osteoblast Differentiation and Bone Matrix Formation In Vivo and In Vitro. *Tissue Eng Part B Rev* **23**, 268–280 (2017).

121. Larrouture, Q. C. *et al.* Chloride–hydrogen antiporters ClC-3 and ClC-5 drive osteoblast mineralization and regulate fine-structure bone patterning in vitro. *Physiol. Rep.* (2015). doi:10.14814/phy2.12607

122. Raggatt, L. J. & Partridge, N. C. Cellular and Molecular Mechanisms of Bone Remodeling * Cells Involved in Bone Remodeling. (2010). doi:10.1074/jbc.R109.041087

123. Bonewald, L. F. The Amazing Osteocyte. doi:10.1002/jbmr.320

124. Nakashima, T. *et al.* Evidence for osteocyte regulation of bone homeostasis through RANKL expression. *Nat. Med.* (2011). doi:10.1038/nm.2452

125. Kölliker, A. *Die normale Resorption des Knochengewebes und ihre Bedeutung für die Entstehung der typischen Knochenformen*. (Vogel, 1873).

126. Walker, D. G. Bone resorption restored in osteopetrotic mice by transplants of normal bone marrow and spleen cells. *Science (80-.).* **190**, 784 LP – 785 (1975).

127. Coccia, P. F. *et al.* Successful Bone-Marrow Transplantation for Infantile Malignant Osteopetrosis. *N. Engl. J. Med.* **302**, 701–708 (1980).

128. Ash, P., Loutit, J. F. & Townsend, K. M. S. Osteoclasts derived from haematopoietic stem cells. *Nature* **283**, 669–670 (1980).

129. Burger, E. H. In vitro formation of osteoclasts from long-term cultures of bone marrow mononuclear phagocytes. *J. Exp. Med.* (2004). doi:10.1084/jem.156.6.1604

130. YAMAGUCHI, A. *et al.* The Bone Marrow-Derived Stromal Cell Lines MC3T3-G2/PA6 and ST2 Support Osteoclast-Like Cell Differentiation in Cocultures with Mouse Spleen Cells. *Endocrinology* **125**, 1805–1813 (1989).

131. Rubin, J. & Greenfield, E. M. *Osteoclast: Origin and Differentiation*.

132. Takahashi, N. *et al. Osteoclast-Like Cell Formation and its Regulation by Osteotropic Hormones in Mouse Bone Marrow Cultures**. (1988).

133. Akatsu, T. *et al.* Role of prostaglandins in interleukin-1-induced bone

resorption in mice in vitro. *J. Bone Miner. Res.* (1991). doi:10.1002/jbmr.5650060212

134. Udagawa, N. *et al.* Origin of osteoclasts: mature monocytes and macrophages are capable of differentiating into osteoclasts under a suitable microenvironment prepared by bone marrow-derived stromal cells. *Proc. Natl. Acad. Sci.* **87**, 7260–7264 (2006).

135. Sabokbar, A., Quinn, J. M., McGee, J. O., Athanasou, N. A. & Fujikawa, Y. The human osteoclast precursor circulates in the monocyte fraction. *Endocrinology* **137**, 4058–4060 (1996).

136. Massey, H. M. & Flanagan, A. M. Human osteoclasts derive from CD14-positive monocytes. *Br. J. Haematol.* (1999). doi:10.1046/j.1365-2141.1999.01491.x

137. Elliott, J., Quinn, J. M. W., Gillespie, M. T. & Martin, T. J. A Combination of Osteoclast Differentiation Factor and Macrophage-Colony Stimulating Factor Is Sufficient for both Human and Mouse Osteoclast Formation in Vitro. *Endocrinology* **139**, 4424–4427 (1998).

138. Pixley, F. J. & Stanley, E. R. CSF-1 regulation of the wandering macrophage: Complexity in action. *Trends in Cell Biology* (2004). doi:10.1016/j.tcb.2004.09.016

139. Jimi, E. *et al.* Modulation of Osteoclast Differentiation and Function by the New Members of the Tumor Necrosis Factor Receptor and Ligand Families. *Endocr. Rev.* **20**, 345–357 (1999).

140. Boyle, W. J., Simonet, W. S. & Lacey, D. L. Osteoclast differentiation and activation. *Nature* **423**, 337–342 (2003).

141. Wiktor Jedrzejczak, W. *et al. Total absence of colony-stimulating factor 1 in the macrophage-deficient osteopetrotic (op/op) mouse*. *Proc. Nad. Acad. Sci. USA* **87**, (1990).

142. Yoshida, H. *et al. The murine mutation osteopetrosis is in the coding region of the macrophage colony stimulating factor gene*.

143. Marks, S. C. *et al. Administration of Colony Stimulating Factor-l Corrects Some Macrophage, Dental, and Skeletal Defects in an Osteopetrotic Mutation (Toothless, tl) in the Rat*. *Bone* **13**, (1992).

144. Yoshida, H. *et al.* The murine mutation osteopetrosis is in the coding region of the macrophage colony stimulating factor gene. *Nature* **345**, 442–444 (1990).

145. Dai, X.-M. *et al.* Targeted disruption of the mouse colony-stimulating factor 1 receptor gene results in osteopetrosis, mononuclear phagocyte deficiency, increased primitive progenitor cell frequencies, and reproductive defects. *Blood* **99**, 111 LP – 120 (2002).

146. Kodama, H. *et al. Brief Definitive Report Congenital Osteoclast Deficiency in Osteopetrotic (oplop) Mice Is Cured by Injections of Macrophage Colony-stimulating Factor*.

147. Kim, J. H. & Kim, N. Signaling Pathways in Osteoclast

Differentiation. *Chonnam Med. J.* **52**, 12–17 (2016).

148. Feng, X. & Teitelbaum, S. L. Osteoclasts: New Insights. *Bone Res* **1**, 11–26 (2013).

149. BOYDE, A. *et al.* Osteoclast-Like Cell Formation and its Regulation by Osteotropic Hormones in Mouse Bone Marrow Cultures*. *Endocrinology* **122**, 1373–1382 (1988).

150. Takahashi, N., Martin, T. J. & Suda, T. Modulation of Osteoclast Differentiation. *Endocr. Rev.* **13**, 66–80 (1992).

151. Dougall, W. C. *et al.* RANK is essential for osteoclast and lymph node development. *Genes Dev.* (1999). doi:10.1101/gad.13.18.2412

152. Kong, Y.-Y. *et al.* Activated T cells regulate bone loss and joint destruction in adjuvant arthritis through osteoprotegerin ligand. *Nature* **402**, 304–309 (1999).

153. Kondo, M., Weissman, I. L. & Akashi, K. *Identification of Clonogenic Common Lymphoid Progenitors in Mouse Bone Marrow*. *Cell* **91**, (1997).

154. Hattersley, G., Owens, J., Flanagan, A. M. & Chambers, T. J. *MACROPHAGE COLONY STIMULATING FACTOR (M-CSF) IS ESSENTIAL FOR OSTEOCLAST FORMATION IN VITRO*. **177**, (1991).

155. Tondravi, M. M. *et al.* Osteopetrosis in mice lacking haematopoietic transcription factor PU.1. *Nature* (1997). doi:10.1038/386081a0

156. Dekoter, R. P., Walsh, J. C. & Singh, H. *PU.1 regulates both cytokine-dependent proliferation and differentiation of granulocyte/ macrophage progenitors*. *The EMBO Journal* **17**, (1998).

157. Yavropoulou, M. P. & Yovos, J. G. Osteoclastogenesis--current knowledge and future perspectives. *J Musculoskelet Neuronal Interact* **8**, 204–216 (2008).

158. Bucay, N. *et al.* Osteoprotegerin-deficient mice develop early onset osteoporosis and arterial calcification. *Genes Dev.* (1998). doi:10.1101/gad.12.9.1260

159. Mizuno, A. *et al.* Severe osteoporosis in mice lacking osteoclastogenesis inhibitory factor/osteoprotegerin. *Biochem. Biophys. Res. Commun.* (1998). doi:10.1006/bbrc.1998.8697

160. Holen, I. & Shipman, C. M. Role of osteoprotegerin (OPG) in cancer. *Clin. Sci.* **110**, 279–291 (2006).

161. Jones, S. J. & Boyde, A. Morphological changes of osteoblasts in vitro. *Cell Tissue Res.* (1976). doi:10.1007/BF00215129

162. Athanasou, N. A. & Quinn, J. Immunophenotypic differences between osteoclasts and macrophage polykaryons: Immunohistological distinction and implications for osteoclast ontogeny and function. *J. Clin. Pathol.* (1990). doi:10.1136/jcp.43.12.997

163. Nesbitt, S., Nesbit, A., Helfrich, M. & Horton, M. Biochemical characterization of human osteoclast integrins. Osteoclasts express alpha v beta 3, alpha 2 beta 1, and alpha v beta 1 integrins. *J. Biol. Chem.* (1993).

164. Blair, H. C. How the osteoclast degrades bone. *Bioessays* **20**, 837–846 (1998).

165. Väänänen, H. K. & Horton, M. The osteoclast clear zone is a specialized cell-extracellular matrix adhesion structure. *J. Cell Sci.* (1995).

166. Hall, T. J. & Chambers, T. J. Optimal bone resorption by isolated rat osteoclasts requires chloride bicarbonate exchange. *Calcif. Tissue Int.* (1989). doi:10.1007/BF02556011

167. Bossard, M. J. *et al.* Proteolytic Activity of Human Osteoclast Cathepsin K. *J. Biol. Chem.* (2002). doi:10.1074/jbc.271.21.12517

168. Lyndon Key, L. & Ries, W. L. Chapter 72 - Osteopetrosis. in (eds. Bilezikian, J. P., Raisz, L. G. & Martin, T. J. B. T.-P. of B. B. (Third E.) 1561–1572 (Academic Press, 2008). doi:https://doi.org/10.1016/B978-0-12-373884-4.00019-7

169. Zhang, Y. *et al.* Analysis of the mineral composition of the human calcified cartilage zone. *Int J Med Sci* **9**, 353–360 (2012).

170. Duer, M. J., Friščić, T., Murray, R. C., Reid, D. G. & Wise, E. R. The Mineral Phase of Calcified Cartilage: Its Molecular Structure and Interface with the Organic Matrix. *Biophys. J.* **96**, 3372–3378 (2009).

171. IMHOF, H. *et al.* Subchondral Bone and Cartilage Disease: A Rediscovered Functional Unit. *Invest. Radiol.* **35**, (2000).

172. Kim, H. K. W. *et al.* Hypoxia and HIF-1α expression in the epiphyseal cartilage following ischemic injury to the immature femoral head. *Bone* **45**, 280–288 (2009).

173. Landínez-Parra, N. S. Mechanical Behavior of Articular Cartilage. in (ed. Garzón-Alvarado, D. A.) Ch. 11 (IntechOpen, 2012). doi:10.5772/48323

174. Arkill, K. P. & Winlove, C. P. Solute transport in the deep and calcified zones of articular cartilage. *Osteoarthr. Cartil.* **16**, 708–714 (2008).

175. Pan, J. *et al.* In situ measurement of transport between subchondral bone and articular cartilage. *J Orthop Res* **27**, 1347–1352 (2009).

176. Hwang, J. *et al.* Increased hydraulic conductance of human articular cartilage and subchondral bone plate with progression of osteoarthritis. *Arthritis Rheum.* **58**, 3831–3842 (2008).

177. Pan, J. *et al.* Elevated cross-talk between subchondral bone and cartilage in osteoarthritic joints. *Bone* **51**, 212–217 (2012).

178. Botter, S. M. *et al.* Osteoarthritis induction leads to early and temporal subchondral plate porosity in the tibial plateau of mice: An in vivo

microfocal computed tomography study. *Arthritis Rheum.* **63**, 2690–2699 (2011).

179. Blaney Davidson, E. N., van der Kraan, P. M. & van den Berg, W. B. TGF-β and osteoarthritis. *Osteoarthr. Cartil.* **15**, 597–604 (2007).

180. Zhen, G. *et al.* Inhibition of TGF-β signaling in mesenchymal stem cells of subchondral bone attenuates osteoarthritis. *Nat. Med.* **19**, 704 (2013).

181. Weng, L.-H., Wang, C.-J., Ko, J.-Y., Sun, Y.-C. & Wang, F.-S. Control of Dkk-1 ameliorates chondrocyte apoptosis, cartilage destruction, and subchondral bone deterioration in osteoarthritic knees. *Arthritis Rheum.* **62**, 1393–1402 (2010).

182. Schenk, R. K., Spiro, D. & Wiener, J. Cartilage resorption in the tibial epiphyseal plate of growing rats. *J Cell Biol* **34**, 275–291 (1967).

183. Ota, N. *et al.* Accelerated cartilage resorption by chondroclasts during bone fracture healing in osteoprotegerin-deficient mice. *Endocrinology* **150**, 4823–4834 (2009).

184. Bertuglia, A. *et al.* Osteoclasts are recruited to the subchondral bone in naturally occurring post-traumatic equine carpal osteoarthritis and may contribute to cartilage degradation. *Osteoarthr. Cartil.* **24**, 555–566 (2016).

185. Lofvall, H. *et al.* Osteoclasts degrade bone and cartilage knee joint compartments through different resorption processes. *Arthritis Res Ther* **20**, 67 (2018).

186. Funck-Brentano, T. & Cohen-Solal, M. Crosstalk between cartilage and bone: when bone cytokines matter. *Cytokine Growth Factor Rev* **22**, 91–97 (2011).

187. Funck-Brentano, T. *et al.* Targeting bone alleviates osteoarthritis in osteopenic mice and modulates cartilage catabolism. *PLoS One* (2012). doi:10.1371/journal.pone.0033543

188. Knowles, H. J. *et al.* Chondroclasts are mature osteoclasts which are capable of cartilage matrix resorption. *Virchows Arch* **461**, 205–210 (2012).

189. Neutzsky-Wulff, A. V *et al.* Alterations in osteoclast function and phenotype induced by different inhibitors of bone resorption--implications for osteoclast quality. *BMC Musculoskelet Disord* **11**, 109 (2010).

190. Merril, C. R., Goldman, D., Sedman, S. A. & Ebert, M. H. Ultrasensitive stain for proteins in polyacrylamide gels shows regional variation in cerebrospinal fluid proteins. *Science (80-.).* **211**, 1437 LP – 1438 (1981).

191. Jinek, M. & Doudna, J. A. A three-dimensional view of the molecular machinery of RNA interference. *Nature* **457**, 405–412 (2009).

192. Dana, H. *et al.* Molecular Mechanisms and Biological Functions of

siRNA. *Int. J. Biomed. Sci.* **13**, 48–57 (2017).

193. Hayami, T. *et al.* The role of subchondral bone remodeling in osteoarthritis: reduction of cartilage degeneration and prevention of osteophyte formation by alendronate in the rat anterior cruciate ligament transection model. *Arthritis Rheum* **50**, 1193–1206 (2004).

194. Bikle, D. D. *et al.* Alendronate increases skeletal mass of growing rats during unloading by inhibiting resorption of calcified cartilage. *J. Bone Miner. Res.* **9**, 1777–1787 (1994).

195. Kadri, A. *et al.* Inhibition of bone resorption blunts osteoarthritis in mice with high bone remodelling. *Ann. Rheum. Dis.* **69**, 1533 LP – 1538 (2010).

196. Shimizu, S. *et al.* Prevention of cartilage destruction with intraarticular osteoclastogenesis inhibitory factor/osteoprotegerin in a murine model of osteoarthritis. *Arthritis Rheum.* **56**, 3358–3365 (2007).

197. Shibakawa, A. *et al.* The role of subchondral bone resorption pits in osteoarthritis: MMP production by cells derived from bone marrow. *Osteoarthr. Cartil.* **13**, 679–687 (2005).

198. Durand, M. *et al.* Monocytes from patients with osteoarthritis display increased osteoclastogenesis and bone resorption: The In Vitro Osteoclast Differentiation in Arthritis study. *Arthritis Rheum.* **65**, 148–158 (2013).

199. Gravallese, E. M. *et al.* Identification of cell types responsible for bone resorption in rheumatoid arthritis and juvenile rheumatoid arthritis. *Am. J. Pathol.* **152**, 943–951 (1998).

200. Bromley, M. & Woolley, D. E. Chondroclasts and Osteoclasts at Subchondral Sites of Erosion in the Rheumatoid Joint. *Arthritis Rheum.* **27**, 968–975 (1984).

201. Kotake, S. *et al. Activated Human T Cells Directly Induce Osteoclastogenesis From Human Monocytes Possible Role of T Cells in Bone Destruction in Rheumatoid Arthritis Patients*. *ARTHRITIS & RHEUMATISM* **44**, (2001).

202. Gravallese, E. M. *et al.* Synovial tissue in rheumatoid arthritis is a source of osteoclast differentiation factor. *Arthritis Rheum.* **43**, 250–258 (2000).

203. Horwood, N. J. *et al.* Activated T Lymphocytes Support Osteoclast Formation in Vitro. *Biochem. Biophys. Res. Commun.* **265**, 144–150 (1999).

204. Seitz, M., Loetcher, P., Fey, M. F. & Tobler, A. CONSTITUTIVE mRNA AND PROTEIN PRODUCTION OF MACROPHAGE COLONY-STIMULATING FACTOR BUT NOT OF OTHER CYTOKINES BY SYNOVIAL FIBROBLASTS FROM RHEUMATOID ARTHRITIS AND OSTEOARTHRITIS PATIENTS. *Rheumatology* **33**, 613–619 (1994).

205. Feldmann, M., Brennan, F. M. & Maini, R. N. ROLE OF CYTOKINES IN RHEUMATOID ARTHRITIS. *Annu. Rev. Immunol.* **14**, 397–440 (1996).

206. Luo, G., Li, F., Li, X., Wang, Z.-G. & Zhang, B. TNF-α and RANKL promote osteoclastogenesis by upregulating RANK via the NF-κB pathway. *Mol. Med. Rep.* **17**, 6605–6611 (2018).

207. Keffer, J. *et al.* Transgenic mice expressing human tumour necrosis factor: a predictive genetic model of arthritis. *EMBO J.* **10**, 4025–4031 (1991).

208. Herrak, P. *et al.* Zoledronic acid protects against local and systemic bone loss in tumor necrosis factor–mediated arthritis. *Arthritis Rheum.* **50**, 2327–2337 (2004).

209. Campanacci, M., Baldini, N., Boriani, S. & Sudanese, A. Giant-cell tumor of bone. *JBJS* **69**, (1987).

210. Kumar Verma, R., Gupta, G., Bal, A. & Yadav, J. Primary Giant Cell Rich Osteosarcoma of Maxilla: An Unusual Case Report. doi:10.1007/s12663-010-0066-z

211. Farjanikish, G., Dezfoulian, O. & Mohammadi, H. Metastatic giant cell osteosarcoma in a cat. *Vet. Res. forum an Int. Q. J.* **9**, 289–292 (2018).

212. Simon, M. A. & Hecht, J. D. Invasion of joints by primary bone sarcomas in adults. *Cancer* **50**, 1649–1655 (1982).

213. Quan, G. M. Y. *et al.* Osteosarcoma near joints: Assessment and implications. *J. Surg. Oncol.* **91**, 159–166 (2005).

214. Wang, C.-S. *et al.* Giant cell-rich osteosarcoma in long bones: clinical, radiological and pathological features. *Radiol. Med.* **118**, 1324–1334 (2013).

215. Yamagishi, T. *et al.* Receptor-Activator of Nuclear KappaB Ligand Expression as a New Therapeutic Target in Primary Bone Tumors. *PLoS One* **11**, e0154680–e0154680 (2016).

216. Fitzgerald, J., Broehm, C., Chafey, D. & Treme, G. Chondroblastoma of the knee treated with resection and osteochondral allograft reconstruction. *Case Rep. Orthop.* **2014**, 543959 (2014).

217. Huang, L., Cheng, Y. Y., Chow, L. T. C., Zheng, M. H. & Kumta, S. M. Receptor activator of NF-kappaB ligand (RANKL) is expressed in chondroblastoma: possible involvement in osteoclastic giant cell recruitment. *Mol. Pathol.* **56**, 116–120 (2003).

218. Odgren, P. R., Witwicka, H. & Reyes-Gutierrez, P. The cast of clasts: catabolism and vascular invasion during bone growth, repair, and disease by osteoclasts, chondroclasts, and septoclasts. doi:10.3109/03008207.2016.1140752

219. Bromley, M., Evanson, J. M. & Woolley, D. E. Chondroclasts and Osteoclasts at Subchondral Sites of Cartilage Erosion in the

Rheumatoid Joint. *Bone* **7**, 146 (1986).

220. Savostin-Asling, I. & Asling, C. W. Transmission and scanning electron microscope studies of calcified cartilage resorption. *Anat. Rec.* **183**, 373–391 (1975).

221. Savostin-Asling, I. & Asling, C. W. Resorption of calcified cartilage as seen in Meckel's cartilage of rats. *Anat. Rec.* **176**, 345–359 (1973).

222. Bromley, M. & Woolley, D. E. Histopathology of the rheumatoid lesion. Identification of cell types at sites of cartilage erosion. *Arthritis Rheum* **27**, 857–863 (1984).

223. Suzumoto, R., Takami, M. & Sasaki, T. Differentiation and function of osteoclasts cultured on bone and cartilage. *J Electron Microsc* **54**, 529–540 (2005).

224. Takito, J., Inoue, S. & Nakamura, M. The Sealing Zone in Osteoclasts: A Self-Organized Structure on the Bone. *Int. J. Mol. Sci.* **19**, 984 (2018).

225. Avnet, S. *et al.* Increased osteoclast activity is associated with aggressiveness of osteosarcoma. *Int. J. Oncol.* (2008). doi:10.3892/ijo_00000113

226. Saltel, F., Destaing, O., Bard, F., Eichert, D. & Jurdic, P. Apatite-mediated Actin Dynamics in Resorbing Osteoclasts. *Mol. Biol. Cell* **15**, 5231–5241 (2004).

227. Chambers, T. J., Thomson, B. M. & Fuller, K. Effect of substrate composition on bone resorption by rabbit osteoclasts. *J Cell Sci* **70**, 61–71 (1984).

228. Nordahl, J., Andersson, G. & Reinholt, F. P. Chondroclasts and osteoclasts in bones of young rats: comparison of ultrastructural and functional features. *Calcif Tissue Int* **63**, 401–408 (1998).

229. Kleinhans, C., Schmid, F. F., Schmid, F. V & Kluger, P. J. Comparison of osteoclastogenesis and resorption activity of human osteoclasts on tissue culture polystyrene and on natural extracellular bone matrix in 2D and 3D. *J. Biotechnol.* **205**, 101–110 (2015).

230. Fisher, J. E. *et al.* Inhibition of osteoclastic bone resorption in vivo by echistatin, an "arginyl-glycyl-aspartyl " (Rgd)-containing protein. *Endocrinology* (1993). doi:10.1210/endo.132.3.8440195

231. Lakkakorpi, P. T., Horton, M. A., Helfrich, M. H., Karhukorpi, E. K. & Vaananen, H. K. Vitronectin receptor has a role in bone resorption but does not mediate tight sealing zone attachment of osteoclasts to the bone surface. *J Cell Biol* **115**, 1179–1186 (1991).

232. Engleman, V. W. *et al.* A peptidomimetic antagonist of the αvβ3 integrin inhibits bone resorption in vitro and prevents osteoporosis in vivo. *J. Clin. Invest.* (1997). doi:10.1172/JCI119404

233. Fuller, K., Ross, J. L., Szewczyk, K. A., Moss, R. & Chambers, T. J. Bone Is Not Essential for Osteoclast Activation. *PLoS One* **5**, e12837

(2010).

234. Lindstrom, E., Grabowska, U., Athanasou, N. A., Fuller, K. & Chambers, T. J. Inhibition of CTX-II release by cathepsin K inhibition in vivo but not in vitro suggests that anti-resorptive therapy protects cartilage. *Osteoarthr. Cartil.* **23**, A310 (2015).

235. Matsuo, K. & Irie, N. Osteoclast–osteoblast communication. *Arch. Biochem. Biophys.* **473**, 201–209 (2008).

236. Blair, H. C. *et al.* Support of bone mineral deposition by regulation of pH. *Am. J. Physiol. Physiol.* (2018). doi:10.1152/ajpcell.00056.2018

237. Sobota, J. A., Bäck, N., Eipper, B. A. & Mains, R. E. Inhibitors of the V0 subunit of the vacuolar H+-ATPase prevent segregation of lysosomal- and secretory-pathway proteins. *J. Cell Sci.* **122**, 3542–3553 (2009).

238. Henriksen, K. *et al.* Characterization of osteoclasts from patients harboring a G215R mutation in ClC-7 causing autosomal dominant osteopetrosis type II. *Am. J. Pathol.* **164**, 1537–1545 (2004).

239. Henriksen, K. *et al.* Degradation of the organic phase of bone by osteoclasts: a secondary role for lysosomal acidification. *J Bone Min. Res* **21**, 58–66 (2006).

240. Motyckova, G. & Fisher, D. Pycnodysostosis: Role and Regulation of Cathepsin K in Osteoclast Function and Human Disease. *Curr. Mol. Med.* (2005). doi:10.2174/1566524023362401

241. Delaisse, J. M. *et al.* Matrix metalloproteinases (MMP) and cathepsin K contribute differently to osteoclastic activities. *Microsc Res Tech* **61**, 504–513 (2003).

242. Everts, V. *et al.* The Bone Lining Cell: Its Role in Cleaning Howship's Lacunae and Initiating Bone Formation. *J. Bone Miner. Res.* **17**, 77–90 (2002).

243. Everts, V. *et al.* Osteoclastic Bone Degradation and the Role of Different Cysteine Proteinases and Matrix Metalloproteinases: Differences Between Calvaria and Long Bone. *J. Bone Miner. Res.* **21**, 1399–1408 (2006).

244. Martínez-Calatrava, M. J. *et al.* RANKL synthesized by articular chondrocytes contributes to juxta-articular bone loss in chronic arthritis. *Arthritis Res. Ther.* **14**, R149 (2012).

245. Guévremont, M. *et al.* Human Adult Chondrocytes Express Hepatocyte Growth Factor (HGF) Isoforms but Not HGF: Potential Implication of Osteoblasts on the Presence of HGF in Cartilage. *J. Bone Miner. Res.* **18**, 1073–1081 (2003).

246. Reboul, P. *et al.* Hepatocyte growth factor induction of collagenase 3 production in human osteoarthritic cartilage: Involvement of the stress-activated protein kinase/c-Jun N-terminal kinase pathway and a sensitive p38 mitogen-activated protein kinase inhibitor cascade.

Arthritis Rheum. **44**, 73–84 (2001).

247. Sanchez, C. *et al.* Osteoblasts from the sclerotic subchondral bone downregulate aggrecan but upregulate metalloproteinases expression by chondrocytes. This effect is mimicked by interleukin-6, -1β and oncostatin M pre-treated non-sclerotic osteoblasts. *Osteoarthr. Cartil.* **13**, 979–987 (2005).

248. Sanchez, C. *et al.* Subchondral bone osteoblasts induce phenotypic changes in human osteoarthritic chondrocytes. *Osteoarthr. Cartil.* **13**, 988–997 (2005).

249. Dreier, R., Wallace, S., Fuchs, S., Bruckner, P. & Grassel, S. Paracrine interactions of chondrocytes and macrophages in cartilage degradation: articular chondrocytes provide factors that activate macrophage-derived pro-gelatinase B (pro-MMP-9). *J Cell Sci* **114**, 3813–3822 (2001).

250. Taylor, L. M., Turksen, K., Aubin, J. E. & Heersche, J. N. Osteoclast differentiation in cocultures of a clonal chondrogenic cell line and mouse bone marrow cells. *Endocrinology* **133**, 2292–2300 (1993).

251. Wang, B., Jin, H., Shu, B., Mira, R. R. & Chen, D. Chondrocytes-Specific Expression of Osteoprotegerin Modulates Osteoclast Formation in Metaphyseal Bone. *Sci. Rep.* **5**, 13667 (2015).

252. Usui, M. *et al.* Murine and chicken chondrocytes regulate osteoclastogenesis by producing RANKL in response to BMP2. *J. Bone Miner. Res.* **23**, 314–325 (2008).

253. Masuyama, R. *et al.* Vitamin D receptor in chondrocytes promotes osteoclastogenesis and regulates FGF23 production in osteoblasts. *J. Clin. Invest.* **116**, 3150–3159 (2006).

254. Kwan Tat, S. *et al.* Modulation of OPG, RANK and RANKL by human chondrocytes and their implication during osteoarthritis. *Rheumatol.* **48**, 1482–1490 (2009).

255. Kafienah, W., Brömme, D., Buttle, D. J., Croucher, L. J. & Hollander, A. P. Human cathepsin K cleaves native type I and II collagens at the N-terminal end of the triple helix. *Biochem. J.* **331 (Pt 3**, 727–732 (1998).

256. Brown, C. J. *et al.* Inhibitors of collagenase but not of gelatinase reduce cartilage explant proteoglycan breakdown despite only low levels of matrix metalloproteinase activity. *J. Clin. Pathol. - Clin. Mol. Pathol.* (1996).

257. Yocum, S. A., Loprestimorrow, L. L., Gabel, C. A., Milici, A. J. & Mitchell, P. G. Bafilomycin A1 Inhibits IL-1-Stimulated Proteoglycan Degradation by Chondrocytes Without Affecting Stromelysin Synthesis. *Arch. Biochem. Biophys.* **316**, 827–835 (1995).

258. Newton, P. T., Vuppalapati, K. K., Bouderlique, T. & Chagin, A. S. Pharmacological inhibition of lysosomes activates the MTORC1 signaling pathway in chondrocytes in an autophagy-independent

manner. *Autophagy* **11**, 1594–1607 (2015).

259. Chamoux, E., Houde, N., L'Eriger, K. & Roux, S. Osteoprotegerin decreases human osteoclast apoptosis by inhibiting the TRAIL pathway. *J. Cell. Physiol.* **216**, 536–542 (2008).

260. Williams, K. E. & Olsen, D. R. Matrix metalloproteinase-1 cleavage site recognition and binding in full-length human type III collagen. *Matrix Biol.* **28**, 373–379 (2009).

261. Farley, J., Dejica, V. M. & Mort, J. S. Proteases and Cartilage Degradation in Osteoarthritis. in

262. Fosang, A. J. *et al.* Fibroblast and neutrophil collagenases cleave at two sites in the cartilage aggrecan interglobular domain. *Biochem. J.* (1993). doi:10.1042/bj2950273

263. Durigova, M., Nagase, H., Mort, J. S. & Roughley, P. J. MMPs are less efficient than ADAMTS5 in cleaving aggrecan core protein. *Matrix Biol.* **30**, 145–153 (2011).

264. Cole, A. A. *et al.* Chondrocyte matrix metalloproteinase-8. Human articular chondrocytes express neutrophil collagenase. *J Biol Chem* **271**, 11023–11026 (1996).

265. Fosang, A. J. *et al.* Neutrophil collagenase (MMP-8) cleaves at the aggrecanase site E373-A374 in the interglobular domain of cartilage aggrecan. *Biochem J* **304 (Pt 2**, 347–351 (1994).

266. Owen, C. A., Hu, Z., Lopez-Otin, C. & Shapiro, S. D. Membrane-Bound Matrix Metalloproteinase-8 on Activated Polymorphonuclear Cells Is a Potent, Tissue Inhibitor of Metalloproteinase-Resistant Collagenase and Serpinase. *J. Immunol.* (2014). doi:10.4049/jimmunol.172.12.7791

267. Quintero, P. A., Knolle, M. D., Cala, L. F., Zhuang, Y. & Owen, C. A. Matrix Metalloproteinase-8 Inactivates Macrophage Inflammatory Protein-1 To Reduce Acute Lung Inflammation and Injury in Mice. *J. Immunol.* (2009). doi:10.4049/jimmunol.0900290

268. Arner, E. C., Decicco, C. P., Cherney, R. & Tortorella, M. D. Cleavage of native cartilage aggrecan by neutrophil collagenase (MMP-8) is distinct from endogenous cleavage by aggrecanase. *J. Biol. Chem.* (1997). doi:10.1074/jbc.272.14.9294

269. Shlopov, B. V *et al.* Osteoarthritic lesions: involvement of three different collagenases. *Arthritis Rheum* **40**, 2065–2074 (1997).

270. Salminen, H. J. *et al.* Differential expression patterns of matrix metalloproteinases and their inhibitors during development of osteoarthritis in a transgenic mouse model. *Ann. Rheum. Dis.* (2002). doi:10.1136/ard.61.7.591

271. Hanemaaijer, R. *et al.* Matrix metalloproteinase-8 is expressed in rheumatoid synovial fibroblasts and endothelial cells: Regulation by tumor necrosis factor-α and doxycycline. *J. Biol. Chem.* (1997).

doi:10.1074/jbc.272.50.31504

272. Qingzhong, X. *et al.* Functional Role of Matrix Metalloproteinase-8 in Stem/Progenitor Cell Migration and Their Recruitment Into Atherosclerotic Lesions. *Circ. Res.* **112**, 35–47 (2013).

273. Fang, C. *et al.* An important role of matrix metalloproteinase-8 in angiogenesis in vitro and in vivo. *Cardiovasc. Res.* **99**, 146–155 (2013).

274. Qingzhong, X. *et al.* Matrix Metalloproteinase-8 Promotes Vascular Smooth Muscle Cell Proliferation and Neointima Formation. *Arterioscler. Thromb. Vasc. Biol.* **34**, 90–98 (2014).

275. Gueders, M. M. *et al.* Matrix Metalloproteinase-8 Deficiency Promotes Granulocytic Allergen-Induced Airway Inflammation. *J. Immunol.* **175**, 2589 LP – 2597 (2005).

276. Wen, G. *et al.* A Novel Role of Matrix Metalloproteinase-8 in Macrophage Differentiation and Polarization. *J Biol Chem* **290**, 19158–19172 (2015).

277. Laxton, R. C. *et al.* A role of matrix metalloproteinase-8 in atherosclerosis. *Circ. Res.* **105**, 921–929 (2009).

278. Van Lint, P. *et al.* Resistance of Collagenase-2 (Matrix Metalloproteinase-8)-Deficient Mice to TNF-Induced Lethal Hepatitis. *J. Immunol.* **175**, 7642 LP – 7649 (2005).

279. Balbín, M. *et al.* Loss of collagenase-2 confers increased skin tumor susceptibility to male mice. *Nat. Genet.* **35**, 252–257 (2003).

280. Tetlow, L. C., Adlam, D. J. & Woolley, D. E. Matrix metalloproteinase and proinflammatory cytokine production by chondrocytes of human osteoarthritic cartilage: associations with degenerative changes. *Arthritis Rheum* **44**, 585–594 (2001).

281. Helminen, H. J., Säämänen, A. -M., Salminen, H. & Hyttinen, M. M. Transgenic mouse models for studying the role of cartilage macromolecules in osteoarthritis. *Rheumatology* **41**, 848–856 (2002).

282. Little, C. B. *et al.* Matrix metalloproteinase 13–deficient mice are resistant to osteoarthritic cartilage erosion but not chondrocyte hypertrophy or osteophyte development. *Arthritis Rheum.* **60**, 3723–3733 (2009).

283. Okada, Y., Nagase, H. & Harris, E. D. A metalloproteinase from human rheumatoid synovial fibroblasts that digests connective tissue matrix components. Purification and characterization. *J. Biol. Chem.* (1986).

284. McCroskery, P. A., Wood, S. & Harris, E. D. Gelatin: A Poor Substrate for a Mammalian Collagenase. *Science (80-.).* **182**, 70 LP – 71 (1973).

285. Sellers, A., Reynolds, J. J. & Meikle, M. C. *Neutral Metallo-Proteinases of Rabbit Bone*. *Biochem. J* **171**, (1978).

286. Klein, T. & Bischoff, • R. Physiology and pathophysiology of matrix metalloproteases. doi:10.1007/s00726-010-0689-x

287. Martignetti, J. A. *et al.* Mutation of the matrix metalloproteinase 2 gene (MMP2) causes a multicentric osteolysis and arthritis syndrome. *Nat. Genet.* **28**, 261–265 (2001).

288. Mosig, R. A. *et al.* Loss of MMP-2 disrupts skeletal and craniofacial development, and results in decreased bone mineralization, joint erosion, and defects in osteoblast and osteoclast growth. *Hum Mol Genet* **16**, 1113–1123 (2007).

289. Farina, A. R. & Mackay, A. R. Gelatinase B/MMP-9 in Tumour Pathogenesis and Progression. *Cancers (Basel).* **6**, 240–296 (2014).

290. Vu, T. H. *et al.* MMP-9/Gelatinase B Is a Key Regulator of Growth Plate Angiogenesis and Apoptosis of Hypertrophic Chondrocytes. *Cell* **93**, 411–422 (1998).

291. Ahrens, D., Koch, A. E., Pope, R. M., Stein-Picarella, M. & Niedbala, M. J. Expression of matrix metalloproteinase 9 (96-kd gelatinase B) in human rheumatoid arthritis. *Arthritis Rheum.* **39**, 1576–1587 (1996).

292. Yoshihara, Y. *et al.* Matrix metalloproteinases and tissue inhibitors of metalloproteinases in synovial fluids from patients with rheumatoid arthritis or osteoarthritis. *Ann. Rheum. Dis.* **59**, 455–461 (2000).

293. Jiang, A. *et al.* Regulation of membrane-type matrix metalloproteinase 1 activity by dynamin-mediated endocytosis. *Proc. Natl. Acad. Sci.* **98**, 13693 LP – 13698 (2001).

294. Zhou, Z. *et al.* Impaired endochondral ossification and angiogenesis in mice deficient in membrane-type matrix metalloproteinase I. *Proc. Natl. Acad. Sci. U. S. A.* **97**, 4052–4057 (2000).

295. Holmbeck, K. *et al. MT1-MMP-Deficient Mice Develop Dwarfism, Osteopenia, Arthritis, and Connective Tissue Disease due to Inadequate Collagen Turnover*. *Cell* **99**, (Nagase, 1999).

296. Stanton, H. *et al.* ADAMTS5 is the major aggrecanase in mouse cartilage in vivo and in vitro. *Nature* **434**, 648–652 (2005).

297. Glasson, S. S. *et al.* Deletion of active ADAMTS5 prevents cartilage degradation in a murine model of osteoarthritis. *Nature* **434**, 644–648 (2005).

298. Little, C. B. *et al.* Blocking aggrecanase cleavage in the aggrecan interglobular domain abrogates cartilage erosion and promotes cartilage repair. *J. Clin. Invest.* **117**, (2007).

299. Bondeson, J., Wainwright, S., Hughes, C. & Caterson, B. *The regulation of the ADAMTS4 and ADAMTS5 aggrecanases in osteoarthritis: a review*. *Clin Exp Rheumatol* **26**, (2008).

300. Song, R. H. *et al.* Aggrecan degradation in human articular cartilage explants is mediated by both ADAMTS-4 and ADAMTS-5. *Arthritis Rheum* **56**, 575–585 (2007).

301. Powell, A. J., Little, C. B. & Hughes, C. E. Low molecular weight isoforms of the aggrecanases are responsible for the cytokine-induced proteolysis of aggrecan in a porcine chondrocyte culture system. *Arthritis Rheum.* **56**, 3010–3019 (2007).

302. Tortorella, M. D., Malfait, A.-M., Deccico, C. & Arner, E. The role of ADAM-TS4 (aggrecanase-1) and ADAM-TS5 (aggrecanase-2) in a model of cartilage degradation. *Osteoarthr. Cartil.* **9**, 539–552 (2001).

303. Bekhouche, M. & Colige, A. The procollagen N-proteinases ADAMTS2, 3 and 14 in pathophysiology. *Matrix Biol.* **44–46**, 46–53 (2015).

304. Fosang, A. J. *et al.* The interglobular domain of cartilage aggrecan is cleaved by PUMP, gelatinases, and cathepsin B. *J. Biol. Chem.* (1992).

305. Fosang, A. J., Last, K., Knäuper, V., Murphy, G. & Neame, P. J. Degradation of cartilage aggrecan by collagenase-3 (MMP-13). *FEBS Lett.* (1996). doi:10.1016/0014-5793(95)01539-6

306. Fosang, A. J., Last, K., Fujii, Y., Seiki, M. & Okada, Y. Membrane-type 1 MMP (MMP-14) cleaves at three sites in the aggrecan interglobular domain. *FEBS Lett.* (1998). doi:10.1016/S0014-5793(98)00667-X

307. Bonassar, L. J. *et al.* Changes in cartilage composition and physical properties due to stromelysin degradation. *Arthritis Rheum.* **38**, 173–183 (1995).

308. Little, C. B. *et al.* Matrix metalloproteinases are involved in C-terminal and interglobular domain processing of cartilage aggrecan in late stage cartilage degradation. *Matrix Biol.* (2002). doi:10.1016/S0945-053X(02)00004-5

309. Struglics, A. & Hansson, M. MMP proteolysis of the human extracellular matrix protein aggrecan is mainly a process of normal turnover. *Biochem. J.* **446**, 213 LP – 223 (2012).

310. Van Meurs, J. B. J. *et al.* Kinetics of aggrecanase- and metalloproteinase-induced neoepitopes in various stages of cartilage destruction in murine arthritis. *Arthritis Rheum.* (1999). doi:10.1002/1529-0131(199906)42:6<1128::AID-ANR9>3.0.CO;2-2

311. Van Meurs, J. *et al.* Cleavage of aggrecan at the ASN341-PHE342 site coincides with the initiation of collagen damage in murine antigen-induced arthritis: A pivotal role for stromelysin 1 in matrix metalloproteinase activity. *Arthritis Rheum.* (1999). doi:10.1002/1529-0131(199910)42:10<2074::AID-ANR7>3.0.CO;2-5

312. Fosang, A. J., Rogerson, F. M., East, C. J. & Stanton, H. ADAMTS-5: The story so far. *European Cells and Materials* (2008). doi:10.22203/eCM.v015a02

313. Büttner, F. H. *et al.* Membrane type 1 matrix metalloproteinase (MT1-MMP) cleaves the recombinant aggrecan substrate rAgg1mut at the

'aggrecanase' and the MMP sites. Characterization of MT1-MMP catabolic activities on the interglobular domain of aggrecan. *Biochem. J.* **333 (Pt 1**, 159–165 (1998).

314. Vankemmelbeke, M. N. *et al.* Expression and activity of ADAMTS-5 in synovium. *Eur. J. Biochem.* **268**, 1259–1268 (2001).

315. Tortorella, M. D., Liu, R.-Q., Burn, T., Newton, R. C. & Arner, E. Characterization of human aggrecanase 2 (ADAM-TS5): substrate specificity studies and comparison with aggrecanase 1 (ADAM-TS4). *Matrix Biol.* **21**, 499–511 (2002).

316. Tortorella, M. D. *et al.* Sites of aggrecan cleavage by recombinant human aggrecanase-1 (ADAMTS-4). *J. Biol. Chem.* (2000). doi:10.1074/jbc.M909383199

317. Vilim, V. & Fosang, A. J. Proteoglycans isolated from dissociative extracts of differently aged human articular cartilage: characterization of naturally occurring hyaluronan-binding fragments of aggrecan. *Biochem. J.* **304**, 887 LP – 894 (1994).

318. Carlos Rodríguez-Manzaneque, J. *et al.* ADAMTS1 cleaves aggrecan at multiple sites and is differentially inhibited by metalloproteinase inhibitors. *Biochem. Biophys. Res. Commun.* **293**, 501–508 (2002).

319. Westling, J. *et al.* ADAMTS4 cleaves at the aggrecanase site (Glu373-Ala374) and secondarily at the matrix metalloproteinase site (Asn341-Phe342) in the aggrecan interglobular domain. *J. Biol. Chem.* **277**, 16059–16066 (2002).

320. Nothnick, W. B. Reduction in reproductive lifespan of tissue inhibitor of metalloproteinase 1 (TIMP-1)-deficient female mice. *Reproduction* (2001). doi:10.1530/rep.0.1220923

321. J. F. Woessner, H. N. *No Title Matrix Metalloproteinases and TIMPs. , Nagase H, 2000, Matrix Metalloproteinases and TIMPs, Oxford, USA, pp: 130 - 131.* (2000).

322. Murphy, G. & Nagase, H. Progress in matrix metalloproteinase research. *Mol. Aspects Med.* **29**, 290–308 (2008).

323. Xue, M. *et al.* Endogenous MMP-9 and not MMP-2 promotes rheumatoid synovial fibroblast survival, inflammation and cartilage degradation. *Rheumatology* **53**, 2270–2279 (2014).

324. Waddell, L. A. *et al.* ADGRE1 (EMR1, F4/80) Is a Rapidly-Evolving Gene Expressed in Mammalian Monocyte-Macrophages. *Front. Immunol.* **9**, 2246 (2018).

325. Yago, T. *et al.* IL-35 inhibits human osteoclastogenesis from monocytes induced by receptor-activator of NF-κB ligand. *Cent. J. Immunol.* **43**, 148–154 (2018).

326. Matsuoka, K., Park, K., Ito, M., Ikeda, K. & Takeshita, S. Osteoclast-Derived Complement Component 3a Stimulates Osteoblast Differentiation. *J. Bone Miner. Res.* **29**, 1522–1530 (2014).

327. Aeschlimann, D. & Evans, B. A. J. The vital osteoclast: how is it regulated? *Cell Death Differ.* **11**, S5 (2004).

328. Steinl, C. *et al.* Release of Matrix Metalloproteinase-8 During Physiological Trafficking and Induced Mobilization of Human Hematopoietic Stem Cells. *Stem Cells Dev.* **22**, 1307–1318 (2012).

329. Angata, T., Nycholat, C. M. & Macauley, M. S. Therapeutic Targeting of Siglecs using Antibody- and Glycan-Based Approaches. *Trends Pharmacol. Sci.* **36**, 645–660 (2015).

330. Macauley, M. S., Crocker, P. R. & Paulson, J. C. Siglec-mediated regulation of immune cell function in disease. *Nat. Rev. Immunol.* **14**, 653–666 (2014).

331. Stuible, M. *et al.* Mechanism and function of monoclonal antibodies targeting siglec-15 for therapeutic inhibition of osteoclastic bone resorption. *J. Biol. Chem.* **289**, 6498–6512 (2014).

332. Edwards, J. R. *et al.* LIGHT (TNFSF14), a novel mediator of bone resorption, is elevated in rheumatoid arthritis. *Arthritis Rheum.* **54**, 1451–1462 (2006).

333. Hemingway, F., Kashima, T. G., Knowles, H. J. & Athanasou, N. A. Investigation of osteoclastogenic signalling of the RANKL substitute LIGHT. *Exp. Mol. Pathol.* **94**, 380–385 (2013).

334. Sandy, J. D., Flannery, C. R., Neame, P. J. & Lohmander, L. S. The structure of aggrecan fragments in human synovial fluid. Evidence for the involvement in osteoarthritis of a novel proteinase which cleaves the Glu 373-Ala 374 bond of the interglobular domain. *J. Clin. Invest.* **89**, 1512–1516 (1992).

335. Stefan Lohmander, L., Neame, P. J. & Sandy, J. D. The structure of aggrecan fragments in human synovial fluid. evidence that aggrecanase mediates cartilage degradation in inflammatory joint disease, joint injury, and osteoarthritis. *Arthritis Rheum.* **36**, 1214–1222 (1993).

336. Loulakis, P., Shrikhande, A., Davis, G. & Maniglia, C. A. N-terminal sequence of proteoglycan fragments isolated from medium of interleukin-1-treated articular-cartilage cultures. Putative site(s) of enzymic cleavage. *Biochem. J.* **284**, 589 LP – 593 (1992).

337. Carter, D. R. & Beaupre, G. S. Endochondral Growth and Ossification. in *Skeletal Function and Form* 106–137 (Cambridge University Press, 2000). doi:10.1017/CBO9780511574993.006

338. Ishida, N. *et al.* Large scale gene expression analysis of osteoclastogenesis in vitro and elucidation of NFAT2 as a key regulator. *J. Biol. Chem.* (2002). doi:10.1074/jbc.M205063200

339. Nakki, A. *et al.* Association study of MMP8 gene in osteoarthritis. *Connect Tissue Res* **57**, 44–52 (2016).

340. McHugh, K. P. *et al.* The role of cell–substrate interaction in regulating osteoclast activation: potential implications in targeting bone loss in rheumatoid arthritis. *Ann. Rheum. Dis.* **69**, i83 LP-i85 (2010).

341. Crotti, T. N. *et al.* Bone matrix regulates osteoclast differentiation and annexin A8 gene expression. *J. Cell. Physiol.* **226**, 3413–3421 (2011).

342. Purdue, P. E. *et al.* Comprehensive profiling analysis of actively resorbing osteoclasts identifies critical signaling pathways regulated by bone substrate. *Sci. Rep.* **4**, 7595 (2014).

343. Strassle, B. W. *et al.* Inhibition of osteoclasts prevents cartilage loss and pain in a rat model of degenerative joint disease. *Osteoarthr. Cartil.* **18**, 1319–1328 (2010).

344. Rother, S. *et al.* Structural and functional insights into the interaction of sulfated glycosaminoglycans with tissue inhibitor of metalloproteinase-3 – A possible regulatory role on extracellular matrix homeostasis. *Acta Biomater.* **45**, 143–154 (2016).

345. Han, Y., You, X., Xing, W., Zhang, Z. & Zou, W. Paracrine and endocrine actions of bone-the functions of secretory proteins from osteoblasts, osteocytes, and osteoclasts. *Bone Res.* **6**, 16 (2018).

346. Pederson, L., Ruan, M., Westendorf, J. J., Khosla, S. & Oursler, M. J. Regulation of bone formation by osteoclasts involves Wnt/BMP signaling and the chemokine sphingosine-1-phosphate. *Proc. Natl. Acad. Sci. U. S. A.* **105**, 20764–20769 (2008).

347. Wang, B. *et al.* Chondrocyte β-Catenin Signaling Regulates Postnatal Bone Remodeling Through Modulation of Osteoclast Formation in a Murine Model. *Arthritis Rheumatol.* **66**, 107–120 (2014).

348. Kwan Tat, S. *et al.* Modulation of OPG, RANK and RANKL by human chondrocytes and their implication during osteoarthritis. *Rheumatology* **48**, 1482–1490 (2009).

349. De Santis, M. *et al.* The Role of Wnt Pathway in the Pathogenesis of OA and Its Potential Therapeutic Implications in the Field of Regenerative Medicine. *Biomed Res. Int.* **2018**, 7402947 (2018).

350. Duan, P. & Bonewald, L. F. The role of the wnt/β-catenin signaling pathway in formation and maintenance of bone and teeth. *Int. J. Biochem. Cell Biol.* **77**, 23–29 (2016).

351. Regard, J. B., Zhong, Z., Williams, B. O. & Yang, Y. Wnt signaling in bone development and disease: making stronger bone with Wnts. *Cold Spring Harb. Perspect. Biol.* **4**, a007997 (2012).

352. Zhou, Y., Wang, T., Hamilton, J. L. & Chen, D. Wnt/β-catenin Signaling in Osteoarthritis and in Other Forms of Arthritis. *Curr. Rheumatol. Rep.* **19**, 53 (2017).

353. Moreno-Rubio, J., Herrero-Beaumont, G., Tardı´o, L., álvarez-Soria, M. ángeles & Largo, R. Nonsteroidal antiinflammatory drugs and prostaglandin E2 modulate the synthesis of osteoprotegerin and

RANKL in the cartilage of patients with severe knee osteoarthritis. *Arthritis Rheum.* **62**, 478–488 (2010).

354. Pettit, A. R. *et al.* TRANCE/RANKL Knockout Mice Are Protected from Bone Erosion in a Serum Transfer Model of Arthritis. *Am. J. Pathol.* **159**, 1689–1699 (2001).

355. Romeo, S. G. *et al.* Endothelial proteolytic activity and interaction with non-resorbing osteoclasts mediate bone elongation. *Nat. Cell Biol.* **21**, (2019).

356. Collin-Osdoby, P. & Osdoby, P. RANKL-mediated osteoclast formation from murine RAW 264.7 cells. *Methods Mol. Biol.* (2012). doi:10.1007/978-1-61779-415-5_13

357. Han, X., Aslanian, A. & Yates 3rd, J. R. Mass spectrometry for proteomics. *Curr. Opin. Chem. Biol.* **12**, 483–490 (2008).

358. Chu, C. R., Szczodry, M. & Bruno, S. Animal models for cartilage regeneration and repair. *Tissue Eng. Part B. Rev.* **16**, 105–115 (2010).

359. Athanasiou, K. A. *et al.* Biomechanical properties of hip cartilage in experimental animal models. *Clin. Orthop. Relat. Res.* (1995).

360. Taylor, S. D. *et al.* Comparison of human and animal femoral head chondral properties and geometries. *Proc. Inst. Mech. Eng. Part H J. Eng. Med.* **226**, 55–62 (2011).

361. Naranda, J., Gradišnik, L., Gorenjak, M., Vogrin, M. & Maver, U. Isolation and characterization of human articular chondrocytes from surgical waste after total knee arthroplasty (TKA). *PeerJ* **5**, e3079–e3079 (2017).

362. Nozaki, T. *et al.* Development of an ex vivo cellular model of rheumatoid arthritis: Critical role of cd14-positive monocyte/macrophages in the development of pannus tissue. *Arthritis Rheum.* **56**, 2875–2885 (2007).

363. Soysa, N. S., Alles, N., Aoki, K. & Ohya, K. Osteoclast formation and differentiation: an overview. *J Med Dent Sci* **59**, 65–74 (2012).

364. Filipowska, J., Tomaszewski, K. A., Niedźwiedzki, Ł., Walocha, J. A. & Niedźwiedzki, T. The role of vasculature in bone development, regeneration and proper systemic functioning. *Angiogenesis* **20**, 291–302 (2017).

365. Fernández-Torres, J., Martínez-Nava, G. A., Gutiérrez-Ruíz, M. C., Gómez-Quiroz, L. E. & Gutiérrez, M. Role of HIF-1α signaling pathway in osteoarthritis: a systematic review. *Rev. Bras. Reumatol. (English Ed.* **57**, 162–173 (2017).

366. Bouaziz, W. *et al.* Interaction of HIF1α and β-catenin inhibits matrix metalloproteinase 13 expression and prevents cartilage damage in mice. *Proc. Natl. Acad. Sci. U. S. A.* **113**, 5453–5458 (2016).

367. Anderson-MacKenzie, J. M. *et al.* Fundamental subchondral bone changes in spontaneous knee osteoarthritis. *Int. J. Biochem. Cell Biol.*

37, 224–236 (2005).